Aus dem
Julius Wolff Institut für Biomechanik und Muskuloskeletale Regeneration der Medizinischen Fakultät Charité – Universitätsmedizin Berlin

DISSERTATION

Knochengewebe unter dem Einfluss eines gealterten/erfahrenen adaptiven Immunsystem

Bone tissue under the influence of an aged/experienced adaptive immune system

zur Erlangung des akademischen Grades

Doctor of Philosophy (PhD)

vorgelegt der Medizinischen Fakultät
Charité – Universitätsmedizin Berlin

von

Christian H. Bucher

aus Udligenswil, Schweiz

Datum der Promotion: 18.09.2020

Table of contents

List of figures

List of tables

Abbreviations

TNFα	tumor necrosis factor alpha
IFNγ	interferon gamma
PBMC	peripheral blood mononuclear cells
FBS	fetal bovine serum
MSC	mesenchymal stromal cells
CD	cluster of differentiation
OD	optical density
SPF	specific pathogen free
M-CSF	macrophage colony-stimulating factor
RANKL	receptor activator of nuclear factor kappa-B ligand
OPG	osteoprotegerin
PBS	phosphate buffered saline
ECM	extracellular matrix
microCT	microcomputed tomoraphy
MMIp	minimum moment of inertia (polar)
DAMP	danger associated molecular pattern
PAMP	pathogen associated molecular pattern
LPS	lipopolysaccharide

Abstract

Deutsch: Erkrankungen des Bewegungsapparates gehören zu den häufigsten Ursachen von Schmerzen, Immobilität und Einschränkungen am Arbeitsplatz. Im Rahmen dieser Studie wurden altersabhängige Veränderungen des Immun- und Skelettsystems untersucht, um den Einfluss der gealterten Immunität auf den Knochen zu bewerten. Bei Patienten mit verzögerter Frakturheilung ist die Häufigkeit eines Subtyps von T Zellen im Vergleich zu normaler Heilung erhöht. Es stellt sich die Frage, ob die Erfahrung in der adaptiven Immunität einen direkten Einfluss auf den Knochen hat.

Das Skelett- und das Immunsystem wurden bei Mäusen im Alter von 3 bis 24 Monaten analysiert. Die Mäuse wurden in einer SPF Umgebung gealtert, wodurch eine relativ naive Immunität aufrechterhalten wurde, oder sie wurden Umweltmikroorganismen exponiert, wodurch das Immunsystem eine Erfahrung aufbauen konnte. Die Mäuse wurden auf ihren Immunstatus untersucht, welcher dann mit ihrer Knochenstruktur und -kompetenz korreliert wurde. Die Regeneration wurde in einem Osteotomiemodell analysiert und der Heilungsverlauf nach 3 und 21 Tagen bewertet. Eine Proteinanalyse wurde durchgeführt, um die Zytokinmuster zu entschlüsseln. Zusätzlich wurden MSCs hinsichtlich ihres Differenzierungspotentials und ihrer ECM-Produktion unter Immunzellsignalen analysiert. Darüber hinaus wurden mehrere immunmodulatorische Interventionen getestet, um die beeinträchtigte Heilung unter dem Einfluss einer gealterten/erfahrenen adaptiven Immunität zu verbessern.

Eine chronologische und biologische Alterung konnte über eine Trennung der immunologischen und knochengewebsspezifischen Alterung unterschieden werden. Das Gedächtnis-Kompartiment der adaptiven Immunität war bei Mäusen unter exponierter Haltung signifikant erhöht. Diese Immunerfahrung führte zu einem signifikant unterschiedlichen Knochenphänotyp in Bezug auf Struktur und Belastbarkeit. Der Verlauf der Knochenregeneration war vom Alter und vom Immunstatus abhängig. Die Heilung war in der Gruppe mit erfahrener adaptiver Immunität beeinträchtigt, und 3 Tage nach der Osteotomie wurden signifikant veränderte Zytokinspiegel beobachtet. Darüber hinaus bildeten die getesteten Interventionen des adaptiven Transfers von regulatorischen T Zellen oder der Aktivierungshemmung von Immunzellen als Immunmodulation den Grundstein für zukünftige Behandlungsoptionen.

Die adaptive Immunität wirkt sich direkt auf die Knochenbildung und den Gewebeumbau aus und führt zu strukturellen Unterschieden in der Knochenmaterialorganisation sowie in der mechanischen Kompetenz. Dieses Wissen ist für die Charakterisierung des Heilungsverlaufs von wesentlicher Bedeutung und bildet die Grundlage für neuartige Diagnostika und Therapeutika, die darauf abzielen, die beeinträchtigte Knochenregeneration bei immunologisch anspruchsvollen Patienten zu verstehen und zu behandeln. Diese Daten zeigen erstmals, dass die Immunerfahrung sowohl in der Diagnostik als auch in der Therapie berücksichtigt werden sollte.

English: Musculoskeletal conditions are the leading cause of pain, suffering and disability in workplaces and have a huge financial burden. Within this study, age-dependent changes in the immune and skeletal system were investigated in parallel to evaluate the impact of aged immunity on bone structures and quality. In patients with delayed fracture healing a subtype of T cells are at higher abundance compared to normal healing patients. This raises the question of whether the experience in the adaptive immunity directly influences bone structure and formation.

The skeletal and immune systems were analyzed in mice aged from 3 months to 24 months. The mice were aged in specific pathogen-free environment thus keeping a relative naïve immunity or exposed to environmental microorganisms allowing the immune system to establish memory. The immune status of the mice was examined via flow cytometry, which was then correlated to their bone structure via microCT and bone competence via biomechanical testing. Bone regeneration was analyzed *in vivo* in a mouse osteotomy model, and healing outcome was evaluated after 3 and 21 days. Protein analysis was done to unravel the diverging cytokine patterns after fracture. In addition, MSCs from these mice were analyzed for their differentiation potential and ECM production in the presence and absence of immune cell signaling *ex vivo*. Furthermore, several immunomodulatory interventions were tested in order to improve bone fracture healing under the influence of an aged/experienced adaptive immunity.

Age-associated alterations in the immune profile and bone tissue could be itemized between chronological and biological aging. The memory/effector compartment of adaptive immunity was significantly increased in mice that were exposed to environmental microorganisms. The immune experience led to a significantly different bone phenotype both in structure and in competence to withstand loads. The *in vivo* bone formation was highly affected by age but also by the immune status. Bone tissue formation during healing was delayed in the experienced adaptive immunity group and significant changes in cytokine levels were observed 3 days post-surgery. Furthermore, the tested interventions of regulatory T cells transfer or inhibition of immune cell activation as immunomodulatory approaches laid the foundation of future treatment options.

Adaptive immunity directly affects bone tissue formation and tissue remodeling leading to structural differences in bone material organization as well as mechanical competence. Such knowledge is essential for the characterization of healing settings and lays the foundation for novel diagnostics and therapeutics that aim to understand and rescue delayed bone regeneration in immunologically challenging patients. This data is the first to show that a patient's immune experience needs to be taken into account, in the context of diagnostics as well as in therapy.

1 Introduction

Self-healing or endogenous regeneration is a remarkable process that our bodies use to overcome injuries and traumas. In humans, the endogenous regeneration capacity is less obvious when compared to other species. Humans however are one of the most efficient combatants against invaders like bacteria or viruses and therefore bear one of the strongest adaptive immune system.

Bone is one of the few tissues in our body with the capacity for regeneration after injury (*restitutio-ad-integrum*). Unfortunately, in almost 10% of fracture cases, this capacity is insufficient and the healing outcome is not satisfactory for patients nor clinicians, eventually leading to pseudoarthrosis or even non-unions (Figure 1B). Geriatric fracture cases more often lead to non-healing situations when compared to young individuals and the fracture incidence is increased in this patient cohort (Figure 1A) [1,2]. Additionally, the population worldwide now tends to live longer, by 2050 the number of people over 60 years will nearly double from about 12% to 22%, to a total of two billion (Figure 1C). There were around 125 million people over 80 years in 2015 and by 2050 there will be around 434 million people over 80 years worldwide. [3] Trauma is also the most expensive medical condition after heart conditions and the number of geriatric trauma cases most likely will further increase due to a more active and recreative elderly population [4]. Thus, this increasing aged population challenges medical care and medical research. Fracture incidence increases with age and the incidence of non-unions correlates with the patient age. Geriatric fracture patients have the highest bed capacity requirement in hospitals, even higher than cardiovascular or stroke patients. The healing outcome of geriatric hip fractures leads in 18,4% of the cases to a re-hospitalization within 30 days, and the mortality rate is 10% after 4 weeks and 30% within one year. [5,6]

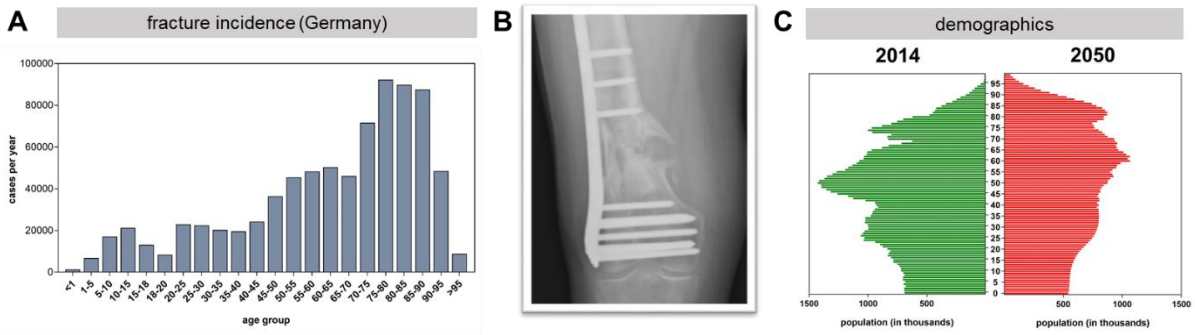

Figure 1 Bone fractures in geriatric patients. (A) Fracture incidence increases with patient ages, challenging the health care system (B) X-ray image from a 6 months old fracture from a 73-year old patient, showing insufficient callus formation leading eventually to a non-union. (B) Demographic distribution of population age in 2014 and provisioned for 2050, showing the increased elderly population. Combination of increased fracture incidence and delayed fracture healing in the aged combined with the demographic changes within the next year depict unmet needs in the clinics. (data: Federal Statistical Office, Wiesbaden, Germany)

Despite the substantial capacity to bear loads, bones can break under extreme external forces and adequate restoration is needed. Bone fractures can heal by two different processes: the direct, primary fracture healing or an indirect, secondary fracture healing. In the case of a secondary fracture healing, bone regeneration follows consecutive, partially overlapping phases. With the injury and rupture of adjacent blood vessels, a hematoma is formed within the fracture gap and clotting occurs. The simultaneously occurring inflammatory phase is characterized by the infiltration of macrophages, granulocytes, mast cells and T lymphocytes with secretion of histamine, heparin and pro-inflammatory cytokines. Cytokines and growth factors secreted within the hematoma are important for the control of cell infiltration, angiogenesis and cell differentiation. After the pro-inflammatory phase has subsided due to secretion of anti-inflammatory cytokines, the hematoma, in which a network of fibrin and collagen as an initial matrix has already formed, is replaced by granulation tissue with fibroblasts, additional collagen fiber and sprouting capillaries. Bone integrity is restored by a preliminary cartilage bridge, which is replaced by woven bone, hypertrophic cartilage and mineralization of the extracellular matrix. Subsequently, in the remodeling phase, the woven bone is transformed into lamellar bone according to the mechanical constraints.

Immune cells have been found to interact with bone cells throughout the healing process. They are the first cells in the hematoma which readily adapt to the harsh surrounding with lack of oxygen [7], and increased lactate levels indicating low pH values [8]. With the rupture of adjacent blood vessels, macrophages and lymphocytes are submerged within the fracture hematoma [9,10]. T cells, a subtype of the adaptive immune system, were especially identified as playing a major role in the regulation of the initial inflammatory cells and in the recruitment of other cells towards the fracture site [11,12]. These cells of the adaptive immune system can undergo significant changes during the ageing process. In the protection against pathogens, the innate immune system provides an early first line of defense with neutrophils, monocytes, macrophages, NK cells and dendritic cells, which all interact with the adaptive immune system. The adaptive immune system gradually matures with age, the innate immune system however is not able to establish an immune memory. As a result of immune challenges naïve T cells undergo significant changes and memory and effector T cells are generated. Through constant exposure to pathogens and antigens a memory and effector immune function is developed [13]. This accumulation of immunological memory is accompanied by the risk of delayed fracture healing [14]. Aged individuals tend to present with a chronic low-grade inflammatory state that has been implicated in the pathogenesis of many age-related diseases (atherosclerosis, Alzheimer's disease, osteoporosis and diabetes) [15,16]. This inflamm-aging is characterized by increased levels of circulating cytokines and pro-inflammatory markers like tumor necrosis factor a (TNFα), Interleukin-1 (IL1), Interleukin-6 (IL6) or Interleukin-8 (IL8) [17].

Apart from in injury situations, the immune system has also been acknowledged to play a major role in bone homeostasis, the formation, resorption and remodeling of bone tissue. Bone progenitor cells (mesenchymal stromal cells/pre-osteoblasts) and immune cells share their tissue

of origin, the bone marrow. Additionally, hematopoietic progenitor cells can divide through discriminative signaling cascades during cell maturation into either osteoclasts (OC) or cells of the monocyte/macrophage lineage, therefore sharing the same ancestors, highlighting the strong interdependency of the musculoskeletal and immune system. Bone homeostasis is a coordinated process between formation and degradation of bone, respectively managed by osteoblasts (OB) and osteoclasts; this ensures the constant adaptation to mechanical loading. In physiological conditions, canonical osteoclast formation requires macrophage colony-stimulating factor (M-CSF) and receptor activator factor of nuclear factor kB ligand (RANKL), which act on cells of the monocyte-macrophage lineage, to induce their fusion to form polynucleated active resorbing cells, the osteoclasts. Osteoprotegerin (OPG) however inhibits the osteoclast formation by binding RANKL and prevent bone formation over resorption. [18,19] Cells of the adaptive immune system are potent producers of OPG and RANKL and can directly interfere with the process of bone homeostasis. Li et al. showed that B- and T-cell-deficient mice exhibit a significantly increased number of OCs and reduced bone density as compared to controls [20]. Other mechanisms induced by the adaptive immune system could be shown in rheumatoid arthritis, a chronic inflammatory disease characterized by excessive bone loss, where T cells infiltrate tissues in the joints and release pro-inflammatory cytokines including IL-17 and TNFα [21]. TNFα subsequently increases the RANKL expression, favoring the differentiation of osteoclasts (osteoclastogenesis) [22]. These data highlight the tight interdependency of the bone and immune system, especially the adaptive immune system in homeostasis and regeneration.

In current research the standard housing conditions for small research animals is under specific pathogens free conditions. Under these conditions the variances between animals has been considered to be small, however, the development of an experienced immune system is abolished [23]. Therefore, studies considering the impact of the experienced adaptive immune system, the so called inflamm-aging, on bone structures and regeneration are scarce.

The immune system performs many regulatory tasks inside the body. With a fracture, the immune system is activated via a sterile inflammation. The effect of inflamm-aging on bone tissue is so far not known. In homeostasis the immune system and their products such as cytokines and growth factors may be involved, but their influence on bone homeostasis and regeneration are often neglected. This study aims to understand the influence of an experienced immune phenotype on bone structures and bone regeneration. Within this study, aging effects were analyzed in a cohort of mice with a more naïve immune phenotype (chronological aging) and compared to a cohort of mice that were allowed to gain an immune memory during aging (biological aging). Thus, bone phenotype changes due to the aged immunity were identified during homeostasis, regeneration and adaptation therefore allowing the distinction between age induced and immune induced changes of the bone. Fractures in elderly people represent a medical need with a high demand for future therapies. Understanding the changes in fracture healing with an aged/experienced immune system, could lead to new therapeutic options for geriatric fracture patients and cut hospital costs.

2 Materials & Methods

2.1 Animal experiments, *in vivo* studies

Female C57BL/6 mice were purchased from Charles River Laboratories with an age of 10 weeks and were used at an age of 3, 12 or 24 months. Animals were imported with a health certificate and kept under obligatory hygiene standards that were monitored according to the FELASA standards. The mice were kept under specific pathogen free (SPF) housing or under nonSPF housing. Food and water was available ad libitum and the temperature (20±2°C) controlled with a 12 h light/dark circle. The nonSPF mice were able to establish an experienced immune system due to surrounding environmental germs/pathogens compared to SPF housed mice in individual ventilated cages (IVC) with restricted environmental exposure. The nonSPF mice did not contract any infections or similar and still exhibited good health when tested according to the FELASA guidelines. All experiments were carried out with ethical permission according to the policies and principles established by the Animal Welfare Act, the National Institutes of Health Guide for Care and Use of Laboratory Animals, and the National Animal Welfare Guidelines, the ARRIVE guidelines and were approved by the local legal representative animal rights protection authorities (Landesamt für Gesundheit und Soziales Berlin: G 0338/13, G 0061/14, G 0008/12, T 0119/14, T 0026/16).

2.1.1 Mouse osteotomy as a model of fracture healing

Bone regeneration was studied by introducing an osteotomy on the left femur. The mice were anesthetized with a mixture of isoflurane (Forene) and oxygen (Induction with 2% Isoflurane and maintenance with 1.5%). First line analgesia was done with Bubrenorphine pre-surgery, antibiotics with clindamycin and eye ointment to protect the eyes. Post-surgery, tramadol (25mg/l) was added to the drinking water for three days. The surgical area was shaved and disinfected, and all surgical procedures were performed on a heating pad. Briefly, a longitudinal, lateral skin incision and dissection of the fasciae allowed to expose the femur. The Musculus vastus lateralis and Musculus biceps femoris were dislodged by blunt preparation with protection of the sciatic nerve. Thereafter, serial drilling for pin placement (diameter: 0.45 mm) through the connectors of the external fixator (MouseExFix, RISystem, Davos, Switzerland) was performed, resulting in a fixation of the external fixator construct strictly parallel to the femur. Following rigid fixation, a 0.70mm osteotomy was performed between the medial pins using a Gigli wire saw (RISystem, Davos, Switzerland). After skin closure, mice were returned to their cages and kept under warming lamps during the period of immediate anesthesia recovery.

2.1.2 Humanization of NSG mice

Humanization of mice was achieved by injection of human peripheral blood immune cells into immunocompromised NOD.Cg-Prkdc^{scid} Il2rg^{tm1Wjl}/SzJ (NSG) mice, a mouse strain deficient in mature lymphocytes and dendritic cells, low NK and macrophages cell activity and absence

of the complement system and serum levels of antibodies. The human immune cells were isolated from characterized donors and stratified into more or less experienced (immunoaged) donors by the effector T cell markers CD8, CD57 and CD28 (ethical approval EA1/125/10). The peripheral blood mononuclear cells (PBMC) were resuspended in PBS and injected via the tail vein at a concentration of $10x10^6$ cells per animal. The cell engraftment was verified at 3 and 21days post-injection and showed a stable infiltration into the bone marrow and other tissues.

2.1.3 Regulatory T cell administration

Regulatory T cells were isolated from the spleen and lymph nodes of donor mice via magnetic cell isolation (MACS). The CD4+T_{Reg} isolation kit (Miltenyi Biotec, Bergisch Gladbach, Germany) was used according to the manufacturer's instructions. The isolated T_{Reg} cells were resuspended in PBS and injected via the tail vein at a concentration of $5\text{-}8x10^5$ cells per animal. The host mice were either kept under SPF or nonSPF conditions.

2.1.4 Immune cell activation pathway blockage

Osteotomized animals were injected intraperitoneally with three different signaling pathways inhibitors post-surgery for 5 days to block the activation pathways of T cells during the initial inflammatory phase. Tacrolimus (Prograf, Astellas Pharma, München, Germany) was injected at a concentration of 1mg/kg BW to block the calcineurin pathway, Rapamycin (Merck, Darmstadt, Germany) at a concentration of 3mg/kg BW to block the mTOR pathway and Pepinh-MYD (Bio-Techne, Minneapolis, USA) at a concentration of 5mg/kg BW to block the MyD88 pathway.

2.1.5 Transgenic mouse RAG/OT

Splenocytes were isolated from Rag2/OT-I mice which are deficient in the recombination activating gene 2 (Rag2) and therefore do not develop mature T or B cells expressing endogenous T cell receptors, but virtually all peripheral CD8+ cells express a transgene for a T cell receptor recognizing a synthetic peptide (SIINFEKL). The CD8+ T cells were isolated via magnetic cell separation (MACS) with the CD8a+ T Cell Isolation Kit (Miltenyi Biotec, Bergisch Gladbach, Germany) according to the manufacturer's instructions. The isolated T cells were verified by flow cytometry by staining with DimerX I, a recombinant soluble dimeric mouse H-2K[b]:Ig fusion protein (BD biosciences, Franklin Lakes, USA) bound with the synthetic peptide and were injected via the tail vein at a concentration of $2x10^6$ cells per animal.

2.1.6 *In vivo* limb loading

The left tibiae of 3 month and 12 month old mice underwent *in vivo* cyclic compressive loading, while the right tibia was not loaded and served as an internal control. The flexed knee and the ankle of the mice were placed in our loading device (Testbench ElectroForceLM1, TA Instruments, USA) and axial dynamic compressive loading was applied 5 days per week for 2 weeks while the mice were anesthetized with isoflurane. The loading protocol consisted of 216 cycles applied at 4 Hz, which is the mean mouse locomotory stride frequency delivering a maximum

force of -7N for the 3 and -9N for the 12 month old mice, engendering 900με at the periosteal surface in the tibia mid-diaphysis. Mice were sacrificed on day 15, 3 days after the last loading session.

2.1.7 Isolation of bones/samples

Osteotomized animals were sacrificed three or 21 days post-surgery by injection of Ketamin and Medetomidine to induce a deep anesthesia and subsequently euthanized by cervical dislocation. Bone and other tissue were excised, stored in PBS on ice or directly fixated in a 4% formaldehyde/PBS mixture.

2.2 Flow cytometry

Samples were either harvested from mouse tissue and isolated from spleen or bone marrow or isolated from human peripheral blood from volunteers (ethical approval EA1/125/10). Mouse spleen and bone marrow was isolated via filtration through a 40µm strainer (Falcon, BD Biosciences, Franklin Lakes, USA) and the single cell suspension was treated with erythrocyte lysis buffer (BioLegend, San Diego, USA) to remove red blood cells. Human peripheral blood was processed via density centrifugation in SepMate tubes and Lymphoprep density gradient medium (both Stemcell Technologies, Vancouver, Canada) to isolate peripheral blood mononuclear cells (PBMC). The cells were then incubated with a live/dead stain and subsequent fc block solution, to remove dead cells from the analysis and unspecific binding of antibodies to fc receptors. The cells were then incubated for 20 min at room temperature (RT) or 4 °C with fluorochrome-coupled antibodies according the multicolor panels in Appendix 1. For intracellular markers, the cells were fixed and permeabilized with the True-Nuclear Transcription Factor Buffer Set (BioLegend, San Diego, USA) according the manufacturer's instructions and subsequently stained for 30 min at RT with fluorochrome-coupled antibodies against the respective epitopes. The cells were measured with a BD LSR Fortessa SORP (BD Biosciences, Franklin Lakes, USA) or CytoFlex LX (Beckman Coulter, Brea, USA) flow cytometer and analyzed with the software FlowJo v10 (TreeStar, Ashland, USA).

2.3 Micro computed tomography

Samples were harvested from mouse tissue, fixed and washed in buffer saline solutions. Micro computed tomography was executed with a Skyscan 1172 (Bruker, Billerica, USA) at a nominal voxel resolution of 8 µm at 70 kV and 142 µA source energy with a maximized power at 10W. A 0.5 mm aluminium filter was employed to reduce the beam hardening effect. Shadow images were reconstructed with an adapted Feldkamp algorithm with the software nRecon (Bruker, Billerica, USA). Analysis was performed via self-made scripts within the CTan software and visualized with CTvox (both Bruker, Billerica, USA).

2.4 Biomechanical testing

The torsional stiffness, the maximum torque, its corresponding angle, workload and post-yield displacement were assessed in a torsional load to failure experiment. Following harvesting, the femora were excised and prepared by removing all adjacent muscles and tendons. Subsequently both epiphyses of the femora were embedded with methylmethacrylate (Technovit 3040, Heraeus Kulzer, Hanau, Germany) in custom made molds. Bones were mounted into a material testing device (Bose ElectroForce LM1, Bose Corporation, Eden Prairie, USA) and tested by first applying an axially preloaded of 0.3 N which remained constant during the following torsional load to failure at a rate of 0.54 °/s. Axial displacement, load, torque and rotation were all acquired at a 100 Hz sample rate. All parameters were calculated by a routine written in MATLAB (The Mathworks Inc., Natick, USA).

2.5 Cell culture, *in vitro* studies

2.5.1 Murine cell culture

Splenocytes and bone marrow cells were isolated from mouse tissue. The spleen was dissected and mashed through a 70 µm mesh to isolate the splenocytes. Erythrocytes were removed by incubation with the ACK Lysing Buffer (Thermo Fisher Scientific, Waltham, USA). The bone marrow was isolated by cutting open both end of femora or tibia and flushing the bone marrow out of the cavity with a 24 G needle and PBS, after filtration through a 40 µm mesh strain, red blood cells were removed with the lysing buffer. The splenocytes were activated with 10 mg/ml plate bound α-CD3 antibody and soluble 2 mg/ml α-CD28 (BioLegend, San Diego USA). After 48 h the conditioned medium was collected, pooled, filtered and stored at -80 °C. Murine mesenchymal stromal cells were obtained via outgrowth culture from bone marrow cells. The isolated single cells from bone marrow were plated in 25 cm^2 cell culture plates with DMEM low glucose medium (Biochrom, Berlin, Germany) supplemented with 10 % FBS (Biochrom, Berlin, Germany). Murine MSC were used between passage 5 and 6 for the experiments. Osteogenic differentiation of mMSC was achieved by the supplementation with 100 nM Dexamethasone, 0.05 mM l-ascorbic acid 2-phosphate and 10 mM β-Glycerolphosphate. Conditioned medium was added at a concentration of one part to three parts osteogenic differentiation medium. Medium was exchanged every 3-4 days. After 14 days the experiment was stopped and the mineralized extracellular matrix was stained with Alizarine Red S (Sigma, St. Louis, USA) and quantification was achieved by resolving the stain with cetylpyridiniumchlorid (Sigma-Aldrich, St. Louis USA). Optical density (OD) was measured with a multimode microplate reader (Tecan, Männedorf, Switzerland) and the collagen fibers were stained with Picrosirius Red (Sigma, St. Louis, USA) and analyzed under polarizing light. Pro-inflammatory stimulation with TNFα (BioLegend, San Diego, USA) and IFNγ (BioLegend, San Diego, USA) was performed for 72 h before cell harvesting and mRNA isolation with TRIzol (Sigma, St. Louis, USA).

2.5.2 Human cell culture

Human mesenchymal stromal cells (hMSC) were isolated from bone marrow of patients undergoing total hip replacement (provided by the Center for Musculoskeletal Surgery, Charité-Universitätsmedizin Berlin and distributed by the "Cell and Tissue Harvesting" Core Facility of the BCRT). All protocols were approved by the Charité-Universitätsmedizin ethics committee and performed according to the Helsinki Declaration. hMSC were cultivated with DMEM low glucose medium (Biochrom, Berlin, Germany) supplemented with 10 % FBS (Biochrom, Berlin, Germany). After three passaging steps, hMSC were characterized by differentiation assays (osteogenic, adipogenic and chondrogenic). Only hMSC that were capable of differentiation in all three lineages were used in the experiment within passage 4-8. Peripheral blood mononuclear cells (PBMC) were isolated from buffy coats (provided with ethical approval by DRK, Berlin, Germany) via density gradient. Naïve T cells were isolated with the naïve pan T cell isolation kit and effector T cells were isolated with the CD8+CD57+ T cell isolation kit (Miltenyi Biotec, Bergisch Gladbach, Germany) according to the manufacturer's protocol. The isolated cells and PBMC were activated with 10 mg/ml plate bound α-CD3 antibody and soluble 2 mg/ml α-CD28 (BioLegend, San Diego, USA). After 48 h the conditioned medium was collected, pooled, filtered and stored at -80 °C until further use. Osteogenic differentiation of hMSC, under the influence of conditioned medium from hPBMC was developed similarly to murine MSC. Activation of CD8+ T cells was achieved after isolation with RosetteSep CD8+ T cell enrichment kit (Stemcell Technologies, Vancouver, Canada) according the manufacturer's protocol and incubation in RPMI 1640 (BioLegend, San Diego, USA) supplemented with 10 % heat-inactivated FBS (Thermo Fisher Scientific, Waltham, USA). The CD8+ T cells were activated for 24 h with either α-CD3/CD28, HMGB1, S100A8/A9, IL-12/IL-18, IL-1a, IL-33 (all BioLegend, San Diego, USA) or LPS (strain O111:B4, Bio-Techne, Minneapolis, USA).

2.6 Cytokine secretion, ELISA

Conditioned medium from activated immune cells was harvested as described and processed for enzyme-linked immunosorbent assay (ELISA). Cardial blood from mice at the finalization step was collected and centrifuged at 3000 x g to isolate the blood serum. ELISAs for TNFα (TNF alpha Human Uncoated ELISA Kit, Thermo Fisher Scientific, Waltham, USA) and IFNγ (Interferon gamma Human Uncoated ELISA Kit, Thermo Fisher Scientific, Waltham, USA) were performed in triplicate according to the manufacturer's instructions and optical density was measured with a microplate reader Tecan Infinite (Tecan, Männedorf, Switzerland). A standard curve was generated with a four parametric logistic curve fit. Muliplexed ELISA was achieved with LegendPlex Kits T Helper Cytokine Panel and Cytokine Panel 2 (BioLegend, San Diego, USA) for mouse serum and the CD8/NK Panel (BioLegend, San Diego, USA) for the human immune cell conditioned medium. The assay was run according the manufacturer's instructions and acquired on a CytoFlex LX (Beckman Coulter, Brea, USA) flow cytometer, analyzed with the LegendPlex software available from BioLegend.

2.7 Gene expression

RNA isolation from TRIzol Reagent dissolved cells was achieved with the RNeasy Mini Kit (Qiagen, Venlo, Netherlands) according to the manufacturer's protocol. DNA was eliminated with DNAse I (Thermo Fisher Scientific, Waltham, USA). One microgram of total RNA of each sample was then used for cDNA synthesis with the iScript Reverse Transcription Super-mix for RT-qPCR (Bio-Rad Laboratories, Hercules, USA). Quantification was performed using Probe assays for real-time PCR including PCR primers and a dual-labeled fluorescent probe with FAM or Cy5 (Bio-Rad Laboratories, Hercules, USA) run on a LightCycler II (Roche, Basel, Switzerland). Analysis of housekeeping genes for Ppia, RPL13A and HPRT was used for normalization of the data.

2.8 Statistics

Due to the small sample sizes of *in vivo* preclinical studies, a normal distribution of the data was excluded. Therefore, the Mann-Whitney U-test was used as statistical test. If more than two samples were compared, the significance value p was corrected by using the Bonferroni correction. *In vitro* data was analyzed using the unpaired Student's t-test (two groups). Data were seen as statistically significant if $p \leq 0.05$.

Graphs and statistics were produced with GraphPad Prism (GraphPad Software Inc., San Diego, USA).

3 Main results

3.1 Characterization of an aged/experienced adaptive immunity

Cells of the adaptive immune system can change phenotype upon activation and in contrast to the innate immune response are able to establish an immune memory. Naïve T cells can form long lasting memory cells through repetitive antigen/pathogen challenge. Memory cells accumulate physiologically with age and the naïve T cells diminish over time. The memory formation is highly individual due to different genetics and behavior of people. Therefore, the variance in memory subpopulations in the T cell compartment increases with age. To adopt this finding of increased experience and interindividual variances in a research setting to develop a close clinical setting, mice were aged up to 24 months and either kept under specific pathogen free (SPF) housing conditions, to keep the immune experience low, or kept in cages without additional hygiene barriers (nonSPF) to allow the development of an experienced immune system. Both aging groups with different housing conditions were compared to young (3 months old) and immunologically naïve mice. A thorough characterization was performed, which included the innate and the adaptive immune compartments. Significant differences in the immune phenotype could be found in the two mouse cohorts upon aging. The most prominent changes due to chronological aging was the observation of a significant myeloid shift, the percentage of lymphocytes is lower in 12 months old mice compared to 3 months old mice. The ratio of CD4+ T cells to CD8+ T cells is also shifted towards CD4+ T cells in the aged animals. The immune experience however had an immense impact on the adaptive immune cell composition during aging. While the mice under SPF conditions only showed a mild increase in memory cells, the mice under nonSPF conditions almost completely exhausted their naïve T cell compartment and memory and effector T cells represented the dominant subpopulations (see Figure 2). The T regulatory (T_{Reg}) cell population within the CD4+ T cell compartment increased with age and significantly increased with experience in the immune system, showing a mechanism of compensation for the experience level in the immune system. However the

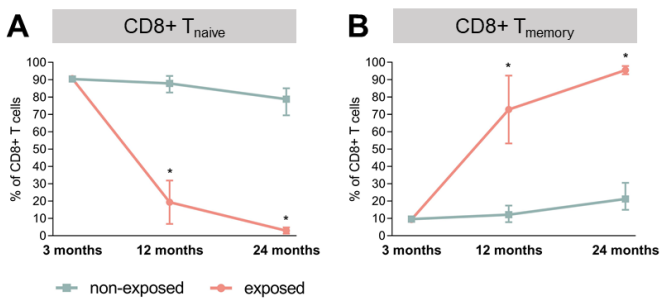

Figure 2 (key results) Experience in the adaptive immunity as a function of age and housing conditions. Flow cytometric analysis of the systemic immune phenotype (spleen tissue). (A) Depending on the housing conditions, a decrease of naïve immune cells could be shown, here shown as percentage of CD8+ T cells and (B) an increase in memory T cells as a function of age and exposition to environmental microorganisms, shown as percentage of CD8+ T cells. N=6 per group, Mann-Whitney U test, * p<0,05 (adapted from Bucher et al. *Front. Immunol.* 2019)

ratio of CD4+ T_{Reg} cells to CD8+ T effector/memory (T_{EM}) cells, a biomarker for a more prone pro-inflammatory status, showed a decline in the aged and especially aged experienced animals, favoring the CD8+ T_{EM} population, resulting in a more pro-inflammatory status. Therefore, the CD4+ T_{Reg} are only able to combat to some extent the CD8+ T_{EM} in the aged animals, as the CD8+ T_{EM} population increased more than the CD4+ T_{Reg} in the experienced mouse cohort.

The memory T cells can be distinguished from central memory cells (T_{CM}) and effector memory cells (T_{EM}) by their surface marker expression. They differ in their homing signals as several markers like CD62L are downregulated for instance in effector memory cells. This allows the T_{EM} cells to be more easily trafficked outside of primary or secondary lymphoid organs. This compartmentalization of memory T cells only allows one to distinguish between trafficking behaviors but does not reflect a functional aspect of these memory cells. Regardless of whether the cells are found in the central or effector memory compartment, both cell types differentially react upon antigen activation. This so-called recall efficacy (activation phenotype) allows one to distinguish between highly reactive strong responders (pronounced IFNγ and Granulysin production), intermediate responders and low responders (low pro-inflammatory and effector cytokine production) [24]. The activation phenotype of the memory CD8+ T cells changed significantly with age and under different housing conditions (antigen exposure). With age and antigen exposure (nonSPF) a potentiation of highly reactive immune cells occurred, the pool of specialized memory immune cells increased (see figure 3). In the immunologically experienced cohort, the CD8+ T memory population was increased compared to the non-experienced cohort (as shown in figure 2) and finally those CD8+ T memory cells were even stronger in their recall efficacy under nonSPF condition, showing an overall increase in the pro-inflammatory signaling and activation behavior in the immunologically experienced cohort.

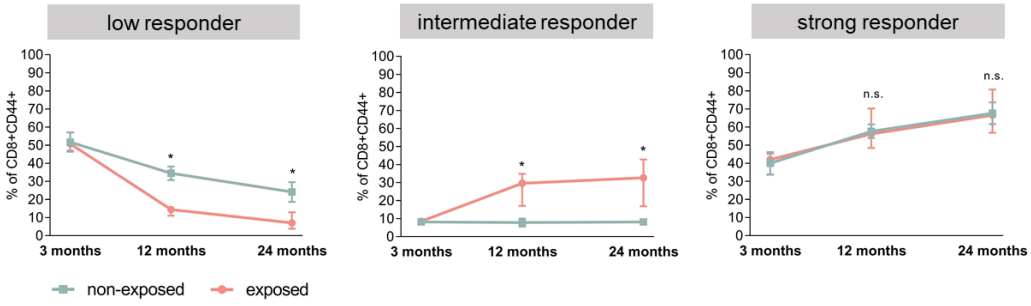

Figure 3 (key results) Recall efficacy (activation phenotype) of memory CD8+ T cells. Flow cytometric analysis of memory CD8+ T cells (gated for CD44+ cells) in the spleen. Memory CD8+ T cells can be distinguished by their response efficacy (activation phenotype) by recall antigen challenge. Strong responders produce high amounts of effector cytokines, whereas low responders are more inert upon activation also they belong to the same memory compartmentalization (T_{EM} or T_{CM}). The intermediate responders are increased under the exposed housing, depicting a potentiation of the experience in the CD8+ T cell compartment. N=6 per group, Mann-Whitney U test, * p<0,05 (adapted from Bucher et al. *Front. Immunol.* 2019)

3.2 Changes in bone tissue due to increased experience in the adaptive immunity

As shown in figure 2 and 3 several and severe changes occur in the immune system due to age and/or antigen exposure. This study aims to reveal the influence of an experienced adaptive immunity on bone homeostasis. The same thoroughly characterized groups of aged and immunologically experienced or non-experienced mice were analyzed for their bone properties. Young 3 month old mice were used as controls compared to 12 month old mice. Age-dependent alterations of the bone tissue are known [25–27], however the results from this study show that the experience level in the adaptive immune system intensified those age-dependent changes. In the diaphyseal region of the bone the cortical thickness increased with age and significantly increased further in the presence of an experienced immune system without significantly changing the mineral density (figure 4A). This increase in cortical thickness, as well as the observed thicker trabecular structures in the metaphyseal bone, led to an overall stiffer bone in the torsional testing for bone competence (figure 4B and C). The smaller post-yield-displacement depicted a brittle fracture manner in the aged femora, with even worsened brittleness under high experience level in the adaptive immune system, compared to a ductile fracture manner in 3 month old femora (figure 4C). Aged bone showed an overall lower bone quality, with the immune experience intensifying the decline in quality upon aging. These immunologically experienced and aged bones can be found in geriatric patients in the clinical setting.

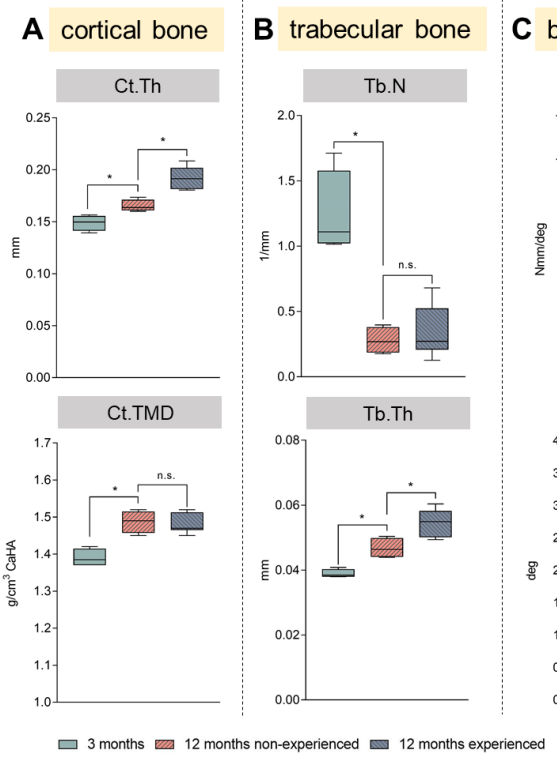

Figure 4 (key results) Cortical and trabecular bone changes with immune experience. (A) MicroCT analyses of femoral cortical bone revealed a thicker (Ct.Th) and denser (Ct.TMD) bone with age, however without changing the mineral density, the immune experienced animal cohort further increased the thickness. (B) Trabecular bone number (Tb.N) decreases with age, the immune experience increased the remaining trabecular bone (Tb.Th). (C) Bone competence by torsional testing revealed an increased stiffness of the femur by age and the immune experience, as well as a lower post-yield-displacement (PYD) depicting that the bone broke in a more brittle manner. N=6 per group, Mann-Whitney U test, * p<0,05 (adapted from Bucher et al. *Front. Immunol.* 2019)

3.3 T cell cytokines alter stromal cell behavior

To understand the crosstalk between immune cells of the adaptive immune system and bone tissue cells, an *in vitro* experimental set up was established, which tested the immune cell products on mesenchymal stromal cells (MSC). The immune cells, here splenocytes, were isolated from mice lacking defined populations of the adaptive immune system: $RAG^{-/-}$ mice lacking both T and B cells, $TCRbd^{-/-}$ mice lacking T cells and $JHT^{-/-}$ mice lacking B cells. All three groups were compared to Wildtype (WT) mice. The isolated immune cells were stimulated with a common activator of the complete immune cell cascade, Lipopolysaccharide (LPS). The obtained conditioned medium was transferred to MSC under osteogenic differentiating conditions to investigate alterations in their capacity to undergo osteogenic differentiation. The conditioned medium obtained from immune cells from mice lacking B and T cells ($RAG^{-/-}$) and T cell deficient mice ($TCRbd^{-/-}$) significantly altered the extracellular matrix (ECM) deposition and the mineralization process of MSC, showing a potential deficiency in the bone healing process, as MSC are required to differentiate into osteoblasts and form adequate ECM during healing. The conditioned medium from mice lacking B cells ($JHT^{-/-}$) however showed no differences compared to the WT conditioned medium (see representative images in figure 5). The differentiation and ECM production of MSC seemed to be dependent on T cells and independent of B cells. This is in correspondence with the osteoblast distribution found *in vivo* in these animals in histological sections.

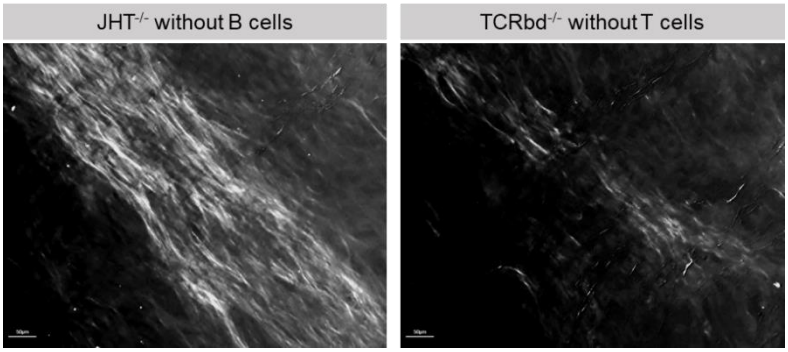

Figure 5 (key results) Extracellular matrix formation under the influence of the adaptive immunity. Representative images of Sirius Red staining of the newly formed collagen fibrils produced by mesenchymal stromal cells (MSC) under the influence of immune cell products. Conditioned medium obtained by stimulated immune cells from B cell deficient mice ($JHT^{-/-}$) stimulated the matrix formation process of MSC, however conditioned medium from T cell deficient mice ($TCRbd^{-/-}$) mice lowered the matrix deposition. (adapted from El Khassawna et al. *Front. Immunol.* 2017)

3.4 Memory T cells alter stromal cell behavior

As T cells were revealed to be key players in the immune cell mediated changes of the bone tissue, the subpopulations of the T cell compartment (naïve or memory) were isolated and tested for their cytokine profile and crosstalk with MSCs. Naïve T cells and memory CD8+ T cells were isolated from peripheral blood from volunteers. Human samples were used to mimic the in-patient situation. The isolated cells were stimulated with α-CD3 and α-CD28, a potent inducer of T cell activation. Both groups were compared to unprocessed isolated and activated peripheral blood mononuclear cells (PBMC). The conditioned medium of naïve T cells did not interfere with the osteogenic differentiation process of MSC, whereas the conditioned medium of activated CD8+ T cells almost completely abolished the differentiation process (see figure 6 A). The cytokines tested in the conditioned medium revealed a distinct production of TNFα and IFNγ from CD8+ T cells, whereas naïve T cells did not produce high amount of pro-inflammatory cytokines (see figure 6 C). The increased pro-inflammatory cytokines from CD8+ T cells induced proliferation rather than differentiation of MSC (see figure 6 B). Resting PBMC especially changed MSC behavior from proliferation towards differentiation, as the mineralized tissue per cell increased in this treatment group compared to the differentiation group without conditioned medium.

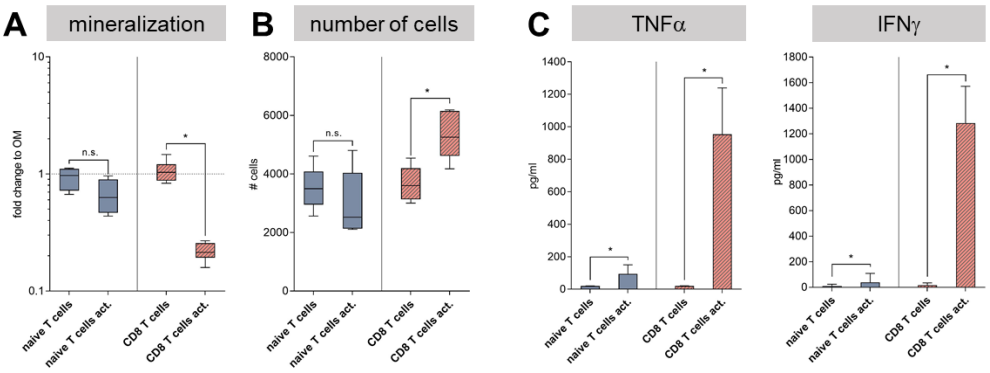

Figure 6 (key results) Mineralization of stromal cells under the influence of experienced adaptive immunity. (A) Osteogenic differentiation of mesenchymal stromal cells (MSC) under the influence of immune cell products. Conditioned medium from naïve T cells did not interfere with the osteogenic differentiation process of MSC, however the conditioned medium from activated experienced CD8+ T cells almost abolished the differentiation process. (B) The increased pro-inflammatory cytokines from CD8+ T cells induced proliferation rather than differentiation of MSC. (C) Cytokine expression analysis of the conditioned medium. Activated naïve T cells only produced low amount of pro-inflammatory cytokines like TNFα and IFNγ, activated experienced CD8+ T cells however produced high amounts of TNFα and IFNγ. N=3 different immune cell donors and N=2 different MSC donors. Student's t-test, * p<0,05 (adapted from Bucher et al. *Front. Immunol.* 2019)

To test the influence of a pro-inflammatory stimulus, reflecting the initial inflammatory phase during fracture healing, mesenchymal stromal cells were stressed with the pro-inflammatory cytokines TNFα and IFNγ. The stimulation of undifferentiated MSCs directly with TNFα and IFNγ led to a decreased production of extracellular matrix components and to an increase of pro-inflammatory cytokines as seen in the gene expression profile (see figure 7). A prolonged pro-inflammatory phase during the bone healing cascade is able to delay the formation of new extracellular matrix and even potentiates the invasion of additional immune cells by production of chemokines and pro-inflammatory cytokines by stimulated MSCs.

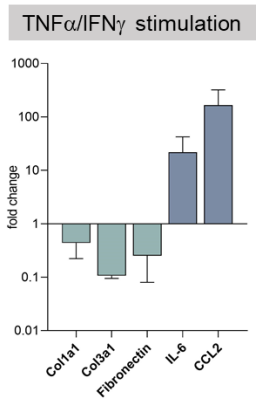

Figure 7 (key results) A pro-inflammatory stimulus hinders extracellular matrix production of stromal cells and amplifies the inflammation. Gene expression analysis after pro-inflammatory stimulus on stromal cells. TNFα and IFNγ stimulation of mesenchymal stromal cells, mirrored from the initial pro-inflammatory phase of fracture healing, showed a decrease of mRNA levels for ECM proteins, but showed an increased pro-inflammatory cytokine mRNA and migratory attractors. N=3 MSC donors in triplicates

3.5 Fracture healing in an experienced or naïve adaptive immune system

To reveal the tremendous effect of T cells on bone properties and mesenchymal stromal cell behavior under regenerative conditions the healing cascade in osteotomized femurs in mice were analyzed. Aged 12 months old mice either immunologically experienced or naïve (non-experienced) were screened for changes in the healing cascade due to the experience of the adaptive immune system. The immunologically experienced group was compared with the non-experienced group at 12 months to determine the healing outcome after 21 days post-surgery by microCT. The altered cytokine levels as well as the immune phenotype was assessed pre-surgery and after 3 days of healing, to determine the immunological experience induced changes of signaling molecules in the initial inflammatory phase of bone healing. At the pre-surgery timepoint, the two groups showed clear differences in the memory and effector T cell compartments as well as a pro-inflammatory cytokine pattern, seen by the systemically elevated TNFα levels in the experienced group compared to the non-experienced group, showing the inflamm-aged status in this cohort. Three days after insertion of an osteotomy the cytokine levels were measured in the blood by a multiplexed ELISA screening approach to detect signs of systemic changes due the injured bone and due to the altered immune status (inflamm-aged status). Three days after introducing the osteotomy the systemic levels of, for example IL-1β, a potent mediator of inflammation, IL-5, a chemotactic cytokine for eosinophils and GM-CSF,

a macrophage stimulating factor for the pro-inflammatory M1 macrophages, were significantly increased in the immunologically experienced group (see figure 8). The cytokine levels demonstrated overall an amplified initial inflammatory reaction to bone fracture in animals with an experienced adaptive immune system. These findings suggest that the healing cascade is altered and delayed due to this modified cytokine pattern, as an altered initial inflammatory phase impacts the healing cascade up to the final stages of bone healing.

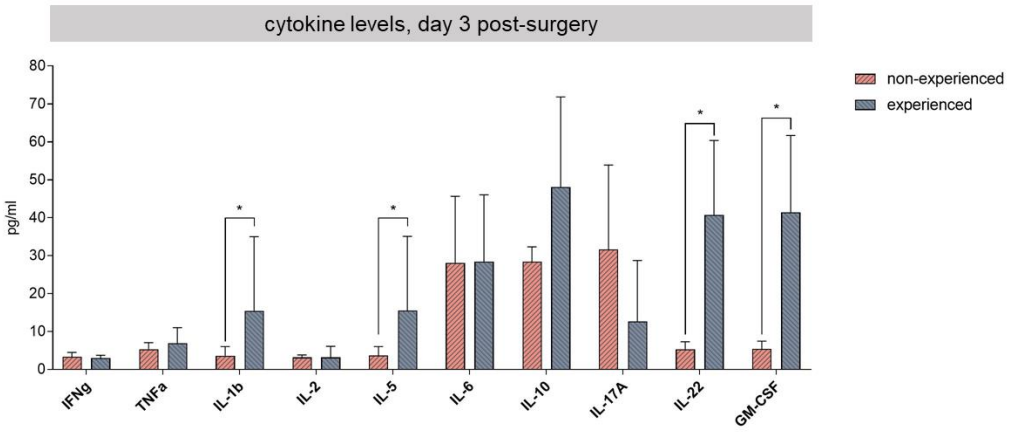

Figure 8 (key results) Altered cytokine levels 3 days post-surgery due to experience in the adaptive immunity. Multiplexed ELISA from mouse plasma 3 days after introduction of an osteotomy. With an immunological experience, the cytokine patterns were shifted, showing a more pronounced inflammatory state within these animals. N=6 per groups, Mann-Whitney U test, * $p<0,05$

These altered cytokine patterns during the initial healing phase appear to be essentially responsible for the altered healing outcome after 21 days in the two cohorts of immunologically experienced or non-experienced mice. Chronological aging showed that, compared to young 3 month old mice, both 12 month old groups showed an age-dependent decrease in newly formed bone tissue. However, bone fracture healing in mice with an experienced adaptive immune system was further significantly altered after 21 day compared to non-experienced mice, reflecting the tremendous effect of immunological experience and altered cytokine patterns in the initial healing phase. Bone healing in the context of an experienced adaptive immune system showed decreased newly formed bone and a decreased callus volume compared to the non-experienced aged cohort. The parameter of torsional stability (MMIp) was significantly decreased in mice with an experienced adaptive immune system, showing less stable calluses compared to those formed in mice with a more naïve/non-experienced adaptive immune system. The thickness of the newly formed bone structures (Tb.Th) showed a trend of increased thickness in the context of an experienced adaptive immune system, which correlated with the bone properties seen during homeostasis (see figure 9 and figure 4). The experience in the adaptive immunity held a deleterious effect on the healing capacity and resulted in a less stable callus and delayed fracture healing.

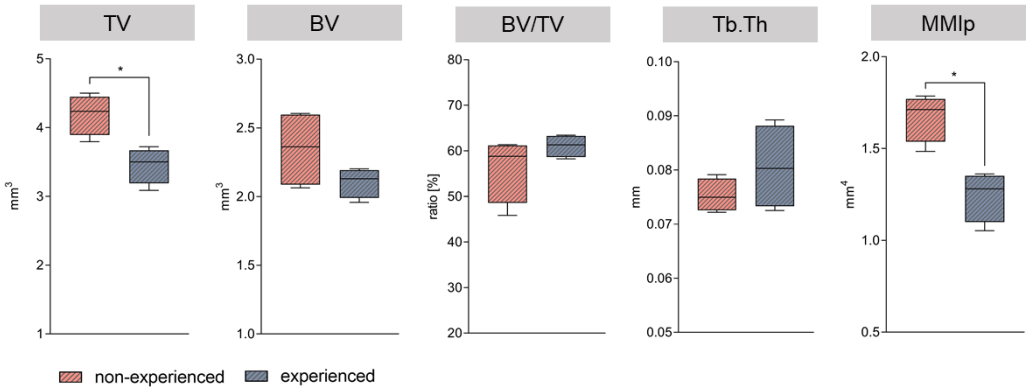

Figure 9 (key results) Healing outcome 21 days post-surgery under the influence of an experienced adaptive immunity. MicroCT analysis of the osteotomized femur 21 days post-surgery in 12 months old mice either with an experienced or a non-experienced adaptive immunity. The immunological experience significantly altered the healing outcome in the 12 months old mice cohort. Reduced callus volume (TV) and bone volume (BV) could be observed, however the ratio of bone inside the callus volume (BV/TV) seemed to be unaltered. However, the mechanical stability measured with the minimal moment of inertia (MMIp) showed a tremendous decrease within the immunologically experienced cohort. The thickness of the newly formed bone structures (Tb.Th) showed a slight increase in the experienced group. N=6 per groups, Mann-Whitney U test, * $p<0,05$

3.6 Activation of CD8+ T cells during bone fracture healing

T cells and especially the CD8+ T cells need to undergo activation in order to secrete their cytokines. As CD8+ T cells are known to execute their function primarily by antigen driven processes, it remains unclear how the adaptive immunity is involved under aseptic conditions like the bone regeneration process. Non-antigen driven activation includes bystander activation (following activation of the innate immune system) or pattern recognition by danger/damage associated molecular patterns (DAMPS). DAMPs are released from necrotic and apoptotic cells, which can be found within a fracture. To investigate CD8+ T cell activation in detail, CD8+ T cells were stimulated with either DAMPs, IL-12 and IL-18, to simulate bystander activation, and α-CD3/CD28 activation, to represent T cell receptor (TCR) activation. Lipopolysaccharide (LPS) stimulation was used to activate the pathogen associated molecular pattern (PAMP) response. Isolated CD8+ T cell secreted differing cytokines and cytokine levels depending on the different activation stimuli used. TCR engaging via α-CD3/CD28 activation unveiled the most pro-inflammatory cytokine pattern with high secretion of TNFα and IFNγ as well as cytolytic proteins like granzymes, perforin and granulysin, which are all potent cytotoxic molecules able to kill parasites and cells. Engaging pattern recognition receptors via LPS stimulation showed the highest IL-6 secretion. Exposure to high mobility group box 1 protein (HMGB1), a well-known DAMP, revealed that CD8+ T cells were able to directly react to molecular patterns, a finding less known in the literature. HMGB1 is an intranuclear protein that is only released upon cell necrosis. Exposure to HMGB1 induced a robust granulysin secretion in CD8+ T cells. IL-12/IL-18 stimulation induced the cytokine secretion in a less pro-

inflammatory manner compared to α-CD3/CD28 (see figure 10). This study showed that the adaptive immune system directly responds to molecular patterns and bystander activation, and is able to execute immune functions within the otherwise sterile fracture environment by reacting to molecules released by the injured tissue. An important step to understand the involvement of T cells in the fracture environment and the deleterious effects of experience in the adaptive immune system on the healing cascade.

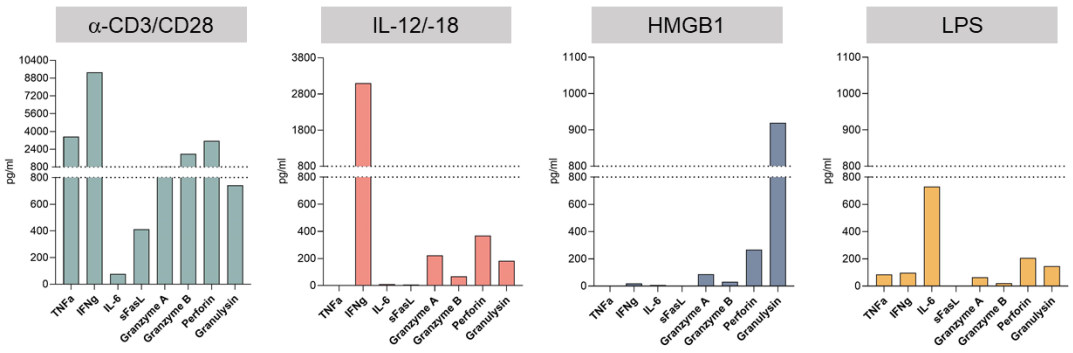

Figure 10 (key results) Cytokine secretion upon activation patterns of CD8+ T cells. Isolated CD8+ T cells were stimulated with danger signals (DAMPs or PAMPs) or activated via bystander molecules like IL-12/IL-18 to simulate the activation patterns during bone fracture. The released cytokine patterns were compared to the α-CD3/CD28 stimulated cells. Activation via TCR involvement (α-CD3/CD28) released the most prominent pro-inflammatory cytokine pattern. The other stimulation however showed a very distinct cytokine pattern upon different stimuli, but revealed the direct activation via pattern recognition receptors on CD8+ T cells. N=1 immune cell donor

To exclude the involvement of the T cell receptor during fracture healing another *in vivo* approach was used to reveal the activation pattern of T cells after bone trauma. Therefore, a cell transfer of wild type or transgenic T cells was used to elucidate the influence of CD8+ T cells in the healing process. Immunologically naïve mice (showing an undisturbed healing cascade) were either adoptively transferred with transgenic CD8+ T cells bearing a transgenic T cell receptor exclusively recognizing ovalbumin, or polyclonal CD8+ T cells from wild type mice. The transgenic CD8+ T cells can only be activated via ovalbumin or bystander and DAMP activation, therefore the TCR involvement can be excluded in this group. The wild type CD8+ T cells are able to be activated via the TCR, bystander or DAMP employment. Healing outcome was assessed 21 days post-surgery via microCT. The healing outcome showed no differences between both groups and only showed a mild decrease in bone volume in the callus of both adoptively transferred groups compared to the control group. The transfer of CD8+ T cells is known to negatively influence the healing process. As no differences between the adoptively transferred groups could be found, an antigen driven process could be excluded. Moreover, either bystander and/or pattern recognition activation might stir the T cell activation during fracture healing.

3.7 A humanized mouse model to mimic the in-patient situation

In order to study experienced adaptive immunity in a setting more closely resembling that found in patients in the clinics, a humanized immune cell mouse model was investigated. Peripheral blood mononuclear cells (PBMC) from patients with either high or low experience in the adaptive immunity were selected (based on the frequency of memory and effector CD8+ T cells) and the immune cells were isolated. The characterized immune cells from the stratified donors were further injected into immunocompromised animals to mirror the in-patient situation. The healing outcome showed a beneficial effect of the transferred immune cells compared to the group without immune cell transfer (control), as a higher bone mineral density was observed in the treated groups. Especially the bone volume in the callus volume (BV/TV) was significantly increased under the influence of a more naïve immune system compared to the control and the experienced immune cells. Furthermore, both groups receiving immune cells showed thicker trabecular structures in the callus (see figure 11). This model partially mimics the in-patient situation and can be used for the investigation of new treatment strategies and options developed for human immune cells and not murine immune cells.

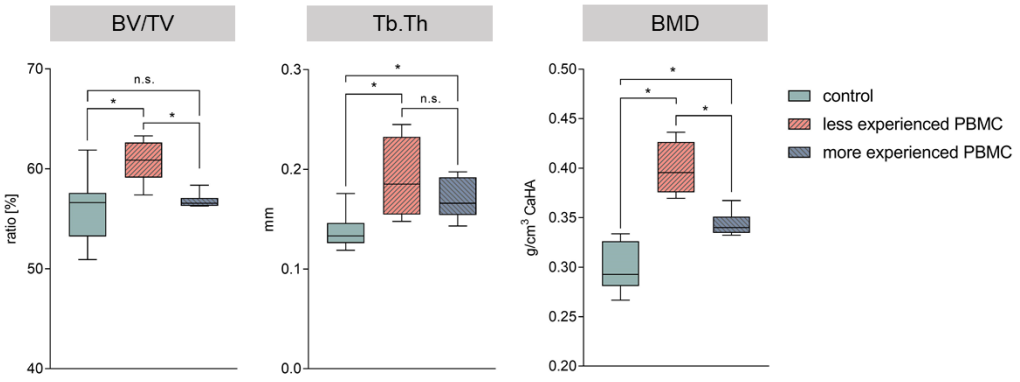

Figure 11 (key results) Humanized mouse model mirroring the in-patient fracture healing. The humanized PBMC mouse model was able to mimic the delayed healing situation found in patients with a strong immune experience (measured via the expression of end stage effector markers on CD8+ T cells). The bone volume in the callus volume (BV/TV) was significantly increased under the influence of a less experienced (more naïve) immune system. Measuring the thickness (Tb.Th) and the mineral density (BMD) of the newly formed bone revealed a beneficial effect of immune cells during the healing process as well as the advantageous influence of less experienced immune cells during the healing process. N=8 mice per group, N=2 different immune cell donors per group, Mann-Whitney U test, * $p<0,05$ (adapted from Bucher et al. *Front. Immunol.* 2019)

3.8 Therapeutic options to modulate the immunity during fracture healing

3.8.1 Inhibition of T cell activation pathways

Targeting immune cells, especially the effector and memory T cells could help to restore age-dependent alterations of the regenerating cascade towards a more juvenile process. Therapeutics to target immune cells during regenerative processes can be either direct or indirect. A direct approach to modulate immune cell function could be via blocking of downstream activation pathways to hinder cytokine secretion or hinder the binding of ligands to their respective receptors. Antigen, bystander or DAMP driven activation of immune cells employs different downstream pathways. For example, antigen activation uses the calcineurin pathway whereas bystander driven activation acts via the mTOR pathway to alter the nuclear transcription of cytokine genes. DAMP activation uses mostly the MyD88 pathway (one of the main pathways in toll-like receptor (TLR) signaling), depending on the danger signals and the receptors on the cell surface. Inhibition of immune cell activation was achieved by systemically blocking each pathway using therapeutics. Rapamycin was used to block the mTOR pathway, tacrolimus was used to block the calcineurin pathway and the Pepinh-MYD inhibitor was used to block pattern recognition activation via MyD88 inhibition. MicroCT analyses of the fracture callus was performed after 21 days of healing, during which time the mice received each therapeutic for 5 days, starting 1 day after introducing of the osteotomy. The fracture callus was difficult to analyze, as some fractured bones had already entered the remodeling phase. Therefore the calculation of callus volume and bone volume led to misleading data. The BV and TV values showed no significant differences between all groups, however the MyD88 inhibited group revealed a more mature healing process under further investigation of the remodeling phase (see figure 12). The MyD88 inhibited group already showed a recanalization of the bone marrow in the fracture area, and while this indicated a progression in the remodeling process a decreased callus and bone volume was observed. By investigating the new “empty” volume due to the recanalization process of the bone marrow a significantly higher recanalization volume was found in the MyD88 inhibited group. The Rapamycin treated group showed overall worsened healing outcome, due to possible adverse effects of systemic rapamycin administration (see figure 12). The treatment with MyD88 inhibitor significantly altered the immune phenotype by switching the ratio of T cells towards CD4+ T cells and the percentage of CD8+ T cells was diminished. A ratio favoring CD4+ T cells was seen to be beneficial for bone healing as this indicates a lower pro-inflammatory status in this treatment group (see figure 12).

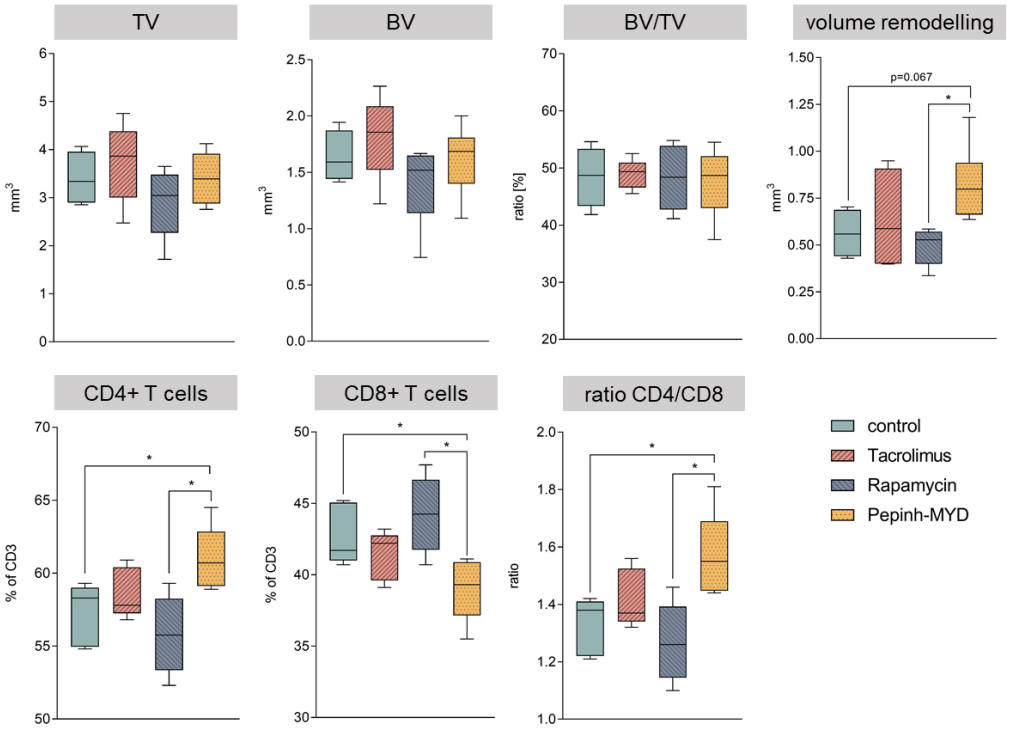

Figure 12 (key results) Immunomodulation by activation pathway blockage improves fracture healing. MicroCT analysis of the osteotomized femur 21 days post-surgery and flow cytometric analysis of the immune cells in the spleen. The analyses of the callus (TV) and bone volume (BV) and the ratio of BV/TV did not show significant differences between the treatment groups. However, the Pepinh-MYD (MyD88 inhibitor) treatment group showed advanced healing by entering the remodeling phase of the fracture callus. The remodeling includes recanalization of the bone marrow, and this newly formed volume (volume remodeling) was significantly increased in the MyD88 inhibited group depicting a more progressed fracture callus. The Pepinh-MYD treatment significantly altered the immune cell composition and favored CD4+ T cells over CD8+ T cells in the MyD88 inhibited group. N=6 mice per group, Mann-Whitney U test, * p<0,05

3.8.2 Adoptive transfer of regulatory T cells

CD8+ T cells are efficiently modulated by CD4+ regulatory T cells (T_{Reg}). T_{Reg} are a counter player to CD8+ T cells by downregulating the pro-inflammatory environment and inhibition of proliferation and activation of CD8+ T cells. Administration of syngeneic T_{Reg} could therefore lead to a favorable immune environment and promote regenerative processes by downregulation/shortening of the initial inflammatory phase during bone healing. The adoptively transferred T_{Reg} to wild type mice (host) showed a significant dependency on the experience level of the host immune system. Administrating CD4+ T_{Reg} in mice with a more naïve immune phenotype (SPF housing) led to a significant increase of bone volume and callus volume after 21 days of healing after osteotomy. T_{Reg} transfer in immune experienced hosts (non-SPF housing) however demonstrated a dependency on the ratio of CD4+ T cells to CD8+ T cells. Only in animals with a lower ratio of effector and memory CD8+ T cells to CD4+ T_{Reg} showed a beneficial effect from treatment with T_{Reg} cells. The healing outcome after 21 days showed a

higher bone to callus volume in T_{Reg}-responder (low CD8+ T_{EM}/CD4+ T_{Reg} ratio) mice. T_{Reg} responsiveness was dependent on the CD8+ T_{EM}/CD4+ T_{Reg} ratio, T_{Reg} responsiveness was only achieved in animals with a ratio favoring CD4+ T cells after T_{Reg} transfer (see figure 13). Employing CD4+ T_{Reg} for bone healing significantly depends on the individual immune status of the host. The dosage of T_{Reg} cells need to be individually evaluated to combat the CD8+ effector and memory T cells.

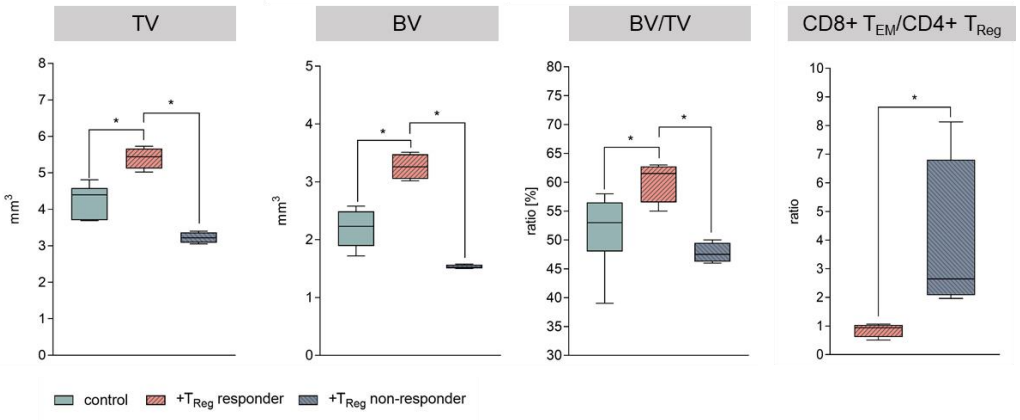

Figure 13 (key results) T_{Reg} administration partially improves the healing outcome. Regulatory T cells (T_{Reg}) isolated from the spleen and lymph nodes of donor mice were adoptively transferred into host animals undergoing an osteotomy surgery. 21 days post-surgery analysis by microCT of the osteotomized femur and flow cytometry analysis of the spleen revealed diverse healing outcomes. Depending on the host's ratio of CD8+ T_{EM} to CD4+ T_{Reg} cells the healing outcome was either progressed (higher TV and BV values), depicted as +T_{Reg} responder, or diminished, depicted as +T_{Reg} non-responder, compared to the control without cell transfer. N=6 mice per group, Mann-Whitney U test, * p<0,05 (adapted from Schlundt et al. *Front. Immunol.* 2019)

3.8.3 Mechanical loading of the bone

Musculoskeletal exercise shows an effect on catabolic, anabolic and metabolic processes in the body. However, the underlying processes are still not completely understood. Loading of bone structures *in vivo* (comparable to exercise) leads to increased bone formation in young individuals. This process is age-dependent and bone loading has less of an effect in elderly individuals. To understand how this process is linked to the altered adaptive immunity in aged subjects, a tibia loading experiment was conducted. Daily loading of the tibia for 2 weeks increased the bone volume in young animals, however there was no significant increase in bone volume in aged animals. In accordance with the anabolic effects seen in the bone structures, the immune system underwent significant changes in the young animals during loading. The CD8+ T cell compartment underwent a significant switch from effector and memory CD8+ T cells towards naïve CD8+ T cells, favoring the bone remodeling and adaptation process (see figure 14).

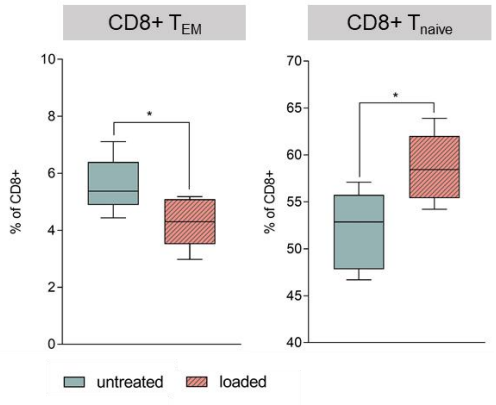

Figure 14 (key results) Loading of the tibia changes the local immune composition. The tibiae from young mice were loaded for 2 weeks to induce the mechanical adaptation and formation of new bone tissue. This loading regimen induced a change of the local immune phenotype by switching to a more naïve phenotype, seen in the higher percentage of naïve CD8+ T cells compared to effector and memory CD8+ T cells (CD8+ T_{EM}). N=6 mice per group, Mann-Whitney U test, * p<0,05 (adapted from Bucher et al. *Front. Immunol.* 2019)

4 Discussion

Age-related alterations on the tissue, matrix, cellular, subcellular, and signaling molecule levels requires more research in order to realize novel treatment approaches to help patients in need such as patients with delayed fracture healing who suffer with long term disability, pain and engender high socio-economical costs. The influence of experience in adaptive immunity seems to be crucial for determining the outcome of interactions between the immune and skeletal systems, and provides new leads for novel therapeutic immunomodulatory options to combat delayed fracture healing and other musculoskeletal conditions.

Bone homeostasis

Bone tissue is highly regulated by the micromilieu of cells in the bone as well as by systemic regulators of bone metabolism. The bone milieu is formed of osteoblasts and osteoclasts and a vast number of different cells like endothelial cells, fibroblasts, immune cells, progenitor cells and others as well as numerous hormones and cytokines. Changes in this bone milieu caused by infections, cancer metastases, drugs, disturbed metabolism (e.g. obesity) or autoimmune reactions often result in massive changes to the bone structure, e.g. loss of bone tissue or even ectopic bone formation. Inflammatory changes in particular significantly affect the balance between bone formation and destruction by osteoblasts or osteoclasts. [28] The bone micromilieu is altered by age, with aged bone being characterized by an increased pro-inflammatory milieu and loss of bone mass. Within my work the loss of bone mass could be linked to regulatory processes of the immune system and immune cell compositions leading to pro-inflammatory conditions. I have shown that the trabecular bone structure was highly diminished in mass in the aged, on the other hand the cortical bone increased in thickness with age. This process resulted in a stiffer bone and therefore one would predict a more brittle fracture manner, which I could prove by biomechanical testing of the bone. Low bone quality in older patients is a major challenge in the treatment of geriatric patients. Until recently bone quality had not been linked to the immune system, however the immune system has been shown to be involved in the process of bone formation and destruction by regulation of osteoblasts and osteoclasts. Changes in the immune phenotype by experience in the adaptive immune system alters this interdependency of bone and immune cells in interrelation. Within this thesis, I have shown that the increase in experience in the immune system, especially in the adaptive immune system, leads to an imbalance in the crosstalk between musculoskeletal and immune system. The experiments have shown that the increased immune experience of T cells leads to a significant aggravation of the age-dependent changes in the bone, which manifest as a thicker cortical bone and a deteriorated mechanical competence. Systemic cytokine analysis revealed a higher and constant pro-inflammatory cytokine milieu in immune experienced subjects, as seen in the increased systemic levels of tumor necrosis factor alpha (TNFα). This process is called inflamm-aging, as the cells are constantly exposed to inflammatory cytokines. [29]

Preclinical studies are important to understand the underlying mechanisms driving patient diseases. Bone healing studies in preclinical models, like mice, rats or sheep are often used to understand the systemic involvement of different cell types or to understand the contribution of metabolism, immunology and/or nutrition. It has become increasingly clear that the immune system plays a major role in the regulation of regenerative processes, as, in most organs, the initial reaction to an injury is guided by immune cells. Immune cells readily adapt to the harsh environment in the fracture hematoma and are potent producers of cytokines and chemoattractants. However to date, in most of the studies addressing the immune system in regenerative processes the phenotype of the immune system is neglected or not stated in the publications [25–27]. Different cell types have been identified to be beneficial or detrimental in the healing process [30]. The adaptive immune system is able to retain a memory upon antigen/pathogen recognition. This memory is reflected by a stronger reaction upon antigen recall, e.g. cytokine production or proliferation, as well as distinct chemokine receptors, enabling a faster migration towards the tissue. The ageing process of organisms is widely studied, including bone properties, which have been studied in preclinical models [25–27]. These studies revealed age-dependent changes in bone structure and competence. However, the immune status of the mice used in these studies was not considered and it is not possible to identify the housing conditions of the animals used. Within this thesis, the involvement of memory in the adaptive immune system has been made clearer and that the changes are significant in bone homeostasis, healing and adaptation. An experienced adaptive immune system interferes with the age-dependent changes as well as with regenerative processes in a significantly negative way as shown in this thesis. Further studies could benefit from more advanced preclinical models (more closely mimicking the in-patient situation) to be able to study the interaction between an experienced/aged adaptive immunity with aged bone structures to reveal potential new targets for the development of novel therapeutics tackling bone loss, osteoporosis or delayed healing. The aged but immunologically naïve animal (often used in aging studies) is an artificial model to decrease the inter-individual variance in research and lacks the translational character required from preclinical models to most closely mimic the in-patient situation.

Bone healing

Bone healing depends on an initial activation of the immune system. Cells from the innate immune system are one of the first cells guiding the process, whilst the adaptive immune system is a potent regulator found in different phases of the bone healing process. The detrimental involvement of T cells in the healing process and especially of CD8+ T cells was correlated with delayed fracture healing in earlier studies [14,31]. The activation of the immune system can occur via antigen, bystander or danger signals such as damage-associated molecular patterns (DAMPs) or pathogen-associated molecular patterns (PAMPs). Within this thesis I have shown that the activation of isolated T cells, especially CD8+ T cells via all three different pathways led to the finding, that T cells can be directly activated via pattern recognition and

can therefore directly interfere in the initial healing process due to the presence of danger signals in the surrounding tissue. DAMPs are released from necrotic tissue, induced by the fracture, or dying cells due to a restricted blood supply as a consequence of the injury. The activation of CD8+ T cells revealed distinct profiles of released cytokines, which were dependent on the molecules used for T cell activation. Activation via the T cell receptor revealed the strongest and most broad cytokine production, however the stimulation with IL-12 and IL-18, a potential bystander activation, and molecular pattern activation, significantly changed the cytokine milieu. The presence of toll-like receptors and other pattern recognition receptors on CD8+ T cells has only recently been described. For example TLR2, TLR3 and TLR9 are known to be involved in the T cell mediated DAMP recognition and subsequent direct activation without the necessity of T cell receptor (TCR) involvement [32,33]. To verify this hypothesis within this study a bone healing experiment with injection of transgenic CD8+ T cell recognizing only one particular antigen (here ovalbumin) was performed. In comparison with injection of polyclonal CD8+ T cell, the transgenic CD8+ T cells did not show any difference, therefore an antigen driven process in the aseptic bone healing process could not be confirmed, rather a bystander or danger signal driven activation of CD8+ T cell can be inferred. Schwacha et al. identified an increase in toll-like receptors on T cells after burn injuries [34], thereby highlighting the importance of danger/damage signals, DAMPS, during an aseptic injury to initiate and modulate the immune response.

CD8+ T cells can undergo phenotypic changes upon activation and can establish an experience level, and are involved in regenerative processes, thus the impact of the immune experience of T cells needs to be elucidated in order to understand the heterogeneity of fracture healing outcomes in elderly patients. Age-dependent decline in regenerative capacity is widely acknowledged. My work in a preclinical model has shown that bone forming capacity in aged mice is diminished when compared to young mice. Additionally, experience in the adaptive immune system significantly worsened the reduced regenerative capacity in the one-year-old mouse cohort. Cytokine analysis revealed a dysregulation of cytokines within the immune experienced mice compared with the non-experienced group. From experiments performed during my PhD, it became apparent that an increased level of granulocyte-macrophage colony-stimulating factor (GM-CSF) could promote a prolonged pro-inflammatory phase during healing, as GM-CSF is a potent stimulator if M1 type macrophages. A prolonged pro-inflammatory phase during healing leads to a delayed fracture healing as shown by Schmidt-Bleek et al and others. [31,35]. My research revealed other cytokines dysregulated during the initial healing phase in the experienced group such as IL-5 or IL-22, which can act directly on mesenchymal cells and can regulate the migration, proliferation and differentiation potential of those cells. IL-22 is bivalent cytokine, and its effect seems to be milieu dependent, as Monasterio et al. showed an association of IL-22 with bone resorption whereas El-Zayadi et al. showed that IL-22 drives the osteogenic differentiation of mesenchymal stromal cells [36,37]. IL-5 however imbalance the bone metabolism as shown by Macias et al. [38]. IL-1b, a cytokine found to be upregulated within

this work, can potentiate the inflammatory phase by stimulating different activation pathways and hinder or delay regeneration when dysregulated. A timely resolving of IL-1b is crucial for an undisturbed regeneration after injury [39]. My research has shown that pro-inflammatory environment has detrimental effects on mesenchymal cells, stimulation with pro-inflammatory cytokines almost abolished collagen production, and contrariwise induced the production of chemokines and inflammatory cytokines in the mesenchymal cells. The oppression of extracellular matrix production and potentiation of inflammatory mediators could explain the delay observed in fracture healing in the context of an experienced adaptive immune system and stresses the importance of timely resolution of the pro-inflammatory phase in regenerative processes. Within my work I have clearly demonstrated the detrimental effect of immune experience on bone fracture healing. To mimic the in-patient situation, more advanced preclinical models are required. Analyzing the fracture healing capacity under the influence of patient derived immune cells in a humanized PBMC mouse model is a promising model. Within this work the injection of experienced patient derived immune cells in a mouse model reflected the delayed healing outcome observed in patients with more experience in the adaptive immune system. The bone healing process benefitted from a more naïve immune phenotype compared to an experienced immune phenotype as seen in patients with high experience level in the CD8+ T cell compartment and delayed fracture healing.

Immunomodulation

Therapeutic approaches to modulate immunity can either directly or indirectly modulate immune cells: Cell products can be up or downregulated, cells can be depleted or hindered in functionality or cells can be used to modulate the environment or directly act on other cells. Depletion of CD8+ T cells has been shown by Reinke et al. to enhance the healing capacity [14]. However, this treatment strategy is not a desirable treatment option for patients, as immune suppression by depletion of a complete T cell subset could lead to infection and severe side effects. Hindering activation pathways or modulating the degree of inflammation is a practicable way to regulate the initial inflammatory phase in bone healing. Immunosuppression after organ transplantation suppresses the activation of the host immune cells in order for the graft to survive and hinder rejection by the host immune system. Within this work, the feasibility of immunosuppression was tested by systemic intervention using known drugs such as Rapamycin or Tacrolimus. However, this suppression did not lead to significant improvement of bone healing; however I could show that blockage of danger signal driven activation of immune cells using a MyD88 inhibitor improved the bone healing outcome. This finding underlines the importance of danger signal recognition in fracture healing and the opportunity for interventions via the signaling pathways for endogenous danger/damage signals. In order to modulate the immune reaction more specifically, regulatory T cells (T_{Reg}) possess a boundless immunomodulatory potential. Within this work it could be shown that administering T_{Reg} cells during the bone healing process enhanced the healing capacity based on the CD8+ effector T cell level of the host organism. The ratio of CD8+ effector to CD4+ regulatory T cells predicted the healing

outcome and T_{Reg} substitution might improve the initial inflammatory response by aiding the timely resolution of the pro-inflammatory environment during bone healing. The quantity of administered T_{Reg} cells will likely have to be calculated on a case by case basis depending on the immune experience level of an individual in order to ensure an effective treatment response. T_{Reg} administration likewise shows beneficial effects in different research fields, especially in solid organ transplantation [40].

Conclusion/Outlook

During the research undertaken during my PhD, I was able to link the adaptive immune system directly to bone tissue formation and tissue remodeling. Changes in the adaptive immune system led to structural differences in bone material organization as well as mechanical competence in intact bones. I could show that the experience in the adaptive immune system influences bone homeostasis by significantly changing the bone phenotype. Experience in the adaptive immune system is an important part of age-dependent changes. The impairment of bone quality due to the immunological experience could be used for the interpretation of age-dependent diseases like osteoporosis. Furthermore, I have shown that immunological experience is detrimental for bone healing and is likely to have an influence on healing processes in other parts of the body.

This study is a promising starting-point to stratify patients who will need additional interventions due to delayed healing processes and need access to new treatment options, which are not yet available in regular standard of care regimes. In regard of the upcoming challenge due to the aging demographic distribution within the next decades the need for treatment options for the immunologically induced delayed healing situations may rise. The experimental reproduction of an experienced immune system showed that adaptive immunity is essential for bone healing success or failure in human patients. Overall, more experienced immunity substantially affected bone tissue formation. The regulation of cytokines and the cytokine profile during the early onset of healing is determined by the experience of the adaptive immune system. Such knowledge is essential not only for pre-clinical characterization of healing settings but lays the foundation for novel diagnostics and therapeutics that aim to understand and rescue delayed bone regeneration. Currently there are no novel therapies available to treat patients with high levels of immune experience that results in delayed healing. New therapeutic approaches are required that address advanced immune experience and modulate the immune system to rejuvenate the regenerative processes.

5 References

1. Einhorn TA, Gerstenfeld LC. Fracture healing: Mechanisms and interventions. Vol. 11, Nature Reviews Rheumatology. NIH Public Access; 2015. p. 45–54.
2. Tzioupis C, Giannoudis P V. Prevalence of long-bone non-unions. Injury. 2007 May 1;38:S3–9.
3. World Health Organization Geneva. World Health Organization. Ageing and Health. 2018.
4. Bishop JA, Palanca AA, Bellino MJ, Lowenberg DW. Assessment of compromised fracture healing. Vol. 20, Journal of the American Academy of Orthopaedic Surgeons. 2012. p. 273–82.
5. Dyer SM, Crotty M, Fairhall N, Magaziner J, Beaupre LA, Cameron ID, Sherrington C. A critical review of the long-term disability outcomes following hip fracture. BMC Geriatr. 2016 Dec 2;16(1):158.
6. Rapp K, Rothenbacher D, Magaziner J, Becker C, Benzinger P, König H-H, Jaensch A, Büchele G. Risk of Nursing Home Admission After Femoral Fracture Compared With Stroke, Myocardial Infarction, and Pneumonia. J Am Med Dir Assoc. 2015 Aug 1;16(8):715.e7-715.e12.
7. Brighton CT, Krebs AG. Oxygen Tension of Healing Fractures in the Rabbit. J Bone Jt Surg. 1972 Mar;54(2):323–32.
8. Walters G, Pountos I, Giannoudis P V. The cytokines and micro-environment of fracture haematoma: Current evidence. Vol. 12, Journal of Tissue Engineering and Regenerative Medicine. Wiley-Blackwell; 2018. p. e1662–77.
9. Hoff P, Gaber T, Strehl C, Schmidt-Bleek K, Lang A, Huscher D, Burmester GR, Schmidmaier G, Perka C, Duda GN, Buttgereit F. Immunological characterization of the early human fracture hematoma. Immunol Res. 2016 Dec 14;64(5–6):1195–206.
10. Baht GS, Vi L, Alman BA. The Role of the Immune Cells in Fracture Healing. Current Osteoporosis Reports Springer; Apr 5, 2018 p. 138–45.
11. Könnecke I, Serra A, El Khassawna T, Schlundt C, Schell H, Hauser A, Ellinghaus A, Volk H-DD, Radbruch A, Duda GN, Schmidt-Bleek K. T and B cells participate in bone repair by infiltrating the fracture callus in a two-wave fashion. Bone. 2014 Jul;64:155–65.
12. Schell H, Duda GN, Peters A, Tsitsilonis S, Johnson KA, Schmidt-Bleek K. The haematoma and its role in bone healing. J Exp Orthop. 2017 Dec 7;4(1):5.
13. Kverneland AH, Streitz M, Geissler E, Hutchinson J, Vogt K, Boës D, Niemann N, Pedersen AE, Schlickeiser S, Sawitzki B. Age and gender leucocytes variances and references values generated using the standardized ONE-Study protocol. Cytometry A. 2016 Jun;89(6):543–64.
14. Reinke S, Geissler S, Taylor WR, Schmidt-Bleek K, Juelke K, Schwachmeyer V, Dahne M, Hartwig T, Akyüz L, Meisel C, Unterwalder N, Singh NB, Reinke P, Haas NP, Volk H-D, Duda GN. Terminally differentiated $CD8^+$ T cells negatively affect bone regeneration in humans. Sci Transl Med. 2013 Mar 20;5(177):177ra36.
15. Griffin WST. Inflammation and neurodegenerative diseases. Am J Clin Nutr. 2006 Feb 1;83(2):470–4.
16. Pradhan AD. C-Reactive Protein, Interleukin 6, and Risk of Developing Type 2 Diabetes

Mellitus. JAMA. 2001 Jul 18;286(3):327.

17. Franceschi C, Bonafè M, Valensin S, Olivieri F, De Luca M, Ottaviani E, De Benedictis G. Inflamm-aging: An Evolutionary Perspective on Immunosenescence. Ann N Y Acad Sci. 2006 Jan 25;908(1):244–54.

18. Knowles HJ, Athanasou NA. Canonical and non-canonical pathways of osteoclast formation. Vol. 24, Histology and Histopathology. 2009. p. 337–46.

19. Schoppet M, Preissner KT, Hofbauer LC. RANK ligand and osteoprotegerin: paracrine regulators of bone metabolism and vascular function. Arterioscler Thromb Vasc Biol. 2002 Apr 1;22(4):549–53.

20. Li Y, Toraldo G, Li A, Yang X, Zhang H, Qian WP, Weitzmann MN. B cells and T cells are critical for the preservation of bone homeostasis and attainment of peak bone mass in vivo. Blood. 2007 May 1;109(9):3839–48.

21. Mellado M, Martínez-Muñoz L, Cascio G, Lucas P, Pablos JL, Rodríguez-Frade JM. T cell migration in rheumatoid arthritis. Vol. 6, Frontiers in Immunology. Frontiers Media SA; 2015. p. 384.

22. Pettit AR, Ji H, Von Stechow D, Müller R, Goldring SR, Choi Y, Benoist C, Gravallese EM. TRANCE/RANKL knockout mice are protected from bone erosion in a serum transfer model of arthritis. Am J Pathol. 2001 Nov 1;159(5):1689–99.

23. Japp AS, Hoffmann K, Schlickeiser S, Glauben R, Nikolaou C, Maecker HT, Braun J, Matzmohr N, Sawitzki B, Siegmund B, Radbruch A, Volk HD, Frentsch M, Kunkel D, Thiel A. Wild immunology assessed by multidimensional mass cytometry. Cytom Part A. 2017 Jan;91(1):85–95.

24. Hikono H, Kohlmeier JE, Takamura S, Wittmer ST, Roberts AD, Woodland DL. Activation phenotype, rather than central- or effector-memory phenotype, predicts the recall efficacy of memory CD8+ T cells. J Exp Med. 2007 Jun 11;204(7):1625–36.

25. Willinghamm MD, Brodt MD, Lee KL, Stephens AL, Ye J, Silva MJ. Age-related changes in bone structure and strength in female and male BALB/c Mice. Calcif Tissue Int. 2010 Jun 20;86(6):470–83.

26. Brodt MD, Ellis CB, Silva MJ. Growing C57B1/6 mice increase whole bone mechanical properties by increasing geometric and material properties. J Bone Miner Res. 1999 Dec 1;14(12):2159–66.

27. Halloran BP, Ferguson VL, Simske SJ, Burghardt A, Venton LL, Majumdar S. Changes in bone structure and mass with advancing age in the male C57BL/6J mouse. J Bone Miner Res. 2002 Jun 1;17(6):1044–50.

28. Schett G. Effects of inflammatory and anti-inflammatory cytokines on the bone. Eur J Clin Invest. 2011 Dec 1;41(12):1361–6.

29. Rea IM, Gibson DS, McGilligan V, McNerlan SE, Alexander HD, Ross OA. Age and Age-Related Diseases: Role of Inflammation Triggers and Cytokines. Front Immunol. 2018 Apr 9;9:586.

30. Tsukasaki M, Takayanagi H. Osteoimmunology: evolving concepts in bone–immune interactions in health and disease. Nat Rev Immunol. 2019 Oct 11;19(10):626–42.

31. Schmidt-Bleek K, Schell H, Schulz N, Hoff P, Perka C, Buttgereit F, Volk H-DD, Lienau J, Duda GN. Inflammatory phase of bone healing initiates the regenerative healing cascade. Cell Tissue Res. 2012 Mar 26;347(3):567–73.

32. Meisel R, Zibert A, Laryea M, Göbel U, Däubener W, Dilloo D. Human bone marrow stromal cells inhibit allogeneic T-cell responses by indoleamine 2,3-dioxygenase-mediated tryptophan degradation. Blood. 2004 Jun 15;103(12):4619–21.

33. Geng D, Zheng L, Srivastava R, Asprodites N, Velasco-Gonzalez C, Davila E. When Toll-like receptor and T-cell receptor signals collide: a mechanism for enhanced CD8 T-cell effector function. Blood. 2010 Nov 4;116(18):3494–504.

34. Schwacha MG, Daniel T. Up-regulation of cell surface Toll-like receptors on circulating γδ T-cells following burn injury. Cytokine. 2008 Dec 1;44(3):328–34.

35. Clark D, Nakamura M, Miclau T, Marcucio R. Effects of Aging on Fracture Healing. Curr Osteoporos Rep. 2017 Dec 16;15(6):601–8.

36. Monasterio G, Budini V, Fernández B, Castillo F, Rojas C, Alvarez C, Cafferata EA, Vicencio E, Cortés BI, Cortez C, Vernal R. IL -22–expressing CD 4 $^{+}$ AhR $^{+}$ T lymphocytes are associated with RANKL -mediated alveolar bone resorption during experimental periodontitis. J Periodontal Res. 2019 Apr 29;jre.12654.

37. El-Zayadi AA, Jones EA, Churchman SM, Baboolal TG, Cuthbert RJ, El-Jawhari JJ, Badawy AM, Alase AA, El-Sherbiny YM, McGonagle D. Interleukin-22 drives the proliferation, migration and osteogenic differentiation of mesenchymal stem cells: A novel cytokine that could contribute to new bone formation in spondyloarthropathies. Rheumatol (United Kingdom). 2017 Dec 10;56(3):488–93.

38. Macias MP, Fitzpatrick LA, Brenneise I, McGarry MP, Lee JJ, Lee NA. Expression of IL-5 alters bone metabolism and induces ossification of the spleen in transgenic mice. J Clin Invest. 2001 Apr 15;107(8):949–59.

39. Hasegawa T, Hall CJ, Crosier PS, Abe G, Kawakami K, Kudo A, Kawakami A. Transient inflammatory response mediated by interleukin-1β is required for proper regeneration in zebrafish fin fold. Elife. 2017 Feb 23;6.

40. Romano M, Fanelli G, Albany CJ, Giganti G, Lombardi G. Past, Present, and Future of Regulatory T Cell Therapy in Transplantation and Autoimmunity. Front Immunol. 2019 Jan 31;10:43.

6 Appendix

Table 1 Flow cytometry antibody panels

murine panel

cytotoxic T cell phenotyping

marker	*clone*
Live/Dead stain	
CD45	30-F11
CD3e	145-2C11
CD4	GK1.5
CD8a	53-6.7
CD335	29A1.4
CD11c	N418
CD45R/B220	RA3-6B2
CD62L	MEL-14
CD44	IM7
CD127	SB/199
KLRG1	2F1/KLRG1
CD205	DEC-205

helper T cell phenotyping

marker	*clone*
Live/Dead stain	
CD45	30-F11
CD3e	145-2C11
CD4	GK1.5
CD8a	53-6.7
TCR gd	GL3
CD62L	MEL-14
CD44	IM7
CD25	PC61
FoxP3	MF23
T-bet	O4-46
GATA3	L50-823
RORγ(t)	Q31-378

T cell activation phenotyping

marker	*clone*
Live/Dead stain	
CD45	30-F11
CD3e	145-2C11
CD4	GK1.5
CD8a	53-6.7
CD44	IM7
CD62L	MEL-14
CD27	LG.3A10
CXCR3 (CD183)	CXCR3-173
CD43	1B11
CD137	17B5
PD-1 (CD279)	29F.1A12
CD107a	1D4B

human and “humanized mouse model” panel

panel 1

marker	*clone*
Live/Dead stain	
CD45	J.33
CD3	UCHT1
CD4	13B8.2
CD8	B9.11
CD45RA	HI100
CD57	NC1
CD28	CD28.2
CD27	1A4CD27
HLA-DR	Immu-357

panel 2

marker	*clone*
Live/Dead stain	
CD45	J.33
CD3	UCHT1
CD4	13B8.2
CD8	B9.11
CD45RA	HI100
CCR7	150503
CD62L	DREG56
CD127	R34.34
CD25	B1.49.9

panel 3

marker	*clone*
Live/Dead stain	
CD42b	HIP1
CD45 human	HI30
CD45 mouse	30-F11
CD3	UCHT1
CD14	M5E2
CD56	5.1H11
CD19	SJ25C1
CD31	WM59

7 Eidesstattliche Versicherung

„Ich, Christian H. Bucher, versichere an Eides statt durch meine eigenhändige Unterschrift, dass ich die vorgelegte Dissertation mit dem Thema: “Knochengewebe unter dem Einfluss eines gealterten/erfahrenen adaptiven Immunsystem”, “Bone tissue under the influence of an aged/experienced adaptive immunity” selbstständig und ohne nicht offengelegte Hilfe Dritter verfasst und keine anderen als die angegebenen Quellen und Hilfsmittel genutzt habe.

Alle Stellen, die wörtlich oder dem Sinne nach auf Publikationen oder Vorträgen anderer Autoren/innen beruhen, sind als solche in korrekter Zitierung kenntlich gemacht. Die Abschnitte zu Methodik (insbesondere praktische Arbeiten, Laborbestimmungen, statistische Aufarbeitung) und Resultaten (insbesondere Abbildungen, Graphiken und Tabellen) werden von mir verantwortet.

Ich versichere ferner, dass ich die in Zusammenarbeit mit anderen Personen generierten Daten, Datenauswertungen und Schlussfolgerungen korrekt gekennzeichnet und meinen eigenen Beitrag sowie die Beiträge anderer Personen korrekt kenntlich gemacht habe (siehe Anteilserklärung). Texte oder Textteilte, die gemeinsam mit anderen erstellt oder verwendet wurden, habe ich korrekt kenntlich gemacht.

Meine Anteile an etwaigen Publikationen zu dieser Dissertation entsprechen denen, die in der untenstehenden gemeinsamen Erklärung mit dem/der Erstbetreuer/in, angegeben sind. Für sämtliche im Rahmen der Dissertation entstandenen Publikationen wurden die Richtlinien des ICMJE (International Committee of Medical Journal Editors; www.icmje.org) zur Autorenschaft eingehalten. Ich erkläre ferner, dass ich mich zur Einhaltung der Satzung der Charité – Universitätsmedizin Berlin zur Sicherung Guter Wissenschaftlicher Praxis verpflichte.

Weiterhin versichere ich, dass ich diese Dissertation weder in gleicher noch in ähnlicher Form bereits an einer anderen Fakultät eingereicht habe.

Die Bedeutung dieser eidesstattlichen Versicherung und die strafrechtlichen Folgen einer unwahren eidesstattlichen Versicherung (§§156, 161 des Strafgesetzbuches) sind mir bekannt und bewusst.“

Datum Unterschrift

Anteilserklärung an den erfolgten Publikationen

Christian H. Bucher hatte folgenden Anteil an den folgenden Publikationen:

Publikation 1: Thaqif El Khassawna, Alessandro Serra, Christian H. Bucher, Ansgar Petersen, Claudia Schlundt, Ireen Könnecke, Deeksha Malhan, Sebastian Wendler, Hanna Schell, Hans-Dieter Volk, Katharina Schmidt-Bleek, Georg N. Duda, *T lymphocytes influence the mineralization process of bone*, Frontiers in Immunology, 2017

Beitrag im Einzelnen (bitte ausführlich ausführen):

Herr Bucher war involviert in der Planung der Experimente und in der Durchführung einzelner Analysen. Herr Bucher hat im Schreibprozess mitgewirkt und insbesondere den Review Prozess des Journals umgesetzt und Korrekturen und Ergänzungen am Manuskript vorgenommen. Herr Bucher hat die biomechanische Testung der Femora geplant, durchgeführt und ausgewertet, die zur Abbildung 1 B geführt hat. Des Weiteren hat Herr Bucher die in vitro Experimente geplant, etabliert und durchgeführt die zur Abbildung 13 C geführt haben, dies beinhaltete die Isolierung der Zellen, die Versuchsdurchführung und die Analyse. Die Ausführungen zu den in vitro Experimenten wurden ebenfalls von Herrn Bucher durchgeführt. Seine durchflusszytometrische Analyse der Immunzellkomposition hat zur Abbildung 12 geführt und seine Zytokinanalyse zur Abbildung 13 B.

Publikation 2: Christian H. Bucher, Claudia Schlundt, Dag Wulsten, F. Andrea Sass, Sebastian Wendler, Agnes Ellinghaus, Tobias Thiele, Ricarda Seemann, Bettina M. Willie, Hans-Dieter Volk, Georg N. Duda, Katharina Schmidt-Bleek, *Experience in the Adaptive Immunity Impacts Bone Homeostasis, Remodeling, and Healing*, Frontiers in Immunology, 2019

Beitrag im Einzelnen (bitte ausführlich ausführen):

Herr Bucher war für die konzeptionelle Durchführung der Experimente zuständig, hat das Manuskript geschrieben und redigiert und den Review Prozess im Journal betreut. Im Einzelnen hat Herr Bucher folgende Experimente durchgeführt: Die in vivo Arbeiten wurden alle von Herrn Bucher in Absprache mit Frau Schmidt-Bleek, Herr Duda und Herr Volk konzipiert und durchgeführt, dies beinhaltet die Vorbereitung sowie die Operation, Nachsorge der Tiere und Aufarbeitung der Proben. Die microCT Aufnahmen und Analysen der Frakturen bei jungen und alten Mäusen hat zu Abbildung 1 B und C geführt. Die Gewebeaufarbeitung und die durchflusszytometrische Färbung, Messung und Analyse der 5 Tiergruppen wurden von Herrn Bucher durchgeführt, dies hat zu Abbildung 2 geführt. Herr Bucher hat alle die in dieser Publikation verwendeten Durchflusszytometrie-Antikörper-Panels selber designt, die Antikörper titriert, die Panel am Zytometer kompensiert und auch optimiert. Die von Herr Bucher erstellten durchflusszytometrischen Analysen haben auch zu Abbildung 3 geführt. Herr Bucher hat die biomechanischen Testungen der Femora der 3 Tiergruppen geplant, durchgeführt und ausgewertet, die führte zur Abbildung 4. Weitere microCT Arbeiten haben zu Abbildung 5 und 6 geführt, dazu war es notwendig, dass Herr Bucher zusätzliche neue Auswertungs-Skripte erstellte und etablierte. In Zusammenarbeit mit Herrn Thiele wurden die Tierexperimente für Abbildung 8 durchgeführt, die durchflusszytometrische Aufarbeitung, Färbung, Messung und Auswertung wurden im Anschluss von Herrn Bucher durchgeführt. Die in vitro Arbeiten aus Abbildung 9 wurden von Herrn Bucher geplant, etabliert und durchgeführt; dies beinhaltete diie Aufreinigung und Isolation humaner Zellen sowie die Versuchsdurchführung der osteogenen Differenzierungsassay. Die Zytokinanalyse aus Abbildung 9 C wurde ebenfalls von Herrn Bucher durchgeführt. Die Abbildung 10 beinhaltet ein großes Projekt, das von Herrn Bucher durchgeführt wurde: Die Isolierung und Charakterisierung humaner Immunzellen, das Etablieren des Tiermodelles mit der

Humanisierung der Mäuse, der Osteotomie, der Aufarbeitung der Gewebe sowie die Analyse des Knochens und der Immunzellen. Dazu wurden ebenfalls neue Durchflusszytometrie-Panels von Herrn Bucher designt, titriert und etabliert.

Publikation 3: Claudia Schlundt, Simon Reinke, Sven Geissler, Christian H. Bucher, Carolin Giannini, Sven Märdian, Michael Dahne, Christian Kleber, Björn Samans, Udo Baron, Georg N. Duda, Hans-Dieter Volk, Katharina Schmidt-Bleek, *Individual Effector/Regulator T Cell Ratios Impact Bone Regeneration*, Frontiers in Immunology, 2019

Beitrag im Einzelnen (bitte ausführlich ausführen):

Herr Bucher war involviert in der Planung der Experimente und in der Durchführung einzelner Analysen. Herr Bucher hat im Schreibprozess mitgewirkt und war maßgeblich beteiligt beim Review Prozess des Artikels. Herr Bucher hat bei den durchflusszytometrischen Analysen Antikörper-Panels geplant und Proben gemessen, die zu den Abbildungen 1 B, 2 E-G und zu Abbildungen 3 A, B und C geführt haben. Herr Bucher war hier mit Aufarbeitung, Färbung, Messungen und Analysen der Tiergruppen betraut. Herr Bucher hat bei den Tieroperationen assistiert und war ebenfalls beim adaptiven Zelltransfer eingebunden.

_____

Unterschrift, Datum und Stempel des erstbetreuenden Hochschullehrers

_____

Unterschrift des Doktoranden

8 Publications

Publication 1: T lymphocytes influence the mineralization process of bone

Thaqif El Khassawna, Alessandro Serra, Christian H. Bucher, Ansgar Petersen, Claudia Schlundt, Ireen Könnecke, Deeksha Malhan, Sebastian Wendler, Hanna Schell, Hans-Dieter Volk, Katharina Schmidt-Bleek, Georg N. Duda, *T lymphocytes influence the mineralization process of bone*, Frontiers in Immunology, 2017

Auszug aus der Journal Summary List

Journal Data Filtered By: **Selected JCR Year: 2017** Selected Editions: SCIE,SSCI
Selected Categories: "**Immunology**" Selected Category Scheme: WoS
Gesamtanzahl: 155 Journale

Rank	Full Journal Title	Total Cites	Journal Impact Factor	Eigenfactor Score
1	NATURE REVIEWS IMMUNOLOGY	39,215	41.982	0.085360
2	Annual Review of Immunology	17,086	22.714	0.028800
3	NATURE IMMUNOLOGY	41,410	21.809	0.102290
4	IMMUNITY	46,541	19.734	0.136360
5	TRENDS IN IMMUNOLOGY	11,204	14.188	0.026850
6	JOURNAL OF ALLERGY AND CLINICAL IMMUNOLOGY	49,229	13.258	0.083800
7	Lancet HIV	1,476	11.355	0.007950
8	JOURNAL OF EXPERIMENTAL MEDICINE	62,537	10.790	0.078310
9	IMMUNOLOGICAL REVIEWS	14,555	9.217	0.028540
10	Cancer Immunology Research	4,361	9.188	0.021180
11	CLINICAL INFECTIOUS DISEASES	61,618	9.117	0.120010
12	AUTOIMMUNITY REVIEWS	8,956	8.745	0.020990
13	Journal for ImmunoTherapy of Cancer	1,675	8.374	0.007130
14	CURRENT OPINION IN IMMUNOLOGY	9,275	7.932	0.020120
15	JOURNAL OF AUTOIMMUNITY	6,410	7.607	0.015490
16	Cellular & Molecular Immunology	3,633	7.551	0.008300
17	EMERGING INFECTIOUS DISEASES	29,657	7.422	0.057980
18	Mucosal Immunology	6,105	7.360	0.021860
19	SEMINARS IN IMMUNOLOGY	4,552	7.206	0.010950
20	EXERCISE IMMUNOLOGY REVIEW	740	7.105	0.001110
21	Journal of Allergy and Clinical Immunology-In Practice	2,802	6.966	0.009670
22	CLINICAL REVIEWS IN ALLERGY & IMMUNOLOGY	2,741	6.442	0.005880
23	Seminars in Immunopathology	2,967	6.437	0.009290
24	BRAIN BEHAVIOR AND IMMUNITY	12,583	6.306	0.026850
25	ALLERGY	16,476	6.048	0.025790
26	Emerging Microbes & Infections	1,318	6.032	0.005910
27	Advances in Immunology	2,423	5.935	0.004250
28	Current Topics in Microbiology and Immunology	5,633	5.829	0.011740
29	World Allergy Organization Journal	1,352	5.676	0.003800
30	Frontiers in Immunology	16,999	5.511	0.067470

frontiers in Immunology

ORIGINAL RESEARCH
published: 24 May 2017
doi: 10.3389/fimmu.2017.00562

T Lymphocytes Influence the Mineralization Process of Bone

Thaqif El Khassawna[1†], Alessandro Serra[2†], Christian H. Bucher[3,4], Ansgar Petersen[3,4], Claudia Schlundt[3,4], Ireen Könnecke[3], Deeksha Malhan[1], Sebastian Wendler[3,4], Hanna Schell[3], Hans-Dieter Volk[4,5], Katharina Schmidt-Bleek[3,4†] and Georg N. Duda[3,4†]*

[1] Experimental Trauma Surgery, Faculty of Medicine, Justus-Liebig University, Giessen, Germany, [2] German Arthritis Research Center (DRFZ), Berlin, Germany, [3] Julius Wolff Institute, Center for Musculoskeletal Surgery, Charité – Universitätsmedizin Berlin, Berlin, Germany, [4] Berlin-Brandenburg Center for Regenerative Therapies, Charité – Universitätsmedizin Berlin, Berlin, Germany, [5] Institute of Medical Immunology, Charité – Universitätsmedizin Berlin, Berlin, Germany

Bone is a unique organ able to regenerate itself after injuries. This regeneration requires the local interplay between different biological systems such as inflammation and matrix formation. Structural reconstitution is initiated by an inflammatory response orchestrated by the host immune system. However, the individual role of T cells and B cells in regeneration and their relationship to bone tissue reconstitution remain unknown. Comparing bone and fracture healing in animals with and without mature T and B cells revealed the essential role of these immune cells in determining the tissue mineralization and thus the bone quality. Bone without mature T and B cells is stiffer when compared to wild-type bone thus lacking the elasticity that helps to absorb forces, thus preventing fractures. In-depth analysis showed dysregulations in collagen deposition and osteoblast distribution upon lack of mature T and B cells. These changes in matrix deposition have been correlated with T cells rather than B cells within this study. This work presents, for the first time, a direct link between immune cells and matrix formation during bone healing after fracture. It illustrates specifically the role of T cells in the collagen organization process and the lack thereof in the absence of T cells.

Keywords: bone healing, collagen I, T lymphocytes, immune cells, mineralization

OPEN ACCESS

Edited by:
Akihiko Yoshimura, Keio University, Japan

Reviewed by:
Ines Pedro Perpetuo, Royal Veterinary College, United Kingdom
Daisuke Kamimura, Hokkaido University, Japan

***Correspondence:**
Katharina Schmidt-Bleek
katharina.schmidt-bleek@charite.de

†These authors have contributed equally to this work.

Specialty section:
This article was submitted to T Cell Biology, a section of the journal Frontiers in Immunology

Received: *26 January 2017*
Accepted: *26 April 2017*
Published: *24 May 2017*

Citation:
El Khassawna T, Serra A, Bucher CH, Petersen A, Schlundt C, Könnecke I, Malhan D, Wendler S, Schell H, Volk H-D, Schmidt-Bleek K and Duda GN (2017) T Lymphocytes Influence the Mineralization Process of Bone. Front. Immunol. 8:562. doi: 10.3389/fimmu.2017.00562

INTRODUCTION

Bone is capable of regeneration, but the process that leads to scarless restoration of form and function is highly complex and prone to failure (1). Even today delayed and non-union following bone injury represent a clinical problem that results in strongly reduced quality of life for affected patients (2). Despite the progress in characterizing molecular and cellular elements of the bone regeneration cascade, the distinct aspects that are altered in compromised patients remain so far unclear. The need to understand the correlation of systemic diseases that influence the immune reaction to bone healing remains.

Only recently the tight interplay of the skeletal and immune system has been described and recognized as a key element of the bone healing cascade (3). The current understanding of this interplay, however, is rather controversially discussed. On one hand, lymphopenic mice display a seemingly better healing after injury (4). On the other hand, several studies attribute either a positive or negative role to T and B cells in bone biology, autoimmunity, and fracture repair. Activated T cells are responsible for causing bone loss during rheumatoid arthritis (5) and postmenopausal

osteoporosis (6), and $CD8^+$ memory/effector T cells have been linked to delayed bone healing (7).

It is also known that fracture repair starts with a pro-inflammatory reaction which is essential for triggering the healing cascade (8), that macrophages are essential for successful bone regeneration (9), that osteoblast maturation is triggered by T-lymphocytes (10), and that regulatory T cells cause higher bone mass (11) and enhance bone repair (12). B and T cells are producers of osteoprotegerin (OPG) and receptor activator of NF-kB ligand (RANKL) influencing the osteoclastogenesis, and they are present in high numbers during the remodeling process that reorganizes bone structure toward its final mechanical strength and competence (13). The above-described detrimental or beneficial effects address different phases of bone formation and healing, but their detailed interplay remains so far unknown. Specifically, the distinct role of T and B cells during bone healing appears to be unclear. From previous experiments, we could identify that the absence of mature B and T lymphocytes accelerated fracture healing (4).

In this work, we ascertain whether such changes in bone repair are dependent on either T or B cells. Furthermore, we analyzed the implications of a changed matrix formation on the quality of newly generated bone and on the underlying osteoblast activity.

MATERIALS AND METHODS

Experimental Design

To assess the global role of T and B cells in bone function, structure, and regeneration process, a mouse model of recombination activating gene 1 homozygous knockout ($RAG1^{-/-}$) (C57BL/6N background; Bundesinstitut für Risikobewertung, Berlin, Germany) was used. $RAG1^{-/-}$ mice lack both mature T and B cells (14). The differentiation of T and B cells in these mice is arrested at an early stage due to their inability to perform V(D)J recombination. Discrepancies in bone architecture and function between the $RAG1^{-/-}$ mice and wild-type (WT) controls (C57BL/6N, Charles River Laboratories, Wilmington, MA, USA) were assessed on various levels: bone biomechanics, by biomechanical torsional testing, morphology by micro computed tomography (microCT) analysis and histological staining, and differential gene expression by microarray, qPCR analysis, and flow cytometry.

Bone healing phases in both groups were investigated by creating a unilateral closed fracture in the diaphysis of the left femur according to Bonnarens and Einhorn (15). Fracture healing was assessed on an 8-week-old male at (day = D) D3, D7, D14, D21, and D28 after surgery.

Furthermore, the individual role of each T and B cells in the cartilaginous callus formation (D7) was investigated. A group of T cell receptor β and δ chain homozygous knockout ($TCR\beta\delta^{-/-}$) mice (16) ($n = 8$) (AG Löhning, Charité – Universitätsmedizin Berlin) was investigated at D7 post fracture. Through knockout of genes in the beta- and delta-chain of the T cell receptor, T cells in these animals were unable to express functional receptors that induce cell apoptosis. Bone healing without the influence of T cell was investigated in this group. On the other hand, a second group of immunoglobulin heavy chain, joining region homozygous knockout ($JHT^{-/-}$) mice (17) ($n = 8$) (Bundesinstitut für Risikobewertung, Berlin, Germany) was investigated 7 days post fracture to analyze healing without B cells. These mice harbor a deletion mediated by cre-loxP resulting in the loss of the exons encoding the joining region and the intron enhancer of the immunoglobulin heavy chain locus (IgH). The $JHT^{-/-}$ mice fail to produce functional B-cells as they lack the gene for the assembly of the heavy chain for the production of antibodies.

Adhering to the 3R principles, sample sizes were kept as small as possible—results were confirmed by using different analyzing methods.

Surgical Procedure

During the operation, mice were anesthetized with 2.5% isoflurane/oxygen and received pain medication [buprenorphine 1 mg/kg BW intraperitoneally (i.p.), Reckitt Benckiser, Mannheim, Germany]. After opening the skin and the knee joint the patella was dislocated to the lateral side. Through the distal end of the femur a passage for the intramedullary pin was created using a hollow needle (Microlance 3, 0.55 mm × 25 mm, BD Drogheda, Ireland). This needle was removed and an intramedullary pin (Thermo spinal needle 17, 0.5 mm × 0.9 mm, TERUMO EUROPE N. V., Leuven, Belgium) was inserted into the bone marrow cavity.

All experiments were carried out with ethical permission according to the policies and principles established by the Animal Welfare Act, the National Institutes of Health Guide for Care and Use of Laboratory Animals, and the National Animal Welfare Guidelines and were approved by the local legal representative animal rights protection authorities (Landesamt für Gesundheit und Soziales Berlin: G 0206/08).

Biomechanical Testing

To study the initial mechanical properties, torsional testing was carried out on the intact contralateral femora of WT and $RAG1^{-/-}$ animals ($n = 18$ per group). The proximal and distal ends of the femur were embedded into the holding pots using polymethyl methacrylate. Using a laser line, femora were aligned parallel to the loading axis and centered into the holding pots. Bones were brought to the point of failure under torsional loading setup of 0.5°/s and 0.3 N axial preload (BOSE ElectroForce 3200 test system, Eden Prairie, MN, USA). Torque of failure (M_max), degree of torsion (angle-at-max), energy at break, and stiffness were evaluated for the intact contralateral bones.

X-Ray Micro Computed Tomography (microCT) Analyses

Mineralized tissue has been analyzed using microCT. Therefore, the femur was isolated from untreated animals or from the contralateral side of animals that received a fracture (WT $n = 56$, $RAG1^{-/-}$ $n = 39$). Femora were scanned with a fixed isotropic voxel size of 10.5 µm (VivaCT, Scanco Medical AG®, Switzerland, 70 kVp, 114 µA). The scan axis equaled the diaphyseal axis of the femora. A diaphyseal volume of interest with a

size of 630 slices was analyzed with a global threshold of 190 mg HA/cm^3. All analyses were performed on the digitally extracted callus tissue using 3D distance techniques (Scanco® software, Switzerland) (18).

Sample Preparation for Histological Analyses

To analyze tissue formation over the course of healing a histological analysis was performed according to the targeted test. Femora were harvested at D3, D7, D14, D21, and D28 of healing from the WT and RAG1$^{-/-}$ mice for paraffin embedding (n = 8 per time point and group). Briefly, bones were harvested with little surrounding muscle tissue and fixated in 4% paraformaldehyde (PFA) at 4°C for 48 h. Afterward, decalcification was done for 3 weeks in a 1:1 solution of 4% PFA and 14% EDTA at 4°C. After dehydration bones were embedded in paraffin and cut into 4 µm sagittal slices.

Furthermore, femora of WT and RAG1$^{-/-}$ mice were also harvested at 7, 14, and 21 days post fracture (n = 3 per group and time point) for plastic embedding. Briefly, femora were fixed with 4% PFA for 48 h, dehydrated, and plastic embedded (Technovit® 9100 neu, Heraeus Kulzer GmbH, Wehrheim, Germany), and then 7 µm sagittal slices were prepared.

Another set of animals from WT, JHT$^{-/-}$, and TCRβδ$^{-/-}$ groups (n = 3 per group) were collected at 7 days post fracture processed for cryo-sectioning. Briefly, bones were harvested and fixed in 4% PFA for 2 h at 4°C. Afterward, the bones were treated in increasing concentrations of sucrose solution 10%, 20%, and finally 30% for 24 h each at 4°C. Bones were then embedded in SCEM cryo-embedding medium (Section Lab Co Ltd., Yokohama, Japan). Cryostat sections of 7 µm were cut sagittal using the Leica CM3050S Cryotom (Leica Microsystems, Nussloch GmbH, Germany) and Cryofilm [Cryofilm type II C (9), Section Lab Co Ltd., Yokohama, Japan].

Histological Assessment and Histomorphometry

Paraffin- and cryo-sections were used for a general overview of the different tissues that are involved in fracture healing using Movat's pentachrome staining. The Movat's pentachrome is a combination of alcian blue solution, Weigert's iron hematoxylin, brilliant crocein acid fuchsin, phosphotungstic acid, and safran du Gatinais solution. The stain differentiates cartilage formation and hypertrophy (green), matrix mineralization (yellow), connective tissue (light blue), muscle (orange), bone marrow (purple), and was used for histomorphometric analyses (19), using a computerized histomorphometric analysis with an image analysis system (KS400 3.0, Zeiss, Eching, Germany).

Triple Fluorochrome Labeling

To label the mineral formation near the fracture gap on the endosteal and periosteal regions *in vivo* fluorescence dyes were injected i.p., (n = 3). Dyes were dissolved in 1.4% $NaHCO_3$ and injected with respect to the time point of euthanasia: calcein blue (blue fluorescence, 30 mg/kg BW, M1255, Sigma, Hamburg, Germany) 12 days pre-euthanasia, calcein green (20 mg/kg i.p.; C0875, Sigma, Hamburg, Germany) 7 days pre-euthanasia, and Alizarin red (30 mg/kg i.p.; A3882, Sigma, Hamburg, Germany) 2 days pre-euthanasia. After sacrifice, femora were dissected and embedded in PMMA as described above. 7 µm thick sections were inspected using fluorescent microscopy and analyzed semiautomated using the provided software (Axioskop 40, and AxioVision software; Carl Zeiss MicroImaging GmbH, Göttingen, Germany).

Immunohistochemical (IHC) and Fluorescent IHC Staining of Bone Matrix and Cells

Immunohistochemical staining was performed on paraffin sections to visualize collagen type I (ColI) at 7 days post fracture (n = 3) in WT and RAG1$^{-/-}$ animals. Briefly, deparaffinized sections were incubated with hyaluronidase for antigen retrieval, rinsed in phosphate-buffered saline (PBS) and incubated with the primary antibody (anti-type I collagen rabbit, C020121, Biologon, 1:500 dilution) overnight at 4°C. Using the avidin/biotin complex method (Alkaline Phosphatase Universal, AK-5200, Vectastain ABC Kit, Vector, CA, USA) binding of the secondary antibody (biotinylated anti-rabbit IgG, made in goat, BA-1000, Vector laboratories, CA, USA) to the primary was visualized by AP substrate (Alkaline Phosphatase Substrate Kit 1, SK-5100, Vector). Counterstaining was performed with hematoxylin. As a negative control, sections were processed for each sample in the absence of the suitable primary antibody.

Fluorescent IHC was performed on cryo-sections of JHT$^{-/-}$, TCRβδ$^{-/-}$, and WT at D7 post fracture (n = 3, for each group). The approach was used to visualize the following components: 1) B cells using anti-mouse B220 (B220/CD45R Alexa Fluor 488-conjugated antibody, Clone # RA3-6B2, R&D Systems GmbH Wiesbaden, Germany); 2) T cells using anti-mouse CD3e (CD3e PE, Clone # eBio500A2, eBioscience, CA, USA); 3) osteocalcin (Ocn) using anti-mouse (rabbit polyclonal, Enzo Life Sciences, cat. no ALX-210-333, 1:4,000); and 4) ColI using anti-mouse ColI (rabbit polyclonal, Bio-Rad). Briefly, sections were brought to room temperature (RT) and washed with PBS. An initial blocking step was performed by applying a solution of PBS containing 5% FCS, 0.1% TWEEN-20, and 10% rat serum for 30 min. For Ocn and ColI staining, sections were blocked with un-labeled Donkey gamma globulin (Jackson). All subsequent washing steps were done using PBS with 5% FCS and 0.1% TWEEN-20. All primary antibodies were incubated for 1 h at RT. Secondary antibodies were used (Alexa Fluor 488, A21206, Invitrogen, 1:500; Alexa 647, Invitrogen, 1:600) for detection. DAPI was used to stain nuclei. After staining was completed the slices were mounted with DAKO fluorescent mounting medium (S3023, DAKO, Hamburg, Germany). To analyze the staining a LSM 710 confocal microscope (Carl Zeiss, Jena, Germany) was used, and pictures were taken using the software Zen 2011 (Carl Zeiss MicroImaging GmbH, Göttingen, Germany). Image analysis was performed using the ImageJ software.

Tartrate-resistant acid phosphatase (TRAP) staining was performed to determine osteoclasts. Counterstaining was done with methyl green. TRAP-positive cells with >3 nuclei and positioned

on the bone surface were considered osteoclasts and included in the evaluation. A total of $N = 8$ animals were analyzed per group, osteoclast numbers were normalized against the bone surface in the analyzed region of interest.

Second Harmonic Generation (SHG) Microscopy

Plastic-embedded samples (WT = 3, RAG1$^{-/-}$ = 4, D7) were used to visualize collagen fibrils in WT and RAG1$^{-/-}$ mice *via* SHG imaging. Collagen fibrils exhibit endogenous SHG signals arising from their well-known non-centrosymmetric molecular structure (20, 21). Imaging was performed using a Leica SP5 II microscope (Leica Microsystems, Wetzlar, Germany). The SHG signal was generated using a Mai Tai® HP Ti:Sapphire oscillator (Spectra Physics, Stahnsdorf, Germany) with 100 fs pulse width at 80 MHz and wavelength of 910 nm. The SHG collagen signal was detected in the range of 450–460 nm. Z-Stacks were recorded with 4 µm *z*-spacing using 25× water immersion objectives with numerical apertures of 0.95. Overview images were created *via* image stitching and maximal intensity projections of z-stacks.

Microarray Analysis

To support our macroscopic findings a gene expression analysis was performed.

mRNA Isolation and Expression Analysis

For RNA preparation from fracture callus, the soft tissue was removed and the fractured bone samples including 1 mm diaphyseal bone on either side of the fracture ($n = 5$ per group and time point) were taken. Same region was also collected from intact femora from both groups to assess indigenous differences. Samples were immediately snap frozen in liquid nitrogen and stored at −80°C until further use. Bones were pulverized in liquid nitrogen and transferred to TRIzol (Invitrogen Life Technologies, Germany) and RNA was isolated according to the manufacturer's protocol with DNAse I (Invitrogen Life Technologies) digestion included. A total of 150 ng RNA per sample was pooled in a given group ($n = 5$ per group). The pooled RNA mixture was distributed as 200 ng samples per tube for technical triplicate in the subsequent microarray analysis.

Microarray Hybridization

Whole genome expression profiling was performed using Illumina's MouseRef-8 v2.0 Expression BeadChips (Illumina, Ambion, TX, USA). Processing RNA for hybridization, including cRNA synthesis and labeling, was done according to standard protocols described in the instruction manual of Illumina TotalPrep RNA amplification kit (Illumina, Ambion, TX, USA). Hybridization of the labeled and fragmented cRNA to the microarray and subsequent staining, washing, and scanning of the arrays was done according to the Illumina Whole-Genome Gene Expression direct Hybridization Assay guide.

Microarray Evaluation

The arrays were pre-processed and normalized using R (22), the bead array (23), and Bioconductor (24) packages. Between arrays, quintile was normalized using the Lumi package (25). Quality assessment of the microarray data was performed by computing the mean Pearson correlation between each array and every other array in the test database. Exclusion of arrays was unnecessary as they did not exceed the mean correlation cutoff of 0.6. Pearson correlation of each pair was used to evaluate replicates. Mean correlation cutoff was set to 0.9—no replicate removal was necessary. Differences between gene expression at each time point in WT and RAG1$^{-/-}$ was calculated using a two-tailed *t*-test. The *p*-values were alpha-error adjusted using the Benjamini–Hochberg method. Fold changes (FCs) were calculated from comparison of the mean expressions between the control (WT) and the treatment (RAG1$^{-/-}$) group. Differentially expressed genes were visualized in a heatmap after applying a *t*-test analysis to reveal the significant gene regulations for each analyzed time point. Significance FC cutoff of >1 and Benjamini and Hochberg-corrected *p*-values (*p*.BH) <0.05 was followed for the guilt-by-association (GBA) analysis and a cutoff of FC > 1 and *p*.BH < 0.01 for the panel analysis. Genes were then clustered (arranged) according to their expression pattern over the course of healing. Gene lists of the expression clusters were then compared to literature and NCBI-DAVID (an online server for the gene annotation) to characterize the major biological processes, molecular functions, and cellular components for these genes.

Quantitative Reverse Transcription Polymerase Chain Reaction (qRT-PCR)

To evaluate the differential expression of collagen I and bone markers [OPG, RANKL, Runt-related transcription factor 2 (RUNX2)] a qRT-PCR was performed. Femora from WT, RAG1$^{-/-}$, TCRβδ$^{-/-}$, and JHT$^{-/-}$ ($n = 4$) were harvested and instantly frozen in liquid nitrogen and then stored at −80°C until processing. RNA was extracted using a Trizol/chloroform (TRIzol® Reagent, Invitrogen, 15596-018; chloroform for molecular biology, VWR, SIALC2432-25ML) and the RNAeasy kit [RNeasy Mini Kit (74104), RNase Free DNase Set (79254), Nuclease Free Water (129114), QIAGEN]. A total of 100 ng RNA per sample have been reverse transcribed using random primer [Random Primers, Invitrogen, 48190-011; Set of four dNTPs (100 mM), BIORON, 110011; Recombinant RNasin® Ribonuclease Inhibitor inkl. M-MLV RT 5× Reactionbuffer, Promega, N2511; M-MLV Reverse Transcriptase RNase H Minus, Point Mutant, Promega, M3683; Ribonuclease H, Promega, M4285]. Primers were tested for the annealing temperature and efficiency prior to use: mCOL1a1 ase: 5′-gttccaggcaatccacgag-3′, mCOL1a1 se: 5′-ggtccacaaggtttc-caagg-3′; mOPG ase: 5′-ctgctctgtggtgaggttcg-3′, mOPG se: 5′-agctgctgaagctgtggaaa-3′; mRANKL ase: 5′-cgaaagcaaatgttg-gcgta-3′, mRANKL se: 5′-gcacacctcaccatcaatgc-3′; mRUNX2 ase: 5′-tgtctgtgccttcttggttcc-3′, and mRUNX2 se: 5′-cgaaatgcctccgct-gttat-3′. Cyclophilin A was used as a house keeping gene. PCR cycle: 40 cycles each consisting of 95°C, 30 s, 62°C, 30 s, 72°C, 30 s. Evaluation was done using the $2^{-\Delta Ct}$ method.

Flow Cytometry

Splenocytes were harvested from WT, RAG1$^{-/-}$, TCRβδ$^{-/-}$, and JHT$^{-/-}$ ($n = 4$) and brought into single cell suspension. Cells were washed and resuspended in FACS buffer (PBS/0.5% BSA/0.1% sodium acid). Staining with the fluorescent coupled antibodies

was performed for live/dead (Invitrogen LIVE/DEAD fixable blue dead cell stain kit, for UV excitation), CD45 (30-F11, V500, BD Horizon), CD3e (145-2C11, PerCP/Cy5.5, BioLegend), and CD8a (53-6.7, BV785, BioLegend). The FACS analysis was done with a BD LSRFortessa (BD Deutschland GmbH). The FlowJo software (TreeStar Inc., Ashland, OR, USA) was used for data evaluation. Gating strategy: lymphocytes, single cells, live cells, CD45-positive cells, CD3e-positive cells, CD8a-positive cells to determine $CD8^+$ T cell percentage in the respective mouse strains.

Protein Expression Analysis

Conditioned media of LPS-activated splenocytes of WT, $TCR\beta\delta^{-/-}$, $JHT^{-/-}$, and $RAG1^{-/-}$ mice ($n = 4$) were pooled and analyzed toward their TNFα and interleukin 10 (IL-10) concentrations. Mouse TNFα ELISA Ready-SET-Go!® and Mouse IL-10 ELISA Ready-SET-Go!® kits (eBioscience, San Diego, CA, USA) were carried out after manufacturer's recommendations. Samples were incubated overnight at 4°C, final staining reactions were stopped with 1 M H_3PO_4 and absorbance was read at 450 nm with 570 nm reference wavelength with Tecan Infinite M200 PRO (Tecan, Männedorf, Switzerland) and analyzed with i-control 1.9 software (Tecan).

Cell Culture

Isolated murine MSCs were cultured in chamber slides with expansion medium for 1 day. Then osteogenic differentiation medium was added which included conditioned medium (1:3 dilution) from LPS (1 µg/ml)-activated splenocytes of WT, $RAG1^{-/-}$, $TCR\beta\delta^{-/-}$, and $JHT^{-/-}$ mice ($n = 4$). Medium change was done twice per week for 14 days. Collagen fibers were stained with Sirius red and analyzed under polarized light.

Statistical Analysis

Tests for statistical significance were performed in SPSS 21.0 (IBM, CA, USA). Data from histomorphometry, biomechanics, and microCT analyses were explored for normality by examining skewness and kurtosis. Data were not normally distributed. Therefore, Bonferroni *post hoc* corrected Mann–Whitney *U* test was used to test the significance between the two groups in a given time point. *p*-Values of <0.05 were chosen to indicate an exact two-tailed significance. Data were presented as box plots (median and interquartile range) or bar graphs (mean ± SEM).

In the analyses of statistical significance, $n \geq 5$ animals were included per group. This was the lowest number of samples needed for the present study based on *a priori* assumption for qualitative statements. For descriptive analyses, samples sizes of $n < 5$ were used. No experimental animals were excluded from the analysis.

RESULTS

$RAG1^{-/-}$ mice are in their gross appearance similar to WT. Without mature T and B cells bone developmental processes, however, are altered and this alteration in organogenesis is reflected in fracture healing. Detailed analysis of structural parameters, functional competence, and expression profiling in intact $RAG1^{-/-}$ bone was performed (Figure S1 in Supplementary Material).

Morphological Differences between $RAG1^{-/-}$ and WT Bones

To characterize phenotypic differences between the $RAG1^{-/-}$ and WT, intact bones were investigated using histological and radiological tests. Movat's pentachrome staining indicated no morphological differences between the femora of both groups. Histomorphological analysis was also performed. However, no significant differences in trabecular number or thickness were found (data not shown). microCT data of unfractured and contralateral bones of WT and $RAG1^{-/-}$ animals showed no differences in total volume, bone volume (BV), or the ratio thereof; however, qualitative bone markers such as tissue mineral density and bone mineral density (BMD) were significantly different (**Figure 1A**).

Discrepant Functional Competence in the $RAG1^{-/-}$ Intact Femora

To determine indigenous discrepancies in material properties resulting from the lack of mature T and B cells, intact bones from $RAG1^{-/-}$ and WT animals were subjected to biomechanical torsional testing. While the moment to failure (M_max) did not differ between $RAG1^{-/-}$ and WT (**Figure 1B**), it became apparent that WT bones endured significantly higher deformation equaled by the angle at maximum force at failure (angle-at-max). This reflects on the energy required to cause the material failure in the form of fracture (energy-to-break), which was lower in $RAG1^{-/-}$ compared to the WT. Therefore, the significantly higher stiffness found in the $RAG1^{-/-}$ compared to the WT controls indicates a stiffer but more brittle bone in $RAG1^{-/-}$.

Gene Expression Data Reveal Discrepancies in Bone Structure due to the Lack of Mature T and B Cells

Differentially expressed genes associated with a role in bone structure and formation and a correlation with T and B cells were analyzed in intact bones. (Detailed data of the initial discrepancies between both the groups are shown in Table S1 in Supplementary Material.) Microarray data of intact bone between WT and $RAG1^{-/-}$ showed changes in bone homeostasis and osteogenic processes (**Figure 1C**). Mesenchymal stem cells (MSCs)-related genes were upregulated: the Sema3f gene [a known chemorepulsant from the Semaphorin protein family (26)] and type 1 collagen alpha one (Col1a1). On the other hand, ubiquitin-D [Ubd, a known cell survival factor (27)] and actin beta (Actb, which is involved in MSC differentiation into osteoblasts) were downregulated. The lack of mature T and B cells also affected osteoblasts through four upregulated genes [Col1a1, Sp7 transcription factor (Sp7), Gpnmb also known as osteoactivin, and insulin growth factor 2 (Igf2)] and another two downregulated genes [transcription factor myocyte enhancer factor 2C (Mef2c) and Ubd]. Osteoclast-related genes were mostly downregulated: Kruppel-like factor 10, bone gamma carboxyglutamate protein (Bglap), and osteopontin (Spp1). One

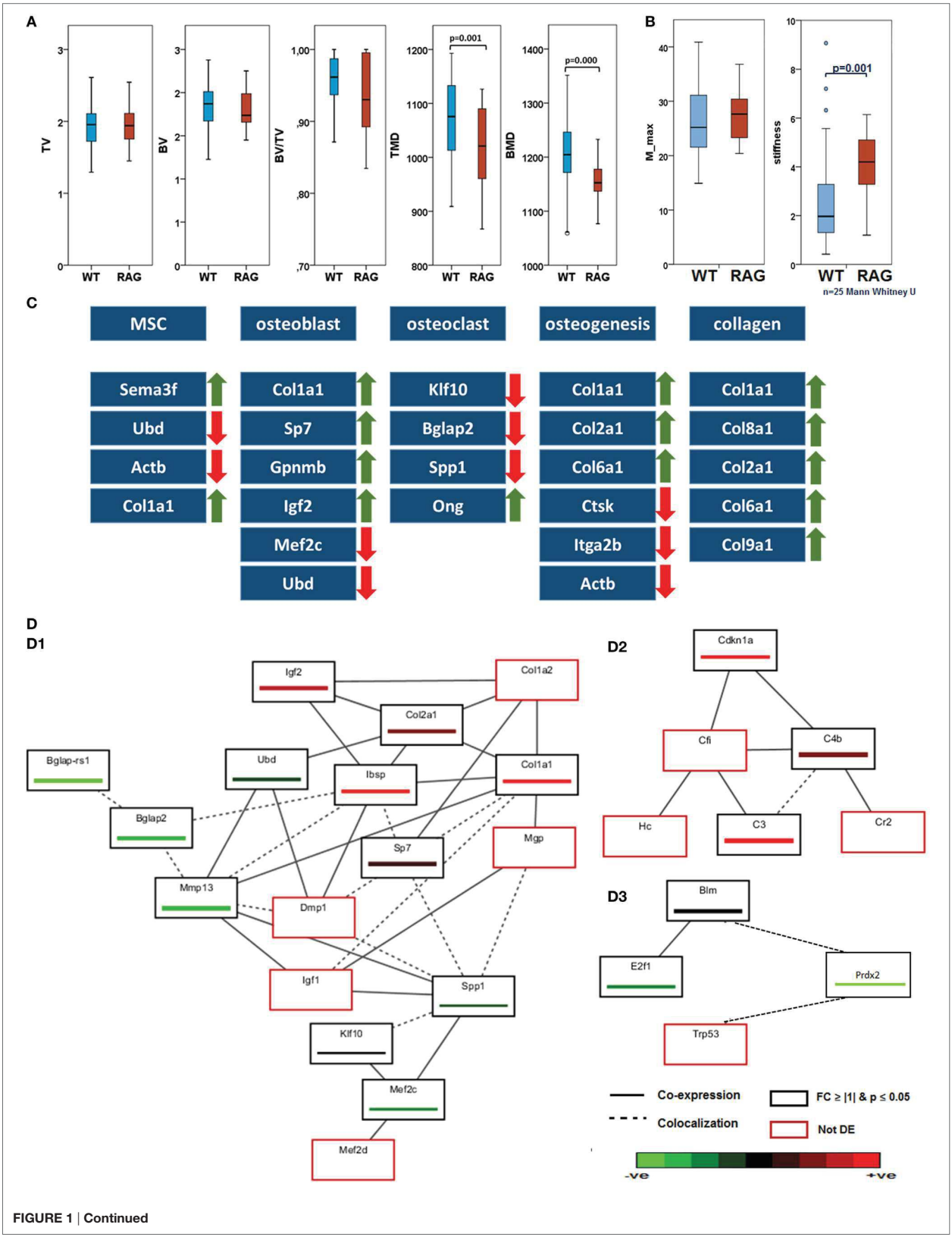

FIGURE 1 | **Continued**

FIGURE 1 | Continued
Intact bone of wild-type (WT) and recombination activating gene 1 homozygous knockout (RAG1$^{-/-}$) while having the same morphology difference in their biomechanical competence and gene expression: (A) micro computed tomography analyses showed no differences in total volume (TV), bone volume (BV), and BV/TV. In those parameters describing the bone quality, tissue mineral density (TMD, $p = 0.001$) and bone mineral density ($p = 0.000$), however, significant differences were found between WT and RAG$^{-/-}$ animals with RAG$^{-/-}$ showing a decreased TMD and BMD (WT $n = 56$, RAG$^{-/-}$ $n = 39$). **(B)** The torque of failure (M_max) is the same in untreated bone of WT and RAG1$^{-/-}$ animals. However, the RAG1$^{-/-}$ bones show significantly higher stiffness when compared with WT bones. **(C)** Differentially expressed genes correlated with T and B cells were analyzed in intact bones. Expression changes were seen on cellular and extracellular matrix (ECM) levels and in bone homeostasis and osteogenic processes. Major expression changes were seen as an increase in collagen genes expression and their subunits. **(D)** Guilt-by-association analysis correlates genes regulation depending on their coexpression and colocalization. (D.1) differentially expressed genes as described in **(C)** were associated with ECM proteins, (D.2) shows upregulation in B cell-related genes and (D.3) shows downregulation of T cell-regulated genes.

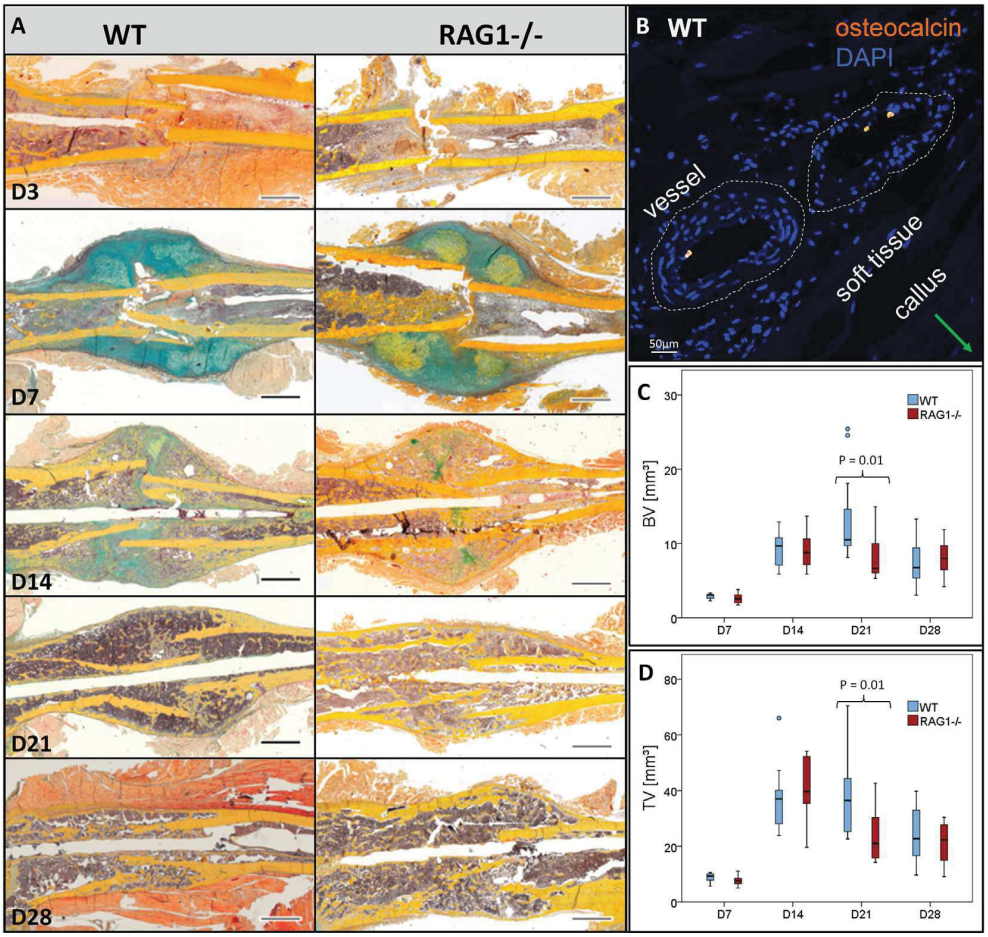

FIGURE 2 | Fracture healing in wild-type (WT) and recombination activating gene 1 homozygous knockout (RAG1$^{-/-}$) animals: (A) fracture healing in the WT animals showed the typical steps of hematoma [day 3 (D3)], soft callus formation (D7), woven bone deposition (D14), and remodeling (21 and 28 days). In the RAG1$^{-/-}$ animals, lack of mature T and B cells has altered this sequence. D3 shows abundant endosteal hematoma, however, periosteal bone formation far from the fracture gap was also seen. 7 days after fracture mineralized batches in the cartilaginous callus indicated enhanced mineralization of the callus, these were more pronounced than in the WT. At D14, the cartilage was vastly calcified and remodeling was enhanced at 21 and 28 days (Movat's pentachrome staining: bone—yellow, cartilage—blue/green, muscle—red, bone marrow—magenta, and connective tissue— light blue; scale = 1 mm). **(B)** Osteocalcin-positive cells were found in WT in the vessel of the soft tissue surrounding the callus. Micro computed tomography analysis (without normalization to the contralateral bone—to analyze the difference in healing only) showed higher bone volume **(C)** and the total volume **(D)** in the WT animal callus at D21.

gene was upregulated: osteoglycin. This differential expression was reflected in osteogenic processes that showed a downregulation in osteoclast-mediated resorption genes such as cathepsin K, integrin alpha-IIb (also known as CD41) and Actb. However, collagen types correlated with bone matrix formation were upregulated (Col1a1, Col2a1, and Col6a1). This increase in collagen genes expression was also found in other collagen subunits such as Col8a1, Col9a1, and Col10a1.

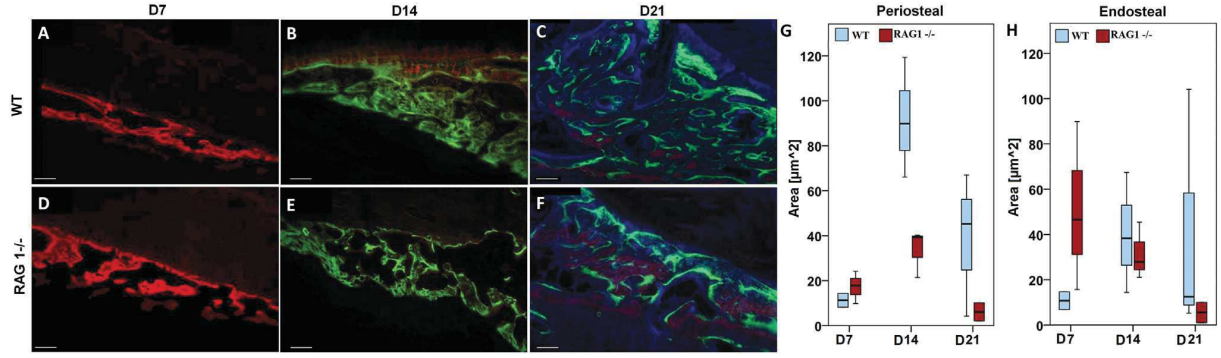

FIGURE 3 | Fracture callus mineralization differs without mature T and B cells. Fluorochrome labeling reflects mineral deposition in bone matrix upon binding to a fluorophore. Red labeled areas show mineral deposition at day 7 (D7) [**(A)** for wild-type (WT) and **(D)** for recombination activating gene 1 homozygous knockout (RAG1$^{-/-}$)], green ones reflect deposition at D14 [**(B)** for WT and **(E)** for RAG1$^{-/-}$], these time points show larger deposition areas in the RAG1$^{-/-}$ compared to the WT. However, the area of mineral deposition (blue area) at D21 was larger in the WT **(C)** than in the RAG1$^{-/-}$ **(F)**. Intramembranous/periosteal mineral deposition was higher in the RAG1$^{-/-}$ only at D7 and then higher in the WT **(G,H)**. Interestingly, mineral deposition in the cartilaginous callus/endosteal ossification was not different at D14 or D21, but was higher in the RAG1$^{-/-}$ only at D7. Scale bar: 100 µm, see Table S3 in Supplementary Material for periosteal/endosteal area values (µm^2) per group and time points.

Guilt-by-association analysis correlates genes regulated in T and B cells and osteogenesis depending on their coexpression and colocalization (**Figure 1D**). The osteogenic process in the RAG1$^{-/-}$ was compared to the WT. Differentially expressed genes as described in **Figure 1C** were associated with the following genes: matrix Gla protein, dentin matrix acidic phosphoprotein 1, insulin growth factor 1 (Igf1), myocyte enhancer factor 2D (Mef2d), and Col1a2 (**Figure 1**, D.1).

Microarray analysis also showed upregulated B cell-related genes (**Figure 1**, D.2), such as cyclin-dependent kinase inhibitor 1A, complement component 4B, and complement component 3. GBA analysis revealed three non-differentially regulated genes: complement component factor i, complement receptor 2, and hemolytic complement genes were coexpressed with the B cell-related network genes.

Interestingly, T cell-related genes (**Figure 1**, D.3) were downregulated (Bloom syndrome, E2F transcription factor 1 and peroxiredoxin 2) in the RAG1$^{-/-}$ compared to the WT. Another gene was found to be colocalized with these genes: transformation-related protein 53.

Bone Healing with and without Mature T and B Cells

To confirm the effects of T and B cells in bone formation processes, bone healing was analyzed in WT and compared to bone healing in RAG1$^{-/-}$ mice: Movat's pentachrome staining was used to quantify dimensions and distribution of callus tissue during the time course of healing. Histomorphometric methods were used to quantify cartilaginous fractions including zones of hypertrophic chondrocytes as well as ossified regions at the periosteal bone surface area in the fracture callus.

The WT showed a typical course of bone healing that consists of consecutive but overlapping phases. The inflammatory reaction that is initiated upon injury and bleeding resulted in visible hematoma formation and maturation (**Figure 2**, WT, D3). It is followed by cartilaginous callus formation (**Figure 2**, WT, D7). Upon hypertrophy of chondrocytes the matrix mineralized and the hard callus evolved, which consisted of woven bone (**Figure 2**, WT, D14). During the final phase of bone healing, remodeling took place thereby slowly rebuilding the form and function of the bone according to its mechanical constraints (**Figure 2**, WT, D21 and D28). When comparing the bone healing sequence in WT mice and mice lacking mature T and B cells it becomes apparent that ossification seems to be accelerated, which can be seen in the earlier onset of mineralization (**Figure 2**, RAG1$^{-/-}$, D7). The earlier callus formation in the RAG1$^{-/-}$ animals lacking mature T and B cells has been reported in detail before (4).

During healing, Ocn visualization showed lower signals in the RAG1$^{-/-}$ than in the WT callus at D7 (**Figure 2B**). Furthermore, microCT analysis of bone healing progression reflected an increased BV and total volume (TV) in the WT animals at D21 (**Figures 2C,D**, respectively). Both, BV and TV showed a decreasing trend between D21 and D28 in the WT but not in the RAG1$^{-/-}$.

Bone Deposition Pattern Changes in the Absence of Mature B and T Lymphocytes

To determine how mature T and B cells influence the material formation of bone, we looked into bone apposition during bone healing. Bone formation was monitored using fluorescent dyes injected 2 days prior to sacrifice at 7, 14, and 21 days after fracture to determine new bone formation in the fracture callus with (WT) and without B and T lymphocytes (RAG1$^{-/-}$).

At D7 post fracture, the RAG1$^{-/-}$ animals showed more bone formation in areas of intramembranous/periosteal ossification (**Figures 3A,D,G,H**). This result supports the finding of

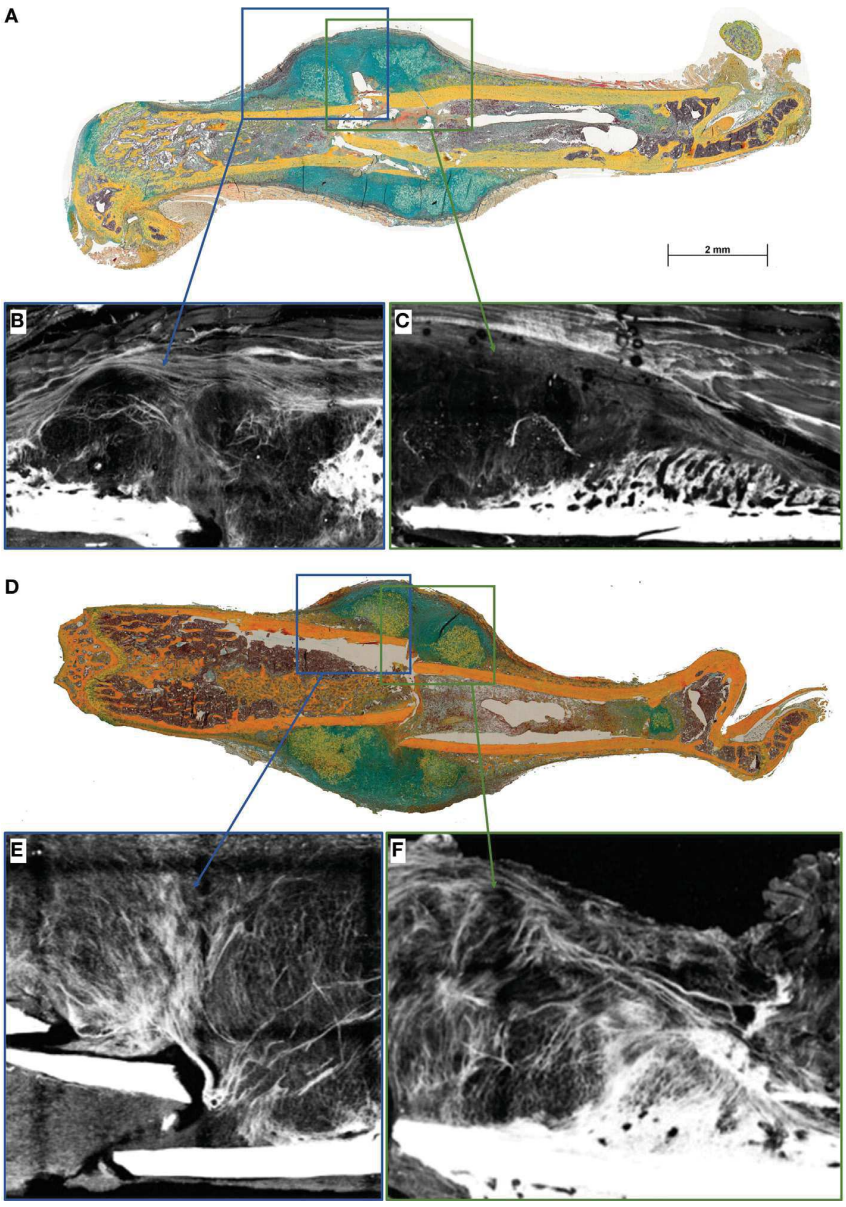

FIGURE 4 | Collagen fibril deposition appears disorganized in recombination activating gene 1 homozygous knockout (RAG1$^{-/-}$) animals' callus at day 7 (D7). Seven days after fracture the callus was imaged to analyze the collagen deposition pattern in wild-type (WT) mice **(A)** and RAG1$^{-/-}$ mice **(D)**. WT animals show an aligned structure of collagen fibrils **(B)** in the callus and on the periosteal surface **(C)**, the imaging also shows structurally sound woven bone on the periosteal surface. Disarrangement of collagen fibrils structure was apparent in the RAG1$^{-/-}$ callus **(E)**, and periosteal bundle arrangement is seen with dense mineral deposition in the periosteal surface without woven bone structure **(F)**. This representative image shows the disorganized collagen deposition occurring without mature T and B cells in the RAG1$^{-/-}$ animals. (Blue rectangles show the central area of the fracture callus while the green outtakes concentrate on the margin and thus periosteal callus area.)

accelerated mechanical stabilization in the absence of mature T and B cells reported earlier (4).

However, this dynamic changed at later healing time points, when WT bone formation exceeded RAG1$^{-/-}$ bone formation at D14 post fracture during the phase of endochondral ossification in normal bone healing (**Figures 3B,E,G,H**). During the remodeling stage, WT bone formation was distinctively higher than in RAG1$^{-/-}$ bone formation, indicating an active bone forming process in a phase where high numbers of T and B cells are present (**Figures 3C,F,G,H**) (13). During the remodeling stage, the bone adapts to its mechanical loading that according to "Wolff's law" determines form and function of the bone.

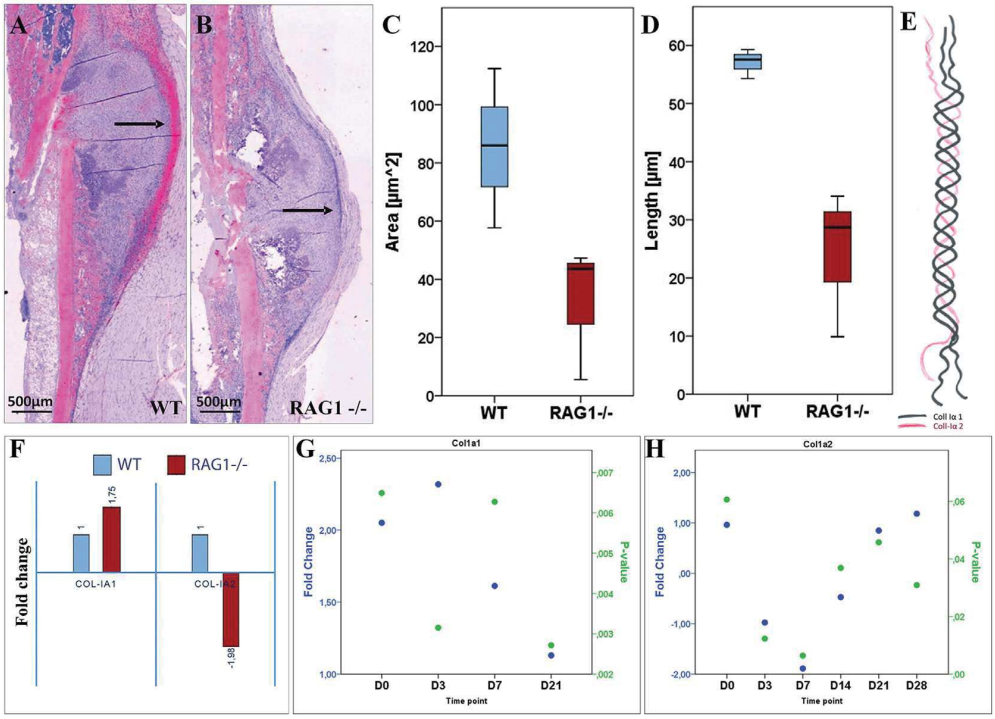

FIGURE 5 | Collagen type I (ColI) deposition and expression pattern are considerably altered in fracture healing when mature T and B cells are absent. **(A)** Histological staining of ColI (2.5× overview) shows higher signal intensity (indicated by black arrows) on the periosteal surface and the callus outer borders in the wild-type (WT) at day 7 (D7). **(B)** Lack of signal location at the callus outer border in the recombination activating gene 1 homozygous knockout (RAG1$^{-/-}$) at D7 with general lower signal intensity. Compared to the RAG1$^{-/-}$, larger ColI-positive area in the WT **(C)** and longer surface in the WT **(D)** are detected. **(E)** ColI composition: two subunits of Collα1 and one subunit of Collα2 form the typical ColI triple helix. **(F)** The expression of the ColI subunits Iα1 and Iα2 at D7 shows a 1.75-fold increase in Collα1, while the expression of Collα2 was decreased by 2. Changed expression patterns for Collα1 **(G)** and Collα2 **(H)** were observed throughout the observed healing period of 28 days.

We conclude that in the presence of T and B cells the bone formation process is guided to allow proper matrix organization leading to distinct bone quality.

Distinctive Changes in Fibril Fibers in Fracture Callus upon Lack of B and T Lymphocytes

To further unravel the impact on matrix formation in animals lacking mature T and B cells, we investigated fibrillar collagen fiber deposition during bone healing in the early fracture callus using second harmonic photon microscopy (D7 post fracture). While fibers in the WT seem to be aligned along the outer callus border and also surrounding the dark areas that would indicate cartilaginous zones, this was not found in the RAG1$^{-/-}$ calluses (**Figure 4**).

For bone formation, ColI deposition proceeds with the binding of hydroxyapatite during matrix mineralization. Since bone formation was affected in RAG1$^{-/-}$, ColI was analyzed during bone healing in both animal types by immunohistochemical staining. In the WT animals, a typical outer callus area was positive for ColI, while this ColI-positive area was missing in the RAG1$^{-/-}$ animals (**Figures 5A–D**).

ColI is a fiber composed of two ColIα1 and one ColIα2 fibrils (**Figure 5E**). Upon analyzing the expression of ColI subunits, a significantly altered expression pattern was detected (**Figures 5G,H**; see Table S2 in Supplementary Material). Interestingly, at D7 ColIα1 expression was nearly two times higher in the RAG1$^{-/-}$, while ColIα2 was nearly two times lower when compared to the WT group (**Figure 5F**). This indicates a severe dysregulation of both subunits of ColI, which represents the most important matrix component of bone. Without mature T and B cells, the synthesis and deposition of ColI were distinctly changed during the early fracture healing stages.

Osteoblast Cell Dynamics Are Distinctly Altered without Mature T and B Cells

With the clear evidence that the lack of mature T and B cells leads to extracellular matrix (ECM) alteration in bone tissues during organogenesis and very pronounced in bone healing, the cells responsible for ColI production were analyzed. ColI is mainly produced by osteoblasts during the bone formation process. Due to the altered ColI pattern in RAG1$^{-/-}$ mice, histological sections were analyzed for Ocn-positive osteoblasts (**Figure 6**). In WT animals, osteoblasts were concentrated in

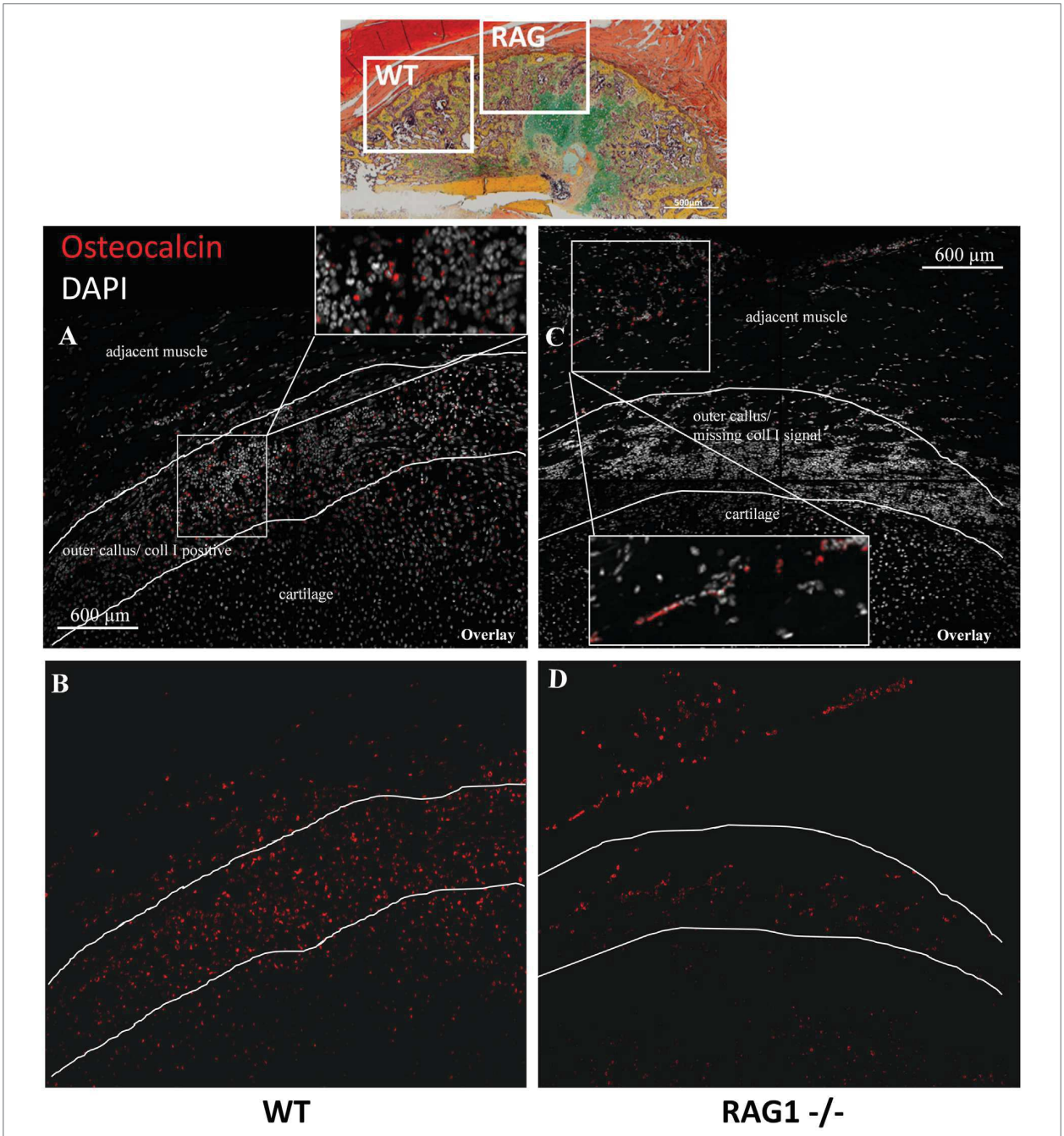

FIGURE 6 | Osteocalcin (Ocn)-positive cells show an aberrant localization in the fracture callus of animals healing without mature T and B cells. Immunohistological images of Ocn-positive cells in the fracture callus of WT **(A,B)** and recombination activating gene 1 homozygous knockout (RAG1$^{-/-}$) animals **(C,D)** at day 14 reveal an abundance of these cells in the collagen type I-positive outer rim of the wild-type callus **(A)** while these cells are scarce in the equivalent location in RAG1$^{-/-}$ animals **(C)**. In the RAG1$^{-/-}$ animals, a layer of Ocn-positive cells appears in the soft tissue adjacent to the fracture callus (red = Ocn; gray = DAPI to stain cell nuclei).

the cell rich outer callus layer jointly with fibrillar fibers and an intense ColI expression (**Figures 6A,B**). In RAG1$^{-/-}$ animals, Ocn-positive cells were concentrated in a distinctly different area, in the connective tissue and muscle layer directly adjacent to the fracture callus but not at the forefront of callus formation (**Figures 6C,D**).

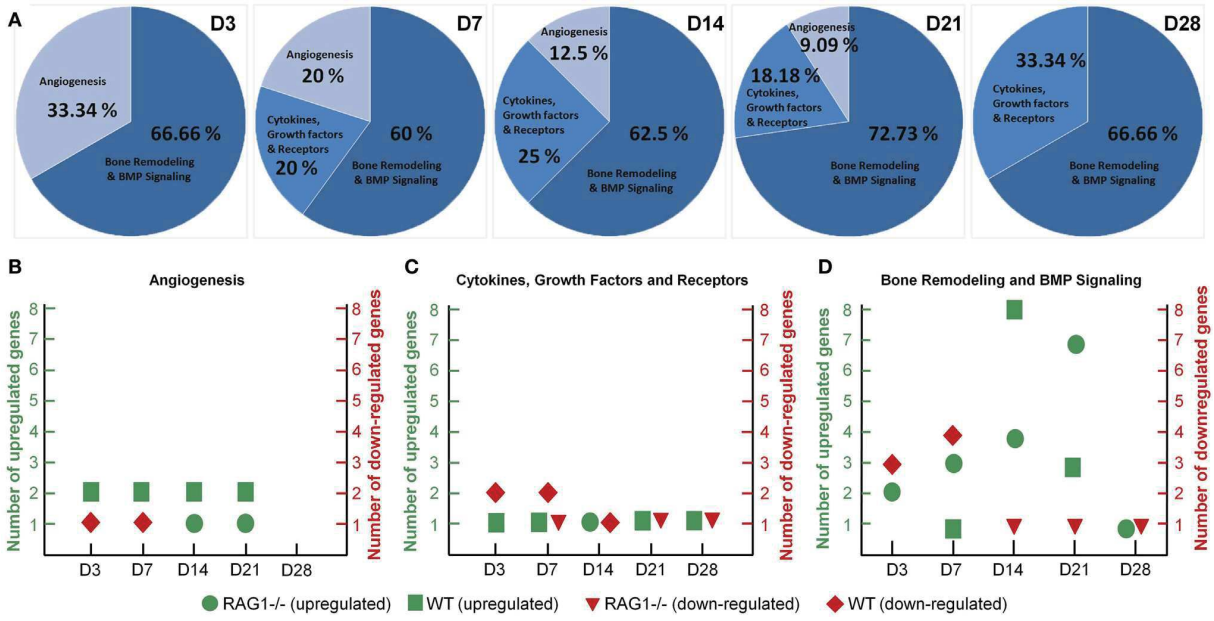

FIGURE 7 | Dysregulated angiogenesis and cytokine expression in the recombination activating gene 1 homozygous knockout (RAG1$^{-/-}$) callus along with chronically shifted (earlier) bone formation and remodeling. (A) Angiogenesis-related genes showed declining numbers of differentially expressed genes with healing progression in the RAG1$^{-/-}$. Cytokines and growth factor gene expression was highest at day 28 (D28). Interestingly, the percentage of bone remodeling and formation differentially expressed genes was almost constant throughout the healing in the RAG1$^{-/-}$ fracture callus. **(B)** Mostly, wild-type (WT) genes were upregulated at all time points, whereas upregulation in the RAG1$^{-/-}$ was only at D14 and D21. **(C)** RAG1$^{-/-}$ genes were upregulated only at D14. **(D)** Number of upregulated genes in the RAG1$^{-/-}$ increased from D3 to D14, however, at D28 upregulated genes were still seen in the RAG1$^{-/-}$.

The abovementioned data suggested that T and B cells are important for the tissue properties of newly formed bone material and that osteoblasts are located distant to the callus tissue formation front if mature T and B cells are missing. Thus, the interdependency of the immune cells and the bone formation signals were analyzed during fracture healing using expression analysis.

A detailed examination of osteoclasts, bone cells responsible for bone degradation revealed no significant difference in osteoclasts numbers in the healing cascade up to D14. At D14, RAG1$^{-/-}$ showed significantly more osteoclasts ($p = 0.037$): at this time point occurs typically the maturation from the soft callus to hard callus and the beginning woven bone deposition in WT animals (Figure S2 in Supplementary Material).

Expression Analysis Confirms That the Changes in RAG1$^{-/-}$ Bone Formation Are Linked to Mature T and B Cells

To identify the discrepancies in bone healing we have limited the comparison of RAG1$^{-/-}$ and the WT callus tissue to the gene sets selected in commercial array panels for angiogenesis, cytokines, and growth factors, and bone remodeling and BMP (bone morphogenetic protein) signaling (Qiagen, Hilden, Germany). In RAG1$^{-/-}$ mice, when D0 was taken as control to look into the changes during the bone healing process, the gene list was compared to the panels for an overview of the change in expression. At D3, over 30% of the differentially expressed genes were related to angiogenesis (**Figure 7A**), the percentage declined from D7 (20%) to D14 (12.5%) to D21 (9%) to 0% at D28. However, the cytokine- and growth factor-related genes showed an irregular pattern with 0 differentially expressed genes at D3, an increase from 20% at D7 to 25% at D14 followed by a decrease at D21 (18%) and again an increase at D28 (33%) (**Figure 7A**). Interestingly, the panel involving bone remodeling and BMP signaling (**Figure 7A**) showed an approximate consistency at all time points from D3 (67%), D7 (60%) through D14 (62.5%), D21 (73%) until D28 (67%).

Additionally, when the RAG1$^{-/-}$ group was compared to the WT group, more genes were seen to be upregulated in the WT group in the angiogenesis panel, whereas genes in the RAG1$^{-/-}$ group on the other side were downregulated at D3 and D7 and upregulated only at D14 and D21 (**Figure 7B**). However, cytokines and growth factors panel showed that more genes were downregulated in the WT group at D3 and D7, but upregulated at all time points in comparison with the RAG1$^{-/-}$ mice (which showed a downregulation of genes at D7, D21, and D28 and an upregulation only at D14) (**Figure 7C**). In the bone remodeling and BMP signaling panel, RAG1$^{-/-}$ mice showed differentially expressed genes at all the time points with the highest number of upregulated genes at D21, while WT showed the highest number of upregulated genes at D14 when compared to RAG1$^{-/-}$ (**Figure 7D**). The gene number blot (**Figure 7D**) showed a shift in upregulation/

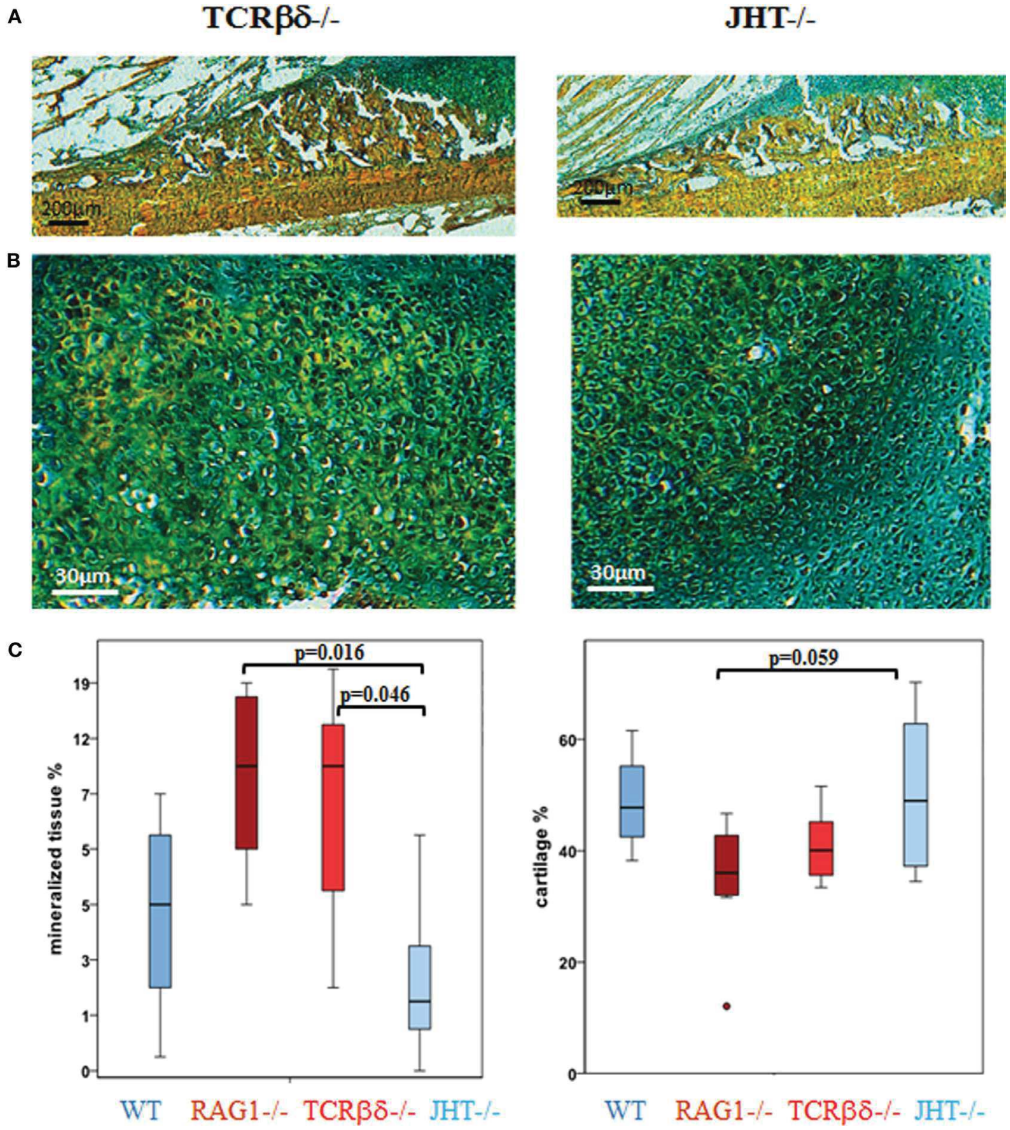

FIGURE 8 | Single knockouts for either T cells or B cells reveal a distinct healing pattern. In T cell-deficient mice healing resembles recombination activating gene 1 homozygous knockout (RAG1$^{-/-}$) animals, while B cell-deficient mice resemble the wild-type (WT) healing more closely. Movat's pentachrome staining of fracture healing 7 days into healing revealed an early mineralization in T [T cell receptor β and δ chain homozygous knockout (TCRβδ$^{-/-}$)] and B [joining region homozygous knockout (JHT$^{-/-}$)] cell-deficient mice **(A,B)** that was also seen in RAG1$^{-/-}$ animals and which exceeds the mineral deposition in B cell-deficient mice. **(C)** A histomorphometrical analysis of the bone and cartilage tissue in the fracture callus confirmed the similarity in RAG1$^{-/-}$ and T cell-deficient mice (red) when compared with WT healing and the healing in B cell-deficient mice (blue).

downregulation patterns in genes related to bone remodeling between the two groups.

The Effect of Changed Healing Pattern in the RAG1$^{-/-}$ Animals Is Predominantly Caused by the Lack of T Cells

Changes in mineralization in RAG1$^{-/-}$ could be dependent on the lack of T cells or B cells independently. Therefore, the 7-day healing process was assessed in animals that lacked either T cells (TCRβδ$^{-/-}$) or B cells (JHT$^{-/-}$). The histological images showed that in the animals that lacked only T cells an earlier mineralization was detected (**Figures 8A,B**, left) and the cartilaginous area showed signs of mineralized matrix earlier as well (**Figure 8C**).

Histomorphometrical analysis showed that mineralized values were similar in RAG1$^{-/-}$ and T cell devoid healing (**Figure 8C**, left). In conclusion, B cell devoid healing was similar to WT healing, while animals without T cells showed healing patterns similar

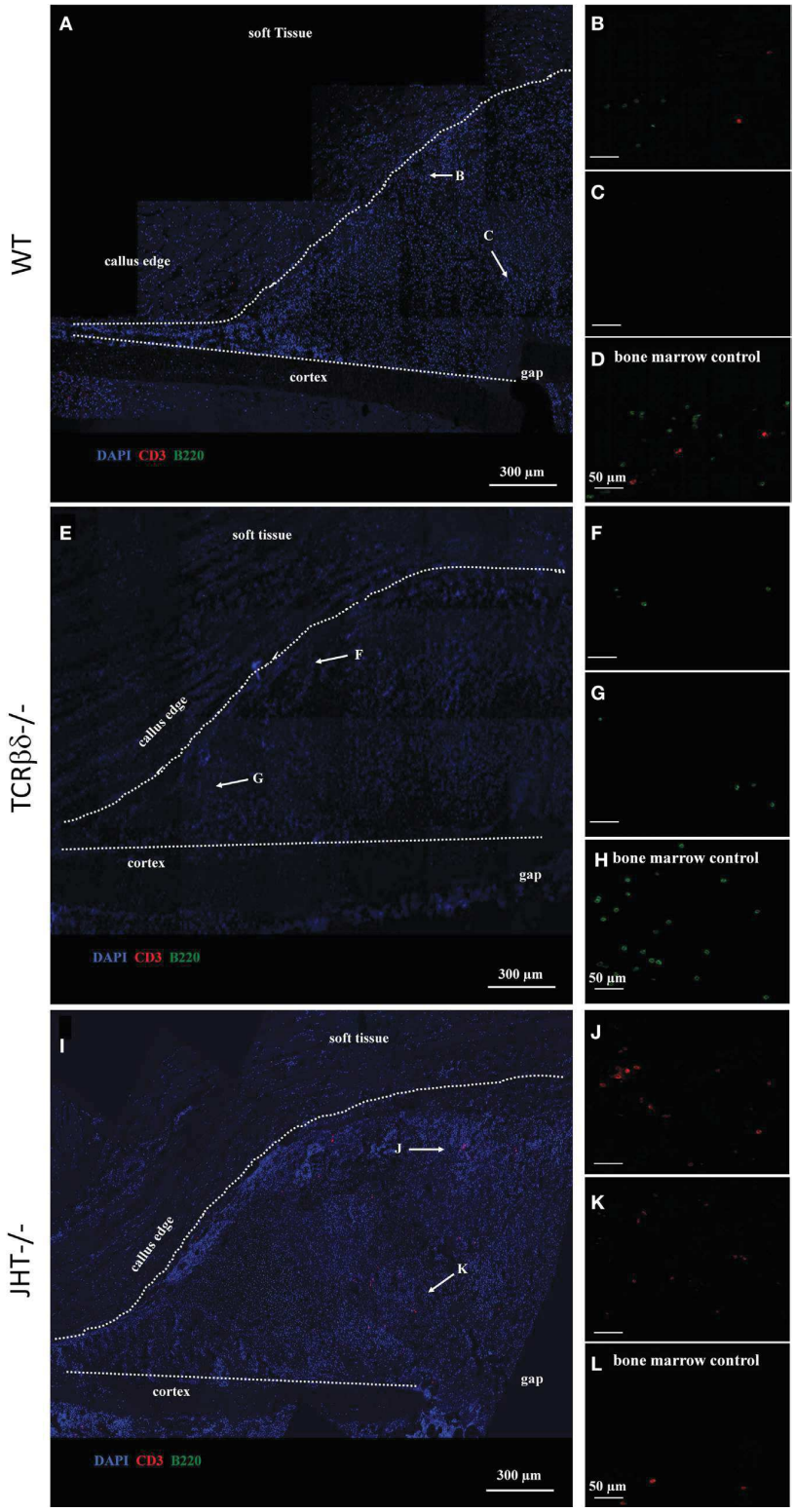

FIGURE 9 | **Continued**

FIGURE 9 | Continued
Altered migration pattern of T cells in the early callus of B cell-deficient mice. Confocal microscope analysis of the callus of wild-type (WT) **(A–D)**, T cell-deficient [T cell receptor β and δ chain homozygous knockout (TCRβδ$^{-/-}$)] **(E–H)** and B cell-deficient [joining region homozygous knockout (JHT$^{-/-}$)] **(I–L)** mice. Sections were stained for the T cell marker CD3 (red), B cell marker B220 (green), and cell nuclei (DAPI, blue). Letters near the white arrows indicate areas that are magnified in the corresponding panels below **(A,E,I)**. **(D,H,L)** Control staining in the bone marrow of WT, T cell—and B cell—mice, respectively. All sections were taken 7 days after fracture.

to the one in RAG1$^{-/-}$ animals. Both groups, RAG1$^{-/-}$ and T cell knockout animals, showed significantly more mineralized tissue in comparison to the B cell knockout group. A similar pattern was found upon analyzing the cartilaginous areas (**Figure 8C**, right). These findings support the assumption that the changes in the bone quality seen in the RAG1$^{-/-}$ bone healing are primarily due to the lack of T cells.

T Cells Drive Normal Deposition of ColI during Fracture Healing

Due to the striking difference in mineralization capacity between mice specifically devoid of either T or B cells, we decided to further analyze bone healing in these animals at the cellular level by confocal microscopy.

At 7 days post fracture and similar to controls, small numbers of B cells were detected in the callus periphery of T cell-deficient mice (**Figures 9E–G**). On the other hand, T cell migration was altered in the callus of B cell-deficient mice (**Figures 9I–K**). In fact, as previously described (13), both T and B cells normally reside in the outer callus edge and not in the inner areas at this time point (**Figures 9A–C**). However, T cells infiltrated in large numbers in the inner callus of B cell-deficient mice, indicating a clear modification of their migratory activity. Control staining in the bone marrow of WT, T cell and B cell deficient mice, respectively (**Figures 9D,H,L**).

In order to test whether this change in lymphocyte migration also influenced the redistribution of cells of the osteoblast lineage in the callus, we stained adjacent sections for Ocn. Interestingly, no evident change in osteoblastic cell migration was visible in either T cell- or B cell-deficient mice (**Figure 10**).

This, however, could not exclude that osteoblastic function was altered in the groups of mice analyzed. In order to test this hypothesis, we stained overlapping sections for ColI. An aberrant pattern of ColI deposition was detected in T cell-deficient mice (**Figures 11C,D**), which strongly resembled what we observed in RAG1$^{-/-}$ mice (**Figures 4** and **5**). In fact, large areas of the callus were devoid of ColI in T cell-deficient mice, giving it a beehive-like appearance (**Figures 11C,D**). Furthermore, collagen did not form the characteristic thick arch of fibers that bridges the cortices across the gap (**Figures 11A,B**). Similar to what was detected using SHG microscopy on RAG1$^{-/-}$ mice fractures (**Figure 4**), the collagen was not deposited across the callus parallel to its edge in T cell-deficient mice, but rather disorderly all over the surface (**Figures 11C,D**).

On the other hand, B cell-deficient mice showed similar expression patterns in immunohistochemistry to WT controls (**Figures 11E,F**). However, large amounts of ColI were detected in the inner areas of the callus where T cells were found to abnormally infiltrate at 7 days after fracture (**Figures 11E,F** and **9I–L**).

To understand the mechanism behind the influence of the T and B cells on the collagen I deposition process, we confirmed the presence of CD8$^+$ T cells in the mouse models (WT, RAG1$^{-/-}$, TCRβδ$^{-/-}$, and JHT$^{-/-}$). CD8$^+$ T cells are present in WT and JHT animals, while they are missing in RAG1$^{-/-}$ and TCRβδ$^{-/-}$ animals (**Figure 12**). The collagen apposition is irregular in the absence of T cells and the mRNA analysis via RT-qPCR underline this abnormality in the absence of T cells (TCRβδ$^{-/-}$ and RAG1$^{-/-}$) but not in the absence of B cells (JHT$^{-/-}$) in the bone marrow. Significant difference in expression of collagen I was detected in bone marrow cells of RAG1$^{-/-}$ and TCRβδ$^{-/-}$ mice when compared to wild-type (WT). Bone markers such as osteoprotegerin (OPG), receptor activator of NF-kB ligand (RANKL), and Runt-related transcription factor 2 (RUNX2), however, were not affected (**Figure 13A**). CD8$^+$ T cells have previously been determined to have an essential impact on the bone healing process, especially in view of TNFα producers (7). Another cytokine, IL10 has been shown as an enhancer of bone healing in an anti-inflammatory context (12). These two cytokines were analyzed in conditioned medium gained from LPS-activated splenocytes of WT, RAG1$^{-/-}$, TCRβδ$^{-/-}$, and JHT$^{-/-}$ animals. Analyzing the protein expression with an ELISA assay showed differential protein expression throughout the mouse models, however, the ratio of TNFα and IL10 showed a more pro-inflammatory cytokine composition for RAG1$^{-/-}$ and TCRβδ$^{-/-}$ (**Figure 13B**). Even though this is only a fraction of the cytokine pattern that guides bone formation it could be an indication of the mechanism behind the changed collagen I deposition. To verify this, we cultivated MSCs with the conditioned medium won from JHT$^{-/-}$ and TCRβδ$^{-/-}$ splenocytes, respectively. Collagen deposition was analyzed using Sirius red staining and polarization microscopy. More collagen was deposited by MSCs cultivated with conditioned medium from JHT$^{-/-}$ splenocytes and this collagen showed a higher orientation when compared with the collagen formation under TCRβδ$^{-/-}$ conditioned medium (**Figure 13C**). These *in vitro* results are in accordance with the above shown *in vivo* results.

Overall, these data suggest that B cells can influence the migratory activity of T cells in the callus and that the latter lymphocytes are essential for normal deposition of ColI in the early stages of fracture healing.

DISCUSSION

Bone healing developed over thousands of years of evolution to a unique and highly successful process of complete regeneration. The faster stabilization observed in mice without mature T and B cells now raises the question on the role of the adaptive immune system in bone healing. A superior healing without adaptive

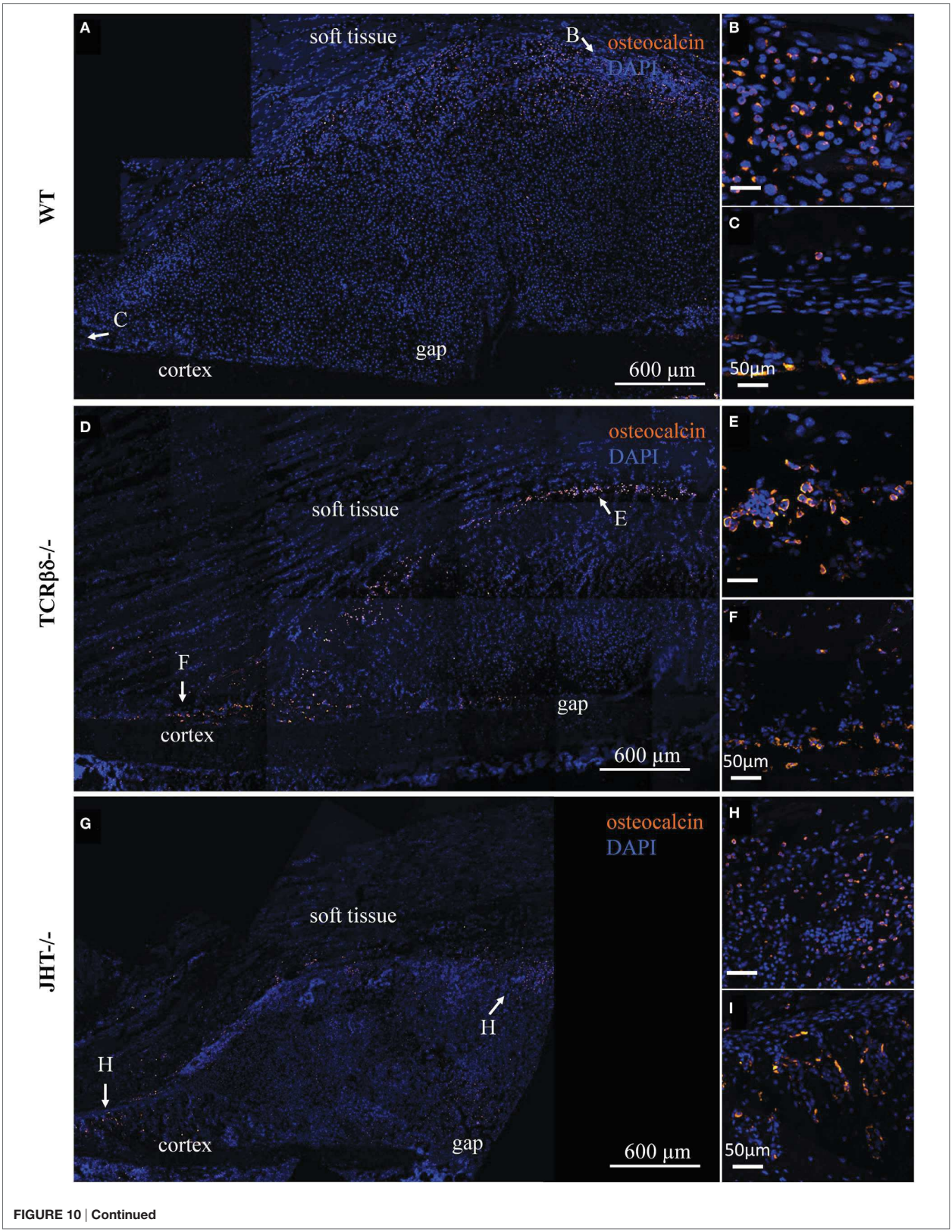

FIGURE 10 | Continued

FIGURE 10 | **Continued**
Infiltration of the soft callus by osteoblast precursors in lymphopenic mice. Confocal microscope analysis of the callus of wild-type (WT) **(A)**, T cell-deficient mice [T cell receptor β and δ chain homozygous knockout (TCRβδ$^{-/-}$)] **(D)** and B cell-deficient [joining region homozygous knockout (JHT$^{-/-}$)] **(G)** mice. Sections were stained for the osteoblast marker osteocalcin (orange) and cell nuclei (DAPI, blue). Letters near the white arrows indicate areas that are magnified in the corresponding panels to the right **(B,C,E,F,H,I)**. All sections were taken 7 days after fracture.

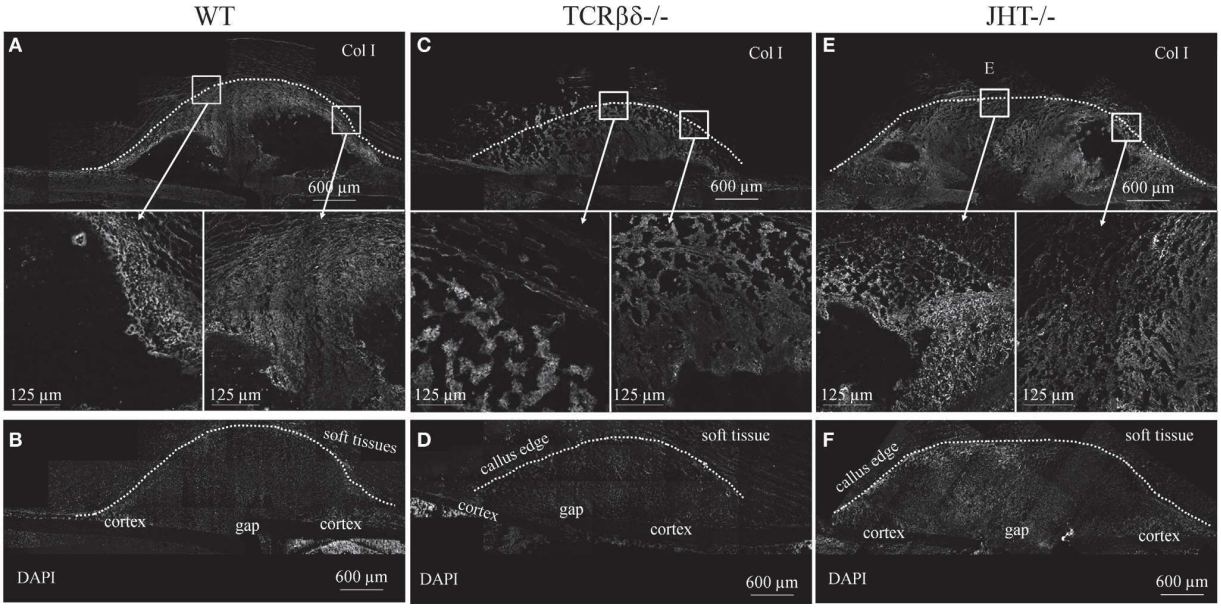

FIGURE 11 | **Aberrant deposition of collagen type I (Coll) in the soft callus of T cell-deficient mice**. Confocal microscope analysis of the callus of wild-type (WT) **(A,B)**, T cell-deficient [T cell receptor β and δ chain homozygous knockout (TCRβδ$^{-/-}$)] **(C,D)** and B cell-deficient [joining region homozygous knockout (JHT$^{-/-}$)] **(E,F)** mice. Sections were stained for the Coll (gray). Areas within the white rectangles are represented below in a higher magnification. **(B,D,F)** show DAPI staining of cell nuclei to highlight the cellular topography corresponding to calluses displayed in **(A,C,E)**, respectively. Soft tissues are visible due to their strong autofluorescence. All sections were taken 7 days after fracture.

immunity seems unlikely as it has evolved within nature's selective evolutionary process. Therefore, we aimed to understand the distinct role adaptive immunity plays in the healing cascade. Why would the apparently retarded immune-mediated healing process be beneficial over the faster healing in the absence of T and B cells? The major changes detected during the healing process without mature T and B cells concerned the faster cartilage mineralization. The deposition of cartilage to bridge the fractured bone offers at least three advantages. First, cartilage can be quickly synthesized to bridge the fracture. Second, —the intermediate cartilage tissue offers the possibility to increase the radius of the bone in the area of injury. Considering the fact that stability increases with the fourth power of the radius increase (28), this is a significant advantage. This phenomenon can be observed in the cases of insufficient fracture stabilization, where a larger callus develops when compared to a stable fixed fracture (29)—an attempt of the body to provide stability. Third, the mechanical properties of the proteins in cartilage tissue. Type II collagen offers tensile strength, while proteoglycans and ECM provide compressive strength (30)—together resulting in a fast recovery of function of the injured bone. For bone healing, the important step of intermediate cartilage formation is still intact in lymphopenic RAG1$^{-/-}$ mice. However, in these animals the subsequent degradation and mineralization of the cartilage were altered, with accelerated mineralization visible at D7 of healing, whereas, in the WT, hyaline cartilage was still predominant (**Figure 2**). The same faster kinetics was seen in animals lacking T cells but not in those devoid of only B cells. Thus, this discussion concentrates on the effect of T cells in the bone healing process.

Previous studies on fracture healing in lymphopenic RAG1$^{-/-}$ mice showed a faster callus formation resulting in quicker bridging and earlier mechanical stability when compared to WT mice, which showed that mature T and B cells are involved in the process (4). Discrepant mechanical characteristics were seen when bone grew with and without B and T cells. The RAG1$^{-/-}$ animals showed stiffer and more brittle bone with less ability to bend and deform when compared to WT bone. This indicates the impact of T and B cells on matrix organization and formation and thus their role in determining bone quality such as the elasticity allowing bone to absorb forces upon impact, thus preventing fractures. The microarray data showed that vitamin D-related gene (Dbp) is upregulated only at D7 and D14 in RAG1$^{-/-}$ compared to WT. Dbp is correlated with T cell proliferation and involved in

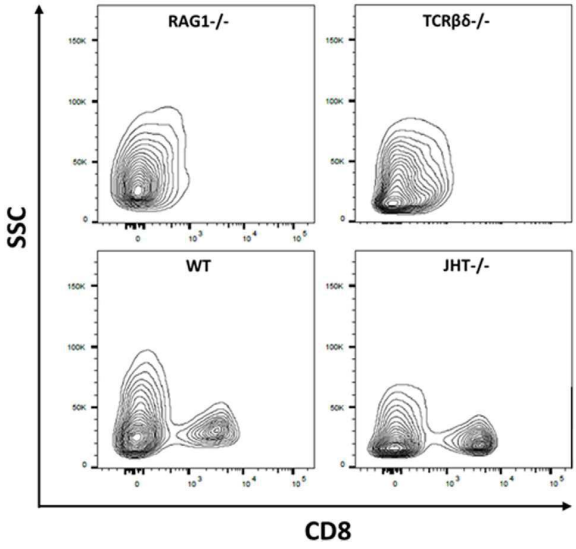

FIGURE 12 | Cellular composition of wild-type (WT), recombination activating gene 1 homozygous knockout (RAG1$^{-/-}$), T cell receptor β and δ chain homozygous knockout (TCRβδ$^{-/-}$), and joining region homozygous knockout (JHT$^{-/-}$) mice. Flow cytometry was used to determine whether CD8$^+$ T cells are present in the mouse strains used in this analysis. CD8$^+$ T cells have been shown to impact bone healing (7). While RAG1$^{-/-}$ and TCRβδ$^{-/-}$ lacked CD8$^+$ T cells these cells were present in WT and JHT$^{-/-}$ animals. Gating: lymphocytes, single cells, live cells, CD45-positive cells, CD3-positive cells, and CD8-positive cells.

maintaining the BMD, which supports the decrease in bone quality under the lack of mature T cell.

Faster mineralization in RAG1$^{-/-}$ mice was apparently contradicted by its defective ColI deposition and displacement of Ocn-positive cells in the callus periphery. ColI is the marker ECM molecule of bone, and Ocn is seen as a marker protein for osteoblasts. Therefore, the lack of mature T and B cells has altered two major contributors to bone formation in the RAG1$^{-/-}$ mice. The GBA analysis correlated Spp1, Ctsk, Bglap, Col1a1, and Igf1. Along with the upregulation of Col1a1 at D3 through D7, D14 until D21 those genes suggest the earlier start of mineralization and end of bone formation in the RAG1$^{-/-}$. The osteoclasts, bone cells important for the bone homeostasis and healing as bone degrading cells, showed no differences in numbers up to day 14 of healing. The changes in collagen I deposition found in our analysis are, therefore, not considered connected to an altered osteoclast function. In addition, our analyses of gene expression in bone marrow cells in mice lacking T cells (TCRβδ$^{-/-}$) or B cells (JHT$^{-/-}$) or mature T and B cells (RAG$^{-/-}$) showed no significant difference for OPG and RANKL, both factors involved in osteoclastogenesis.

During endochondral ossification in WT, mineralization starts in the cartilaginous layer with chondrocytes shifting from ColII toward ColX expression. Chondrocytes become hypertrophic and express a number of ECM proteins including osteonectin, fibronectin, and osteopontin (31–33). At this stage, chondrocytes actively express alkaline phosphatase-rich matrix vesicles that are associated with matrix mineralization (34, 35).

Even today tissue mineralization during bone formation is not fully understood (36) but evidence is increasing that mineralization *per se* is not a challenge [as illustrated by ectopic bone formation (37–39), fibrodysplasia ossificans progressiva, or uncontrolled bone formation after limb amputation (40)]. For healthy functional bone to form and to harbor the best quality to withstand strains and stresses of daily life, a controlled, structure-optimizing, and directed bone formation is key to success. Immune cells seem to play an important role in this process (7, 13, 41).

Immune cells are present during the various phases of bone healing (13) (Figure S3 in Supplementary Material). T cells are able to migrate into and through the ECM (42, 43), a process dependent on integrins and actin–myosin activity. Motile cells are thought to be important for the structure of the ECM (44), which is constantly being reorganized in young, transitional tissue, only becoming more stable in mature tissues (45). The major function of the ECM is to provide structural support for cells and tissues, but it is also a storage for growth factors [transforming growth factor β (TGFβ), BMPs, fibroblast growth factor, and insulin-like growth factor] and thus is involved in regulating their bioavailability and in modulating growth signaling events (44). Integrins expressed on T cells can release TGFβ from the ECM *via* their RGD motif (46). With TGFβ being a known regulator of bone formation (47) this indicates the importance of T cells in regulating the bone forming process. Comparing WT and RAG1$^{-/-}$ animal bone healing we saw a faster callus formation from cartilage in the RAG1$^{-/-}$ animals indicating an earlier change toward hypertrophic chondrocytes. TGFβ decreases chondrocyte hypertrophy (48), which could explain the faster maturation in RAG1$^{-/-}$ animals, where TGFβ would be bound in the ECM because the release through T cell action is missing. Another factor which could be responsible for the faster mineralization could be the downregulation of osteopontin (OPN/SPP1) in the RAG1$^{-/-}$ animals. OPN has been reported to inhibit the mineral crystal growth (49) and with a downregulation of OPN being observed in the RAG1$^{-/-}$ animals this could lead to faster callus mineralization. Furthermore, without T cells, TNFα in the fracture callus would be lowered. This pro-inflammatory cytokine has been reported to suppress the expression of bone sialoprotein (BSP) (50). BSP is a crystal nucleator for hydroxyapatite and upon binding of BSP to ColI calcium deposition increases 10-fold (51). Lower TNFα in RAG1$^{-/-}$ animals would cause higher BSP expression and thus increase the calcium deposition on present ColI fibers. Indeed, the data showed lower expression of tumor necrosis factor receptor superfamily, member 11a, NFKB activator, when compared to the WT at D3 and D7 ($p = 0.0102$ and $p = 0.0071$, respectively). The above are some explanations on how the regulation of T cells impacts matrix mineralization and concurs with our results in animals lacking mature T and B cells. T cells appear to affect cartilage mineralization by slowing the process itself down (when compared to lymphopenic mice), giving matrix organization and mineral deposition adequate time to enable callus structure to concomitant mechanical strains.

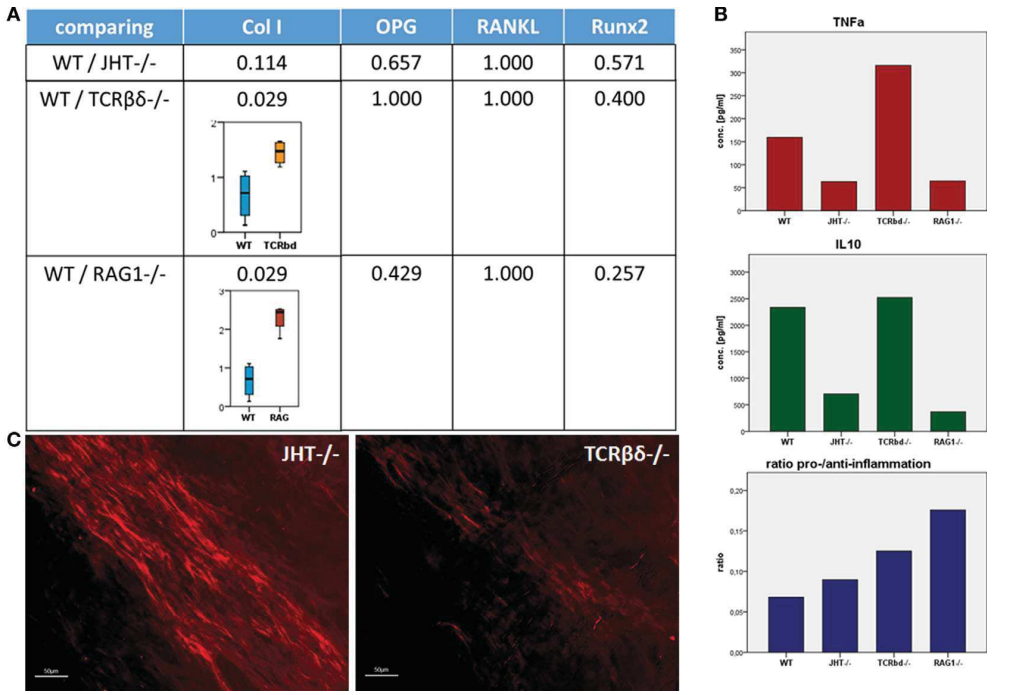

FIGURE 13 | Collagen I deposition is irregular in recombination activating gene 1 homozygous knockout (RAG1$^{-/-}$) and T cell receptor β and δ chain homozygous knockout (TCRβδ$^{-/-}$) mice. **(A)** Using quantitative reverse transcription polymerase chain reaction a significant difference in expression of collagen I was detected in bone marrow cells of RAG1$^{-/-}$ and TCRβδ$^{-/-}$ mice when compared to wild-type (WT). Bone markers such as osteoprotegerin (OPG), receptor activator of NF-kB ligand (RANKL), and Runt-related transcription factor 2 (RUNX2), however, were not affected. **(B)** Splenocytes were activated with LPS, and conditioned medium was analyzed to determine pro-inflammatory (TNFα) and anti-inflammatory (interleukin 10) cytokines. While these factors showed no correlation in itself, the ratio of pro- and anti-inflammatory signals showed higher pro-inflammatory signaling in RAG1$^{-/-}$ and TCRβδ$^{-/-}$ when compared to WT and JHT$^{-/-}$. This indicates an influence of the cytokine pattern of T and B cells on the bone forming process. **(C)** Conditioned medium was added in an *in vitro* assay of mesenchymal stem cells (MSCs), and collagen deposition was analyzed using a Sirius red staining and polarization microscopy. Collagen deposition by MSCs cultivated with conditioned medium of JHT$^{-/-}$ splenocytes showed a stronger and more regular orientation than collagen deposition of MSCs cultivated with conditioned medium of TCRβδ$^{-/-}$ splenocytes.

In the RAG1$^{-/-}$ animals, we detected lower Ocn expression in the fracture callus. With Ocn binding to hydroxyapatite this could indicate a disturbed bone healing, however, Ocn knockout animals only show a mild bone phenotype and prove that mineralization without Ocn is still possible (52). Ocn, however, is also a marker for osteoblasts and the altered distribution of these cells in the RAG1$^{-/-}$ animal fracture callus indicates another role for T cells in the bone healing process. T cells seem to be essential for osteoblast maturation. Expression of IL17F and wingless-type MMTV integration site family, member 10B by T cells has been reported to be essential in the osteoblasts maturation process (10, 53). The close spatial proximity observed between T and B cells and osteoprogenitors in the bone marrow previously reported from our group (13) is another confirmation for the interdependency of these cells. It cannot be excluded that T cell-specific surface molecules like CTLA-4 (12) and its ligands CD80 and CD86 on the surface of osteoblasts (54) might be involved. It could be argued that our result depends on an indirect effect on B cells due to the lack of CD40-CD40L engagement between these and T cells. This pathway has been shown to be important for bone homeostasis (55). However, if this was the case, the phenotype of T cell- and B cell-deficient mice should have overlapped. Still, it has been shown that murine primary osteoblasts do express CD40 and that its engagement protects them from TNFα-induced apoptosis (56). It seems conceivable that lack of CD40-CD40L engagement between T cells and osteoblast precursors would have a major effect on ColI deposition by these cells in the soft callus.

The curious finding that Ocn-positive cells line up on the outside of the RAG1$^{-/-}$ fracture callus could be an indication of another function of immune cells during the bone healing process. Previous studies showed that the lymphatic draining in the injured bone is activated upon fracture and that prolonged lymphonodal activity is associated with successful healing (57, 58). Ocn -positive cells accumulate in the peripheral blood after an injury (59) and osteoblastic precursors have been reported to invade fractured bone *via* blood vessels (60). However, it is unclear whether osteoblast precursors, which reach the callus from vasculature of the surrounding soft tissues (**Figure 2**), require interaction with lymphocytes in secondary lymphoid organs or *in situ* for proper trafficking. Further studies should be carried out to elucidate the complete mobilization pathway of these cells

during bone repair. This is in accordance with the upregulation of VEGF and the downregulation of Serpinf1 as seen at D7 and D14, which both play a role in osteoblast regulation (61).

To partake in the healing process, osteoblastic cells would be required to invade the fracture side which directly after the injury would be filled with a hematoma. The hematoma has an unfavorable milieu for cells to survive and being active due to the low oxygen levels, lower pH value, and higher Na^+ and K^+ values (62–64), however, immune cells, including T cells, are able to survive and thrive in this surrounding (65). Therefore, the immune cells are essential for the chemoattractant pattern responsible for cell recruitment during this early stage of healing (66). Among those cells recruited during early healing phases are again immune cells, including T cells. With the above finding, it can be hypothesized that T cells are essential players in orchestrating the matrix forming osteoblasts, specifically in the phase of endochondral ossification. With T cells missing at this early stage the cellular composition during initiation of healing is altered, the ECM that is formed and necessary for cell invasion is, therefore, different and perhaps is no longer favorable for invasion of Ocn-positive cells. This would indicate that an important source of osteoblast precursors cannot be accessed in mature T- and B cell deficient mice. The Ocn-postive cells stay lined up outside of the fracture callus.

CONCLUSION

This work for the first time presents a direct link between immune cells and matrix formation during regeneration using bone healing as an example. It illustrates specifically the role of T cells in the collagen organization process and the lack thereof in the absence of T cells.

The importance of immune cells during the fracture healing process has already been established. Here, we show that immune cells play an essential part in the regulation of the mineralization in endochondral ossification, which is necessary to generate bone with an elastic quality able to withstand forces. In detail, immune cells are needed to slow down the mineralization process in order to build quality bone, and immune cells are needed to recruit osteogenic precursors and aid their differentiation.

Even though callus formation in itself is faster without T and B cells the ensuing bone callus and organ tissue do not have the sufficient quality and thus functionality that is achieved when these immune cells take their active role in the bone organization and formation process.

ETHICS STATEMENT

This study was carried out in accordance with the recommendations of the Animal Welfare Act, the National Institutes of Health Guide for Care and Use of Laboratory Animals, and the National Animal Welfare Guidelines and was approved by the local legal representative animal rights protection authorities: Landesamt für Gesundheit und Soziales Berlin. The protocol was approved by the Landesamt für Gesundheit und Soziales Berlin: G 0206/08.

AUTHOR CONTRIBUTIONS

TK contributed data acquisition: data evaluation, study design, and manuscript writing; AS contributed data acquisition: histology, data evaluation, and manuscript writing; AP contributed data acquisition: second harmonic imaging and manuscript writing; CB contributed data acquisition: biomechanics, cell culture, and data evaluation; CS contributed data acquisition: histology and manuscript writing; IK contributed data acquisition: histology, data evaluation, and study design; DM contributed data acquisition: data evaluation; SW contributed data acquisition: in cell culture and ELISA, data evaluation, and manuscript writing; HS contributed study design, manuscript writing; H-DV contributed to study design and manuscript writing; KS-B contributed data acquisition: biomechanics study design, data evaluation, and manuscript writing; GD contributed study design and manuscript writing.

ACKNOWLEDGMENTS

We would like to acknowledge Norma Schulz, Dag Wulsten, Daniel Toben, and Jan Frisch for their excellent assistance.

FUNDING

This study was funded by the DFG (SCHE 1594, SCHM 2977, DU 298/22) and the BCRT. Thaqif El Khassawna and Deeksha Malhan are funded by the SFB TRR 79 Subproject 1.

SUPPLEMENTARY MATERIAL

The Supplementary Material for this article can be found online at http://journal.frontiersin.org/article/10.3389/fimmu.2017.00562/full#supplementary-material.

REFERENCES

1. Einhorn TA. The cell and molecular biology of fracture healing. *Clin Orthop Relat Res* (1998) (355 Suppl):S7–21. doi:10.1097/00003086-199810001-00003
2. Mundi R, Bhandari M. Devastating impact of fracture nonunions: the need for timely identification and intervention for high-risk patients: commentary on an article by Patrick C. Schottel, MD, et al.: "time trade-off as a measure of health-related quality of life: long bone nonunions have a devastating impact". *J Bone Joint Surg Am* (2015) 97:e62. doi:10.2106/JBJS.O.00722
3. Schmidt-Bleek K, Petersen A, Dienelt A, Schwarz C, Duda GN. Initiation and early control of tissue regeneration – bone healing as a model system for tissue regeneration. *Expert Opin Biol Ther* (2014) 14:247–59. doi:10.1517/14712598.2014.857653
4. Toben D, Schroeder I, El Khassawna T, Mehta M, Hoffmann JE, Frisch JT, et al. Fracture healing is accelerated in the absence of the adaptive immune system. *J Bone Miner Res* (2011) 26:113–24. doi:10.1002/jbmr.185
5. Kong YY, Feige U, Sarosi I, Bolon B, Tafuri A, Morony S, et al. Activated T cells regulate bone loss and joint destruction in adjuvant arthritis through osteoprotegerin ligand. *Nature* (1999) 402:304–9. doi:10.1038/46303
6. Pacifici R. Role of T cells in ovariectomy induced bone loss – revisited. *J Bone Miner Res* (2012) 27:231–9. doi:10.1002/jbmr.1500
7. Reinke S, Geissler S, Taylor WR, Schmidt-Bleek K, Juelke K, Schwachmeyer V, et al. Terminally differentiated CD8+ T cells negatively affect bone regeneration

in humans. *Sci Transl Med* (2013) 5:177ra136. doi:10.1126/scitranslmed.3004754
8. Claes L, Recknagel S, Ignatius A. Fracture healing under healthy and inflammatory conditions. *Nat Rev Rheumatol* (2012) 8:133–43. doi:10.1038/nrrheum.2012.1
9. Wu AC, Raggatt LJ, Alexander KA, Pettit AR. Unraveling macrophage contributions to bone repair. *Bonekey Rep* (2013) 2:373. doi:10.1038/bonekey.2013.107
10. Nam D, Mau E, Wang Y, Wright D, Silkstone D, Whetstone H, et al. T-lymphocytes enable osteoblast maturation via IL-17F during the early phase of fracture repair. *PLoS One* (2012) 7:e40044. doi:10.1371/journal.pone.0040044
11. Zaiss MM, Axmann R, Zwerina J, Polzer K, Guckel E, Skapenko A, et al. Treg cells suppress osteoclast formation: a new link between the immune system and bone. *Arthritis Rheum* (2007) 56:4104–12. doi:10.1002/art.23138
12. Liu Y, Wang L, Kikuiri T, Akiyama K, Chen C, Xu X, et al. Mesenchymal stem cell-based tissue regeneration is governed by recipient T lymphocytes via IFN-gamma and TNF-alpha. *Nat Med* (2011) 17:1594–601. doi:10.1038/nm.2542
13. Konnecke I, Serra A, El Khassawna T, Schlundt C, Schell H, Hauser A, et al. T and B cells participate in bone repair by infiltrating the fracture callus in a two-wave fashion. *Bone* (2014) 64:155–65. doi:10.1016/j.bone.2014.03.052
14. Mombaerts P, Iacomini J, Johnson RS, Herrup K, Tonegawa S, Papaioannou VE. RAG-1-deficient mice have no mature B and T lymphocytes. *Cell* (1992) 68:869–77. doi:10.1016/0092-8674(92)90030-G
15. Bonnarens F, Einhorn TA. Production of a standard closed fracture in laboratory animal bone. *J Orthop Res* (1984) 2:97–101. doi:10.1002/jor.1100020115
16. Mombaerts P, Clarke AR, Rudnicki MA, Iacomini J, Itohara S, Lafaille JJ, et al. Mutations in T-cell antigen receptor genes alpha and beta block thymocyte development at different stages. *Nature* (1992) 360:225–31. doi:10.1038/360225a0
17. Chen J, Trounstine M, Alt FW, Young F, Kurahara C, Loring JF, et al. Immunoglobulin gene rearrangement in B cell deficient mice generated by targeted deletion of the JH locus. *Int Immunol* (1993) 5:647–56. doi:10.1093/intimm/5.6.647
18. Hildebrand T, Ruegsegger P. Quantification of bone microarchitecture with the structure model index. *Comput Methods Biomech Biomed Engin* (1997) 1:15–23. doi:10.1080/01495739708936692
19. El Khassawna T, Toben D, Kolanczyk M, Schmidt-Bleek K, Koennecke I, Schell H, et al. Deterioration of fracture healing in the mouse model of NF1 long bone dysplasia. *Bone* (2012) 51:651–60. doi:10.1016/j.bone.2012.07.011
20. Roth S, Freund I. Second harmonic-generation in collagen. *J Chem Phys* (1979) 70:1637–43. doi:10.1063/1.437677
21. Williams RM, Zipfel WR, Webb WW. Interpreting second-harmonic generation images of collagen I fibrils. *Biophys J* (2005) 88:1377–86. doi:10.1529/biophysj.104.047308
22. Team V, Canaway R, Manderson L. Integration of complementary and alternative medicine information and advice in chronic disease management guidelines. *Aust J Prim Health* (2011) 17:142–9. doi:10.1071/PY10013
23. Dunning MJ, Smith ML, Ritchie ME, Tavare S. beadarray: R classes and methods for Illumina bead-based data. *Bioinformatics* (2007) 23:2183–4. doi:10.1093/bioinformatics/btm311
24. Gentleman RC, Carey VJ, Bates DM, Bolstad B, Dettling M, Dudoit S, et al. Bioconductor: open software development for computational biology and bioinformatics. *Genome Biol* (2004) 5:R80. doi:10.1186/gb-2004-5-10-r80
25. Smyth GK, Michaud J, Scott HS. Use of within-array replicate spots for assessing differential expression in microarray experiments. *Bioinformatics* (2005) 21:2067–75. doi:10.1093/bioinformatics/bti270
26. Mammoto T, Mammoto A, Torisawa YS, Tat T, Gibbs A, Derda R, et al. Mechanochemical control of mesenchymal condensation and embryonic tooth organ formation. *Dev Cell* (2011) 21:758–69. doi:10.1016/j.devcel.2011.07.006
27. Bates EE, Ravel O, Dieu MC, Ho S, Guret C, Bridon JM, et al. Identification and analysis of a novel member of the ubiquitin family expressed in dendritic cells and mature B cells. *Eur J Immunol* (1997) 27:2471–7. doi:10.1002/eji.1830271002
28. Chan TY, Davidson T. Femoral nerve block after intra-operative subcutaneous bupivacaine injection. *Anaesthesia* (1990) 45:163–4. doi:10.1111/j.1365-2044.1990.tb14289.x
29. Mehta M, Strube P, Peters A, Perka C, Hutmacher D, Fratzl P, et al. Influences of age and mechanical stability on volume, microstructure, and mineralization of the fracture callus during bone healing: is osteoclast activity the key to age-related impaired healing? *Bone* (2010) 47:219–28. doi:10.1016/j.bone.2010.05.029
30. Carroll R. The shoulder. In: Wiesel S, Delahay J, editors. *Essentials of Orthopedic Surgery*. New York: Springer (2007). p. 333–63.
31. Horton WA, Machado MM. Extracellular matrix alterations during endochondral ossification in humans. *J Orthop Res* (1988) 6:793–803. doi:10.1002/jor.1100060603
32. Mark MP, Butler WT, Prince CW, Finkelman RD, Ruch JV. Developmental expression of 44-kDa bone phosphoprotein (osteopontin) and bone gamma-carboxyglutamic acid (Gla)-containing protein (osteocalcin) in calcifying tissues of rat. *Differentiation* (1988) 37:123–36. doi:10.1111/j.1432-0436.1988.tb00804.x
33. Pacifici M, Oshima O, Fisher LW, Young MF, Shapiro IM, Leboy PS. Changes in osteonectin distribution and levels are associated with mineralization of the chicken tibial growth cartilage. *Calcif Tissue Int* (1990) 47:51–61. doi:10.1007/BF02555866
34. Anderson HC. Electron microscopic studies of induced cartilage development and calcification. *J Cell Biol* (1967) 35:81–101. doi:10.1083/jcb.35.1.81
35. Bonucci E. Fine structure of early cartilage calcification. *J Ultrastruct Res* (1967) 20:33–50. doi:10.1016/S0022-5320(67)80034-0
36. Hashimoto A, Yamaguchi Y, Chiu LD, Morimoto C, Fujita K, Takedachi M, et al. Time-lapse Raman imaging of osteoblast differentiation. *Sci Rep* (2015) 5:12529. doi:10.1038/srep12529
37. Muheim G, Donath A, Rossier AB. Serial scintigrams in the course of ectopic bone formation in paraplegic patients. *Am J Roentgenol Radium Ther Nucl Med* (1973) 118:865–9. doi:10.2214/ajr.118.4.865
38. Bakker XR, Nicolai JP. Ectopic bone formation after temporal muscle transposition for facial paralysis. *Plast Reconstr Surg* (2000) 105:2079–81. doi:10.1097/00006534-200005000-00023
39. Franz M, Berndt A, Wehrhan F, Schleier P, Clement J, Hyckel P. Ectopic bone formation as a complication of surgical rehabilitation in patients with Moebius' syndrome. *J Craniomaxillofac Surg* (2007) 35:252–7. doi:10.1016/j.jcms.2007.05.002
40. Dudek NL, Dehaan MN, Marks MB. Bone overgrowth in the adult traumatic amputee. *Am J Phys Med Rehabil* (2003) 82:897–900. doi:10.1097/01.PHM.0000087459.94599.2D
41. Schmidt-Bleek K, Kwee BJ, Mooney DJ, Duda GN. Boon and bane of inflammation in bone tissue regeneration and its link with angiogenesis. *Tissue Eng Part B Rev* (2015) 21(4):354–64. doi:10.1089/ten.TEB.2014.0677
42. Ivanoff J, Talme T, Sundqvist KG. The role of chemokines and extracellular matrix components in the migration of T lymphocytes into three-dimensional substrata. *Immunology* (2005) 114:53–62. doi:10.1111/j.1365-2567.2004.02005.x
43. Overstreet MG, Gaylo A, Angermann BR, Hughson A, Hyun YM, Lambert K, et al. Inflammation-induced interstitial migration of effector CD4(+) T cells is dependent on integrin alphaV. *Nat Immunol* (2013) 14:949–58. doi:10.1038/ni.2682
44. Dallas SL, Chen Q, Sivakumar P. Dynamics of assembly and reorganization of extracellular matrix proteins. *Curr Top Dev Biol* (2006) 75:1–24. doi:10.1016/S0070-2153(06)75001-3
45. Dallas SL. Dynamics of bone extracellular matrix assembly and mineralization. *J Musculoskelet Neuronal Interact* (2006) 6:370–1.
46. Yang Z, Mu Z, Dabovic B, Jurukovski V, Yu D, Sung J, et al. Absence of integrin-mediated TGFbeta1 activation in vivo recapitulates the phenotype of TGFbeta1-null mice. *J Cell Biol* (2007) 176:787–93. doi:10.1083/jcb.200611044
47. Rahman MS, Akhtar N, Jamil HM, Banik RS, Asaduzzaman SM. TGF-beta/BMP signaling and other molecular events: regulation of osteoblastogenesis and bone formation. *Bone Res* (2015) 3:15005. doi:10.1038/boneres.2015.5
48. Iwamoto M, Yagami K, Shapiro IM, Leboy PS, Adams SL, Pacifici M. Retinoic acid is a major regulator of chondrocyte maturation and matrix mineralization. *Microsc Res Tech* (1994) 28:483–91. doi:10.1002/jemt.1070280604
49. Gericke A, Qin C, Spevak L, Fujimoto Y, Butler WT, Sorensen ES, et al. Importance of phosphorylation for osteopontin regulation of biomineralization. *Calcif Tissue Int* (2005) 77:45–54. doi:10.1007/s00223-004-1288-1
50. Samoto H, Shimizu E, Matsuda-Honjo Y, Saito R, Yamazaki M, Kasai K, et al. TNF-alpha suppresses bone sialoprotein (BSP) expression in ROS17/2.8 cells. *J Cell Biochem* (2002) 87:313–23. doi:10.1002/jcb.10301

51. Gorski JP. Biomineralization of bone: a fresh view of the roles of non-collagenous proteins. *Front Biosci (Landmark Ed)* (2011) 16:2598–621. doi:10.2741/3875
52. Ducy P, Desbois C, Boyce B, Pinero G, Story B, Dunstan C, et al. Increased bone formation in osteocalcin-deficient mice. *Nature* (1996) 382:448–52. doi:10.1038/382448a0
53. Geginat J, Sallusto F, Lanzavecchia A. Cytokine-driven proliferation and differentiation of human naive, central memory, and effector memory CD4(+) T cells. *J Exp Med* (2001) 194:1711–9. doi:10.1084/jem.194.12.1711
54. Reyes-Botella C, Montes MJ, Vallecillo-Capilla MF, Olivares EG, Ruiz C. Antigenic phenotype of cultured human osteoblast-like cells. *Cell Physiol Biochem* (2002) 12:359–64. doi:10.1159/000067905
55. Li Y, Toraldo G, Li A, Yang X, Zhang H, Qian WP, et al. B cells and T cells are critical for the preservation of bone homeostasis and attainment of peak bone mass in vivo. *Blood* (2007) 109:3839–48. doi:10.1182/blood-2006-07-037994
56. Ahuja SS, Zhao S, Bellido T, Plotkin LI, Jimenez F, Bonewald LF. CD40 ligand blocks apoptosis induced by tumor necrosis factor alpha, glucocorticoids, and etoposide in osteoblasts and the osteocyte-like cell line murine long bone osteocyte-Y4. *Endocrinology* (2003) 144:1761–9. doi:10.1210/en.2002-221136
57. Szczesny G, Olszewski WL, Gorecki A. Lymphoscintigraphic monitoring of the lower limb lymphatic system response to bone fracture and healing. *Lymphat Res Biol* (2005) 3:137–45. doi:10.1089/lrb.2005.3.137
58. Szczesny G, Olszewski WL, Gewartowska M, Zaleska M, Gorecki A. The healing of tibial fracture and response of the local lymphatic system. *J Trauma* (2007) 63:849–54. doi:10.1097/01.ta.0000236641.51515.8f
59. Yang X, Tao XA, Liang JQ, Huang YJ, Yang XP. The dynamic changes of circulating OCN+ cells versus insulin-like growth factor-I during primary healing of orthognathic surgeries. *Oral Surg Oral Med Oral Pathol Oral Radiol* (2012) 113:734–40. doi:10.1016/j.tripleo.2011.05.044
60. Maes C, Kobayashi T, Selig MK, Torrekens S, Roth SI, Mackem S, et al. Osteoblast precursors, but not mature osteoblasts, move into developing and fractured bones along with invading blood vessels. *Dev Cell* (2010) 19:329–44. doi:10.1016/j.devcel.2010.07.010
61. Liu Y, Berendsen AD, Jia S, Lotinun S, Baron R, Ferrara N, et al. Intracellular VEGF regulates the balance between osteoblast and adipocyte differentiation. *J Clin Invest* (2012) 122:3101–13. doi:10.1172/JCI61209
62. Street J, Winter D, Wang JH, Wakai A, Mcguinness A, Redmond HP. Is human fracture hematoma inherently angiogenic? *Clin Orthop Relat Res* (2000) (378):224–37. doi:10.1097/00003086-200009000-00033
63. Kolar P, Schmidt-Bleek K, Schell H, Gaber T, Toben D, Schmidmaier G, et al. The early fracture hematoma and its potential role in fracture healing. *Tissue Eng Part B Rev* (2010) 16:427–34. doi:10.1089/ten.TEB.2009.0687
64. Kolar P, Gaber T, Perka C, Duda GN, Buttgereit F. Human early fracture hematoma is characterized by inflammation and hypoxia. *Clin Orthop Relat Res* (2011) 469:3118–26. doi:10.1007/s11999-011-1865-3
65. Gaber T, Haupl T, Sandig G, Tykwinska K, Fangradt M, Tschirschmann M, et al. Adaptation of human CD4+ T cells to pathophysiological hypoxia: a transcriptome analysis. *J Rheumatol* (2009) 36:2655–69. doi:10.3899/jrheum.090255
66. Yellowley C. CXCL12/CXCR4 signaling and other recruitment and homing pathways in fracture repair. *Bonekey Rep* (2013) 2:300. doi:10.1038/bonekey.2013.34

Conflict of Interest Statement: The authors declare that the research was conducted in the absence of any commercial or financial relationships that could be construed as a potential conflict of interest.

Publication 2: Experience in the Adaptive Immunity Impacts Bone Homeostasis, Remodeling, and Healing

Christian H. Bucher, Claudia Schlundt, Dag Wulsten, F. Andrea Sass, Sebastian Wendler, Agnes Ellinghaus, Tobias Thiele, Ricarda Seemann, Bettina M. Willie, Hans-Dieter Volk, Georg N. Duda, Katharina Schmidt-Bleek, *Experience in the Adaptive Immunity Impacts Bone Homeostasis, Remodeling, and Healing*, Frontiers in Immunology, 2019

Auszug aus der Journal Summary List

Journal Data Filtered By: **Selected JCR Year: 2017** Selected Editions: SCIE,SSCI
Selected Categories: "**Immunology**" Selected Category Scheme: WoS
Gesamtanzahl: 155 Journale

Rank	Full Journal Title	Total Cites	Journal Impact Factor	Eigenfactor Score
1	NATURE REVIEWS IMMUNOLOGY	39,215	41.982	0.085360
2	Annual Review of Immunology	17,086	22.714	0.028800
3	NATURE IMMUNOLOGY	41,410	21.809	0.102290
4	IMMUNITY	46,541	19.734	0.136360
5	TRENDS IN IMMUNOLOGY	11,204	14.188	0.026850
6	JOURNAL OF ALLERGY AND CLINICAL IMMUNOLOGY	49,229	13.258	0.083800
7	Lancet HIV	1,476	11.355	0.007950
8	JOURNAL OF EXPERIMENTAL MEDICINE	62,537	10.790	0.078310
9	IMMUNOLOGICAL REVIEWS	14,555	9.217	0.028540
10	Cancer Immunology Research	4,361	9.188	0.021180
11	CLINICAL INFECTIOUS DISEASES	61,618	9.117	0.120010
12	AUTOIMMUNITY REVIEWS	8,956	8.745	0.020990
13	Journal for ImmunoTherapy of Cancer	1,675	8.374	0.007130
14	CURRENT OPINION IN IMMUNOLOGY	9,275	7.932	0.020120
15	JOURNAL OF AUTOIMMUNITY	6,410	7.607	0.015490
16	Cellular & Molecular Immunology	3,633	7.551	0.008300
17	EMERGING INFECTIOUS DISEASES	29,657	7.422	0.057980
18	Mucosal Immunology	6,105	7.360	0.021860
19	SEMINARS IN IMMUNOLOGY	4,552	7.206	0.010950
20	EXERCISE IMMUNOLOGY REVIEW	740	7.105	0.001110
21	Journal of Allergy and Clinical Immunology-In Practice	2,802	6.966	0.009670
22	CLINICAL REVIEWS IN ALLERGY & IMMUNOLOGY	2,741	6.442	0.005880
23	Seminars in Immunopathology	2,967	6.437	0.009290
24	BRAIN BEHAVIOR AND IMMUNITY	12,583	6.306	0.026850
25	ALLERGY	16,476	6.048	0.025790
26	Emerging Microbes & Infections	1,318	6.032	0.005910
27	Advances in Immunology	2,423	5.935	0.004250
28	Current Topics in Microbiology and Immunology	5,633	5.829	0.011740
29	World Allergy Organization Journal	1,352	5.676	0.003800
30	Frontiers in Immunology	16,999	5.511	0.067470

frontiers in Immunology

ORIGINAL RESEARCH
published: 12 April 2019
doi: 10.3389/fimmu.2019.00797

Experience in the Adaptive Immunity Impacts Bone Homeostasis, Remodeling, and Healing

Christian H. Bucher[1,2], Claudia Schlundt[1,2], Dag Wulsten[1], F. Andrea Sass[1,2], Sebastian Wendler[1,2], Agnes Ellinghaus[1], Tobias Thiele[1], Ricarda Seemann[1], Bettina M. Willie[3], Hans-Dieter Volk[2,4], Georg N. Duda[1,2,5†] and Katharina Schmidt-Bleek[1,2†]*

[1] Julius Wolff Institute and Center for Musculoskeletal Surgery, Charité — Universitätsmedizin Berlin, Berlin, Germany, [2] Berlin-Brandenburg Center for Regenerative Therapies, Charité — Universitätsmedizin Berlin, Berlin, Germany, [3] Department of Pediatric Surgery, Faculty of Medicine, McGill University, Shriners Hospital for Children, Montreal, QC, Canada, [4] Institute of Medical Immunology, Charité — Universitätsmedizin Berlin, Berlin, Germany, [5] Berlin Institute of Health Center for Regenerative Therapies, Berlin, Germany

OPEN ACCESS

Edited by:
Claudine Blin-Wakkach,
UMR7370 Laboratoire de Physio Médecine Moléculaire (LP2M), France

Reviewed by:
Danka Grcevic,
University of Zagreb, Croatia
Kurt David Hankenson,
University of Michigan, United States

***Correspondence:**
Katharina Schmidt-Bleek
katharina.schmidt-bleek@charite.de

† These authors have contributed equally to this work

Specialty section:
This article was submitted to Inflammation, a section of the journal Frontiers in Immunology

Received: 30 November 2018
Accepted: 26 March 2019
Published: 12 April 2019

Citation:
Bucher CH, Schlundt C, Wulsten D, Sass FA, Wendler S, Ellinghaus A, Thiele T, Seemann R, Willie BM, Volk H-D, Duda GN and Schmidt-Bleek K (2019) Experience in the Adaptive Immunity Impacts Bone Homeostasis, Remodeling, and Healing. Front. Immunol. 10:797. doi: 10.3389/fimmu.2019.00797

Bone formation as well as bone healing capacity is known to be impaired in the elderly. Although bone formation is outpaced by bone resorption in aged individuals, we hereby present a novel path that considerably impacts bone formation and architecture: Bone formation is substantially reduced in aged individual owing to the experience of the adaptive immunity. Thus, immune-aging in addition to chronological aging is a potential risk factor, with an experienced immune system being recognized as more pro-inflammatory. The role of the aging immune system on bone homeostasis and on the bone healing cascade has so far not been considered. Within this study mice at different age and immunological experience were analyzed toward bone properties. Healing was assessed by introducing an osteotomy, immune cells were adoptively transferred to disclose the difference in biological vs. chronological aging. *In vitro* studies were employed to test the interaction of immune cell products (cytokines) on cells of the musculoskeletal system. In metaphyseal bone, immune-aging affects bone homeostasis by impacting bone formation capacity and thereby influencing mass and microstructure of bone trabeculae leading to an overall reduced mechanical competence as found in bone torsional testing. Furthermore, bone formation is also impacted during bone regeneration in terms of a diminished healing capacity observed in young animals who have an experienced human immune system. We show the impact of an experienced immune system compared to a naïve immune system, demonstrating the substantial differences in the healing capacity and bone homeostasis due to the immune composition. We further showed that *in vivo* mechanical stimulation changed the immune system phenotype in young mice toward a more naïve composition. While this rescue was found to be significant in young individuals, aged mice only showed a trend toward the reconstitution of a more naïve immune phenotype.

Considering the immune system's experience level in an individual, will likely allow one to differentiate (stratify) and treat (immune-modulate) patients more effectively. This work illustrates the relevance of including immune diagnostics when discussing immunomodulatory therapeutic strategies for the progressively aging population of the industrial countries.

Keywords: osteoimmunology, regeneration, bone healing, T cells, adaptive immunity, immune experience, inflamm-aging, biological aging

INTRODUCTION

Beginning in adulthood, age-associated alterations of the musculoskeletal system progress and eventually result in a loss of bone mass (1, 2). With increasing life expectancy, such structural alterations represent a growing clinical challenge: By 2050 people over 60 years will nearly double from about 12 to 22%, to a total of two billion (3). In parallel, trauma and associated bone injuries increase in number and already today represent the second most expensive medical condition (after cardio-vascular diseases) with further increases predicted due to a more active elderly population (4). Bone tissue is, in addition to its role within the musculoskeletal system, the home of major parts of the immune system. Therefore, it is not surprising that recent research acknowledged the significant role of the immune system in bone homeostasis (5).

The interdependency between the immune and skeletal system has gained more and more importance in recent orthopedic research (6–12). Bone cells require positive and negative regulators to maintain homeostasis. Cytokines are involved in the homeostatic and regenerative regulation and communication between the immune system and musculoskeletal system. Cytokines are potent mediators of osteoclast/osteoblast function and differentiation. Classically the cytokine regulation of bone resorption, like tumor necrosis α (TNFα), interleukin 1 α (IL-1α), interferon γ (IFNγ), and interleukin 17A (IL-17A), is discussed and studied but bone forming cells are tightly regulated by cytokines as well (13–15). Subsequent studies have identified several cytokines whose activities inhibit bone resorption and promote bone formation, like the IL-1 receptor antagonist (IL-1Ra), interleukin 4 (IL-4), interleukin 10 (IL-10), interleukin 13 (IL-13), and transforming growth factor β (TGFβ) (16). T and B cells are relevant producers of these inflammatory cytokines but also of cytokines impacting bone homeostasis, like osteoprotegerin (OPG) and RANK ligand (RANKL) (17). With a better understanding of the sequential events of the bone healing cascade, the essential role of the initial pro-inflammatory reaction as an initiator of the healing process has been recognized. Also, the consecutive anti-inflammatory signaling has been acknowledged as essential in order to proceed toward the next healing phase, the revascularization of the fracture zone (18–20). Without reestablishing the supply, the healing will seize. However, immune processes are not only essential during the early healing phase. Recent research showed that immune cells are present throughout the entire healing process with a heightened abundance during the remodeling phase (21) and that T cells are tightly interlinked with the process of collagen I deposition by osteoblasts, thus defining the structure of the newly formed bone tissue (22).

Age-related changes in the immune system have so far not been considered in this context: Specifically, the adaptive immune system is changing with age as a result of repetitive pathogen/ antigen exposure (23). Due to such pathogen/antigen exposures, there is a shift from a more naïve T/B lymphocyte system with a huge polyclonal repertoire of antigen receptors in young individuals toward a well-experienced (memory) T/B lymphocyte system with only a limited antigen receptor repertoire and thus a diminishing naïve lymphocyte pool in aged individuals (24). Such increase in immune experience is not directly linked to the chronological aging of an individual and therefore described as immune-aging. An "aged" adaptive immune system, particularly the T cells, are more pro-inflammatory due to various reasons, including: altered properties of memory/effector T cells in respect to tissue infiltration, lower activation threshold and the associated bystander activation, cytokine memory, and a diminished control by regulatory T cells (25). In consequence, immune-aging is accompanied with an inflamm-aging, a term recently coined in osteoimunological research that refers to an elevated inflammatory state in elderly (26). The heightened pro-inflammatory capacity of an experienced adaptive immune system is further enhanced by its effect on the innate immune response. Pro-inflammatory cytokines such as IFNg produced by T cells elicit a pro-inflammatory reaction through a pattern recognition receptor mediated inflammatory response from the innate immune system (27). Moreover, within an experienced immune system the memory/effector T cell pool forms a self-renewing population of tissue-resident cells which reside within the bone marrow (28, 29). Thus, long-lived memory/effector T cells that are fast pro-inflammatory responders to challenges such as injuries are present in the immediate proximity of a bone fracture and are likely to influence the healing process. We hypothesized that immune-aging impacts bone tissue structural properties directly, in bone homeostasis as well as in healing.

Although adaptive immunity seems to play such a central role in homeostasis and healing, it is surprising that age-associated changes of the immune system are so far rarely considered (30, 31). To overcome this limitation, we present herein a novel approach that includes animal age with and without antigen exposure, to understand the role of adaptive immunity in bone. Thus, the presented study aims at revealing the influence of an experienced immune phenotype in comparison to a

naïve immune phenotype on the tissue formation processes in bone adaptation as well as during bone regeneration to unravel the relevance of immune-aging and inflamm-aging on the bone structure and thereby lay the foundation for a more comprehensive understanding of patient treatment with impaired bone regeneration (11).

MATERIALS AND METHODS

Animals to Study Immune-Aging

Female C57BL/6N mice were purchased from Charles River Laboratories with an age of 8–10 weeks and were used at an age of 12, 52, and 102 weeks, respectively. Animals were imported with a health certificate and kept under obligatory hygiene standards that were monitored according to the FELASA standards. The mice were kept under specific pathogen free (SPF) housing or under non-SPF housing. Food and water was available *ad libitum* and the temperature (20 ± 2°C) controlled with a 12 h light/dark circle. All experiments were carried out with ethical permission according to the policies and principles established by the Animal Welfare Act, the National Institutes of Health Guide for Care and Use of Laboratory Animals, and the National Animal Welfare Guidelines, the ARRIVE guidelines and were approved by the local legal representative animal rights protection authorities (Landesamt für Gesundheit und Soziales Berlin).

Mouse Osteotomy as a Model of Fracture Healing

Bone regeneration was studied by introducing an osteotomy on the left femur. Therefore, the mice were anesthetized with a mixture of isoflurane (Forene) and oxygen (Induction with 2% Isoflurane and maintenance with 1.5%). First line analgesia was done with Bubrenorphine pre surgery, antibiotics with clindamycine and eye ointment to protect the eyes. Post-surgery, tramadol (Tramal) was added to the drinking water for 3 days. The surgical area was shaved and disinfected, and all surgical procedures were performed on a heating pad (37°C). The osteotomy was performed as previously published (32). Shortly, a longitudinal, lateral skin incision and dissection of the fasciae allowed to expose the femur. The *Musculus vastus lateralis* and *Musculus biceps femoris* were dislodged by blunt preparation with protection of the sciatic nerve. Thereafter, serial drilling for pin placement (diameter: 0.45 mm) through the connectors of the external fixator (MouseExFix, RISystem, Davos, Switzerland) was performed, resulting in a fixation of the external fixator construct strictly parallel to the femur. Following rigid fixation, a 0.70 mm osteotomy was performed between the medial pins using a Gigli wire saw (RISystem, Davos, Switzerland). After skin closure, mice were returned to their cages and kept under warming lamps for the period of immediate anesthesia recovery.

Bone Tissue Sample Preparation and Flow Cytometry

Animals were intraperitoneally injected with a mixture of medetomidine and ketamine to induce a deep anesthesia, thereafter euthanized by cervical dislocation. Blood, spleen, and the hind limbs were removed and stored for transportation in ice cold phosphate-buffered saline (PBS). For flow cytometry the spleen was dissected and mashed through a 70 μm mesh to isolate the splenocytes. Erythrocytes were removed by incubation with the RBC Lysis Buffer (BioLegend, San Diego, CA USA). The bone marrow was isolated by cutting open both end of femora or tibia and flushing the bone marrow out of the cavity with a 24G needle and PBS. The single cell suspension was incubated with a fixable live/dead stain (LIVE/DEAD™ Fixable Blue Dead Cell Stain Kit, for UV excitation (Invitrogen™, Waltham, MA USA) and subsequently washed with PBS, 0.5% BSA, and 0.1% NaN_3. Before incubation with the antibodies, the fc receptors were blocked with the TruStain fcX™ (anti-mouse CD16/32) Antibody (BioLegend, San Diego, CA USA). Surface epitopes were stained with fluorochrome coupled antibodies for 20 min on ice. For intracellular staining the surface stained cells were incubated with the eBioscience™ Foxp3/Transcription Factor Staining Buffer Set (Invitrogen™, Waltham, MA USA) according to the manufacture's protocol. Intracellular epitopes were stained for 30 min at room temperature. Stained cells were analyzed on a BD LSRFortessa™ cell analyzer (BD Biosciences, Franklin Lakes, NJ USA). For a list of used antibodies and conjugates please refer to the **Supplementary Table 1**.

Biomechanical Analyses of Femur Tissue Competence

The torsional stiffness, the maximum torque, its corresponding angle and workload were assessed in a torsional load to failure experiment. Following harvesting, the femora were excised and prepared by removing all adjacent muscles and tendons. Subsequently both epiphyses of the femora were embedded with methylmethacrylate (Technovit 3040, Heraeus Kulzer, Hanau, Germany) in custom made molds. Eventually, bones were mounted into a material testing device (Bose ElectroForce LM1, TA Instruments, Eden Prairie, MN USA) and tested by first applying an axially preloaded of 0.3N which remained constant during the following torsional load to failure at a rate of 0.54°/s. Axial displacement, load, torque, and rotation were all acquired at a 100 Hz sample rate. All parameters were calculated by a routine written in MATLAB (The Mathworks, Inc. Natick, MA USA).

3D Structural Analysis of Cortical and Trabecular Bone Using microCT Technology

Following harvesting, structural intact bones were cleaned of excess soft tissue and fixed in buffered formalin and directly loaded on a custom made sample holder and scanned at a nominal resolution of 8 and 1 μm, respectively, with a Bruker SkyScan 1172 high-resolution microCT (Bruker, Kontich, Belgium). A 0.5 mm aluminum filter was employed and an x-ray tube voltage of 70 kV. Camera pixel binning of 2 x 2 was applied and the scan orbit was 180 degrees for 8 μm and 360 degrees for 1 μm, respectively, with a rotation step of 0.2 degree. Reconstruction was carried out with a modified Feldkamp algorithm using the SkyScan NRecon software accelerated by GPU. Gaussian smoothing, ring artifact reduction, misalignment compensation, and beam hardening correction were applied.

The cortical bone was analyzed 4 mm cranial from the knee growth plate and a volume of interest (VOI) of the height of 1.6 mm was extracted. The VOI for the trabecular bone was set 0.4 mm above the growth plate and had a height of 5.2 mm, as this VOI included also the most cranial trabecular structures. The cortical bone region was binarised with a global threshold and for the trabecular bone an adaptive thresholding was applied based on localized analysis of density, to minimize partial volume effect and thickness biasing.

Osteotomized femora were mechanically fixed within a serological pipette (to support integrity of the fractured bone) and the external fixator was removed. Those bones were handled likewise as structural intact bones. Global thresholds were selected by the Otsu algorithm. The same global threshold values were applied to all measured bone samples corresponding to bone mineral density (BMD) value of 590 mg/cm^3 calcium hydroxyapatite (CaHA), calibrated by reference phantoms (Bruker-microCT, Kontich, Belgium) containing 0.25 and 0.75 g/cm^3 CaHA evenly mixed in epoxy resin rods which were of similar diameter to the scanned bones to minimize beam hardening error.

In vitro Assays to Analyze the Osteogenic Differentiation

Murine Cell Culture

Splenocytes and bone marrow cells were isolated from spleen and bone tissue from mice with different ages. The spleen was dissected and mashed through a 70 µm mesh to isolate the splenocytes. Erythrocytes were removed by incubation with the ACK Lysing Buffer (Gibco, Waltham, MA USA). The bone marrow was isolated by cutting open both end of femora or tibia and flushing the bone marrow out of the cavity with a 24G needle and PBS, after filtration through a 40 µm mesh strain, red blood cells were removed with the ACK Lysing Buffer (Gibco, Waltham, MA USA). The splenocytes were activated at a density of 2×10^6 cells/ml with 10 mg/ml plate bound anti-CD3 antibody and soluble 2 mg/ml anti-CD28 (BioLegend, San Diego, CA USA) in RPMI-1640 medium supplemented with 10% heat-inactivated FBS. After 48 h the conditioned medium was collected, pooled, filtered through a 0.22 µm hydrophobic filter (Sartorius) and stored at −80°C. Murine mesenchymal stromal cells were obtained via outgrowth culture from bone marrow cells. The isolated single cells from bone marrow was plated in 25 cm^2 cell culture plates with DMEM low glucose medium (Biochrom, Berlin, Germany) supplemented with 10% FBS (Biochrom, Berlin, Germany), 1% GlutaMAX (Gibco, Waltham, MA USA), and 1% penicillin/streptomycin (Biochrom, Berlin, Germany). After reaching confluency, the cells were detached with TrypLE Express Enzyme (Gibco, Waltham, MA USA) and cultured in passage 1 again in a 25 cm^2 culture flask. By passage 2 the cells were transferred gradually with higher passage number in 75, 150, and 300 cm^2 cell culture flasks. Murine mesenchymal stromal cells (mMSC) were used between passage 5 and 6 for the experiments. Osteogenic differentiation of mMSC was achieved by the supplementation with 100 nM Dexamethasone, 0.05 mM l-ascorbic acid 2-phosphate, and 10 mM β-Glycerolphosphate (33). Conditioned medium was added at a dilution of one to three (1:3). Medium was exchanged every 3–4 days. After 14 days the experiment was stopped and the mineralized extracellular matrix was stained with Alizarin Red S (Sigma-Aldrich, St. Louis, MO USA) and quantification was achieved by resolving the stain with cetylpyridiniumchlorid (Sigma-Aldrich, St. Louis, MO USA). Optical density (OD) was measured with a multimode microplate reader (Tecan Infinite, Männedorf, Switzerland).

Human Cell Culture

Human mesenchymal stromal cells (hMSC) were isolated from bone marrow of patients undergoing total hip replacement (provided by the Center for Musculoskeletal Surgery, Charité - Universitätsmedizin Berlin and distributed by the "Cell and Tissue Harvesting" Core Facility of the BCRT). All protocols were approved by the Charité - Universitätsmedizin Ethics Committee and performed according to the Helsinki Declaration. Human MSC were cultivated with DMEM low glucose medium (Biochrom, Berlin, Germany) supplemented with 10% FBS (Biochrom, Berlin, Germany), 1% GlutaMAX (Gibco, Waltham, MA USA), and 1% penicillin/streptomycin (Biochrom, Berlin, Germany). After three passaging steps, hMSC were characterized by differentiation assays (osteogenic, adipogenic, chondrogenic). Only hMSC that were capable of differentiation in all three lineages were used in the experiment within passage 4–8. Human peripheral blood mononuclear cells (hPBMC) were isolated from buffy coats (provided with ethical approval by DRK, Berlin, Germany) via density gradient centrifugation on Histopaque-1077 (Sigma-Aldrich, St. Louis, MO USA). The buffy coats were separated from blood donor volunteers by the Deutsches Rotes Kreuz (DRK) and fulfilled the criteria of age >30 years old and cytomegalovirus (CMV) positive. Isolation of naïve T cells was achieved with the Naïve T Cell Isolation Kit (Miltenyi Biotec, Bergisch Gladbach, Germany) and CD8+ T cells were isolated via CD8a microbeads (Miltenyi Biotec, Bergisch Gladbach, Germany). The hPBMC were activated at a density of 2×10^6 cells/ml with 10 mg/ml plate bound anti-CD3 antibody and soluble 2 mg/ml anti-CD28 (BioLegend, San Diego, CA USA) in RPMI-1640 medium supplemented with 10% heat-inactivated FBS. After 48 h the conditioned medium was collected, pooled, filtered through a 0.22 µm hydrophobic filter (Sartorius) and stored at −80°C until further use. Osteogenic differentiation of hMSC, under the influence of conditioned medium from hPBMC was developed likewise to murine MSC.

Enzyme-Linked Immunosorbent Assay (ELISA)

Conditioned medium from activated murine splenocytes were harvested as described and processed for enzyme-linked immunosorbent assay (ELISA). ELISA for TNFα (Mouse TNFalpha ELISA ReadySet-Go! 10x #88-7324-86, eBioscience), IFNγ (Mouse IFN gamma ELISA Ready-SET-Go! 10x #88-7314-86, eBioscience), and IL-10 (Mouse IL-10 ELISA Ready-SET-Go! #88-7105-86, eBioscience) was performed according to the manufacturer's instructions in triplicates and optical density was measured with a microplate reader Tecan Infinite (Tecan,

Männedorf, Switzerland). A standard curve was generated with a four parametric logistic curve fit.

Conditioned medium from activated human PBMC were harvested as described and processed for quantitative cytokine detection via ELISA. ELISA for human TNFα (Human TNF alpha Uncoated ELISA, 88-7346, Invitrogen) and human IFNγ (Human IFN gamma Uncoated ELISA, 88-7316, Invitrogen) was performed according to the manufacturer's instructions in triplicates and optical density was measured with a microplate reader Tecan Infinite (Tecan, Männedorf, Switzerland). A standard curve was generated with a four parametric logistic curve fit.

Mechano-Therapeutics: *in vivo* Hind Limb Loading to Analyze Bone Adaptation and Homeostasis

The left tibiae of 10 week (young) and 52 week (aged) old C57Bl/6J mice ($N = 6$/age) underwent *in vivo* cyclic compressive loading, while the right tibia was not loaded and served as an internal control. The flexed knee and the ankle of the mice were placed in our loading device (Bose ElectroForce LM1, TA Instruments, Eden Prairie, MN USA) and axial dynamic compressive loading was applied 5 days/week for 2 weeks while the mice were anesthetized with isoflurane (2.5%). Refer to Willie et al. (34) for further information. Shortly, the loading protocol consisted of 216 cycles applied at 4 Hz, which is the mean mouse locomotory stride frequency (35) delivering a maximum force of −7N for the 10 and −9N for the 52 week old mice, engendering 900 με at the periosteal surface in the tibia mid-diaphysis determined by prior *in vivo* strain gauging studies (36). This strain level equates to about two to three times the strains engendered on the medial tibia when mouse ambulates (37, 38). Mice were sacrificed on day 15, 3 days after the last loading session.

Humanized PBMC Mouse Model to Assess the Osteo-Immune Crosstalk

The humanized peripheral blood mononuclear cell (hPBMC) mouse model is described elsewhere (39–41). Shortly, human PBMC were isolated from venous blood from volunteers via density gradient centrifugation with Histopaque-1077 (Sigma-Aldrich, St. Louis, MO USA). Immune phenotype was characterized with flow cytometry. Cells were incubated with a fixable live/dead stain (LIVE/DEAD™ Fixable Blue Dead Cell Stain Kit, for UV excitation, Invitrogen™, Waltham, MA USA) and subsequently washed with phosphate-buffered saline (PBS), 0.5% BSA, and 0.1% NaN_3. Before incubation with the antibodies, the fc receptors were blocked with the Fc Receptor Blocking Solution (Human TruStain fcX™, BioLegend, San Diego, CA USA). Surface epitopes were stained with fluorochrome coupled antibodies for 20 min. Stained cells were analyzed on a BD LSRFortessa™ cell analyzer (BD Biosciences, Franklin Lakes, NJ USA). For a list of used antibodies and conjugates please refer to the **Supplementary Table 2**. Experience level for stratification was achieved via the CD8+ T_{EMRA} level: 36% [the level was set corresponding to Reinke et al. (42)] and higher were classified as experienced and below 20% as naïve donors. Donor immune phenotype characterization can be found in the **Supplementary Table 3**. Ten million freshly isolated and characterized hPBMCs were transferred at a density of 5×10^6 cells/ml PBS via tail vein injection 1 day before surgery. After 3 or 21 days the organs were harvested and analyzed. An osteotomy was introduced as described in the preceding paragraph. For the analysis 21 days after surgery the callus region of the osteotomized femur was defined as a region of 1.4 mm (double the size of the fracture gap to include the complete callus) around the middle of the fracture gap. The cell transfer has been confirmed by blood sampling and consecutive flow cytometry analysis at day 3 and day 21 after osteotomy surgery.

Statistics

Statistical analysis was carried out with SPSS V.22 and GraphPad Prism V.7 software. All values including animal data are expressed as boxplot distribution giving interquartile ranges, a median, and whiskers representing min and max. All data including *in vitro* studies are expressed with mean ± SD. For animal experiments Mann-Whitney *U* was used as an unpaired, non-parametric test to compare ranks (no normal distribution of the data), for *in vitro* studies an unpaired *t*-test with Welch's correction was employed. Two-tailed and exact *p*-value are calculated with a confidence level of 95%. $P < 0.05$ was considered as statistically significant and marked with an asterisk in all graphics. ROUT test was used to exclude outliers ($Q = 1\%$).

RESULTS

Fracture Healing Deteriorates With Age

While it is frequently discussed that bone healing is impaired in the aged population, it is so far not well-understood how healing is impaired with increased chronological age apart from the age-associated decline in bone mass and quality. It is also recognized that bone fractures tend to heal more effectively in young patients compared to those in elderly (**Figure 1A**). To better understand how bone healing is altered with chronological age, a clinically relevant mouse osteotomy model was employed and bone healing was compared in young, 3 month old and elderly, 24 month old mice. Both groups of mice received a 0.7 mm osteotomy in the left femur which was stabilized by a unilateral external fixator (MouseExFix, RISystem, Davos, Switzerland). To quantify bone healing outcome, mice were analyzed at 21 days post-osteotomy using microcomputed tomography (microCT). 3D structural data analysis revealed a more mature callus in young mice compared to aged mice. The newly formed bone (BV) volume slightly decreased and the total callus volume (TV) showed a trend to be increased, whereas the ratio of bone to total callus volume decreased significantly from 48.5(±5.2) to 38.6(±1.0)%.The number of newly formed trabecular structures (Trabecular number, Tb.N) within the callus decreased significantly from 4.7(±0.5) to 3.6(±0.6)/mm in aged animals (**Figures 1B,C**). Thus, the comparison of young vs. elderly mice clearly demonstrated a diminished healing capacity of bone and matches the casual observations made in elderly patients suffering delays in bone healing.

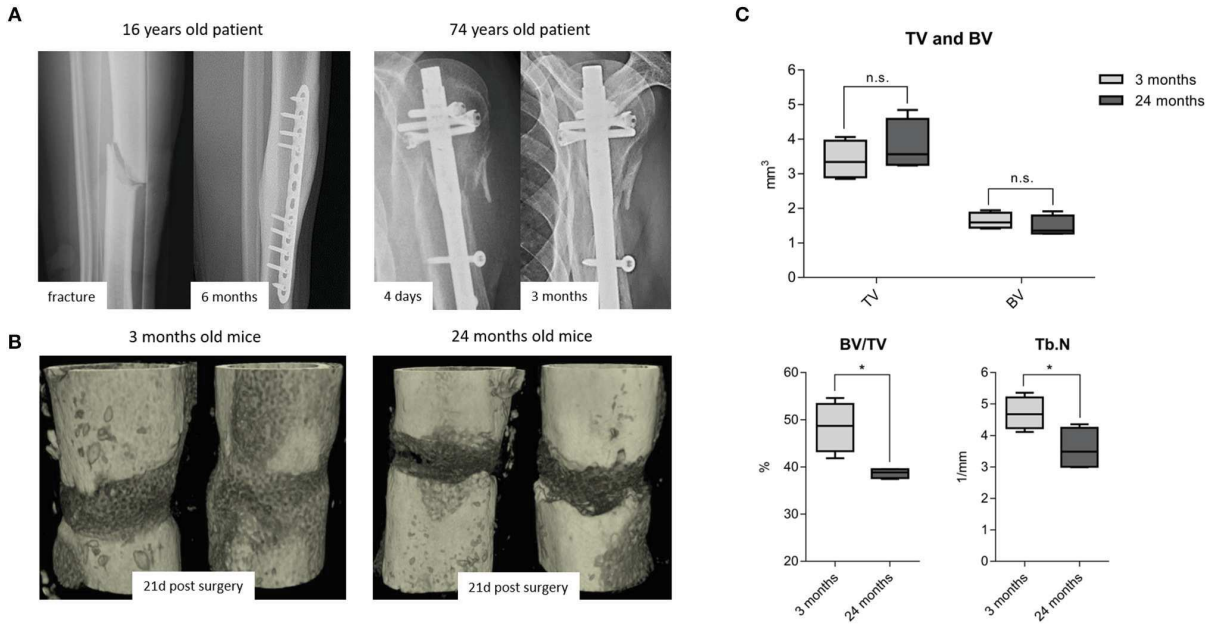

FIGURE 1 | Fracture healing among young and old subjects: (**A** left) X-ray images from a young patient with adequate callus formation after 6 months and (**A** right) from an old patient with no signs of healing after 3 months, leading to delayed fracture healing and revision surgery. This x-ray images are representative images from the clinical routine and depict the need to understand the altered processes within the elderly population. **(B)** 3D rendered x-ray images from 3 to 24 month old mice, respectively, at 21 days post-surgery. Bone healing was delayed in 24 month old compared to the 3 month old mice. **(C)** microCT analysis from the osteotomy gap 21 days post-surgery. Bone volume in total volume (BV/TV) and trabecular number (Tb.N) were diminished in 24 month old fracture callus. TV and BV were not significantly affected by age, but the ratio of newly formed bone in the callus volume was significantly lowered. $N = 6$ animals in the 3 months old group and $N = 5$ in the 24 months old group, boxplot data distribution with median, Mann-Whitney U-test, $^*p < 0.05$.

Antigen Exposure Over Time Alters the Immune Cell Composition

Standard preclinical models use in the majority of cases mice kept under specific pathogen free (SPF) housing conditions—minimizing the exposure to antigens. SPF housing significantly demagnifies the intra-individual variabilities through abolishing the pathogen/antigen exposure. In order to understand the immune-aging process and the development of an immune memory with effector and effector memory cells that are apt to protect the organism from recurrent pathogen exposure, mice were exposed to non-SPF housing conditions. Comparing mice held under SPF conditions with mice that were housed in non-SPF conditions revealed changes within the immune cell composition that mirror the immune-aging that commonly occurs to people while they grow old. These two groups allow one to distinguish between the changes in bone that occur by chronological aging and those changes that are due to the immunological aging. For quantification, the immune composition was characterized by flow cytometry analysis of the spleen from 3, 12, and 24 month old mice, respectively. Antigen exposure primarily influenced the memory compartment of the adaptive immunity over age/time. In both groups, the adaptive immune cell compartment, consisting primary of CD4+ and CD8+ T cells, acquired a more experienced memory phenotype while aging. The naïve cell pool of CD8+ cytotoxic T cells in the SPF mice diminished over time from 90.7(±1.3) to 77.8(±8.3)% within 2 years. However, a more drastic change was observed in the exposed mice: Under non-SPF conditions the memory pool increased to 95.5(±2.4)% of CD8+ T cells whereas the naïve pool was almost completely exhausted with a remnant of 3.0(±1.8)%. Only under non-SPF conditions such nearly complete exhausting of the naïve T cell pool in aged mice could be observed. Similar phenotypical changes could be observed in the CD4+ T helper cell pool (**Figure 2A**).

The memory and effector pool (CD44+) can be distinguished by the CD62L marker into central memory (T_{CM}) and effector memory (T_{EM}) T cells. Both compartments of CD8+ T cells increase with age, but only under non-SPF conditions the inter-individual variance of comparentalization could be seen (see **Figure 2B**). In the CD4+ T cell pool a similar picture could be observed compared to CD8+ T cells with less variance between individual animals. Interestingly, the CD4+ T central memory pool was constant among age and housing condition groups (**Figure 2B**). An increase in memory and effector function of the adaptive immune system was revealed with age and correlated with the housing conditions, which defined the antigen exposure and thus the development of an immune memory.

The classification in T effector/memory (T_{EM}), T central memory (T_{CM}) and T naïve cells in the CD8+ T cell pool describes the compartmentalization, but lacks a description

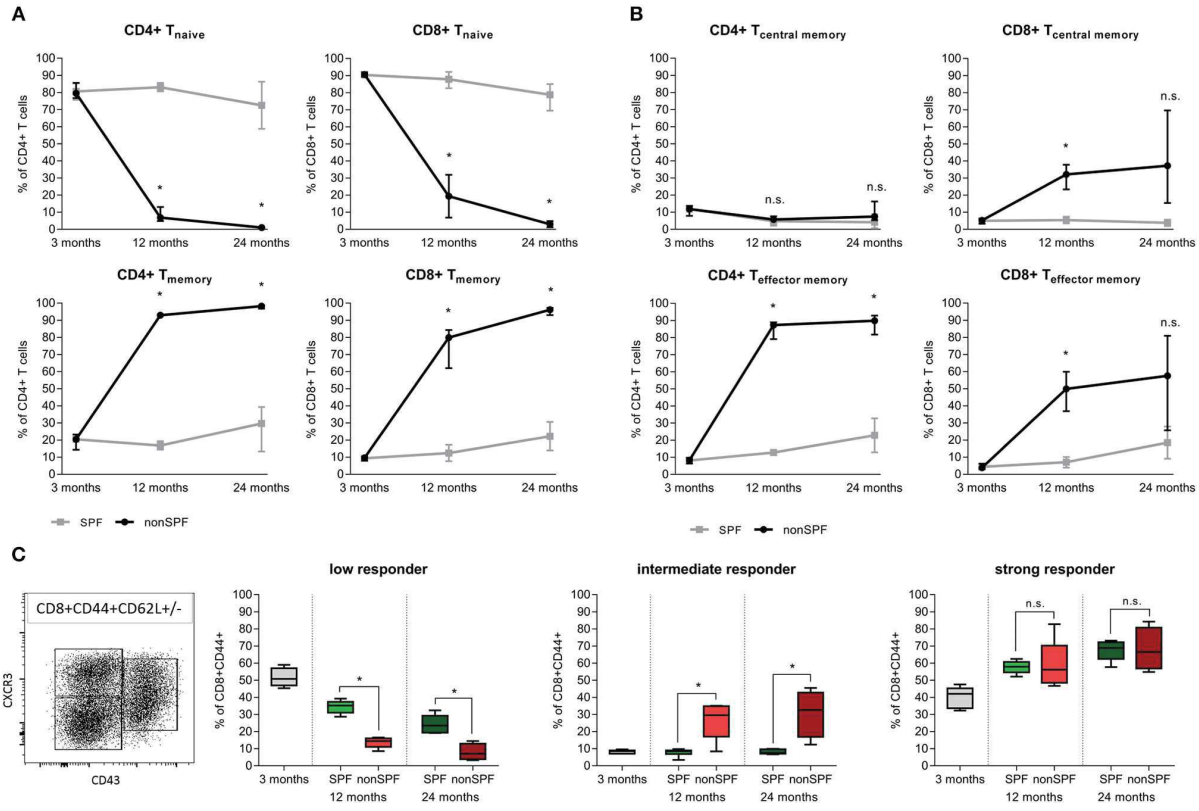

FIGURE 2 | Adaptive immunity changes level of experience among housing conditions (SPF vs. non-SPF) and aging. **(A)** Naïve level of CD4+ and CD8+ T cells diminished and the memory level increased with aging. Exposing the animals to antigens boosts the memory formation significantly. **(B)** Classification of T cells into central memory (T_{CM}) and effector memory (T_{EM}) revealed a different picture for CD4+ and CD8+ T cells: CD8+ T cells increased both compartments under non-SPF conditions, whereas the CD4+ central memory T cells were constant among ages and housing conditions. Keeping mice under SPF conditions oppressed the effect of memory formation. **(C)** CD8+ memory T cells differ in the recall efficiency after antigen encounter. Strong responder CD8+ memory T cells were not affected by non-SPF housing, whereas intermediate responder could only be found under non-SPF conditions (intermediate responder are proven to show fast proliferation and vast cytokine production). The low responder fraction diminished further under non-SPF conditions compared to SPF housing. $N = 6$ animals per age group and housing conditions, **(A,B)** shows median with interquartile range, **(C)** shows boxplot distribution with median, Mann Whitney U-test, $^*p < 0.05$.

of the activation phenotype. Memory CD8+ T cells differ in their capacities to realize a recall response. To quantify the activation potential of immune cells, the spleen of mice under SPF or non-SPF conditions was analyzed in the different age groups. The recall efficiency was classified by surface markers CXCR3 (CD183), CD27, and CD43. CD8+CD44+ memory T cells can be divided in 3 groups of low, intermediate and strong responders. An increase in CXCR3 on the cell surface correlates with an increased proliferative capacity and an increased IL-2 production. Whereas, the low responder characterized by low CXCR3 and CD43 marker show low proliferative capacity and reduced IL-2 production but an increase Granzyme B secretion. Intermediate responder upregulate the CD43 protein on the cell surface and are characterized by a very pronounced proliferation and an elevated secretion of cytokines. The low responder group of CD8+ memory T cells decreased with age and the strong responder increased, almost doubling their population quantity. The increase of strong responder within the memory CD8+ T cells amplifies the earlier finding of an accumulation of memory cells over time. Intermediate responders were almost exclusively found in higher numbers under non-SPF conditions. Under antigen exposure the low responder immune cells decreased over time being replaced by intermediate and strong responder indicating a pronounced inflammatory reaction (**Figure 2C**). Thus, the activation phenotype revealed a higher proliferative and secretory phenotype in mice kept under non-SPF conditions undergoing an immune-aging that consecutively lead to an amplified response capacity upon recall.

Immune-aging (antigen exposure) became further apparent by an in-depth immune phenotyping of these two mice groups kept under different (SPF vs. non-SPF) housing conditions. Strikingly, if mice were kept outside of the SPF housing, a shift occurred from lymphoid toward myeloid immune cells and a shift of the ratio of B and T cells toward T cells (**Figure 3A**). T cells themselves underwent a shift

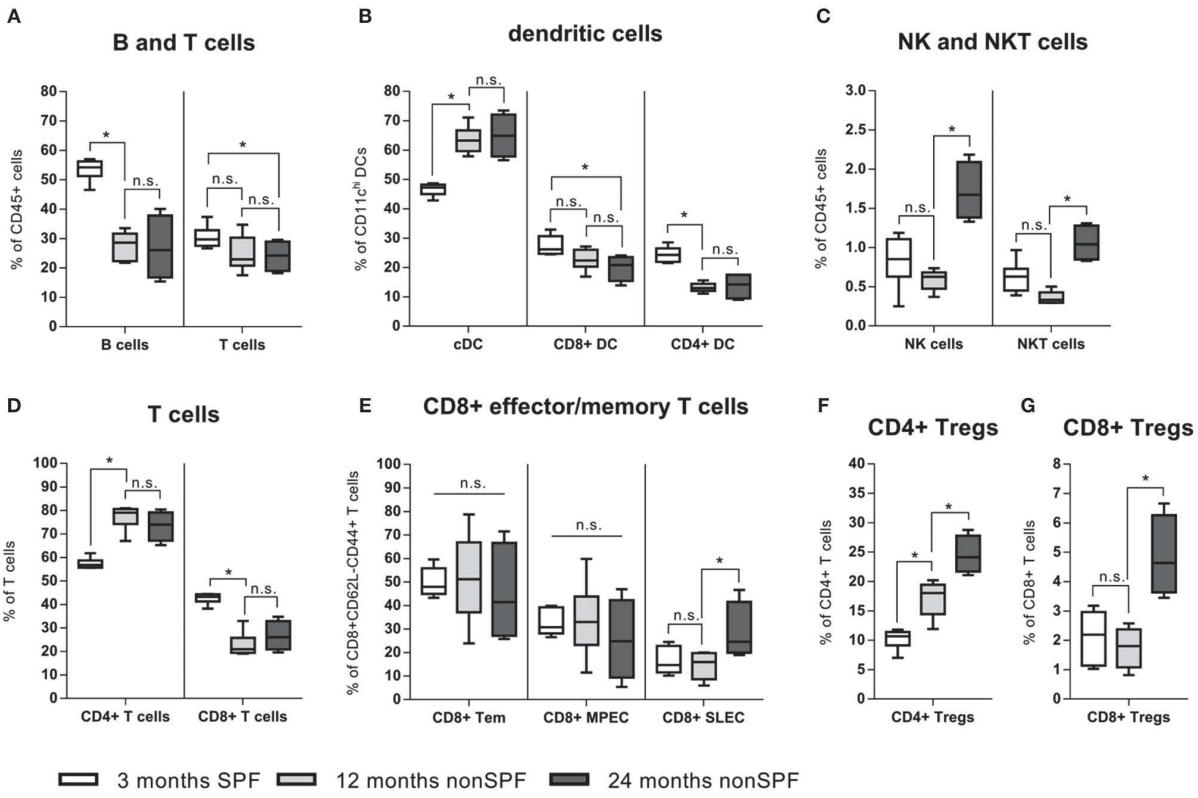

FIGURE 3 | In-depth immune phenotyping showed, that keeping mice under non-SPF conditions significantly changes the immune phenotype with age. **(A)** A shift from lymphoid toward myeloid immune cells could be seen in a lowered B and T cell fraction in the spleen, accompanied by a change of the ratio of B and T cells toward T cells. **(B)** Dendritic cells increased under non-SPF conditions and a shift toward conventional DCs (cDC) occurred. **(C)** Natural killer cells (NK cells) and especially Natural killer T cells (NKT) increased with higher age. **(D)** Under non-SPF conditions a shift from CD8+ T cells toward CD4+ T cells occurred, being stable thereafter throughout aging. **(E)** CD8+ effector memory T cells can further be divided into memory (Tem), memory precursor effector cells (MPEC) and short-lived effector cells (SLEC). The diversity of effector cells increased with age. **(F)** CD4+ T regulatory cells (Treg) increased with age. **(G)** CD8+ T regulatory cells (Treg) are a rare cell population, but could be found in relevant amounts in 24 months old mice. $N = 6$ animals per group, boxplot distribution with median, Mann-Whitney U-test, $^*p < 0.05$.

of the CD4/CD8 ratio toward a more pronounced CD4+ compartment: CD4+ T cells represented ∼70–80% of all CD3+ cells under non-SPF conditions, whereas under SPF conditions the CD4+ T cell pool represented only around 60% of all CD3+ cells (**Figure 3D**). The CD8+ T effector memory pool (CD8+CD44+CD62L-) can further be divided in T effector memory, memory precursor (MPEC), and short-lived effector cells (SLEC) via the markers CD127 and KLRG1. In all three compartments, the inter-individual variance increased with age under non-SPF housing (**Figure 3E**). Within the CD4+ T cell pool the T regulatory cells (Tregs) are of great interest and this immune cell compartment underwent significant changes with age. With 3 month of age 10.2(±1.7)% of CD4+ T cells were Tregs (FoxP3+CD25high), which further increased to 17.1(±3.1)% at 12 and to 23.8(±4.4)% at 24 months (**Figure 3F**). While the proportion of CD8+ Tregs seemed to be stable in the two younger groups, at 24 months the level of CD8+ Tregs increased (**Figure 3G**). As professional antigen presenting cells (APCs) dendritic cells (DCs) are unrivaled in their capability to activate T cells. We found that specifically the dendritic cells underwent a shift from splenic CD8+ and CD4+ DCs toward conventional splenic DCs in non-SPF housing conditions (**Figure 3B**). Regarding the compartments of NK and NKT cells, both cell subpopulations showed a significant increase in the 24-months-aged mice under non-SPF conditions (**Figure 3C**).

In summary, antigen exposure appears to be very crucial for the development of a diversified immune system, especially impacting the development of a specific memory functionality of the immune system.

To distinguish between changes within the bone that occur during chronological aging and those that are caused by the immune-aging, bones of mice with a more naïve immune composition (aged within an SPF surrounding) were compared, using microCT and biomechanical testing, to bones of mice aged with the possibility to develop an immune memory (immune-aging within non-SPF housing).

The Immune Signature Changes the Mechanical Competence of Bone

Biomechanical testing of the femora was conducted with a mechanical testing machine (Bose ElectroForce LM1, TA Instruments, Eden Prairie, MN USA), and loaded to failure in torsion to characterize the mechanical competence of bone under the influence of differently experienced immune phenotypes and in different age groups. Three groups of six animals each were analyzed: 3 month old were considered as young mice without an experienced immune system. Two groups with 12 month old middle age mice were set as aged groups. One group of aged mice was housed under SPF and one group under non-SPF conditions to gain an experience level in the adaptive immunity. Thus, the two aged groups only differed in their immune cell composition and thus any changes of the mechanical competence are due to the difference in the immune phenotype. The stiffness of the femora increased by age from initial 5.4(±0.5) Nmm/deg at 3 months to 7.0(±0.3) Nmm/deg at 12 months. This change was accredited to the chronological aging. The excessive increase to 8.4(±0.9) Nmm/deg seen in animals in non-SPF housing had to be attributed to the more experienced immune system. Torque at the yield point increased with age and was significant higher under non-SPF conditions. The failure torque increased with chronological age, but also showed a further increase with an experienced immune phenotype (however lacking statistical significance): Maximal torque at failure at 3 months of age 20.4(±2.6) Nmm increased to 28.3(±5.3) Nmm at 12 months SPF and 31.2(±6.1) Nmm at 12 months non-SPF, respectively. The post-yield displacement analysis revealed a ductile fracture manner in 3 month old mice and changed to a brittle fracture manner with age and a significant change under non-SPF housing (**Figure 4**). An experienced, immune-aged system, characterized by a higher pro-inflammatory environment resulted in changed biomechanical competences of the bone. To further investigate the underlying structural causes of this difference in mechanical competence, bone structure was analyzed using microCT analysis.

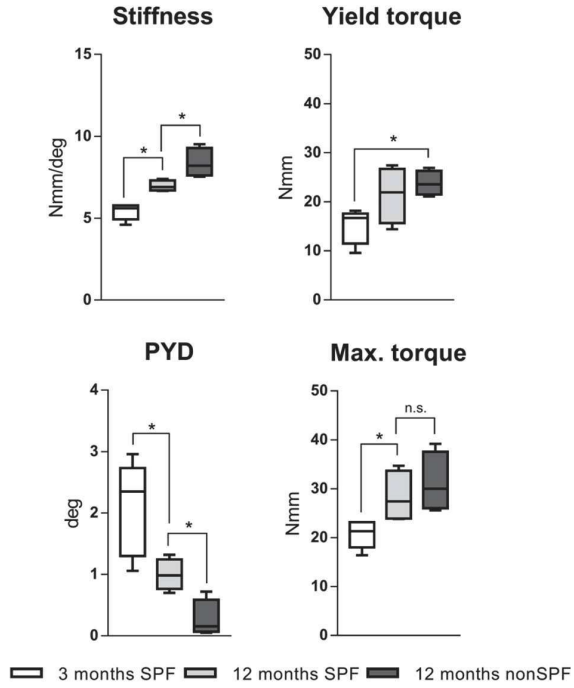

FIGURE 4 | Torsional testing of mouse femora with different immune phenotype. Keeping mouse under non-SPF conditions increased the torsional stiffness compared to 12 months old SPF mice. Yield torque and maximal torque increased by age and was further affected by non-SPF housing. The post-yield displacement (PYD) revelaed a more brittle fracture manner at 12 months under non-SPF compared to 12 months under SPF housing, the 3 month old bone fractured in a more ductile manner. $N = 6$ per group, boxplot distribution with median, Mann-Whitney U-test, $^*p < 0.05$.

The Immune Signature Impacts the Bone Structures

MicroCT analysis was performed on femora of 3 months young mice and two 12 months old groups with one kept under SPF housing (called 12 months SPF) and one kept in non-SPF housing (called 12 months non-SPF) to allow for analyses of chronological aging vs. immune-aging with an increased immunological memory. Both of the old groups showed an aged bone phenotype, additional changes of the bone structure were found within the old mice with an experienced immune phenotype (non-SPF).

Cortical Bone Structure

Total area (Tt.Ar) and bone area (Ct.Ar) increased with age, however both outcome measures were significantly increased in the 12 months non-SPF group compared to the 12 months SPF group. The medullary area (Ma.Ar) did not significantly differ between the groups, leaving the bone marrow canal mostly unaffected. The ratio of bone area inside the tissue area (Ct.Ar/Tt.Ar) was also only different in the aged experienced mouse group, showing an increased ratio of Ct.Ar/Tt.Ar. Strikingly, the total mineral density (TMD) of the cortical bone increased only by age and was not altered by the immune experience (**Figure 5A**). One micrometer resolution scans revealed a periosteal thickness increase with age, specifically on the lateral aspect of the cortex (**Figure 5B**). While in chronological aging, the cortical thickness increased from initial 149(±7) μm at 3 months to 165(±6) μm at 12 months, it increased under the influence of an experienced immune system to 192(±11) μm. Interestingly, this effect was very pronounced on the lateral cortex and demonstrates the general impact of altered immune experience on bone structures such as cortical periosteal perimeter and cortical area.

To judge the mechanical competence of the structure, the mean polar moment of inertia (MMI-polar) was calculated to quantify the bone's capability to resist against rotational loads. The MMI-polar increased with age, reflecting the bone phenotype and age associated adaptation of its mechanical competence like the stiffness of long bones. Surprisingly, this effect of age associated changes in polar moment of inertia were further pronounced in a more experienced immune system.

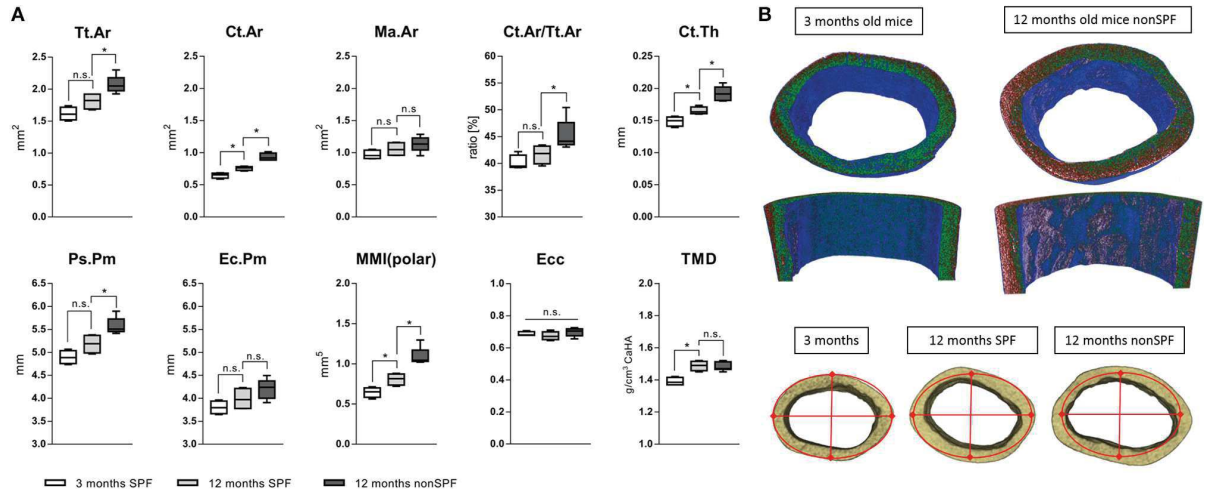

FIGURE 5 | MicroCT analysis of femoral cortical bone. **(A)** Mean total area (Tt.Ar) and cortical area (Ct.Ar) increased under non-SPF conditions compared to SPF conditions. The medullary area (Ma.Ar) and endocortical perimeter (Ec.Pm) are slightly increased, but the periosteal perimeter (Ps.Pm) and cortical thickness (Ct.Th) are significantly increased, demonstrating growth in lateral directions. The ratio of cortical to total area (Ct.Ar/Tt.Ar) was significantly increased in 12 months old mice under non-SPF conditions. Therefore, polar moments of inertia (MMI-polar) were significantly higher under non-SPF conditions. The eccentricity (Ecc) was constant throughout all groups, indicating a constant shape of the cortical femoral bone. Most strikingly the total mineral density (TMD) of the cortical bone was not affected by the housing condition. (**B** top) A density map of the cortical bone comparing a 3 months old mouse with a biologically aged 12 months old mouse. (**B** bottom) Representative images of the cortical bone of a 3 months old mouse compared to 12 months old mice either under SPF or non-SPF conditions. $N = 6$ per group, boxplot distribution with median, Mann-Whitney U-test, $^*p < 0.05$.

Eccentricity (Ecc) is a shape analysis used to define structural deformation of the scanned bones. This parameter was the same for all three analyzed groups indicating that the shape of the cortical bone did not differ among all three groups. The overall mean eccentricity of 0.686(±0.022) indicates a generally elongated, more elliptical object but did not differ neither in chronological nor immunological aged groups (**Figure 5A**).

Trabecular Bone Structure

Bone volume (BV/TV) and trabecular number (Tb.N) decreased with age, independent of the immune experience. However, the trabecular thickness (Tb.Th) was highly effected by the immune cell composition. The trabeculae of 3 month old mice showed a mean thickness of 38(±1) μm and 12 month SPF mice showed an increased thickness to 47(±3) μm, while 12 month non-SPF mice had an even further increased thickness to 53(±5) μm. Trabecular separation indicates the distance between bony structures and revealed that with age the distance increased reflecting the loss of the number of structures, but the two aged groups did not differ. The bone mineral density (BMD) is not affected and the BMD decreases only by age and not by the immune status (**Figures 6A,B**).

The femur length only differed by age, but not with exposure to non-SPF housing conditions. Three months old mice showed a femur length of 14.54 mm ± 0.07, the aged 12 months old mice under SPF conditions showed a femur length of 16.59 mm ± 0.13 comparable to the non-SPF housed mice with 16.86 mm ± 0.27. The weight increased from roughly 22 g at 3 months of age to 27 g in both of the 12 months old group of mice.

In summary, the results show clearly an impact of the immune experience on bone structures but not on bone mineral density. This is a new and so far not reported link between the immune system and the bone structural properties, apparently impacting mechanical competence of bone. The immune experience in 12 month old mice had a significant impact on cortical and trabecular bone microstructure. An experienced immune system led to increases in thickness of the trabecular and cortical bone.

So far, our data illustrate the relevant impact of immune experience on the bone structure. To determine the underlying mechanism, the influence of the immune cell signaling on the osteogenic differentiation of mesenchymal stromal cells had to be investigated. To simulate the immune reaction of an inexperienced vs. an experienced immune system, conditioned medium of activated cells from respective donors was used in osteogenic differentiation assays.

Immune Cells Influence Differentiation and Proliferation of Stromal Cells

To understand why cortical and trabecular microstructure was affected by the adaptive immunity, the interdependency of the immune cells and the bone forming osteoblasts was investigated using mesenchymal stromal cells as an *in vitro* model. To differentiate between the influence of chronological age and experience of the immune system, immune cells from 3 to 12 month old mice were isolated from the spleen, while mesenchymal stromal cells were isolated from bone marrow. Aged mesenchymal stromal cells showed an alleviated ability to differentiate toward the osteogenic lineage: Intensity of the

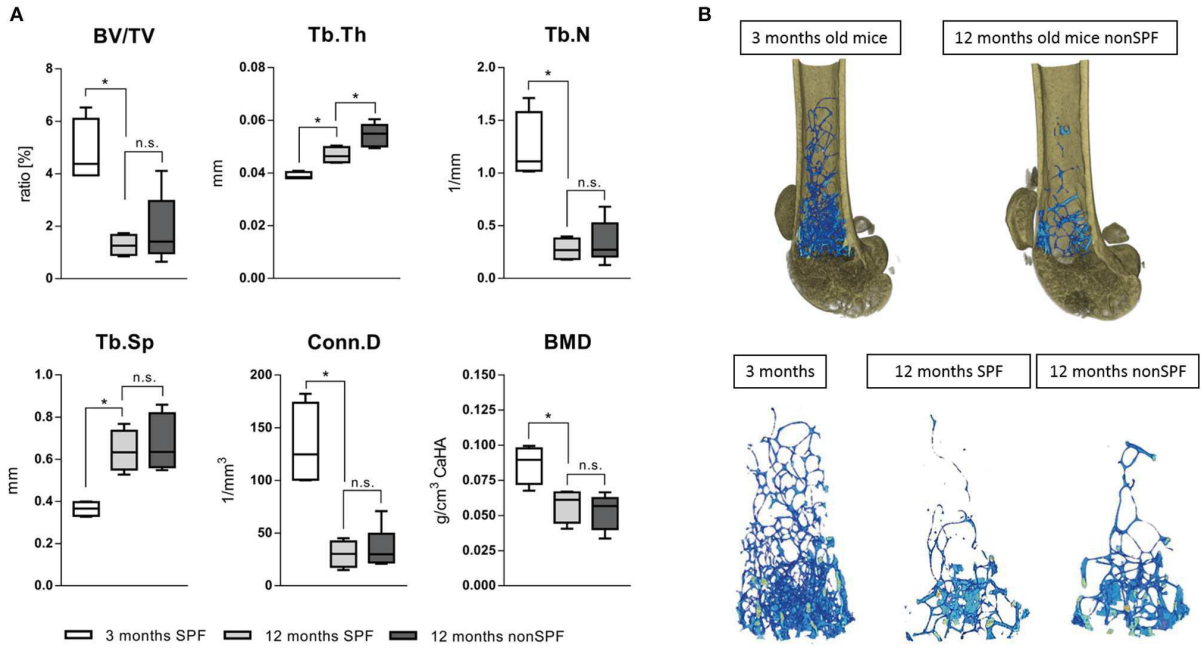

FIGURE 6 | MicroCT analysis of femoral trabecular bone. **(A)** The ratio of bone volume in total volume (BV/TV) and the number of trabecular structures (Tb.N) were both lowered with age, the separation (Tb.Sp) thereafter increased with age. The age dependent loss of trabecular bone was not affected by housing conditions, but the diversity significantly increased under non-SPF conditions. Most strikingly, the trabecular thickness (Tb.Th) not only increased by age but further increased under non-SPF conditions. The connectivity (Conn.D) was not affected by the housing conditions. As seen in the cortical bone analysis the mineral density (BMD) was only affected by age but not by housing conditions. (**B** top) Representative 3D rendered images of trabecular bone comparing a 3 months old mouse with a biologically aged 12 months old mouse. (**B** bottom) Representative images of 3D rendered images of trabecular bone of a 3 months old mouse compared to 12 months old mice either under SPF or non-SPF conditions. $N = 6$ per group, these are the same samples analyzed for the cortical bone parameters (**Figure 5**), boxplot distribution with median, Mann-Whitney *U*-test, $^{*}p < 0.05$.

Alizarin red S staining of the extracellular matrix decreased with age (**Figure 7**). To represent an immunologically inexperienced immune setting, splenocytes of 3 month old, young mice were stimulated and conditioned medium was harvested. The experienced immune composition was simulated by gaining conditioned medium from splenocytes of 12 month old, immunologically experienced mice. The respective conditioned medium was then added to young or old mesenchymal stromal cells which underwent osteogenic differentiation. As a control conditioned medium from non-activated splenocytes, from both ages was used. Conditioned medium (CM) from activated immune cells decreased the osteogenic differentiation of mMSCs in both age groups compared to non-activated CM and osteogenic medium control (OM). The conditioned medium was either added to 3 months old mMSCs or to the less competent 12 months old mMSCs. In both mMSC groups the conditioned medium gained from the experienced immune cells decreased the osteogenic differentiation significantly **(Figure 7)**. Analyses of the conditioned medium with enzyme-linked immunosorbent assay (ELISA) revealed an increase in pro-inflammatory cytokines like interferon γ (IFNγ) and tumor necrosis factor α (TNFα) (**Figure 7C**). Amazingly, interleukin 10 (IL-10), known to have anti-inflammatory properties, was also increased (**Figure 7C**). These results confirmed that an experienced immune system shows an increased pro-inflammatory capacity—that is negatively affecting the osteogenic potential of MSCs. Hence, osteogenic differentiation of mesenchymal stromal cells is damped under the influence of an aged immune system.

The influence of the immune composition on osteogenic processes further confirm that bone formation, mechanical competence, and structure are dependent on the age/experience of the immune cells. But how would a perturbation alter the interplay of immune and bone system, such as in a homeostatic setting? During bone homeostasis, a key modulator of tissue formation and resorption is the mechanical loading experienced by the bone. Bone adapts to the experienced mechanical loads (43). Is such a mechanically induced bone formation process also affected by the experience of the immune system? A well-established limb-loading model was used in young and aged animals and the changes in the immune cell composition in the bone marrow of loaded bones were monitored.

In vivo Perturbation: Mechanical Loading as a Rescue for Immune Experience?

The bone's capability to adapt its mass and architecture to changes in the mechanical loading environment is a remarkable function. While mechanical loading enhances bone mass in young mice,

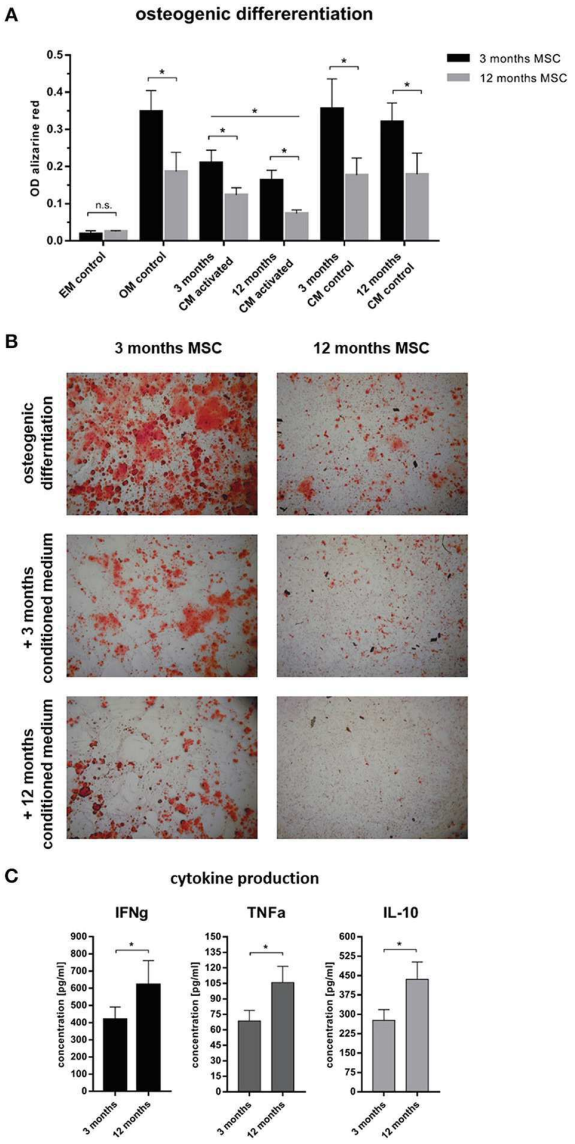

FIGURE 7 | Osteogenic differentiation after 14 days under the influence of conditioned medium from immune cells. **(A)** 3 months old mesenchymal stromal cells (MSC) were compared to 12 months old MSC. The 12 months old MSC showed a reduced osteogenic differentiation potential compared to 3 months old MSC. Adding conditioned medium from immune cells (conditioning for 48 h) that were not activated did not affect the osteogenic differentiation, but adding conditioned medium from activated immune cells lowered the differentiation potential. The conditioned medium from 12 months old mice worsened the ability to differentiate into the osteogenic lineage. **(B)** Representative images of the calcium deposition stained by Alizarin Red S comparing 3 and 12 months old MSC under the influence of different conditioned medium. Twelve months old MSC under the influence of activated 12 months old conditioned medium almost abolished the ability for calcium deposition. **(C)** Analysis of the conditioned medium showed an increase of pro- (IFNγ and TNFα) and anti-inflammatory (IL-10) cytokines from 12 months old immune cells. N = 6 animals per age, conditioned medium was pooled and added at a ratio of 1:3 to the osteogenic differentiation medium, assays were performed in triplicates, mean ± SD, unpaired *t*-test, $^*p < 0.05$.

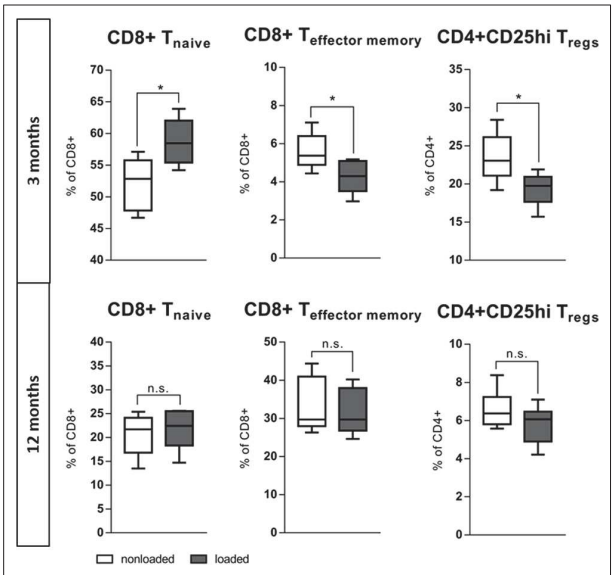

FIGURE 8 | *In vivo* rescue of experience level in the immune system with mechanical loading. The left tibia of 3 and 12 month old mice underwent daily (Monday–Friday) *in vivo* axial compressive cyclic loading for 2 week, thereafter the bone marrow was flow cytometric analyzed. In 3 month old mice the mechanical loading of the tibia increased the population of naïve CD8+ T cells and decreased the effector memory population locally in the bone marrow. CD4+ Tregs decreased comparably to the effector memory T cells. This more naïve immune milieu created under mechanical loading is not viable in 12 months old mice. $N = 6$ animals per age, boxplot distribution with median, Mann-Whitney *U*-test, $^*p < 0.05$.

this effect is reduced in aged individuals (36, 44). The question arose whether this also relates to the immune response involved. The left tibia of 3 and 12 month old mice underwent daily (Monday-Friday) *in vivo* axial compressive cyclic loading for 2 weeks. After 2 weeks, the bone marrow from the loaded and from the non-loaded contralateral tibia was harvested and analyzed with flow cytometry. Strikingly, within the loaded tibia of the young 3 months old mice a more naïve immune phenotype arose when compared to the contralateral non-loaded bone. In the bone marrow of the loaded tibia from the 3 months old mice, the naïve CD8+ T cells increased to 58.7(±3.8)% of all CD8+ T cells compared to 52.2(±4.1)% in the contralateral non-loaded control tibia. In addition, the percentage of CD8+ effector/memory T cells significantly decreased under the influence of loading. This data suggests that a less inflammatory immune cell composition supports bone formation in response to loading of young mice (similar to what we observed in our *in vitro* experiments). This more naïve immune cell milieu did not coincide with loading in the aged, 12 months old mice. CD4+ Tregs, ascribed as potent anti-inflammatory cells, reacted contrariwise to loading with a decrease of their proportion within the bone marrow of the loaded tibia (**Figure 8**). These findings show that the positive effect that mechanical loading had in young mice was absent in the aged animals, and that could indeed be related to differences in the immune response to the mechanical stimulus.

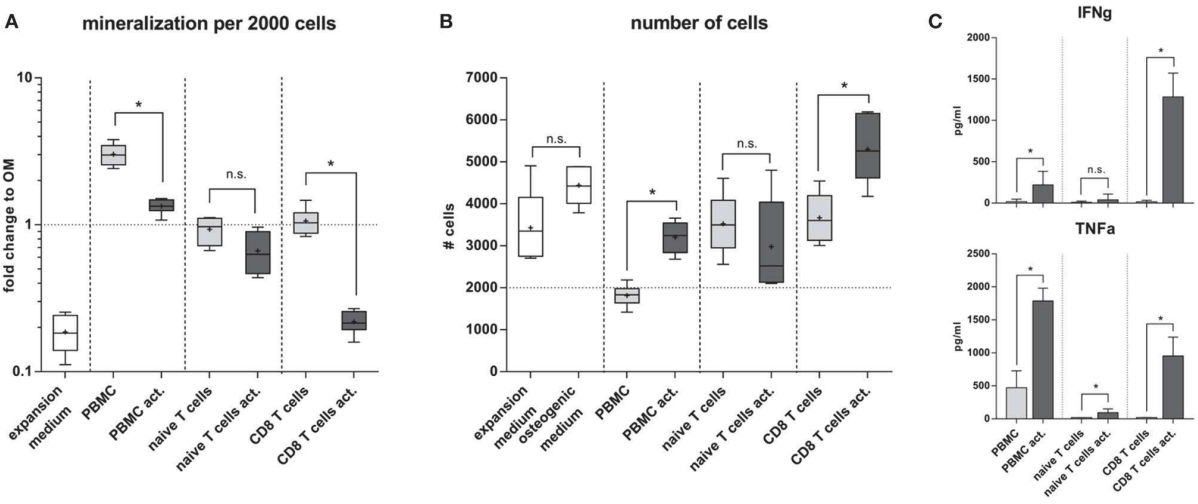

FIGURE 9 | Osteogenic differentiation under the influence of immune cell subsets. **(A)** Naïve T cells compared to CD8+ T cells did not alter the osteogenic differentiation. Activated CD8+ T cells significantly lowered the calcium deposition. Peripheral blood mononuclear cells (hPBMC) increased the mineralization of the extracellular matrix compared to the osteogenic medium without immune cells. This is due to a decreased proliferation **(B)**. Conditioned medium from CD8+ T cells increased proliferation but hindered the osteogenic differentiation of hMSC. **(C)** Cytokine production of activated CD8+ T cells was strong pro-inflammatory, activated PBMC mainly produced TNFα but not IFNγ, whereas activated naïve T cells did not produce significant amounts of IFNγ and TNFα. $N = 3$ immune cell donors, naïve and CD8+ T cell isolation was performed for each donor, $N = 2$ hMSC donors, assay was run in triplicates, boxplot distribution with median, mean depicted with a +, ELISA data shown as mean ± SD, unpaired *t*-test, $^*p < 0.05$.

To further understand the interdependency of an experienced immune system and the osteogenic capacity of mesenchymal stromal cells an *in vitro* "rescue experiment" was performed by analyzing specific cellular subsets in view of their effect on the osteogenic capacity. For this experiment the mouse model where age and immune experience were distinguishable was changed to human cells to model the patient situation more closely *in vitro*.

Naïve and Experienced Human Immune Cell Subsets Differently Affect Osteogenic Differentiation and Proliferation

To further elucidate the interrelation between bone structure and immune experience we selected a more clinically relevant situation by isolating naïve and experienced immune cells directly from human peripheral blood. Distinctly different immune subsets were tested for their influence on the differentiation capacity of human mesenchymal stromal cells (MSC). From density gradient isolated human peripheral blood mononuclear cells (hPBMC) either CD8+ T cells or naïve T cells were isolated and stimulated *in vitro* with CD3 and CD28. Mesenchymal stromal cells were isolated from bone marrow aspirates from patients undergoing hip surgery with written consent. The osteogenic differentiation outcome was calculated per 2000 cells to account for difference between proliferation and differentiation. Our data clearly showed that conditioned medium from naïve T cells did not dampen the osteogenic differentiation ability of MSC, whereas the conditioned medium from CD8+ T cells almost abolished the osteogenic differentiation (**Figure 9A**). Interestingly conditioned medium from activated CD8+ T cells induced proliferation in MSC. In contrast the conditioned medium from whole hPBMC hindered proliferation while supporting osteogenic differentiation (**Figure 9B**). Apparently, signaling patterns from specific immune cell subsets play an important role in distinguishing whether cell proliferation or differentiation is supported and activated. Thus, immune cells appear essential in guiding tissue formation—such as bone formation—and thereby impact the resulting tissue structure. Quantitative cytokine detection revealed an inert cytokine pattern in activated naïve T cells compared to activated CD8+ T cells, which produced a high concentration of IFNγ and TNFα. PBMC already produced a faint milieu of TNFα functionally inhibiting the proliferation of MSCs and therefore promoting the differentiation process as described within other studies (45) (**Figure 9C**).

Determining that the immune cell composition influences the osteogenic potential from mesenchymal stromal cells indicates that the immune signature will also influence the bone healing capacity. Thus, the initial observation that aged patients show a reduced healing capacity (confirmed in a mouse model with an experienced non-SPF immune cell composition) could be related to an experienced immune signature. To further investigate this hypothesis, bone healing was analyzed in a mouse model with a humanized immune system that was either more naive or already more experienced.

In vivo: Bone Regeneration Benefits From a Naïve Immune Milieu

To monitor the behavior of different immune phenotypes on the *in vivo* bone regeneration, a humanized peripheral blood mononuclear cell (hPBMC) mouse model was used: the

humanized PBMC NOD scid gamma (NSG) mice. NOD.Cg-Prkdc^{scid} Il2rg^{tm1Wjl}/SzJ (NSG) mice lack the ability to activate their own immune system and some immune subsets are even completely missing. Human PBMC from different donors were analyzed toward the immune phenotype and an experience level for stratification was achieved via the CD8+ T_{EMRA} level. CD8+ T_{EMRA} cells are known from earlier studies to be predictive for delayed bone healing as published by Reinke et al. (42). Donors with a CD8+ T_{EMRA} level above 30% of total CD8+ T cells were considered as immunologically experienced. NSG mice received intravenously either naïve or experienced hPBMCs from stratified donors and consecutively underwent surgery to introduce a 0.7 mm osteotomy gap stabilized with a unilateral external fixator (MouseExFix, RISystem, Davos, Switzerland). Healing outcome was assessed 21 days post-surgery with microCT. Three groups were analyzed: one group did not receive human immune cells (control), one group received naïve hPBMCs and one group received experienced hPBMCs. The transfection efficacy and accumulation of the human immune cells inside the tissue was verified after 3 and 21 days with flow cytometry (**Figures 10A,B**). The callus 21 days post-surgery showed an increased bone volume fracture (BV/TV) under the influence of naïve hPBMCs compared to the control as well as compared to experienced hPBMC. The bone volume fraction for the group receiving experienced hPBMC did not differ to the control. Quantifying the bone mineral density (BMD) revealed a benefit of immune cells on newly formed bone with an increased mineral density even with experienced immune cells compared to the control. Remarkably, the group with naïve hPBMC showed the highest density of mineralization among all groups. Under the influence of injected hPBMCs newly formed bone revealed a decrease in trabecular numbers while the thickness of those structures significantly increased. The naïve hPBMCs significantly increased the deposition of mineral tissue showing the positive effect of a young/ naïve immune system on the bone healing process (**Figure 10C**). These findings show that bone regeneration benefits from a more naïve immune system.

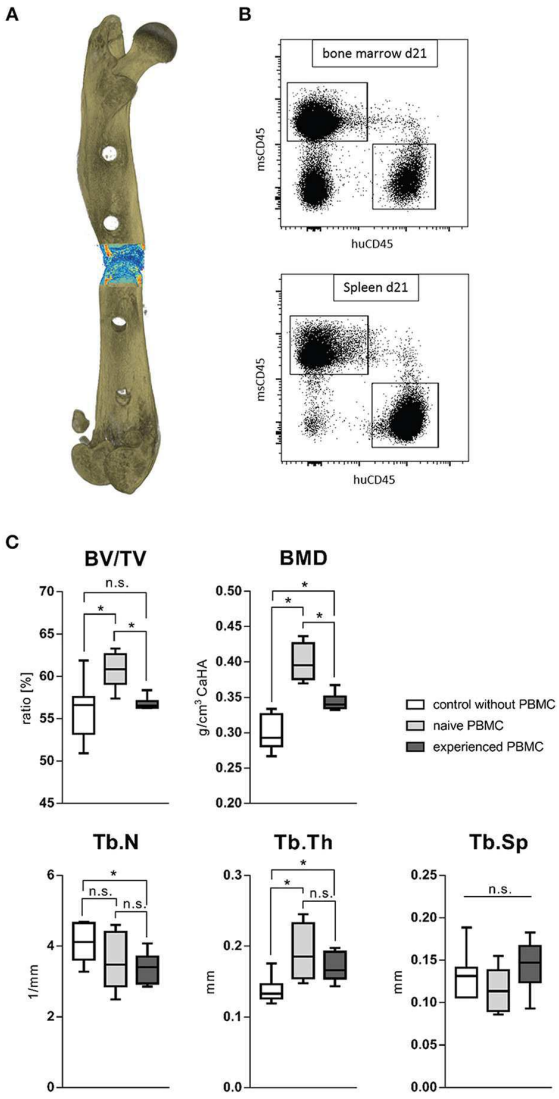

FIGURE 10 | Fracture healing outcome of humanized PBMC mice. **(A)** Representative image of a 21 days old fracture gap. **(B)** Human immune cells settled to spleen and bone marrow in significant levels after transfer. **(C)** Healing under the influence of either experienced or more naïve peripheral blood mononuclear cells (hPBMC) showed a beneficial effect of a more naïve immune phenotype. The bone volume in total volume (BV/TV) was significantly increased under the influence of more naïve hPBMC compared to the control without hPBMC and more experienced hPBMC. The bone mineral density (BMD) and trabecular thickness (Tb.Th) stood to benefit from immune cells. The more naïve hPBMC further increased the mineral density within the fracture gap compared to more experienced hPBMC. The number of newly formed trabecular structures (Tb.N) seemed to decrease under the influence of more experienced hPBMC. $N = 6$ animals in the naïve hPBMC group, $N = 8$ each in control and experienced hPBMC group, boxplot distribution with median, Mann-Whitney U-test, $^*p < 0.05$.

DISCUSSION

Changes within the skeletal system upon aging have been widely acknowledged. This study showed for the first time that not only the chronological age but also the immunological age substantially impacts bone mass and microstructure and should be considered in assessing patient's risk factors and healing potential (42). The immunological age is mostly determined by changes in the adaptive immune system. With increasing antigen exposure, the effector and effector memory pool within the adaptive immunity of an individual increases, while simultaneously the naïve lymphocyte pool diminishes. This process of immune-aging is greatly influenced by time but not *per se* comparable among individuals, specifically if they have seen different immune challenges. This is also mirrored in our data where the immune composition of exposed mice show an increasing standard deviation in the CD8+ T central and effector memory cell population after 2 years of environmental exposure (in a still relatively standardized environment of animal housing). The direction of the immune aging process is comparable among people, however, the pace

with which it proceeds differs due to the living environment and personal habits.

As a first example to illustrate the relevance of the immune experience, we focused on the common assumption that bone healing in the elderly is impaired (46), albeit most studies do not properly document reasons for lack of healing in the aged population (47). There is a paucity of supportive data within the scientific literature on the immune experience or its effect on various biological processes (mainly due to a lack of proper documentation in preclinical studies). Only recently have questionnaires such as the ARRIVE guidelines for preclinical studies included questions related to housing and husbandry that allow one to determine the immunological age of an animal. To analyze the effect of the immune experience on bone homeostasis and healing, immune aging had to be characterized within a mouse model. By dividing mice into two groups and keeping those under specific pathogen free conditions and antigen exposed conditions, respectively, during aging it became possible to distinguish between skeletal changes caused by chronological aging vs. changes that were dependent on the immunological age/state of the animals (biological aging).

Analyzing immune-aging in mice showed an increase in memory and effector function with age. The exposure to antigens in non-SPF housings led to an amplified age-associated phenotype of the immune system, reflecting the changes seen in humans (23). One-year-old non-SPF housed mice appeared to be able to reflect roughly a 40–50 years old human while 2-year-old non-SPF mice reflected humans of around 50–60 years of age. Using such approach, a mouse model was established that allowed the analysis of immune-aging on the bone.

For the analysis of the impact of the immune experience within the study a model was chosen that enabled the investigation of mice of the same age but with a differently developed adaptive immune system due to a difference in housing (SPF vs. non-SPF). While the animals were held as similar as possible in order to determine the immune experience as the source of the changes detected in the bone, additional influences could have had an impact. The influences of the changed immune composition could lead to a change in other cell compartments (e.g., the more pro-inflammatory signaling could induce higher M1 macrophage percentages), epigenetic changes could also occur which were not considered within this study. Also, the microbiota is a potent modulator of the immune system and vice versa, an influence that would offer future research opportunities (9, 48, 49). To overcome this possible bias the humanized PBMC mouse model was applied within this study—these mice were identical up to the day before osteotomy when they received the human immune cells and were kept under identical conditions thereafter for the observation time of 21 days—a time period where the above mentioned changes would not occur in a meaningful way.

It is well-known that biomechanical properties of bone, specifically the energy to mechanical failure decreases with age (50). While our data confirmed the age related changes in biomechanical properties this is the first study to depict that some of these changes are intensified by the immune experience level. This loss in mechanical properties is usually associated with age-related bone microstructural changes in both the cortical and trabecular compartments (51–53) So far, a link between age-related bone loss and adaptive immunity, specifically the experience of the immune system had not been investigated (50–54).

On the other hand, cellular senescence occurring in elderly individuals is a major hallmark of age associated processes representing various types of stress that cause distinct cellular alterations, including major changes in gene expression and metabolism, eventually leading to the development of a pro-inflammatory secretome (55). In accordance with the literature the monocyte-macrophage-osteoclast lineage and the mesenchymal stem cell-osteoblast lineage are affected by increasing age, which is associated with higher baseline levels of inflammatory mediators, and therefore a significant reduction in osteogenic capabilities can be observed (56). This inflamm-aging affects different signaling pathways, gene expression, cellular events like proliferation and differentiation, chemotaxis of precursor cells, expression of growth regulatory factors and the production of bone structural proteins. All these affected processes represent the complex orchestration of interdependent biological events that occur during fracture repair (57).

For the first time, our study clearly illustrates the influence of the experienced immune phenotype on changes in bone mass, microstructure, and mechanical properties that go beyond those attributed to chronological aging. Keeping mice under non-SPF conditions lead to increased cortical thickness. The stiffness and maximal force at failure increased with age due to an increased mineralization density. However, the cortical thickness changed in conjunction with the altered immune composition. The experienced immune signature led to an altered and a more stiff bone structure and a more brittle fracture. Such brittleness increases the risk of fracture upon low-impact loads or injuries—a phenomenon frequently seen in aged patients (58). For the first time, the reduced bone structure and phenotype of an aged bone found in elderly patients can be seen to be even worsened by an immune-aged or inflamm-aged setting. The strong link between immune experience and structural properties makes an immune diagnostic approach to stratify patients according to their immune status a relevant perspective, so far widely ignored in bone treatment and research. Studies from Zhao et al. using a bioinformatics approach revealed likewise significant changes in the inflammatory response during fracture healing upon aging. The inflammatory response was shown to be enriched in the elderly compared to the younger population. In addition changes in the Wnt signaling pathway, vascularization-associated processes, and synaptic-related functions may account for delayed fracture healing in the elderly (59).

The interdependency of the immune and bone compartment has been investigated from different perspectives. Concerning the interplay of osteoclasts and immune cells the pro-inflammatory cytokines TNFα and IFNγ which were analyzed within this study as cytokines delaying the healing/ osteogenesis have been discussed as promoting osteoclastogenesis (60). Bone loss in postmenopausal osteoporosis has been addressed by anti-TNFα treatments (61). This indicates the elevated TNFα levels

could be causative for the postmenopausal bone loss. So far, the immune experience and the higher TNFα levels going hand in hand with higher levels of effector memory T cells has however not yet been considered. That the more pro-inflammatory state of the experienced immune system with high numbers of TNFα producing effector memory T cells could be responsible for reduced bone formation or even bone loss is also mirrored in previous studies where activated T cells have been correlated to bone loss in conditions of inflammation and autoimmune disorders (62, 63), osteoporosis models (64, 65), or even periodontitis and cancer (66–68).

So far, the age-related alteration in mechano-response was solely explained by the mechanical signal losing its specificity to activate osteoblasts or inhibit osteoclasts (69). The here presented data suggest a reprograming of immunity toward a more naïve phenotype and thus a potential rescue mode in young animals. Interestingly, the rescue was only significant in young individuals but showed similar trends in the older animals, suggesting the immune system may play a role in the bones reduced mechano-response with age. The impact of mechanical loading on adaptive immunity illustrates the immune-structure relationship, and thus identifies a re-gain in ones naïve immunity as an additional route that could be exploited therapeutically in the future. In a clinical study moderate intensity exercise in adult subjects revealed a decrease of osteoclastogenic cytokines, showing that biomechanical loading could represent a potential immune modulator (70).

How is bone healing impacted by the immune status? Upon a bone fracture, a cascade of sterile inflammatory reactions are initiated which determine a successful, delayed or failed bone healing (12, 19, 71–73). Earlier studies have shown that a prolonged pro-inflammatory response delays the healing process. Such a prolonged pro-inflammatory cascade could be further enhanced by the here reported immune-aged or inflamm-aged status resulting in a more severe delay of healing. The reported data in the present study demonstrates clearly that a naïve immune system leads to an effective healing while an experienced immunity significantly delays bone formation, as demonstrated by the humanized PBMC mouse models. Again, patient stratification early on would allow for the identification of patients at risk of delayed healing due to an immune-aged status. Preemptive measures could be initiated in these patients to compensate for their healing deficit. A biomarker study is currently ongoing to threshold patients by the level of CD8+ T_{EMRA} cells for a high risk of delayed bone healing (42). As a potential measure to reprogram immunity toward a more naïve phenotype, a mechanical limb loading stimulation such as those experienced in physical exercise was presented. Although a "rescue" toward a more naïve phenotype could clearly be found in young (leading also to an enhanced bone homeostasis) the effect was substantially reduced in a more aged mouse model. Thus, the effect of mechano-therapeutics as measures to reprogram the immune system may alone not be completely sufficient yet. Further in depth understanding of

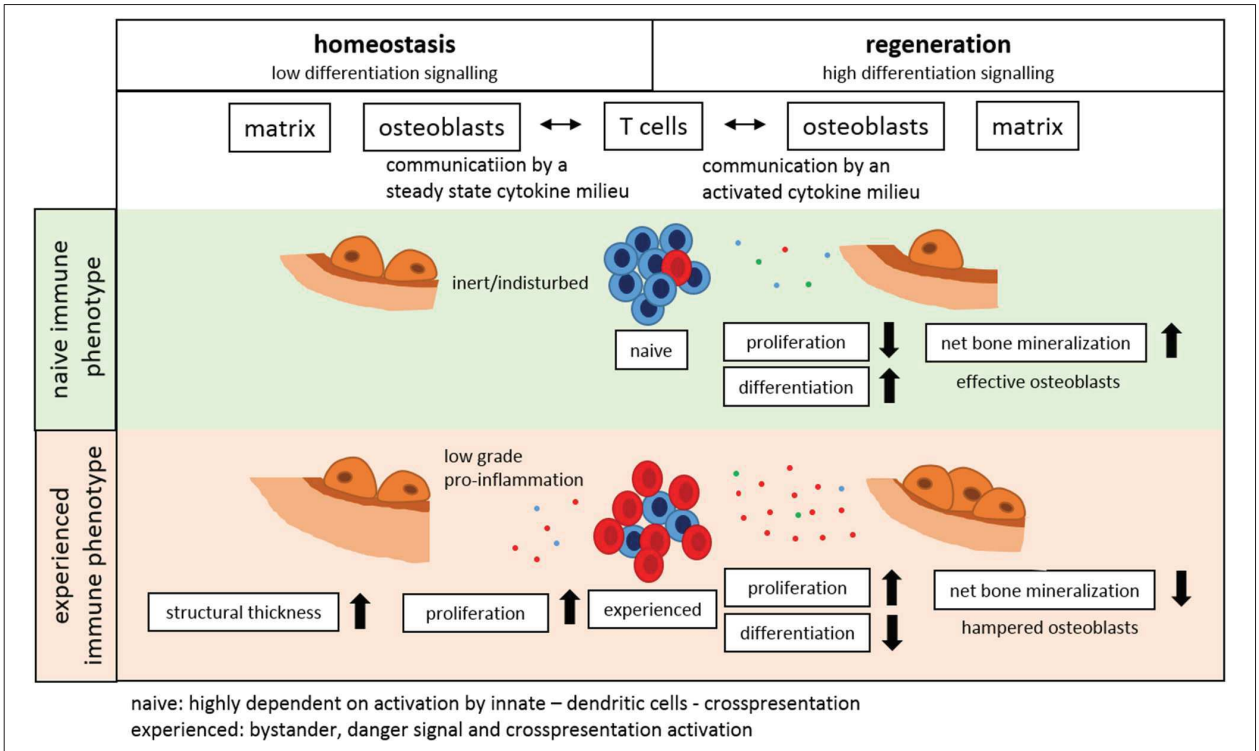

FIGURE 11 | The immune system impacts bone formation.

the processes of re-programming the immune compartment, specifically in inflamm-aged situations seems to be important to further elucidate the therapeutic potential of mechanical loading in the senescent skeleton.

CONCLUSION

In conclusion, our data presented here clearly shows for the first time a distinct link of the immune system to the structural properties of bone as those involved in bone homeostasis, regeneration and adaptation. The experience of the immune system directly impacts bone formation capability and thereby affects structural properties of trabecular and cortical bone as well as overall mechanical competence (**Figure 11**).

ETHICS STATEMENT

This study was carried out in accordance with the recommendations of the ARRIVE and institutional guidelines. The protocol was approved by the Landesamt für Gesundheit und Soziales, LaGeSo, Berlin.

AUTHOR CONTRIBUTIONS

CB, KS-B, GD, BW, and H-DV: conceptual idea and design of the study; CB, CS, SW, DW, FS, and TT: data collection, analysis, and interpretation; CB, KS-B, and AE: animal surgeries; CB, KS-B, CS, GD, H-DV, and BW: drafting of the manuscript; RS: clinical data. All authors revised the manuscript.

FUNDING

This work was supported by a grant from the German Research Foundation (FG 2195: DFG SCHM 2977, DU 298/21-1), the FriedeSpringer Stiftung, the Berlin-Brandenburg Center for Regenerative Therapies, the Berlin-Brandenburg School for Regenerative Therapies and the Einstein Center for Regenerative Therapies.

ACKNOWLEDGMENTS

We would like to acknowledge the Open Access Publication Fund of Charité – Universitätsmedizin Berlin.

We would like to thank Norma Schulz, Anke Dienelt, Christine Figge, Mario Thiele, Anne Seliger and the core unit "Cell and Tissue harvesting."

SUPPLEMENTARY MATERIAL

The Supplementary Material for this article can be found online at: https://www.frontiersin.org/articles/10.3389/fimmu.2019.00797/full#supplementary-material

REFERENCES

1. Manini T. Development of physical disability in older adults. *Curr Aging Sci.* (2011) 4:184–91. doi: 10.2174/1874609811104030184
2. Kiel DP, Rosen CJ, Dempster D. Chapter 20: Age-related bone loss. In: *Primer on the Metabolic Bone Diseases and Disorders of Mineral Metabolism.* Hoboken, NJ: John Wiley & Sons, Inc. (2008) p. 98–102. doi: 10.1002/9780470623992.ch20
3. World Health Organization. *Ageing Heal.* Geneva: Wolrd Health Organization (2018). Available online at: http://www.who.int (accessed February 5, 2018).
4. Bishop JA, Palanca AA, Bellino MJ, Lowenberg DW. Assessment of compromised fracture healing. *J Am Acad Orthop Surg.* (2012) 20:273–82. doi: 10.5435/JAAOS-20-05-273
5. Schmidt-Bleek K, Marcucio R, Duda G. Future treatment strategies for delayed bone healing: an osteoimmunologic approach. *J Am Acad Orthop Surg.* (2016) 24:e134–5. doi: 10.5435/JAAOS-D-16-00513
6. Ono T, Takayanagi H. Osteoimmunology in bone fracture healing. *Curr Osteoporos Rep.* (2017) 15:367–75. doi: 10.1007/s11914-017-0381-0
7. Limmer A, Wirtz D. Osteoimmunology: influence of the immune system on bone regeneration and consumption. *Z Orthop Unfall.* (2017) 155:273–80. doi: 10.1055/s-0043-100100
8. Takayanagi H. New developments in osteoimmunology. *Nat Rev Rheumatol.* (2012) 8:684–9. doi: 10.1038/nrrheum.2012.167
9. Walsh MC, Takegahara N, Kim H, Choi Y. Updating osteoimmunology: regulation of bone cells by innate and adaptive immunity. *Nat Rev Rheumatol.* (2018) 14:146–56. doi: 10.1038/nrrheum.2017.213
10. Ginaldi L, De Martinis M. Osteoimmunology and beyond. *Curr Med Chem.* (2016) 23:3754–74. doi: 10.2174/0929867323666160907162546
11. Schlundt C, Schell H, Goodman SB, Vunjak-Novakovic G, Duda GN, Schmidt-Bleek K. Immune modulation as a therapeutic strategy in bone regeneration. *J Exp Orthop.* (2015) 2:1–10. doi: 10.1186/s40634-014-0017-6
12. Schmidt-Bleek K, Kwee BJ, Mooney DJ, Duda GN. Boon and bane of inflammation in bone tissue regeneration and its link with angiogenesis. *Tissue Eng Part B Rev.* (2015) 21:354–64. doi: 10.1089/ten.teb.2014.0677
13. Schett G. Effects of inflammatory and anti-inflammatory cytokines on the bone. *Eur J Clin Invest.* (2011) 41:1361–6. doi: 10.1111/j.1365-2362.2011.02545.x
14. Pfeilschifter J, Chenu C, Bird A, Mundy GR, Roodman DG. Interleukin-1 and tumor necrosis factor stimulate the formation of human osteoclastlike cells *in vitro*. *J Bone Miner Res.* (2009) 4:113–8. doi: 10.1002/jbmr.5650040116
15. Adamopoulos IE, Bowman EP. Immune regulation of bone loss by Th17 cells. *Arthritis Res Ther.* (2008) 10:225. doi: 10.1186/ar2502
16. Akdis M, Burgler S, Crameri R, Eiwegger T, Fujita H, Gomez E, et al. Interleukins, from 1 to 37, and interferon-γ: receptors, functions, and roles in diseases. *J Allergy Clin Immunol.* (2011) 127:701–21.e70. doi: 10.1016/J.JACI.2010.11.050
17. Li Y, Toraldo G, Li A, Yang X, Zhang H, Qian WP, et al. B cells and T cells are critical for the preservation of bone homeostasis and attainment of peak bone mass *in vivo*. *Blood.* (2007) 109:3839–48. doi: 10.1182/blood-2006-07-037994
18. Schell H, Duda GN, Peters A, Tsitsilonis S, Johnson KA, Schmidt-Bleek K. The haematoma and its role in bone healing. *J Exp Orthop.* (2017) 4:5. doi: 10.1186/s40634-017-0079-3
19. Schmidt-Bleek K, Schell H, Schulz N, Hoff P, Perka C, Buttgereit F, et al. Inflammatory phase of bone healing initiates the regenerative healing cascade. *Cell Tissue Res.* (2012) 347:567–73. doi: 10.1007/s00441-011-1205-7
20. Schmidt-Bleek K, Schell H, Lienau J, Schulz N, Hoff P, Pfaff M, et al. Initial immune reaction and angiogenesis in bone healing. *J Tissue Eng Regen Med.* (2014) 8:120–30. doi: 10.1002/term.1505
21. Könnecke I, Serra A, El Khassawna T, Schlundt C, Schell H, Hauser A, et al. T and B cells participate in bone repair by infiltrating the fracture callus in a two-wave fashion. *Bone.* (2014) 64:155–65. doi: 10.1016/j.bone.2014.03.052

22. El Khassawna T, Serra A, Bucher CH, Petersen A, Schlundt C, Könnecke I, et al. T lymphocytes influence the mineralization process of bone. *Front Immunol.* (2017) 8:562. doi: 10.3389/fimmu.2017.00562
23. Kverneland AH, Streitz M, Geissler E, Hutchinson J, Vogt K, Boës D, et al. Age and gender leucocytes variances and references values generated using the standardized ONE-Study protocol. *Cytometry A.* (2016) 89:543–64. doi: 10.1002/cyto.a.22855
24. Qi Q, Liu Y, Cheng Y, Glanville J, Zhang D, Lee J-Y, et al. Diversity and clonal selection in the human T-cell repertoire. *Proc Natl Acad Sci USA.* (2014) 111:13139–44. doi: 10.1073/pnas.1409155111
25. Weyand CM, Goronzy JJ. Aging of the immune system. Mechanisms and therapeutic targets. *Ann Am Thorac Soc.* (2016) 13:S422–8. doi: 10.1513/AnnalsATS.201602-095AW
26. Clark D, Nakamura M, Miclau T, Marcucio R. Effects of aging on fracture healing. *Curr Osteoporos Rep.* (2017) 15:601–8. doi: 10.1007/s11914-017-0413-9
27. Schoenborn JR, Wilson CB. Regulation of interferon-γ during innate and adaptive immune responses. *Adv Immunol.* (2007) 96:41–101. doi: 10.1016/S0065-2776(07)96002-2
28. Becker TC, Coley SM, Wherry EJ, Ahmed R. Bone marrow is a preferred site for homeostatic proliferation of memory CD8 T cells. *J Immunol.* (2005) 174:1269–73. doi: 10.4049/JIMMUNOL.174.3.1269
29. Di Rosa F, Gebhardt T. Bone marrow T cells and the integrated functions of recirculating and tissue-resident memory T cells. *Front Immunol.* (2016) 7:51. doi: 10.3389/fimmu.2016.00051
30. Badylak S. Perspective: work with, not against, biology. *Nature.* (2016) 540:S55. doi: 10.1038/540S55a
31. Badylak S, Rosenthal N. Regenerative medicine: are we there yet? *npj Regen Med.* (2017) 2:2. doi: 10.1038/s41536-016-0005-9
32. Tsitsilonis S, Seemann R, Misch M, Wichlas F, Haas NP, Schmidt-Bleek K, et al. The effect of traumatic brain injury on bone healing: an experimental study in a novel *in vivo* animal model. *Injury.* (2015) 46:661–5. doi: 10.1016/j.injury.2015.01.044
33. Jaiswal N, Haynesworth SE, Caplan AI, Bruder SP. Osteogenic differentiation of purified, culture-expanded human mesenchymal stem cells *in vitro*. *J Cell Biochem.* (1997) 64:295–312. doi: 10.1002/(SICI)1097-4644(199702)64:2<295::AID-JCB12>3.0.CO;2-I
34. Willie BM, Birkhold AI, Razi H, Thiele T, Aido M, Kruck B, et al. Diminished response to *in vivo* mechanical loading in trabecular and not cortical bone in adulthood of female C57Bl/6 mice coincides with a reduction in deformation to load. *Bone.* (2013) 55:335–46. doi: 10.1016/J.BONE.2013.04.023
35. Clarke K., Still J. Gait analysis in the mouse. *Physiol Behav.* (1999) 66:723–9. doi: 10.1016/S0031-9384(98)00343-6
36. Birkhold AI, Razi H, Duda GN, Weinkamer R, Checa S, Willie BM. Mineralizing surface is the main target of mechanical stimulation independent of age: 3D dynamic *in vivo* morphometry. *Bone.* (2014) 66:15–25. doi: 10.1016/j.bone.2014.05.013
37. De Souza RL, Matsuura M, Eckstein F, Rawlinson SCF, Lanyon LE, Pitsillides AA. Non-invasive axial loading of mouse tibiae increases cortical bone formation and modifies trabecular organization: a new model to study cortical and cancellous compartments in a single loaded element. *Bone.* (2005) 37:810–8. doi: 10.1016/j.bone.2005.07.022
38. Sugiyama T, Meakin LB, Browne WJ, Galea GL, Price JS, Lanyon LE. Bones' adaptive response to mechanical loading is essentially linear between the low strains associated with disuse and the high strains associated with the lamellar/woven bone transition. *J Bone Miner Res.* (2012) 27:1784–93. doi: 10.1002/jbmr.1599
39. Spranger S, Frankenberger B, Schendel DJ. NOD/scid IL-2Rg(null) mice: a preclinical model system to evaluate human dendritic cell-based vaccine strategies *in vivo*. *J Transl Med.* (2012) 10:30. doi: 10.1186/1479-5876-10-30
40. Ishikawa Y, Usui T, Shiomi A, Shimizu M, Murakami K, Mimori T. Functional engraftment of human peripheral T and B cells and sustained production of autoantibodies in NOD/LtSzscid/IL-2Rγ $^{-/-}$ mice. *Eur J Immunol.* (2014) 44:3453–63. doi: 10.1002/eji.201444729
41. King M, Pearson T, Rossini AA, Shultz LD, Greiner DL. Humanized mice for the study of type 1 diabetes and beta cell function. *Ann N Y Acad Sci.* (2008) 1150:46–53. doi: 10.1196/annals.1447.009
42. Reinke S, Geissler S, Taylor WR, Schmidt-Bleek K, Juelke K, Schwachmeyer V, et al. Terminally differentiated $CD8^+$ T cells negatively affect bone regeneration in humans. *Sci Transl Med.* (2013) 5:177ra36. doi: 10.1126/scitranslmed.3004754
43. Chen J-H, Liu C, You L, Simmons CA. Boning up on Wolff's Law: mechanical regulation of the cells that make and maintain bone. *J Biomech.* (2010) 43:108–18. doi: 10.1016/J.JBIOMECH.2009.09.016
44. Birkhold AI, Razi H, Duda GN, Weinkamer R, Checa S, Willie BM. The influence of age on adaptive bone formation and bone resorption. *Biomaterials.* (2014) 35:9290–301. doi: 10.1016/j.biomaterials.2014.07.051
45. Mountziaris PM, Spicer PP, Kasper FK, Mikos AG. Harnessing and modulating inflammation in strategies for bone regeneration. *Tissue Eng Part B Rev.* (2011) 17:393–402. doi: 10.1089/ten.TEB.2011.0182
46. Gruber R, Koch H, Doll BA, Tegtmeier F, Einhorn TA, Hollinger JO. Fracture healing in the elderly patient. *Exp Gerontol.* (2006) 41:1080–93. doi: 10.1016/J.EXGER.2006.09.008
47. Goldhahn J, Suhm N, Goldhahn S, Blauth M, Hanson B. Influence of osteoporosis on fracture fixation - a systematic literature review. *Osteoporos Int.* (2008) 19:761–72. doi: 10.1007/s00198-007-0515-9
48. Gibon E, Loi F, Córdova LA, Pajarinen J, Lin T, Lu L, et al. Aging affects bone marrow macrophage polarization: relevance to bone healing. *Regen Eng Transl Med.* (2016) 2:98–104. doi: 10.1007/s40883-016-0016-5
49. Albright JM, Dunn RC, Shults JA, Boe DM, Afshar M, Kovacs EJ. Advanced age alters monocyte and macrophage responses. *Antioxid Redox Signal.* (2016) 25:805–15. doi: 10.1089/ars.2016.6691
50. Willinghamm MD, Brodt MD, Lee KL, Stephens AL, Ye J, Silva MJ. Age-related changes in bone structure and strength in female and male BALB/c Mice. *Calcif Tissue Int.* (2010) 86:470–83. doi: 10.1007/s00223-010-9359-y
51. Ferguson VL, Ayers RA, Bateman TA, Simske SJ. Bone development and age-related bone loss in male C57BL/6J mice. *Bone.* (2003) 33:387–98. doi: 10.1016/S8756-3282(03)00199-6
52. Glatt V, Canalis E, Stadmeyer L, Bouxsein ML. Age-related changes in trabecular architecture differ in female and male C57BL/6J mice. *J Bone Miner Res.* 22:1197–207. doi: 10.1359/jbmr.070507
53. Halloran BP, Ferguson VL, Simske SJ, Burghardt A, Venton LL, Majumdar S. Changes in bone structure and mass with advancing age in the male C57BL/6J mouse. *J Bone Miner Res.* (2002) 17:1044–50. doi: 10.1359/jbmr.2002.17.6.1044
54. Weiss A, Arbell I, Steinhagen-Thiessen E, Silbermann M. Structural changes in aging bone: osteopenia in the proximal femurs of female mice. *Bone.* (1991) 12:165–72. doi: 10.1016/8756-3282(91)90039-L
55. Farr JN, Khosla S. Cellular senescence in bone. *Bone.* (2019) 121:121–33. doi: 10.1016/j.bone.2019.01.015
56. Gibon E, Lu L, Goodman SB. Aging, inflammation, stem cells, and bone healing. *Stem Cell Res Ther.* (2016) 7:44. doi: 10.1186/s13287-016-0300-9
57. Hadjiargyrou M, O'Keefe RJ. The Convergence of fracture repair and stem cells: interplay of genes, aging, environmental factors and disease. *J Bone Miner Res.* (2014) 29:2307–22. doi: 10.1002/jbmr.2373
58. Zimmermann EA, Schaible E, Bale H, Barth HD, Tang SY, Reichert P, et al. Age-related changes in the plasticity and toughness of human cortical bone at multiple length scales. *Proc Natl Acad Sci USA.* (2011) 108:14416–21. doi: 10.1073/pnas.1107966108
59. Zhao S-J, Kong F-Q, Fan J, Chen Y, Zhou S, Xue M-X, et al. Bioinformatics analysis of the molecular mechanism of aging on fracture healing. *Biomed Res Int.* (2018) 2018:7530653. doi: 10.1155/2018/7530653
60. Mori G, D'Amelio P, Faccio R, Brunetti G. The Interplay between the bone and the immune system. *Clin Dev Immunol.* (2013) 2013:720504. doi: 10.1155/2013/720504
61. Charatcharoenwitthaya N, Khosla S, Atkinson EJ, McCready LK, Riggs BL. Effect of blockade of TNF-α and interleukin-1 action on bone resorption in early postmenopausal women. *J Bone Miner Res.* (2007) 22:724–9. doi: 10.1359/jbmr.070207
62. Kong Y-Y, Feige U, Sarosi I, Bolon B, Tafuri A, Morony S, et al. Activated T cells regulate bone loss and joint destruction in adjuvant arthritis through osteoprotegerin ligand. *Nature.* (1999) 402:304–9. doi: 10.1038/46303
63. Colucci S, Brunetti G, Cantatore F, Oranger A, Mori G, Quarta L, et al. Lymphocytes and synovial fluid fibroblasts support osteoclastogenesis

through RANKL, TNFα, and IL-7 in an *in vitro* model derived from human psoriatic arthritis. *J Pathol.* (2007) 212:47–55. doi: 10.1002/path.2153
64. Faienza MF, Brunetti G, Colucci S, Piacente L, Ciccarelli M, Giordani L, et al. Osteoclastogenesis in children with 21-hydroxylase deficiency on long-term glucocorticoid therapy: the role of receptor activator of nuclear factor-κB ligand/osteoprotegerin imbalance. *J Clin Endocrinol Metab.* (2009) 94:2269–76. doi: 10.1210/jc.2008-2446
65. Weitzmann MN, Pacifici R. Estrogen deficiency and bone loss: an inflammatory tale. *J Clin Invest.* (2006) 116:1186–94. doi: 10.1172/JCI28550
66. Tsukasaki M, Komatsu N, Nagashima K, Nitta T, Pluemsakunthai W, Shukunami C, et al. Host defense against oral microbiota by bone-damaging T cells. *Nat Commun.* (2018) 9:701. doi: 10.1038/s41467-018-03147-6
67. Teng YT, Nguyen H, Gao X, Kong YY, Gorczynski RM, Singh B, et al. Functional human T-cell immunity and osteoprotegerin ligand control alveolar bone destruction in periodontal infection. *J Clin Invest.* (2000) 106:R59–67. doi: 10.1172/JCI10763
68. Colucci S, Brunetti G, Rizzi R, Zonno A, Mori G, Colaianni G, et al. T cells support osteoclastogenesis in an *in vitro* model derived from human multiple myeloma bone disease: the role of the OPG/TRAIL interaction. *Blood.* (2004) 104:3722–30. doi: 10.1182/blood-2004-02-0474
69. Razi H, Birkhold AI, Weinkamer R, Duda GN, Willie BM, Checa S. Aging leads to a dysregulation in mechanically driven bone formation and resorption. *J Bone Miner Res.* (2015) 30:1864–73. doi: 10.1002/jbmr.2528
70. Smith JK, Dykes R, Chi DS. The effect of long-term exercise on the production of osteoclastogenic and antiosteoclastogenic cytokines by peripheral blood mononuclear cells and on serum markers of bone metabolism. *J Osteoporos.* (2016) 2016:1–11. doi: 10.1155/2016/5925380
71. Hoff P, Gaber T, Schmidt-Bleek K, Sentürk U, Tran CL, Blankenstein K, et al. Immunologically restricted patients exhibit a pronounced inflammation and inadequate response to hypoxia in fracture hematomas. *Immunol Res.* (2011) 51:116–22. doi: 10.1007/s12026-011-8235-9
72. Schlundt C, El Khassawna T, Serra A, Di-Enelt A, Wendler S, Schell H, et al. Macrophages in bone fracture healing: their essential role in endochondral ossification. *Bone.* (2015) 106:78–89. doi: 10.1016/j.bone.2015.10.019
73. Bucher CH, Lei H, Duda GN, Volk H-D, Schmidt-Bleek K. The role of immune reactivity in bone regeneration. In: *Advanced Techniques in Bone Regeneration* (London: InTech). doi: 10.5772/62476

Conflict of Interest Statement: The authors declare that the research was conducted in the absence of any commercial or financial relationships that could be construed as a potential conflict of interest.

Publication 3: Individual Effector/Regulator T Cell Ratios Impact Bone Regeneration

Claudia Schlundt, Simon Reinke, Sven Geissler, Christian H. Bucher, Carolin Giannini, Sven Märdian, Michael Dahne, Christian Kleber, Björn Samans, Udo Baron, Georg N. Duda, Hans-Dieter Volk, Katharina Schmidt-Bleek, *Individual Effector/Regulator T Cell Ratios Impact Bone Regeneration*, Frontiers in Immunology, 2019

Auszug aus der Journal Summary List

Journal Data Filtered By: **Selected JCR Year: 2017** Selected Editions: SCIE,SSCI
Selected Categories: "**Immunology**" Selected Category Scheme: WoS
Gesamtanzahl: 155 Journale

Rank	Full Journal Title	Total Cites	Journal Impact Factor	Eigenfactor Score
1	NATURE REVIEWS IMMUNOLOGY	39,215	41.982	0.085360
2	Annual Review of Immunology	17,086	22.714	0.028800
3	NATURE IMMUNOLOGY	41,410	21.809	0.102290
4	IMMUNITY	46,541	19.734	0.136360
5	TRENDS IN IMMUNOLOGY	11,204	14.188	0.026850
6	JOURNAL OF ALLERGY AND CLINICAL IMMUNOLOGY	49,229	13.258	0.083800
7	Lancet HIV	1,476	11.355	0.007950
8	JOURNAL OF EXPERIMENTAL MEDICINE	62,537	10.790	0.078310
9	IMMUNOLOGICAL REVIEWS	14,555	9.217	0.028540
10	Cancer Immunology Research	4,361	9.188	0.021180
11	CLINICAL INFECTIOUS DISEASES	61,618	9.117	0.120010
12	AUTOIMMUNITY REVIEWS	8,956	8.745	0.020990
13	Journal for ImmunoTherapy of Cancer	1,675	8.374	0.007130
14	CURRENT OPINION IN IMMUNOLOGY	9,275	7.932	0.020120
15	JOURNAL OF AUTOIMMUNITY	6,410	7.607	0.015490
16	Cellular & Molecular Immunology	3,633	7.551	0.008300
17	EMERGING INFECTIOUS DISEASES	29,657	7.422	0.057980
18	Mucosal Immunology	6,105	7.360	0.021860
19	SEMINARS IN IMMUNOLOGY	4,552	7.206	0.010950
20	EXERCISE IMMUNOLOGY REVIEW	740	7.105	0.001110
21	Journal of Allergy and Clinical Immunology-In Practice	2,802	6.966	0.009670
22	CLINICAL REVIEWS IN ALLERGY & IMMUNOLOGY	2,741	6.442	0.005880
23	Seminars in Immunopathology	2,967	6.437	0.009290
24	BRAIN BEHAVIOR AND IMMUNITY	12,583	6.306	0.026850
25	ALLERGY	16,476	6.048	0.025790
26	Emerging Microbes & Infections	1,318	6.032	0.005910
27	Advances in Immunology	2,423	5.935	0.004250
28	Current Topics in Microbiology and Immunology	5,633	5.829	0.011740
29	World Allergy Organization Journal	1,352	5.676	0.003800
30	Frontiers in Immunology	16,999	5.511	0.067470

frontiers in Immunology

ORIGINAL RESEARCH
published: 16 August 2019
doi: 10.3389/fimmu.2019.01954

Individual Effector/Regulator T Cell Ratios Impact Bone Regeneration

Claudia Schlundt[1,2†], Simon Reinke[1,2†], Sven Geissler[1,2], Christian H. Bucher[1,2], Carolin Giannini[2,3], Sven Märdian[4], Michael Dahne[4], Christian Kleber[5], Björn Samans[6], Udo Baron[6], Georg N. Duda[1,2,7,8], Hans-Dieter Volk[2,3,7,8‡] and Katharina Schmidt-Bleek[1,2‡]*

[1] Julius Wolff Institut and Center for Musculoskeletal Surgery, Charité – Universitätsmedizin Berlin, Berlin, Germany, [2] Berlin-Brandenburg Center for Regenerative Therapies, Charité – Universitätsmedizin Berlin, Berlin, Germany, [3] Institute of Medical Immunology, Charité – Universitätsmedizin Berlin, Berlin, Germany, [4] Center for Musculoskeletal Surgery, Charité – Universitätsmedizin Berlin, Berlin, Germany, [5] University Center of Orthopaedics and Traumatology, University Medicine Carl Gustav Carus Dresden, Dresden, Germany, [6] Epiontis GmbH, Precision for Medicine Group, Berlin, Germany, [7] Berlin Center for Advanced Therapies (BeCAT), Charité – Universitätsmedizin Berlin, Berlin, Germany, [8] Berlin Institute of Health Center for Regenerative Therapies, Berlin, Germany

OPEN ACCESS

Edited by:
Loretta Tuosto, Sapienza University of Rome, Italy

Reviewed by:
Gilberto Filaci, University of Genoa, Italy
Jason R. Mock, University of North Carolina at Chapel Hill, United States

***Correspondence:**
Georg N. Duda
georg.duda@charite.de

[†] These authors have contributed equally to this work as first authors

[‡] These authors have contributed equally to this work as senior authors

Specialty section:
This article was submitted to T Cell Biology, a section of the journal Frontiers in Immunology

Received: *10 May 2019*
Accepted: *02 August 2019*
Published: *16 August 2019*

Citation:
Schlundt C, Reinke S, Geissler S, Bucher CH, Giannini C, Märdian S, Dahne M, Kleber C, Samans B, Baron U, Duda GN, Volk H-D and Schmidt-Bleek K (2019) Individual Effector/Regulator T Cell Ratios Impact Bone Regeneration. Front. Immunol. 10:1954. doi: 10.3389/fimmu.2019.01954

There is increasing evidence that T lymphocytes play a key role in controlling endogenous regeneration. Regeneration appears to be impaired in case of local accumulation of CD8+ effector T cells (T_{EFF}), impairing endogenous regeneration by increasing a primary "useful" inflammation toward a damaging level. Thus, rescuing regeneration by regulating the heightened pro-inflammatory reaction employing regulatory CD4+ T (T_{Reg}) cells could represent an immunomodulatory option to enhance healing. Hypothesis was that CD4+ T_{Reg} might counteract undesired effects of CD8+ T_{EFF}. Using adoptive T_{Reg} transfer, bone healing was consistently improved in mice possessing an inexperienced immune system with low amounts of CD8+ T_{EFF}. In contrast, mice with an experienced immune system (high amounts of CD8+ T_{EFF}) showed heterogeneous bone repair with regeneration being dependent upon the individual T_{EFF}/T_{Reg} ratio. Thus, the healing outcome can only be improved by an adoptive T_{Reg} therapy, if an unfavorable T_{EFF}/T_{Reg} ratio can be reshaped; if the individual CD8+ T_{EFF} percentage, which is dependent on the individual immune experience can be changed toward a favorable ratio by the T_{Reg} transfer. Remarkably, also in patients with impaired fracture healing the T_{EFF}/T_{Reg} ratio was higher compared to uneventful healers, validating our finding in the mouse osteotomy model. Our data demonstrate for the first time the key-role of a balanced T_{EFF}/T_{Reg} response following injury needed to reach successful regeneration using bone as a model system. Considering this strategy, novel opportunities for immunotherapy in patients, which are at risk for impaired healing by targeting T_{EFF} cells and supporting T_{Reg} cells to enhance healing are possible.

Keywords: bone healing, regeneration, effector T cell, regulatory T (Treg) cell, mouse model

INTRODUCTION

The most promising healing scenario for a damaged tissue would be self-repair, thus to regenerate. Bone is able to heal without scar formation and therefore has a high regenerative capacity (1). Therefore, the healing process after bone injury could serve as a blue print for understanding underlying mechanisms guiding successful tissue regeneration. The majority of bone fractures heal

by endochondral ossification, which is usually divided into five distinct but overlapping stages. Bone healing starts with an initial hematoma formation and inflammation (further divided into pro- [1] and anti-inflammation [2]), subsequent revascularization of the fracture area and cartilage formation (soft callus formation [3]) occurs. Chondrocyte hypertrophy and matrix calcification proceed its replacement by newly formed woven bone (hard callus formation [4]). The final step of the healing cascade is the remodeling [5] of the new formed bone in dependence on the mechanical stimuli during loadbearing. In this generally successful healing of bone, immunological cells play a core role and impact the cascades of regeneration across all of these stages.

Despite its significant endogenous regeneration potential, in a meaningful proportion of humans (10–15%) fracture healing does not succeed and results in delayed union or persistent non-union (2, 3). This still represents a considerable health care problem, specifically in the aging industrial societies (4). After fracture, the initial pro-inflammatory reaction dominated by M1 macrophages and Th1 T cells and their chemokine and cytokine release pattern initiates the infiltration of cells needed for a successful repair process (5, 6).The switch from an initial pro-inflammatory to a subsequent anti-inflammatory state has been proven to be the key to any successful healing (7). There is growing evidence that the adaptive immunity, in particular, T cells, contributes to endogenous regeneration even in the absence of infections (8, 9) by modulating the local cytokine milieu in the fracture gap (8, 10–15) and thus during this early inflammatory phase. Using samples from fracture patients, it was recently shown that a higher amount of CD8+ effector T cells (T_{EFF}) is associated with a prolonged pro-inflammatory reaction and impaired fracture repair (16, 17). Accordingly, systemic depletion of CD8+ T cells in a mouse osteotomy model enhanced endogenous fracture regeneration, whereas the adoptive transfer of CD8+ T cells impaired the regeneration process. Therefore, high CD8+ T effector cell percentages are critical for an uneventful healing.

Important counterparts of an unfavorable pro-inflammatory immune response are CD4+ regulatory T cells (T_{Reg}). CD4+ T_{Reg} are a highly specialized cell population with immunomodulatory functions and are characterized by the expression of the surface marker CD25 and the transcription factor Forkhead-Box-Protein P3 (FOXP3) (7, 18–21). These cells are essential for the maintenance of the immunological self-tolerance, but also to prevent overwhelming inflammation in response to pathogens and in response to tissue injury. Several studies show that CD4+ T_{Reg} might control osteoclast activity and as result osteoarthritis, and enhance bone formation as well as inhibit bone loss under physiological and pathological conditions (19–21). CD4+ T_{Reg} execute immunomodulatory functions by multiple mechanisms, such as cell-cell contact dependent and independent ones. Their direct impact on the ATP metabolism via the surface molecules CD39 and CD73 results in the generation of strong immunomodulatory ATP derivatives, such as adenosine, and might be of particular interest for their immune-regulatory potency in inflamed tissues. Adenosine inhibits cytokine secretion by and proliferation of activated T_{EFF} cells as well as the switch of tissue resident M2 macrophages to pro-inflammatory M1 macrophages (22–24).

With the growing evidences that activated T_{EFF} negatively impact regenerative processes, their counterparts, the CD4+ T_{Reg} might have a positive regulatory impact on endogenous regeneration. In fact, there are a couple of studies showing their pro-regenerative potency e.g., after myocardial infarction or in regeneration from myocarditis (22).

We hypothesize that CD4+ T_{Reg} possess the potential to reshape and further to rebalance an initial unfavorable and "anti-regenerative" immune status (e.g., created by an increased CD8+ T_{EFF} level) into a pro-regenerative state promoting successful bone healing after fracture.

The role of the adaptive immunity in regeneration was overlooked for a long time, mainly because of using mouse models with a naïve T cell phenotype (23). Conventionally, specific pathogen free (SPF) housing is applied to have more standardized conditions. However, this housing is silencing the adaptive immunity, and even >1 year old SPF mice express an almost naive immune system lacking T_{EFF} cells as seen in newborns or babies but not comparable to adult human beings who are permanently exposed to environmental challenges (24). We further hypothesize that immune experienced mice kept under non-SPF, and thus pathogen exposed, conditions are the clinically more relevant model for studying the role of the T_{EFF}/T_{Reg} balance in bone regeneration.

Within this study the interplay of CD8+ T_{EFF} and CD4+ T_{Reg} was analyzed using immunologically naïve SPF housed mice (low CD8+ T_{EFF}) and non-SPF housed animals (high percentage of T_{EFF}) to mimic the impact of immune experience. Finding were compared to human fracture samples from patients with a known undisturbed healing and a diagnosed delayed healing outcome. Findings demonstrate the significant impact of a balanced T_{EFF}/T_{Reg} ratio on bone regeneration and at the same time opens novel avenues for personalized immunomodulatory therapies.

MATERIALS AND METHODS

Study Design

To evaluate the potential of CD4+ T_{Reg} to reshape an initial unfavorable and "anti-regenerative" immune state into a "pro-regenerative" one, we went into our well-established mouse osteotomy model system. Freshly isolated murine CD4+ T_{Reg} were adoptively transferred into mice prior to osteotomy. The healing outcome was investigated 21 d post-surgery. To have a clinically more relevant mouse model, we included for the immunomodulatory approach an osteotomy model using mice possessing a more experienced adaptive immune system (n = 20; control: n = 6, with adoptive CD4+ T_{Reg} transfer: n = 15 [non-SPF housing]) compared to the classically used naïve mice (n = 12; control: n = 6, with adoptive CD4+ T_{Reg} transfer: n = 6 [SPF housing]). One mouse was excluded from the study due to a non-evaluable healing outcome as a consequence of a failed fixation. In the non-SPF housed mice, the CD8+ T_{EFF} to CD4+ T_{Reg} ratio was evaluated by flow cytometry pre- as well as post-osteotomy to investigate the interplay of the cell

ratio and the healing outcome (**Figure S1**: Study design of the mouse experiment).

We included data from human fracture patients to confirm the murine findings in a patient setting. Thirty-five patients (aged 19–77 years, 19 male, and 16 female) were included in this study. Due to the assessment of immunological parameters, patients with human immunodeficiency virus infection, hepatitis infection, ongoing, or past (within 5 years) malign diseases/treatments were excluded from the study. To ensure a similar post-surgery physiotherapeutically mobilization, patients with polytrauma or several fractures (>2 fractures) were also excluded from the study (see **Table 1**, **Tables S1, S2**). Based on the radiological data, fracture patients were divided into normal ($n = 23$) and impaired ($n = 12$) healing fractures. To analyze the interplay of the CD8+ T_{EFF} to CD4+ T_{Reg} ratio and the healing outcome, peripheral blood samples were taken prior to surgery, and the T_{EFF}/T_{Reg} was analyzed by flow cytometry. In addition, the cell ratio was also investigated in fracture hematoma samples, taken during the surgery.

Characteristics of the Animal Model Used for Immune Intervention Approaches

Female C57BL/6 mice (Charles River Laboratories, Wilmington, USA) of an age of 12 weeks were used for the animal experiments. Mice were kept in small groups under specific pathogen free (SPF) or non-SPF (area in the animal facility without an additional barrier and filtered air supply for the mice cages) housing conditions. A controlled temperature (20 ± 2°C) and a 12 h light/dark circle were present. Food and water were available *ad libitum*. All animal experiments were approved by the local legal representatives (Landesamt für Gesundheit und Soziales Berlin: G0008/12; T0119/14; T0249/11) and done accordingly to the guidelines of the Animal Welfare Act, the National Institutes of Health Guide for Care and Use of Laboratory Animals, and the National Animal Welfare and ARRIVE Guidelines. Health monitoring followed the FELASA guidelines for both housing conditions—no health risks were monitored for those animals housed under non-SPF conditions.

CD4+ T_{Reg} were enriched by cell sorting (see below) and adoptively transferred (5–8 × 10^5 cells) via the tail vein prior to surgical intervention. Mice were randomly allocated to the treatment groups.

TABLE 1 | Characterization of the patients.

Parameter	Impaired healing patients ($n = 12$)	Normal healing patients ($n = 23$)	Significance
Age (y)	54.58 ± 12.7	52.17 ± 13.3	0.6
Sex (male/female)	7/5	12/11	0.7
Height (m)	1.71 ± 0.09	1.74 ± 0.09	0.3
Weight (kg)	79.63 ± 18.52	76.43 ± 15.79	0.6
BMI	27.3 ± 5.9	25.2 ± 4.2	0.2

Surgical Approach and Performing the Mouse Osteotomy

A non-critical sized osteotomy was set in the left femur of the mice as described before (6). In short, mice were anesthetized by inhalation of isoflurane and received a subcutaneous injection of the analgesic Buprenorphine (0.03 mg/kg) and of the antibiotic Clindamycin (45 mg/kg). After shaving the surgery field and disinfection, a longitudinal cut of the skin was performed. The femur was bluntly exposed and the external fixator, consisting of four pins and a bar (RISystem, Davos, Switzerland), was mounted on the lateral side of the femur. An osteotomy of 0.7 mm was created between the two middle pins using a wire saw. The skin was sutured, and the mice were brought back into their cages. As post-operative analgesia, tramadol hydrochloride (25 mg/l) was added to the drinking water for 3 days post-surgery.

Isolation of Murine Regulatory T Cells for Immunotherapy

Murine CD4+ regulatory T cells (T_{Reg}) were isolated by magnetic activated cell sorting (MACS) from pooled cells derived from the spleen and the lymph nodes: inguinal nodes, axillary nodes, brachial nodes, and mesenteric nodes. A single cell suspension was prepared and erythrocytes were lysed. The isolation procedure was carried out with the CD4+ T_{Reg} isolation kit (Miltenyi Biotec GmbH, Bergisch Gladbach, Germany), according to the manufactures instructions. Briefly, the cell suspension was incubated with a biotin-labeled antibody mix to stain all non-CD4+ T cells. Afterwards, α-biotin magnetic beads, as well as a PE-labeled α-CD25 antibody were added to the cells. After incubation, cells were washed (8 min, 1,500 rpm, 4°C), resuspended in MACS buffer (1x PBS + 0.5% BSA + 2 mM EDTA) and transferred to an LD column (Miltenyi Biotec GmbH, Bergisch Gladbach, Germany), which was placed in a magnetic field. The flow through was collected, washed, resuspended in MACS buffer and incubated with an α-PE antibody. Cells were washed, resuspended in MACS buffer and transferred to an MS column (Miltenyi Biotec GmbH, Bergisch Gladbach, Germany), which was placed in a magnetic field. CD4+ T_{Reg}, which were kept in the magnetic field in the column, were flushed out, washed and counted. Subsequently, CD4+ T_{Reg} were isolated with a purity of ≥85%.

Regulatory T Cell Suppression Assay

The suppressive capacity of freshly isolated CD4+ T_{Reg} was tested in a co-culture setup with CD4+CD25- responder T cells ($T_{Responder}$). $T_{Responder}$ were labeled with a cell proliferation dye (Cell Proliferation Dye (CPD) eF450, eBioscience, San Diego, USA) following the protocol. In short, MACS isolated $T_{Responder}$ were washed (8 min, 1,500 rpm, RT) twice with PBS and resuspended in a solution consisting of pre-warmed PBS and a 10 mM CPD eF450 solution to a final concentration of 10 × 10^6 cells/ ml. Cells were incubated for 20 min at RT in the dark and the staining was stopped by the addition of ice cold cell culture media [RPMI 1640 (Biochrom AG, Berlin, Germany) + 10% FBS superior (Biochrom AG, Berlin, Germany) + 1% penicillin/streptomycin (Sigma-Aldrich Chemie

GmbH, München, Germany), and 50 μM β-Mercaptoethanol (Sigma-Aldrich Chemie GmbH, München, Germany)]. Cells were incubated for 5 min on ice, washed three times with pre-warmed cell culture media and counted. For the suppression assay, 0.75×10^5 labeled $T_{Responder}$ were co-cultured in cell culture media with (1) 1.5×10^5 or (2) 0.15×10^5 CD4+ T_{Reg} in a 96 well plate. $T_{Responder}$ were also cultured alone. In order to stimulate the proliferation of $T_{Responder}$, α-CD3 and α-CD28 (both eBioscience, San Diego, USA) were plate-bound (each 5 μg/ml) to the wells before adding the co-culture setups. After 2–3 days, cells were harvested, and the proliferation of the $T_{Responder}$ was analyzed by flow cytometry. The suppression of the CD4+ T_{Reg} was calculated based on the proliferation of the $T_{Responder}$ which were cultured alone. Their proliferation was set to 100, and the proliferation of the co-cultured $T_{Responder}$ was calculated relative to it. Finally, the percentage of suppression was defined as 100 minus the (relative) proliferation.

Flow Cytometry Analysis of Murine Immune Cells in Tissue Samples

The sample preparation for flow cytometry was done as follows: from the spleen, the bone marrow, and the lymph nodes, single cell suspensions were prepared. The spleen was cut into small pieces and carefully pushed through a cell strainer. For the bone marrow, the ends of the bones were cut and the marrow was flushed out with a syringe. Afterwards, the bone marrow cells were also carefully pushed through a cell strainer. Lymph nodes were directly pushed through a cell strainer. All single cell suspensions were washed in PBS, and the erythrocytes were lysed. Blood samples were centrifuged (10 min, 2,000 rpm, RT), the supernatant was removed, and erythrocytes were lysed. Cells were washed in PBS (10 min, 1,500 rpm, 4°C) and stained. Lysed and washed cells were resuspended in PBS and incubated with a LIVE/DEAD staining kit (Thermo Fisher Scientific, Waltman, USA) for 30 min on ice. For the evaluation of the adoptive CD4+ T_{Reg} transfer (1 and 21 days post-osteotomy) and the amount of CD4+ T_{Reg} in the harvested tissues after 21 days of healing, cells were washed, resuspended in PBS/BSA (1x PBS + 1% BSA and 0.1% sodium azide) and stained with the following antibody mix for 20 min on ice: α-CD3 PerCP (BioLegend, San Diego, USA), α-CD4 AF700 (eBioscience, San Diego, USA) and α-CD25 APC (BioLegend, San Diego, USA). For the evaluation of the CD4+ and CD8+ effector T cell subset, cells were washed, resuspended in PBS/BSA and stained with the following antibody mix for 20 min on ice: α-CD3 PerCP (BioLegend, San Diego, USA), α-CD4 AF700 (eBioscience, San Diego, USA), α-CD8 eF450 (eBioscience, San Diego, USA), α-CD44 PE-Cy7 (Becton Dickinson Bioscience, Heidelberg, Germany), α-CD62L APC (BioLegend, San Diego, USA) and α-CD25 APC (BioLegend, San Diego, USA). Cells were washed, resuspended, and either fixed for 20 min at RT with a 2% formaldehyde solution (evaluation of adoptive CD4+ T_{Reg} transfer) or permeabilized with a fixation/permeabilization buffer (eBioscience, San Diego, USA) for 1 h on ice (evaluation of the amount of CD4+ T_{Reg} after 21 days). Cells were washed twice with permeabilization buffer (eBioscience, San Diego, USA), resuspended and incubated for 30 min on ice with α-Foxp3 FITC (eBioscience, San Diego, USA). After fixation and permeabilization, cells were washed, resuspended and analyzed with the LSR II flow cytometer (Becton Dickinson Bioscience, Heidelberg, Germany) (for the gating strategy please refer to **Figure S2**).

Micro-Computed Tomography of Osteotomized Mouse Bones

To evaluate the formation of newly formed bone, μCT analyses were performed with the osteotomized bones 21 days post-surgery. The harvested bones were scanned in a μCT Viva 40 (SCANCO Medical AG, Brüttisellen, Switzerland). The volume of interest (VOI) included 190 slices around the former osteotomy gap. The following parameters were used for the scan: 10.5 μm voxel size, 55 keVp peak voltage energy and an applied current of 145 μA. In order to be able to distinguish between non-mineralized and mineralized bone, a gray value threshold was used (25). A defined threshold of 396.9 mg hydroxyapatite per cm^2 identified mineralized bone.

Patients and Study Protocol

The study was performed in compliance with the International Conference on Harmonization Guidelines for Good Clinical Practice and the Declaration of Helsinki. All patients participated with a written informed consent, and the study was approved by the Institutional Review Board (IRB) of the Charité – Universitätsmedizin Berlin (IRB approval EA2/096/11). All patients received a complete study follow up rate including all clinical investigation time points and radiological assessments. Moreover, all patients were matched according to age, sex, fracture type and initial surgical treatment strategy. The demographic and clinical characteristics of the included patients are shown in **Table 1**, **Tables S1, S2**. To monitor the fracture healing process and in consensus with established clinical examination time points, the patients were investigated pre-surgery and after 4–6, 12, 17–19, 24, and 52 weeks. Regarding the fracture treatment, the only significant difference between the healing groups was the number of surgical interventions required ($p = 0.003$; **Table S2**).

Healing Classification and Data Collection

Time-dependent criteria: A fracture was categorized as impaired healing when it was not completely healed after 17–19 post-operative weeks based on the callus formation. *Radiological criteria:* Different criteria were applied to identify an impaired healing fracture by radiological analyses: (A) incomplete fracture healing or the absence of visible bone consolidation on a simple X-ray after 17–19 post-operative weeks; (B) the presence of a resorption zone or incomplete callus formation; (C) incomplete bridging, which means one to three cortices bridged; or (D) no bridging, which means no cortex is bridged.

Every patient underwent consecutive x-ray analyses to assess the stability of the implant and to observe the fracture gap throughout the study time. Appraisal of x-rays was performed by three independent, blinded specialists (two orthopedic surgeons and one radiologist), to ensure the healing outcome and the classification of patients as shown in **Table 1**. To fulfill the

definition of impaired healing, patients had to meet one or more of the time dependent- and/or radiological criteria as stated above (26–29).

Flow Cytometry Analysis of Human Blood Samples to Characterize Immune Status in Fracture Patients

Blood samples were taken before the surgery after 15 min rest in a supine position. All blood samples were immediately moved into a dark, air-conditioned room, and sent to the laboratory within 2 h. Additionally, plasma and serum samples were collected in aliquots and frozen at −80°C. Full blood count and standard clinical variables (erythrocytes, hemoglobin, hematocrit, thrombocytes, creatinine, sodium, potassium, urea, chloride, GPT, GOT, gamma-GT, TSH, CRP) were measured immediately in plasma and serum samples according to the laboratory standard operating procedures.

To evaluate the adaptive immunity of the patients, we applied our recently developed and extensively validated pre-cocktailed dried DuraClone T cell panels (Beckman Coulter), including the "T cell panel" CD45RA, CCR7, CD28, PD1, CD27, CD4, CD8, CD3, CD57, CD45, and "regulatory T cell panel" (Beckman Coulter), including CD45RA, CD25, CD127, CD39, CD4, FOXP3, CD3, CD45 were used. Flow cytometry analysis was performed using the BC NAVIOS 10/3 flow cytometer and data were analyzed using BC Kaluza analysis software (Beckman Coulter).

Human Genomic DNA (gDNA) Purification for Epigenetic Analysis

Frozen human fracture hematoma samples ($n = 8$) were thawed in a 37°C water bath and further kept on ice. To dissolve the hematoma samples, Clotspin® Baskets from Qiagen were used according the manufacturing protocol: Purification of archive-quality gDNA from clotted whole blood using Clotspin® Baskets and the Gentra® Puregene® blood kit provided by Qiagen. All protocol steps were followed according to the manufacturer's instructions. Steps included the usage of isopropanol and Glycogen Solution (20 mg/ml from Qiagen) and washing of gDNA pellets with 70% ethanol. gDNA was further air dried at room temperature until no remaining fluids remained. gDNA was incubated with 500 µl DNA hydration solution provided within the kit (www.qiagen.com/literature/handbooks/default.aspx). gDNA was incubated at 65°C until it was dissolved.

gDNA quality and quantity were confirmed using the NanoDrop-ND-1000 system (PEQLAB GmbH). Samples were stored at −80°C until further experiments.

Epigenetic qPCR Analysis (Patients)

Purified genomic DNA from the fracture hematoma ($n = 8$) was converted using the EpiTect Fast Bisulfite Conversion Kit (Qiagen) following the manufacturer's instructions. CD3+, T_{Reg} -specific and CD8B+ T cell-specific epigenetic qPCR analyses were performed as previously described (30–32).

Statistics

For the statistical evaluation of the data, the program SPSS (Version 22; IBM Deutschland GmbH, Ehningen, Germany) was used. Unless otherwise stated, all data were represented as means ± SD.

Human Data

The Levene test was used to assess the homogeneity of variances of the data for the indicated groups and the data were then analyzed using the unpaired Student's *t*-test (two groups).

Mouse Data

Due to the small sample sizes, a normal distribution of the data was excluded. Therefore, the Mann-Whitney *U*-test was used as statistical test. If more than two samples were compared, the significance value p was corrected by using the Bonferroni correction. Data were seen as statistically significant if $p \leq 0.05$ or if $p \leq 0.05/n$ (n = number of compared samples) (Bonferroni corrected data). Data are presented as scatter or boxplot graphs. Usage of the Bonferroni correction is indicated in the respective figures.

Data and Materials Availability

All data needed to evaluate the conclusions in the paper are presented within the paper and/or in the **Supplementary Materials**. Additional data related to this paper may be requested from the corresponding author.

RESULTS

In a small cohort of patients, we previously showed that CD57+ CD8+ T_{EMRA} cells were markedly elevated in peripheral blood of patients suffering from an impaired bone healing (17). T cell receptor stimulation or IL-12 (bystander activation) can trigger T_{EMRA} cells to produce inflammatory cytokines, like IFNγ and TNFα, without the need of antigen-presenting cells (independent on co-stimulatory signals via CD28 or CD40L), making those ideal candidates for enhancing intra-tissue inflammation if they accumulate after injury. It is well-established that T_{Reg} play a crucial role in controlling immune response at multiple levels to prevent undesired immune reactivity, such as auto/allo-immunity and infection-related pathogenesis (33). There is increasing evidence that they are also pivotal in controlling regenerative processes (34). Therefore, we wondered whether adoptive transfer of CD4+ T_{Reg} might be a relevant option to enhance fracture healing. To address this we applied a well-defined mouse osteotomy model (35) and adoptively transferred CD4+ T_{Reg}.

Application of CD4+ Regulatory T Cells as Potential Agent to Improve Bone Fracture Healing in SPF Mice

Prior to adoptively transferring the CD4+ T_{Reg}, we tested the functionality of *ex vivo* enriched murine CD4+ CD25++ Foxp3+ T_{Reg}. Using an established CD4+ T_{Reg} suppression assay in which freshly isolated CD4+ T_{Reg} (purity ≥85%, **Figure S3**)

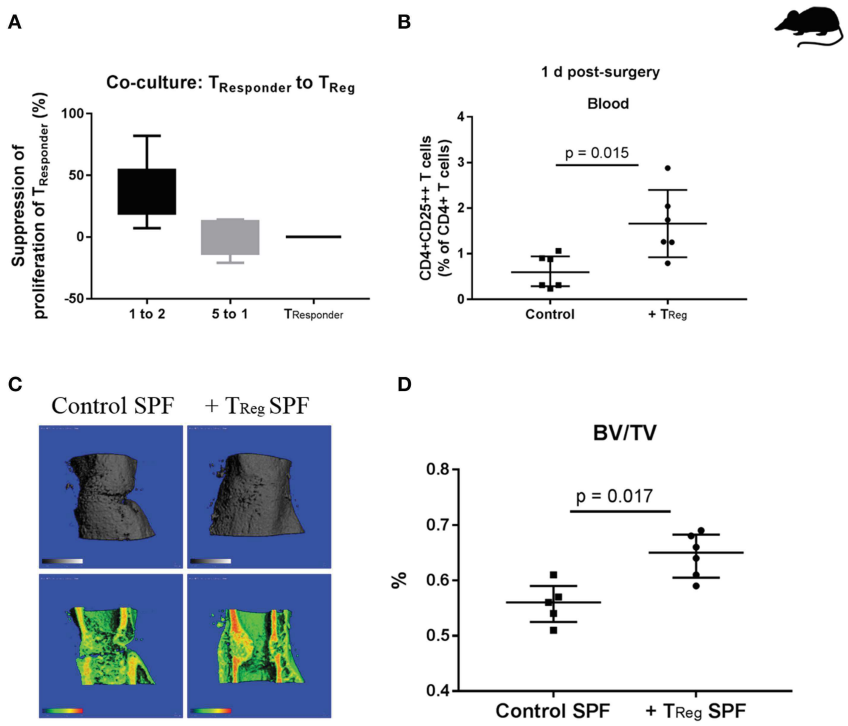

FIGURE 1 | Enhancing bone healing by adoptive transfer of murine CD4+ T_{Reg} in SPF mice. **(A)** Demonstration of the functionality of isolated murine CD4+ T_{Reg} in a suppression assay, illustrated is the suppression of the proliferation of CD4+CD25- $T_{Responder}$ cells by using freshly isolated CD4+ T_{Reg} ($n = 6$). **(B)** Status of CD4+ T_{Reg} in the peripheral blood of the experimental mice 1 d after adoptive transfer, control ($n = 6$) vs. CD4+ T_{Reg} enriched mice ($n = 6$). **(C,D)** Improved bone healing by adoptive CD4+ T_{Reg} transfer as demonstrated by μCT evaluation after 21 d, control (**C**, left, control SPF) vs. T_{Reg} enriched mice (**C**, right, +T_{Reg} SPF). Quantification of the μCT data revealed a significantly higher BV/TV in the mice that received a CD4+ T_{Reg} transfer (+T_{Reg}) ($n = 6$) compared to the control SPF mice ($n = 5$) **(D)**. BV, bone volume; TV, total callus volume; BV/TV, ratio of BV to TV; Mann-Whitney *U*-test.

and stimulated $T_{Responder}$ (non-T_{Reg}) cells were co-cultured, we confirmed their suppressive properties (**Figure 1A**).

In order to confirm the successful transfer of the CD4+ T_{Reg} their fate was analyzed in the recipient mice. After infusion of CD4+ T_{Reg} into the tail vein of C57BL/6 mice prior to osteotomy, a blood sample for counting circulating CD4+ T_{Reg} was taken 1 day (1 d) after surgery. A significantly higher percentage of CD4+CD25++ T cells (representing CD4+ T_{Reg}) was found in animals that received an adoptive transfer in comparison to control mice (**Figure 1B**) illustrating the efficacy of adoptive transfer of T_{Reg} ($p = 0.015$).

After proving the feasibility of isolation, transfer and functionality of adoptively transferred CD4+ T_{Reg}, we tested our hypothesis that these cells had a positive impact on bone healing.

Initially we used SPF mice (12 weeks), where skeletal growth was nearly completed and peak bone mass has almost been reached (36). Further, an osteotomy model was used that did not results in complete healing within 21 days and thus allows to detect improvements in healing in comparison to control mice. As expected, all control mice expressed a healing with a partly visible osteotomy gap, as documented by μCT data (**Figure 1C**). The experiment confirmed our hypothesis showing improved bone healing at 21 d as indicated by a significantly increased ratio of bone volume to total callus volume (BV/TV) in the osteotomized femura of mice that received an adoptive transfer of CD4+ T_{Reg} (**Figure 1D**; $p = 0.017$).

In summary, the elevation of the CD4+ T_{Reg} in recipient mice showed a positive effect on bone healing. However, these mice were kept under the usual SPF housing conditions resulting in a "naïve" T cell system. In contrast, human beings are permanently exposed to environmental antigens shifting their T cell composition to higher T_{EFF} cell counts in an age-dependent manner (32). Therefore, alternative murine osteotomy models are required that better reflect the situation in human patients.

Establishment of a Clinically More Relevant Murine Model Applying Non-SPF Housing to Generate an "Experienced" T Cell Immunity Reflected by Enhanced T_{EFF} Cell Counts

Recently, we established a new model of non-SPF housing conditions inducing a fast switch to a more "experienced" T cell immunity with enhanced levels of T_{EFF} cells (24, 37). Briefly,

mice were transferred toward a non-barrier housing exposing them to environmental pathogens. Thus, the environmental microbial exposure was raised in comparison to the SPF housed mice and the adaptive immune system was challenged. TNAIVE/TMEMORY/T_{EFF} counting in a blood sample before osteotomy allows individual proof of "immune aging," of immune experience. It is worth mentioning that after 5 years of experience with this model, no clinical abnormality was reported in these mice nor has any serological disease status been recorded in this cohort outside of an SPF barrier.

After a minimal exposure of 4 weeks, the immune cell composition in these non-SPF housed animals was analyzed and compared to that of SPF housed animals. Although there is a significant individual variation, mice developed a higher level of T_{EFF} (both CD4+ and CD8+) in immune tissues, e.g., spleen. Thus, the exposure led to an altered CD8+ T_{EFF}/CD4+ T_{Reg} ratio in non-SPF mice compared to SPF mice (spleen: $p = 0.008$; **Figure S4**).

In the next step, we asked whether an adoptive transfer of CD4+ T_{Reg} could enhance bone healing in these mice with a more experienced immune system and a consecutively higher percentage of CD8+ T_{EFF}.

Adoptive Transfer of CD4+ T_{Reg} in Mice With an Experienced Adaptive Immunity Results in Heterogeneous Bone Healing Outcome

Similar to the T_{Reg} transfer in SPF housed animals, we used mice with an experienced adaptive immunity to evaluate the therapeutic potential of CD4+ T_{Reg} to further bone regeneration. Animals received CD4+ T_{Reg} isolated from pooled donor mice to prevent heterogeneity of individual T_{Reg} donors (**Figure 2A**; $+T_{Reg}$). In contrast to the clear data received from the SPF housed mice, non-SPF housed animals displayed a heterogeneous clustered healing outcome after CD4+ T_{Reg} transfer and osteotomy (**Figures 2A–D**). Remarkably, in half of the mice, referred to as $+T_{Reg}$ responders, healing was significantly enhanced compared to control animals, illustrated by an increased TV ($p = 0.01$), BV ($p = 0.01$) and ratio of BV to TV ($p = 0.038$). In contrast, in the other half of the mice, the healing was not improved, but even showed a worsening (named "$+T_{Reg}$ non-responders") with significantly reduced TV ($p = 0.01$) and BV ($p = 0.01$).

In order to determine the reason behind the distinct healing differences of + T_{Reg} responders and non-responders several

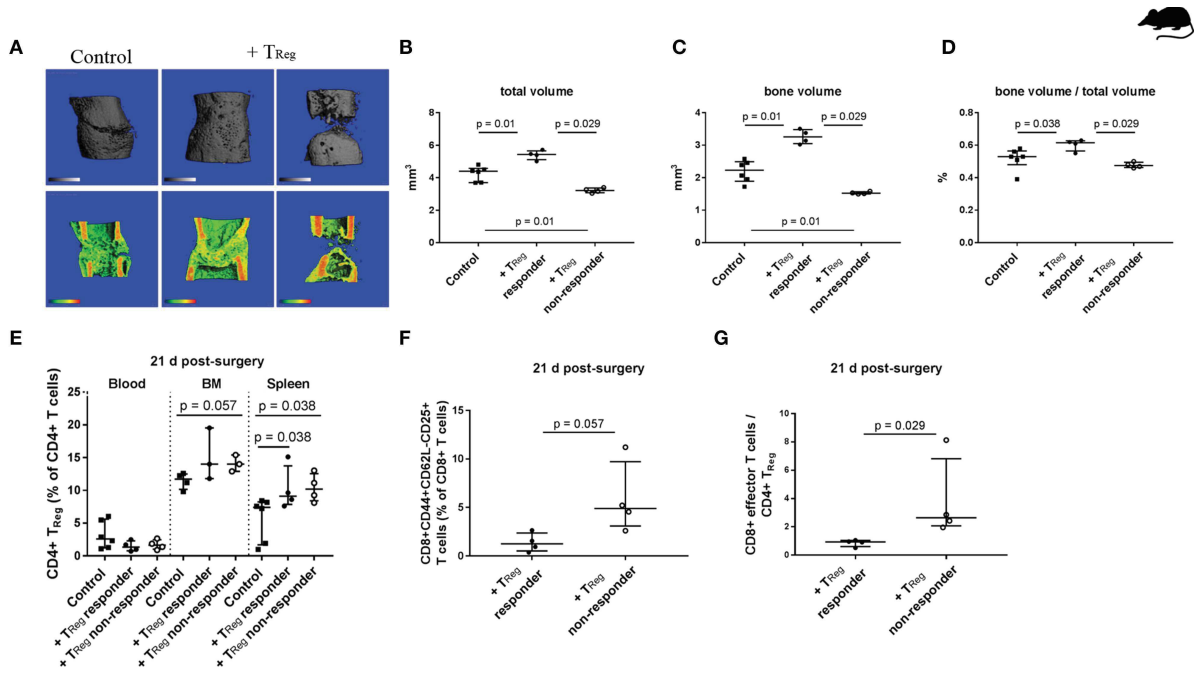

FIGURE 2 | Heterogeneous impact of adoptive transfer of CD4+ T_{Reg} on bone healing outcome in mice kept under non-SPF housing conditions. **(A–D)** μCT evaluation of the healing outcome after adoptive CD4+ T_{Reg} transfer after 21 d. **(A)** Representative images of the analyzed volume of interest of the healing bones are shown. $+T_{Reg}$ treated mice clustered into responder ($+T_{Reg}$ left, $n = 4$) and non-responder ($+T_{Reg}$ right, $n = 4$). Control mice showed no complete bridging after 21 d (left, control, $n = 6$). In contrast, $+T_{Reg}$ responder showed complete bridging, whereas non-responder showed no bridging. **(B–D)** Quantification of the μCT analysis, + T_{Reg} responder vs. + T_{Reg} non-responder vs. control mice. **(E–G)** Evaluation of the immune cell composition of $+T_{Reg}$ responder vs. non-responder 21 d post-surgery. **(E)** Confirmation of CD4+ T_{Reg} engraftment in both, $+T_{Reg}$ responder and non-responder compared to the control. **(F,G)** $+T_{Reg}$ non-responder showed an elevated percentage of CD8+ T_{EFF} **(F)** as well as a significantly higher ratio of CD8+ T_{EFF} /CD4+ T_{Reg} **(G)** in the peripheral blood in comparison to the $+T_{Reg}$ responder. TV, total volume; BV, bone volume; BV/TV, ratio of BV to TV; Mann–Whitney *U*-test, Bonferroni correction **(B–E)**.

possibilities were analyzed. Differences in the functionality of the transferred T_{Reg} can be ruled out as we used pooled cells from several donor animals and saw responders and non-responders among the recipients of the same cell pool. Recipients were chosen from the same cage and randomly placed within the treatment groups—no correlation with responder or non-responder were found. Up to four animals were operated on at each surgery day and no correlation with the surgical sequence was found. Subsequently, we analyzed whether adoptively transferred T_{Reg} showed reduced engraftment in the non-responder mice. However, as shown in **Figure 2E**, the number of T_{Reg} detectable at day 21 post T_{Reg} infusion and osteotomy did not show a heterogeneous distribution and non-responder and responder mice showed comparably elevated T_{Reg} level.

Interestingly, upon analysis of the immune cell composition higher frequencies of CD62L-CD44+CD25+ activated CD8+ T_{EFF} cells were found in the non-responder animals, demonstrating that the immune experience within the group of mice even within the same cage was highly individual. A significantly elevated T_{EFF}/T_{Reg} ratio in peripheral blood of $+T_{Reg}$ non-responder vs. responder mice ($p = 0.029$; **Figures 2F,G**), indicating that the T_{Reg} treatment was not sufficient to reshape the negative effect of the CD8+T_{EFF} cells in the non-responder animals.

To test this assumption, we analyzed this ratio of T_{EFF}/T_{Reg} pre-operatively in the peripheral blood of another cohort of seven non-SPF housed mice. We performed the adoptive CD4+ T_{Reg} transfer, set the osteotomy and evaluated the healing outcome after 21 d as described before. Within this second cohort of osteotomized mice the heterogeneous healing outcome of the previous experiment was confirmed. The healing outcome 21 days after osteotomy again showed $+T_{Reg}$ responder and $+T_{Reg}$ non-responder. Four mice could be clearly categorized as $+T_{Reg}$ responders (good healing outcome: bridging of the cortices in progress) and three mice were classified as $+T_{Reg}$ non-responders (poor healing outcome: no bridging of the cortices). Based on this grouping, we compared values of the pre-surgery CD8+T_{EFF}/CD4+T_{Reg} cell ratio with the µCT evaluation after 21 d (BV/TV) (**Figure 3A**). Notably, all four responder mice had a pre-surgery ratio of CD8+ T_{EFF}/CD4+ T_{Reg} of <0.07 (below the dashed line) which consistently correlated with a higher BV/TV in comparison with the non-responder mice which showed a ratio of 0.08–0.23 (above the dashed line). We further evaluated this CD8+ T_{EFF}/CD4+ T_{Reg} ratio at 1 d post-surgery. Remarkably, CD4+ T_{Reg} transfer could not reverse the unfavorable ratio in the non-responder mice (**Figure 3B**). Again, we could exclude unsuccessful engraftment of the adoptively transferred CD4+ T_{Reg} as shown in **Figure 3C**.

The presented data suggest that successful bone regeneration depends on the balance between CD8+ T_{EFF}/CD4+ T_{Reg}. The cut off between $+T_{Reg}$ responder and $+T_{Reg}$ non-responder however is not pronounced. In order to confirm the results from the mouse experiment that the CD8+ T_{EFF}/CD4+ T_{Reg} ratio is a decisive factor for the bone healing outcome the immune cell composition in a patient cohort with a known healing outcome was analyzed.

Elevated CD8+ T_{EMRA} Level in the Peripheral Blood of Patients With Impaired Healing After Bone Fracture

In accordance with the mouse experiment, a patient cohort with a high CD8+ T_{EFF} level should be included in the experiment to confirm our mouse data. Therefore, a new patient cohort was recruited applying our previously published (17) strategy to define delayed healing by functional and radiological methods (**Figures 4C,D**). In a first step elevated CD8+ T_{EFF} level were confirmed in the new patient cohort, the cells were further subtyped as T_{EMRA} cells CD45+CD3+CD8+CD57+CD28- (**Figure 4A**). The impaired healing group showed an almost three times higher proportion of circulating CD45+CD3+CD8+CD57+CD28- T_{EMRA} cells ($p < 0.001$).

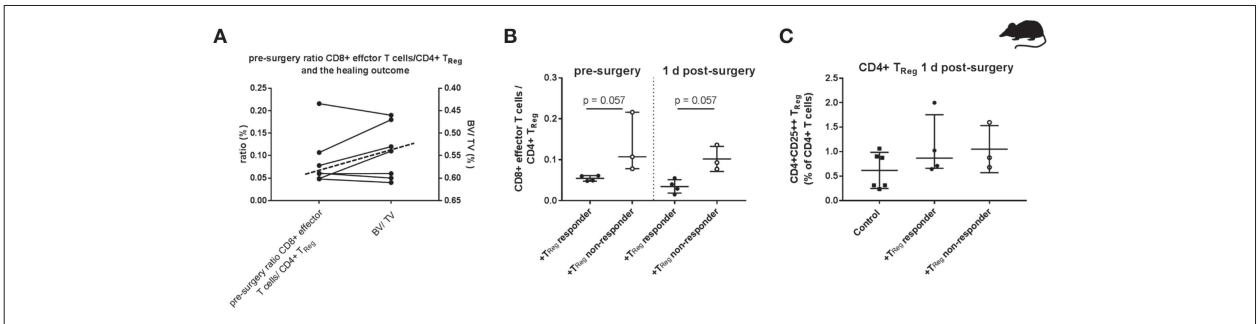

FIGURE 3 | Individual effector/regulatory T cell ratio pre-osteotomy determines the healing outcome in mice. **(A)** Mice having a lower pre-surgery CD8+ T_{EFF} to CD4+ T_{Reg} ratio (left y-axis) showed a higher BV/TV (right y-axis, axis is reversed for a clearer depiction). Dashed line indicates the cut off between the $+T_{Reg}$ responder (below the dashed line) and the $+T_{Reg}$ non-responder (above the dashed line). **(B)** Adoptive CD4+ T_{Reg} transfer did not reshape the unfavorable CD8+ T_{EFF}/CD4+ T_{Reg} ratio. **(C)** Engraftment of CD4+CD25++ T cells 1 d post-surgery is elevated in both, the $+T_{Reg}$ responder ($n = 4$) and $+T_{Reg}$ non-responder ($n = 3$) in comparison to the control group ($n = 6$). 45BV, total bone volume; TV, total callus volume; BV/TV, ratio of BV to TV; Mann–Whitney *U*-test.

Enhanced Accumulation of CD8+ T Cells in the Fracture Hematoma of Patients With Impaired Fracture Healing

To further confirm the effect of the systemically found elevated T_{EMRA} cell count the fracture hematoma of these patient was evaluated for these cells. To address this issue, we applied a recently developed, easily applicable advanced technology to analyze immune cell subset composition from tissue samples based on CD3+-, T_{Reg}- and CD8+-specific epigenetic pattern at tissue-derived DNA (30–32). Fracture hematoma composition does not simply reflect the repertoire of blood leukocytes but is enriched by T_{EFF} cells attracted actively to the fracture environment. The almost two times higher levels of CD8+ T cells in the hematoma of impaired vs. normal healing patients support the hypothesis that CD8+ T_{EFF} accumulate in the fracture hematoma, although statistical significance was not yet reached as only a low number of fracture hematoma samples was available for the analysis (**Figure 4B**).

In a next step, we analyzed the observed tight interconnectivity between the CD8+ T_{EFF} and CD4+ T_{Reg} ratio and the bone healing outcome in our human patient cohort. Interestingly, we observed an elevated percentage of CD4+ T_{Reg} in the peripheral blood of impaired healing patients. This could be interpreted as an intrinsic effort to counteract the higher CD8+ T_{EFF} level that was however, not able to reverse the negative impact of the high CD8+ T_{EMRA}/CD4+ T_{Reg} ratio in those patients (**Figure 5A**; $p < 0.001$). This result is in accordance with the data of the mouse experiment. Remarkably, this imbalance of CD8+ T_{EFF}/CD4+ T_{Reg} was also reflected in the facture hematoma (**Figure 5B**). Impaired fracture healing

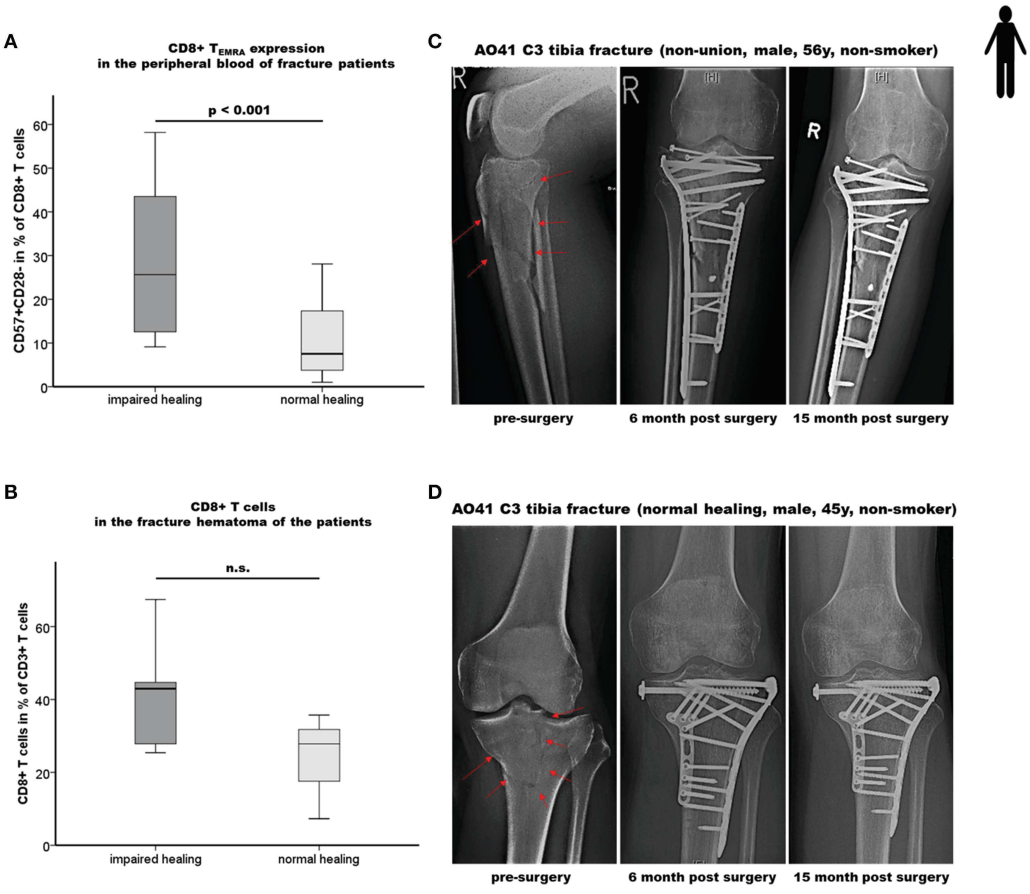

FIGURE 4 | Impaired bone healing correlates with an elevated CD8+ T_{EMRA} level in both the peripheral blood as well as in the local fracture hematoma of patients. **(A)** Results of the flow cytometry analyses of terminally differentiated CD8+ effector T cells (CD8+T_{EMRA}) in the peripheral blood of fracture patients at the time of operation are shown. Impaired fracture healing patients showed a significantly higher frequency of CD45+CD3+CD8+CD57+CD28- T cells (CD57+CD28-+ in % of CD45+CD3+CD8+ T cells) compared to the normal healing patients indicates a dramatic increase of CD8+ T_{EMRA}: n = 12 for the impaired healing group, n = 23 for the normal healing group. **(B)** Quantification of CD8+ T cells in the hematoma region of fracture healing patients by epigenetic qPCR analysis. Impaired fracture healing patients showed an elevated level of CD8+ T cells in the local fracture area: n =5 for the impaired healing group, n = 3 for the normal healing group **(C,D)** Representative x-ray images from the study cohort over a period of 15 months including the pre-surgery as well as the 6 and 15 months post-surgery states of fracture healing of an impaired healing **(C)** and a normal healing **(D)** patient, respectively. Student's t-test.

patients showed a significantly higher CD8+ T cells/CD4+ T_{Reg} ratio without overlap between the two groups, ranging from 3.0 to 6.0 and 1.2 to 2.7 in patients who showed an impaired and normal healing outcome, respectively ($p = 0.043$).

These findings demonstrate that the ratios of CD8+ T_{EFF} to CD4+ T_{Reg} in the peripheral blood are mirrored by those within the fracture hematoma. This cellular correlation between the periphery and the site of injury further highlights the significance of the balance of pro-inflammatory CD8+ T_{EFF} to anti-inflammatory CD4+ T_{Reg} for a successful bone healing process.

DISCUSSION

Our study demonstrates the relevance of the T cell subset composition for regeneration using bone healing in a murine osteotomy model as well as in patients. Enhanced CD8+ T_{EFF}/CD4+ T_{Reg} ratios both in peripheral blood and locally in the fracture hematoma were associated with an impaired bone healing outcome.

The data indicates that the T_{EFF}/T_{Reg} ratio could be a predictive biomarker for bone healing. However, as flow cytometry analysis from hematoma is hardly applicable for the clinical routine, we applied a recently developed fast epigenetic method allowing T cell subset quantification in tissue specimen (30–32) that could be further developed into an intraoperative diagnostic tool. This would enable a stratification of patients in potential need of additional treatments at the time of the initial fracture treatment.

This study clearly demonstrated that the model used for an experimental evaluation of a hypothesis should be carefully considered. While the results in the SPF housed mice indicated that a treatment enhancing T_{Reg} percentages shows 100% healing enhancement changing the model to one with a higher immune experience (and thus a model that is closer to the patient situation) changed this result to only 50% healing success. What is even more alarming is that the other 50% instead of showing an unchanged healing outcome revealed a significantly impaired healing. This indicates that in cases of an unbalanced immune response otherwise supportive immune cells can turn into detrimental cells for the healing process.

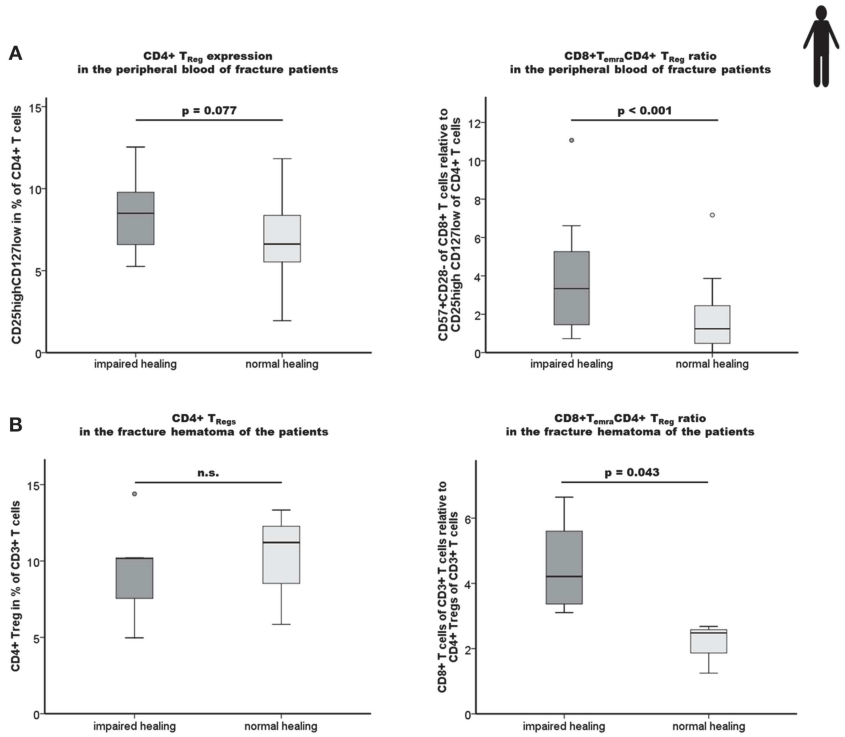

FIGURE 5 | Impaired fracture healing correlates with an elevated level of CD4+ T_{Reg} and a higher ratio of CD8+ T_{EMRA}/CD4+ T_{Reg}. **(A)** Results of the flow cytometry analyses of the CD4+ T_{Reg} and the ratio CD8+T_{EMRA}/CD4+T_{Reg} in the peripheral blood of fracture patients at the time of operation are shown. Impaired fracture healing patients showed slightly elevated levels of CD45+CD3+CD4+CD25highCD127low T_{Reg} (CD25highCD127low in % of CD45+CD3+CD4+) compared to the normal healing patients indicates a partial, but not sufficient compensatory effect. The ratio of CD8+T_{EMRA}/CD4+T_{Reg} was significantly higher in patients with a delayed healing: $n = 12$ for the impaired healing group, $n = 23$ for the normal healing group. **(B)** Impaired fracture healing patients showed a significantly higher ratio of CD8+T cells/CD4+ T_{Reg} in the hematoma region demonstrating an insufficient compensatory effect of the CD4+ T_{Reg} in the impaired fracture healing patients: $n = 5$ for the impaired healing group, $n = 3$ for the normal healing group. Student's *t*-test.

As in human beings, non-SPF housed mice, even if kept in the same cage, show an intragroup heterogeneity regarding the T_{EFF}/T_{Reg} balance in the blood and secondary immune organs. In mice with very high T_{EFF}/T_{Reg} ratio the adoptive transfer of T_{Reg} could not rescue this imbalance measured immediately after cell transfer in blood samples as well as at the end of 21 d follow-up in immune organs even though engraftment was confirmed. This unsuccessful rebalancing of the T_{EFF}/T_{Reg} ratio was associated not only with a lack of benefit of the T_{Reg} transfer but worsened the healing even more. For our immune-experienced mice, we applied a relative short exposure time of 4 weeks in the non-SPF housing. Therefore, the observed findings and differences in the non-SPF mice in comparison to the SPF mice are even more astonishing. In comparison, the changes in the adaptive immune system visible after 4 weeks of exposure were not as pronounced as seen in an aged human being. Therefore, the ratios in the mouse model cannot be transferred toward patients.

How can T_{EFF} cells affect bone healing? In fact, we could recently show (17) that CD8+ T_{EFF} produce high amounts of inflammatory cytokines, such as IFNγ and TNFα even without costimulatory signals. Their strong inflamed tissue homing properties allow them to deliver those cytokines at fracture sites. Although some local inflammation is beneficial for triggering endogenous regeneration post-fracture (38), too much of "a beautiful thing" can have worsening effects, as shown by inhibition of differentiation of osteogenic precursors in the presence of supernatants of CD8+ T_{EFF}, an effect that could be converted by neutralizing TNFα and IFNγ (17).

How might T_{Reg} control the T_{EFF} response in at least half of the immune-experienced mice with pre-established T_{EFF} cells? The positive effects of T_{Reg} might be explained by the prevention of an imbalanced T_{EFF}/T_{Reg} ratio as a result of T_{Reg} blocking memory/effector T cells at multiple checkpoints (34): T_{Reg} can inhibit the cytokine release and proliferation of T_{EFF} cells by cell-cell contact dependent and independent mechanisms. This seems to be related at least partly to adenosine formation and metabolic competition (e.g., tryptophan pathway) as shown before (34).

In summary, our findings confirm our recent data that suggested a negative impact of CD8+ T_{EMRA} on bone fracture healing in patients (17) but extend these observations further by demonstrating the relevance of the systemic and local balance between effector and regulatory mechanisms (T_{EFF}/T_{Reg} ratio). Moreover, our data indicate that a CD4+ T_{Reg} based immunomodulation is feasible to further bone regeneration but its efficiency is dependent on the recipient's immune status, especially of a balanced adaptive immunity (**Figure 6**).

The strong link between the pre-surgery immune cell ratio and the healing outcome was clearly demonstrated in our animal model.

Considering the fact that the non-responder mice show the tendency of even worse healing compared to the responder and even compared to the control mice the following considerations could be made. It is already well-known that CD4+ T_{Reg} are not a committed stable T cell subpopulation. Dependent on the inflammatory environment, several studies reported a loss of FOXP3 expression by CD4+ T_{Reg} accompanied by the loss of their suppressive activity (39, 40). Furthermore, CD4+ T_{Reg} cannot only lose their suppressive capacity but can also convert to CD4+ T_{EFF} cells such as Th17 cells (40–42). For Th17 cells controversial effects on bone cells have been reported. They can stimulate the formation of osteoclasts by the production of Receptor Activator of NF-κB Ligand (RANKL), either directly by themselves or indirectly via osteoblasts or synovial fibroblasts. Furthermore, it is described that Th17

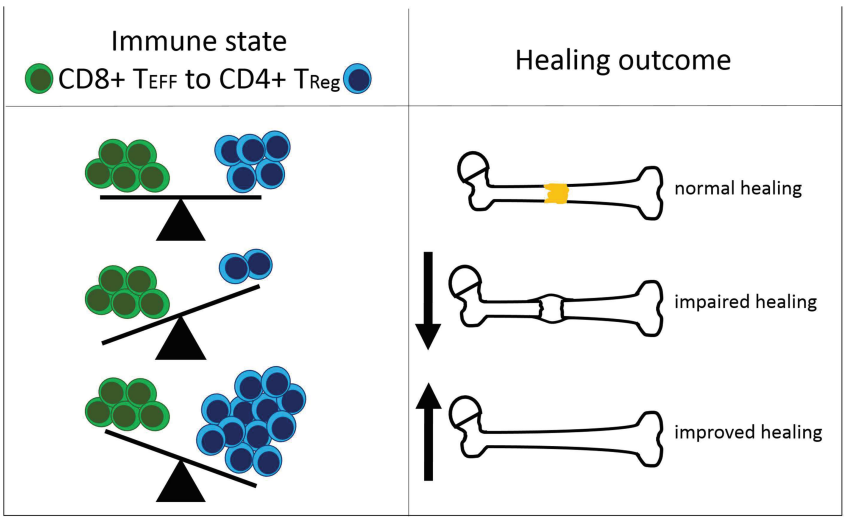

FIGURE 6 | Interdependency of the immune status and the healing outcome after bone fracture. The ratio of CD8+ effector T cells (CD8+ T_{EFF}) to CD4+ regulatory T cells (CD4+ T_{Reg}) affects the healing outcome after bone fracture. Under normal healing conditions, the T cell ratio is balanced. An elevated amount of CD8+ T_{EFF} relative to CD4+ T_{Reg} is unfavorable for successful healing. A shifted balance in the CD4+ T_{Reg} direction improves bone fracture healing.

cells act pro-osteogenic. Additionally, in the context of several bone related disorders, the underlying cause is postulated to be an imbalance of the ratio between Th17 cells and CD4+ T_{Reg} (43, 44).

In vitro studies using murine or human CD4+ T_{Reg} have demonstrated a possible transition between CD4+ T_{Reg} and IL-17 producing (Th17) T cells. For example, Xu et al. reported that this transition is IL-6 dependent (41). Using co-culture setups, another study showed that murine CD4+ T_{Reg} can obtain the expression of Rorγt, the master transcription factor of Th17 cells (45). Studies with human CD4+ T_{Reg} also revealed this conversion between CD4+ T_{Reg} and Th17 cells (46, 47). One possible explanation for the observed non-responsiveness of some CD4+ T_{Reg} enriched animals could, therefore, be a potential transition of the pro-regenerative CD4+ T_{Reg} into an anti-regenerative Th17-like phenotype. This hypothesis could be more directly verified by findings from Zhou and colleagues (*40*). They evaluated the stability and fate of (initially) Foxp3+ CD4+ T_{Reg} under homeostatic as well as pathogenic conditions *in vivo* by using a combined Foxp3-GFP-Cre/ R26-YFP mice system. This mouse model enables the detection of the induction or downregulation of Foxp3 expression and further allows to track the cell fate of Foxp3+ CD4+ T_{Reg}. Zhou and colleagues showed that the strength of loss of Foxp3 expression from CD4+ T_{Reg} was dependent on the microenvironment and was stronger in inflamed tissues in autoimmune conditions. Furthermore, they showed that these converted Foxp3- "CD4+ T_{Reg}" express memory cell marker and pro-inflammatory cytokines like IFNγ and IL-17. Thus, there is evidence that a strong pro-inflammatory microenvironment bears the risk to promote the transition of Foxp3+ to Foxp3- CD4+ T cells. If such a transition is happening during bone fracture healing in elevated pro-inflammatory conditions, this could explain the observed impaired healing in our mice where CD4+ T_{Reg} transfer did not overcome the pro-inflammatory microenvironment resulting from the high T_{EFF} levels.

CONCLUSION

Bone fracture healing is a highly complex process. The presented and discussed human and mice data demonstrate the strong interdependency between the adaptive immunity and the bone system in the context of bone healing. They further highlight how well-regulated the interplay of different (immune) cell subtypes has to be to promote regeneration. Due to the observed findings at both sides, locally at the fracture as well as systemically in the peripheral blood, this cellular interplay is probably not only crucial for bone fracture repair but also for the healing capacity of other injured tissues. With regard to clinical translation, our data indicate the advantage of a T_{EFF}/T_{Reg} ratio analysis, allowing to identify patients at risk in an early stratification and thereby predict already preoperatively the healing potential after bony injury. A prospective multicenter study (>600 patients) is currently ongoing to confirm the promising potential of the CD8+ T_{EMRA}/CD4+ T_{Reg} ratio as a potential biomarker for predicting the healing outcome in human bone fracture patients. Therefore, the cellular interplay could be used to better understand regulatory mechanisms guiding regenerative processes and thus could reveal possible novel target points for (immunomodulatory) treatment strategies to therapeutically support and improve impaired tissue repair.

DATA AVAILABILITY

All datasets generated for this study are included in the manuscript/**Supplementary Files**.

ETHICS STATEMENT

The study was performed in compliance with the International Conference on Harmonization Guidelines for Good Clinical Practice and the Declaration of Helsinki. All patients participated with a written informed consent, and the study was approved by the Institutional Review Board (IRB) of the Charité – Universitätsmedizin Berlin (IRB approval EA2/096/11). All animal experiments were approved by the local legal representatives (Landesamt für Gesundheit und Soziales Berlin: G0008/12; T0119/14; T0249/11) and done accordingly to the guidelines of the Animal Welfare Act, the National Institutes of Health Guide for Care and Use of Laboratory Animals, and the National Animal Welfare and ARRIVE Guidelines.

AUTHOR CONTRIBUTIONS

CS, KS-B, SR, SG, GD, and H-DV: conceptual idea and design of the study and drafting manuscript. CS and SR: data collection, analysis, and interpretation. CS and KS-B: clinically relevant osteotomy model. CG: hematoma preparation. BS, UB, and CG: epigenomic DNA data collection and analysis. SM, MD, and CK: clinical evaluation of patients and sample harvesting. CB: flow cytometry. All authors revised the final version of the manuscript.

FUNDING

This study was supported by grants from the German Research Foundation (DFG SCHE1594, DFG SCHM 2977) and by the Federal Ministry of Education and Research (BMBF: BCRT 2015-18 and EPILYZE 031A191B). We acknowledge support from the Open Access Publication Fund of Charité – Universitätsmedizin Berlin.

ACKNOWLEDGMENTS

We would like to acknowledge Norma Schulz, Janine Mikutta and Antje Blankenstein for her excellent technical support and Mathias Streitz and Birgit Sawitzki for their advice in flow cytometry analyses and murine T_{Reg} preparation, respectively.

SUPPLEMENTARY MATERIAL

The Supplementary Material for this article can be found online at: https://www.frontiersin.org/articles/10.3389/fimmu.2019.01954/full#supplementary-material

REFERENCES

1. Einhorn TA, Gerstenfeld LC. Fracture healing: mechanisms and interventions. *Nat Rev Rheumatol*. (2015) 11:45–54. doi: 10.1038/nrrheum.2014.164
2. Dimitriou R, Tsiridis E, Giannoudis PV. Current concepts of molecular aspects of bone healing. *Injury*. (2005) 36:1392–404. doi: 10.1016/j.injury.2005.07.019
3. Schlundt C, Bucher CH, Tsitsilonis S, Schell H, Duda GN, Schmidt-Bleek K. Clinical and research approaches to treat non-union fracture. *Curr Osteoporos Rep*. (2018) 16:155–68. doi: 10.1007/s11914-018-0432-1
4. Bucher CH, Lei H, Duda GN, Volk HD, Schmidt-Bleek K. The role of immune Reactivity in bone regeneration. In: Zorzi AR, editor. *Advanced Techniques in Bone Regeneration*. IntechOpen. (2016). Available online at: https://www.intechopen.com/books/advanced-techniques-in-bone-regeneration/the-role-of-immune-reactivity-in-bone-regeneration
5. Shapouri-Moghaddam A, Mohammadian S, Vazini H, Taghadosi M, Esmaeili SA, Mardani F, et al. Macrophage plasticity, polarization, and function in health and disease. *J Cell Physiol*. (2018) 233:6425–40. doi: 10.1002/jcp.26429
6. Schlundt C, El Khassawna T, Serra A, Dienelt A, Wendler S, Schell H, et al. Macrophages in bone fracture healing: their essential role in endochondral ossification. *Bone*. (2018) 106:78–89. doi: 10.1016/j.bone.2015.10.019
7. Schmidt-Bleek K, Schell H, Lienau J, Schulz N, Hoff P, Pfaff M, et al. Initial immune reaction and angiogenesis in bone healing. *J Tissue Eng Regen Med*. (2014) 8:120–30. doi: 10.1002/term.1505
8. Barbul A, Breslin RJ, Woodyard JP, Wasserkrug HL, Efron G. The effect of in vivo T helper and T suppressor lymphocyte depletion on wound healing. *Ann Surg*. (1989) 209:479–83. doi: 10.1097/00000658-198904000-00015
9. Efron JE, Frankel HL, Lazarou SA, Wasserkrug HL, Barbul A. Wound healing and T-lymphocytes. *J Surg Res*. (1990) 48:460–3. doi: 10.1016/0022-4804(90)90013-R
10. Hauser CJ, Zhou X, Joshi P, Cuchens MA, Kregor P, Devidas M, et al. The immune microenvironment of human fracture/soft-tissue hematomas and its relationship to systemic immunity. *J Trauma*. (1997) 42:895–903; discussion 903–894. doi: 10.1097/00005373-199705000-00021
11. Könnecke I, Serra A, El Khassawna T, Schlundt C, Schell H, Hauser A, et al. T and B cells participate in bone repair by infiltrating the fracture callus in a two-wave fashion. *Bone*. (2014) 64:155–65. doi: 10.1016/j.bone.2014.03.052
12. Naik AA, Xie C, Zuscik MJ, Kingsley P, Schwarz EM, Awad H, et al. Reduced COX-2 expression in aged mice is associated with impaired fracture healing. *J Bone Miner Res*. (2009) 24:251–64. doi: 10.1359/jbmr.081002
13. Schlundt C, Schell H, Goodman SB, Vunjak-Novakovic G, Duda GN, Schmidt-Bleek K. Immune modulation as a therapeutic strategy in bone regeneration. *J Exp Orthop*. (2015) 2:1. doi: 10.1186/s40634-014-0017-6
14. Schmidt-Bleek K, Petersen A, Dienelt A, Schwarz C, Duda GN. Initiation and early control of tissue regeneration - bone healing as a model system for tissue regeneration. *Exp Opin Biol Therap*. (2014) 14:247–59. doi: 10.1517/14712598.2014.857653
15. Schmidt-Bleek K, Schell H, Kolar P, Pfaff M, Perka C, Buttgereit F, et al. Cellular composition of the initial fracture hematoma compared to a muscle hematoma: a study in sheep. *J Orthop Res*. (2009) 27:1147–51. doi: 10.1002/jor.20901
16. Schmidt-Bleek K, Schell H, Schulz N, Hoff P, Perka C, Buttgereit F, et al. Inflammatory phase of bone healing initiates the regenerative healing cascade. *Cell Tissue Res*. (2012) 347:567–73. doi: 10.1007/s00441-011-1205-7
17. Reinke S, Geissler S, Taylor WR, Schmidt-Bleek K, Juelke K, Schwachmeyer V, et al. Terminally differentiated CD8(+) T cells negatively affect bone regeneration in humans. *Sci Transl Med*. (2013) 5:177ra136. doi: 10.1126/scitranslmed.3004754
18. Liu Y, Wang L, Kikuiri T, Akiyama K, Chen C, Xu X, et al. Mesenchymal stem cell-based tissue regeneration is governed by recipient T lymphocytes via IFN-gamma and TNF-alpha. *Nat Med*. (2011) 17:1594–601. doi: 10.1038/nm.2542
19. Zaiss MM, Axmann R, Zwerina J, Polzer K, Gückel E, Skapenko A, et al. Treg cells suppress osteoclast formation: a new link between the immune system and bone. *Arthritis Rheum*. (2007) 56:4104–12. doi: 10.1002/art.23138
20. Zaiss MM, Frey B, Hess A, Zwerina J, Luther J, Nimmerjahn F, et al. Regulatory T cells protect from local and systemic bone destruction in arthritis. *J Immunol*. (2010) 184:7238–46. doi: 10.4049/jimmunol.0903841
21. Zaiss MM, Sarter K, Hess A, Engelke K, Böhm C, Nimmerjahn F, et al. Increased bone density and resistance to ovariectomy-induced bone loss in FoxP3-transgenic mice based on impaired osteoclast differentiation. *Arthritis Rheum*. (2010) 62:2328–38. doi: 10.1002/art.27535
22. Pappritz K, Savvatis K, Miteva K, Kerim B, Dong F, Fechner H, et al. Immunomodulation by adoptive regulatory T-cell transfer improves Coxsackievirus B3-induced myocarditis. *FASEB J*. (2018) fj201701408R. doi: 10.1096/fj.201701408R. [Epub ahead of print].
23. Geissler S, Textor M, Stumpp S, Seitz S, Lekaj A, Brunk S, et al. Loss of murine Gfi1 causes neutropenia and induces osteoporosis depending on the pathogen load and systemic inflammation. *PLoS ONE*. (2018) 13:e0198510. doi: 10.1371/journal.pone.0198510
24. Bucher CH, Schlundt C, Wulsten D, Sass FA, Wendler S, Ellinghaus A, et al. Experience in the Adaptive Immunity Impacts Bone Homeostasis, Remodeling, and Healing. *Front Immunol*. (2019)10:797. doi: 10.3389/fimmu.2019.00797
25. Bouxsein ML, Boyd SK, Christiansen BA, Guldberg RE, Jepsen KJ, Müller R. Guidelines for assessment of bone microstructure in rodents using micro-computed tomography. *J Bone Miner Res*. (2010) 25:1468–86. doi: 10.1002/jbmr.141
26. Gollwitzer H, Karampour K, Hauschild M, Diehl P, Busch R, Mittelmeier W. Biomechanical investigation of the primary stability of intramedullary compression nails in the proximal tibia: experimental study using interlocking screws in cryopreserved human tibias. *J Orthop Sci*. (2004) 9:22–8. doi: 10.1007/s00776-003-0731-x
27. Hasenboehler E, Rikli D, Babst R. Locking compression plate with minimally invasive plate osteosynthesis in diaphyseal and distal tibial fracture: a retrospective study of 32 patients. *Injury*. (2007) 38:365–70. doi: 10.1016/j.injury.2006.10.024
28. Moghaddam A, Zimmermann G, Hammer K, Bruckner T, Grützner PA, von Recum J. Cigarette smoking influences the clinical and occupational outcome of patients with tibial shaft fractures. *Injury*. (2011) 42:1435–42. doi: 10.1016/j.injury.2011.05.011
29. Yang KH, Patel A. Significance of fracture gap in open tibial fracture. *Yonsei Med J*. (1995) 36:130–6. doi: 10.3349/ymj.1995.36.2.130
30. Türbachova I, Schwachula T, Vasconcelos I, Mustea A, Baldinger T, Jones KA, et al. The cellular ratio of immune tolerance (immunoCRIT) is a definite marker for aggressiveness of solid tumors and may explain tumor dissemination patterns. *Epigenetics*. (2013) 8:1226–35. doi: 10.4161/epi.26334
31. Wieczorek G, Asemissen A, Model F, Turbachova I, Floess S, Liebenberg V, et al. Quantitative DNA methylation analysis of FOXP3 as a new method for counting regulatory T cells in peripheral blood and solid tissue. *Cancer Res*. (2009) 69:599–608. doi: 10.1158/0008-5472.CAN-08-2361
32. Baron U, Werner J, Schildknecht K, Schulze JJ, Mulu A, Liebert UG, et al. Epigenetic immune cell counting in human blood samples for immunodiagnostics. *Sci Transl Med*. (2018) 10:eaan3508. doi: 10.1126/scitranslmed.aan3508
33. Apostolou I, von Boehmer H. *In vivo* instruction of suppressor commitment in naive T cells. *J Exp Med*. (2004) 199:1401–8. doi: 10.1084/jem.20040249
34. Lei H, Schmidt-Bleek K, Dienelt A, Reinke P, Volk HD. Regulatory T cell-mediated anti-inflammatory effects promote successful tissue repair in both indirect and direct manners. *Front Pharmacol*. (2015) 6:184. doi: 10.3389/fphar.2015.00184
35. Lang A, Schulz A, Ellinghaus A, Schmidt-Bleek K. Osteotomy models - the current status on pain scoring and management in small rodents. *Lab Ani*. (2016) 50:433–41. doi: 10.1177/0023677216675007
36. Klein RF, Mitchell SR, Phillips TJ, Belknap JK, Orwoll ES. Quantitative trait loci affecting peak bone mineral density in mice. *J Bone Min Res*. (1998) 13:1648–56. doi: 10.1359/jbmr.1998.13.11.1648
37. Sbierski-Kind J, Kath J, Brachs S, Streitz M, von Herrath MG, Kühl AA, et al. Distinct housing conditions reveal a major impact of adaptive immunity on the course of obesity-induced type 2 diabetes. *Front Immunol*. (2018) **9**:1069. doi: 10.3389/fimmu.2018.01069
38. El Khassawna T, Serra A, Bucher CH, Petersen A, Schlundt C, Könnecke I, et al. T lymphocytes influence the mineralization process of bone. *Front in immunology*. (2017) 8:562 doi: 10.3389/fimmu.2017.00562

39. Rubtsov YP, Niec RE, Josefowicz S, Li L, Darce J, Mathis D, et al. Stability of the regulatory T cell lineage *in vivo*. *Science*. (2010) 329:1667–71. doi: 10.1126/science.1191996
40. Zhou X, Bailey-Bucktrout SL, Jeker LT, Penaranda C, Martínez-Llordella M, Ashby M, et al. Instability of the transcription factor Foxp3 leads to the generation of pathogenic memory T cells *in vivo*. *Nat Immunol*. (2009) 10:1000–7. doi: 10.1038/ni.1774
41. Xu L, Kitani A, Fuss I, Strober W. Cutting edge: regulatory T cells induce CD4+CD25-Foxp3- T cells or are self-induced to become Th17 cells in the absence of exogenous TGF-beta. *J Immunol*. (2007) 178:6725–9. doi: 10.4049/jimmunol.178.11.6725
42. Yang XO, Nurieva R, Martinez GJ, Kang HS, Chung Y, Pappu BP, et al. Molecular antagonism and plasticity of regulatory and inflammatory T cell programs. *Immunity*. (2008) 29:44–56. doi: 10.1016/j.immuni.2008.05.007
43. Niu Q, Cai B, Huang ZC, Shi YY, Wang LL. Disturbed Th17/Treg balance in patients with rheumatoid arthritis. *Rheumatol Int*. (2012) 32:2731–6. doi: 10.1007/s00296-011-1984-x
44. Tyagi AM, Srivastava K, Mansoori MN, Trivedi R, Chattopadhyay N, Singh D. Estrogen deficiency induces the differentiation of IL-17 secreting Th17 cells: a new candidate in the pathogenesis of osteoporosis. *PLoS ONE*. (2012) **7**:e44552. doi: 10.1371/journal.pone.0044552
45. Osorio F, LeibundGut-Landmann S, Lochner M, Lahl K, Sparwasser T, Eberl G, et al. DC activated via dectin-1 convert Treg into IL-17 producers. *Eur J Immunol*. (2008) 38:3274–81. doi: 10.1002/eji.200838950
46. Beriou G, Costantino CM, Ashley CW, Yang L, Kuchroo VK, Baecher-Allan C, et al. IL-17-producing human peripheral regulatory T cells retain suppressive function. *Blood*. (2009) 113:4240–9. doi: 10.1182/blood-2008-10-183251
47. Koenen HJ, Smeets RL, Vink PM, van Rijssen E, Boots AM, Joosten I. Human CD25highFoxp3pos regulatory T cells differentiate into IL-17-producing cells. *Blood*. (2008) 112:2340–52. doi: 10.1182/blood-2008-01-133967

Conflict of Interest Statement: BS and UB were employed by the company Epiontis GmbH, Precision for Medicine Group, Berlin, Germany.

The remaining authors declare that the research was conducted in the absence of any commercial or financial relationships that could be construed as a potential conflict of interest.

9 Curriculum vitae

Mein Lebenslauf wird aus datenschutzrechtlichen Gründen in der elektronischen Version meiner Arbeit nicht veröffentlicht.

10 Publication list

2019

Schlundt C, Reinke S, Geissler S, Bucher CH, Giannini C, Märdian S, Dahne M, Kleber C, Samans B, Baron U, Duda GN, Volk H-D, Schmidt-Bleek K. Individual Effector/Regulator T Cell Ratios Impact Bone Regeneration. Front Immunol. 2019 Aug 16;10:1954. IF: 5.51

Bucher CH, Schlundt C, Wulsten D, Sass FA, Wendler S, Ellinghaus A, Thiele T, Seemann R, Willie BM, Volk H-D, Duda GN, Schmidt-Bleek K. Experience in the Adaptive Immunity Impacts Bone Homeostasis, Remodeling, and Healing. Front Immunol. 2019;10:797. IF: 5.51

Wendler S, Schlundt C, Bucher CH, Birkigt J, Schipp CJ, Volk H-D, Duda GN, Schmidt-Bleek K. Immune Modulation to Enhance Bone Healing—A New Concept to Induce Bone Using Prostacyclin to Locally Modulate Immunity. Front Immunol. 2019 Apr 5;10:713. IF: 5.51

2018

Schlundt C, Bucher CH, Tsitsilonis S, Schell H, Duda GN, Schmidt-Bleek K. Clinical and Research Approaches to Treat Non-union Fracture. Curr Osteoporos Rep. 2018 Apr 13;16(2):155–68. IF: 3.93

Bucher CH, Schmidt-Bleek K. Knochenheilung bei geriatrischen Patienten – die Rolle des Immunsystems. M&K kompakt Sonderheft von Management & Krankenhaus, Wiley-VCH. 2018

2017

Khassawna T El, Serra A, Bucher CH, Petersen A, Schlundt C, Könnecke I, Malhan D, Wendler S, Schell H, Volk HD, Schmidt-Bleek K, Duda GN. T lymphocytes influence the mineralization process of bone. Front Immunol. 2017 May 24;8(MAY):562. IF: 5.51

Bucher CH, Schlundt C, Elmiger J, Reinke S, Duda GN, Geissler S, Schmidt-Bleek K. Das Zusammenspiel des Knochen- und Immunsystems, Osteoporose & Rheuma aktuell, MedienDiensteMedizin. 2017;4

2016

Bucher CH, Lei H, Duda GN, Volk H-D, Schmidt-Bleek K. The Role of Immune Reactivity in Bone Regeneration. In: Advanced Techniques in Bone Regeneration. InTech; 2016.

2013

Bucher CH, Gazdhar A, Benneker LM, Geiser T, Gantenbein-Ritter B. Nonviral Gene Delivery of Growth and Differentiation Factor 5 to Human Mesenchymal Stem Cells Injected into a 3D Bovine Intervertebral Disc Organ Culture System. Stem Cells Int. 2013 Jan;2013:326828. IF: 2.80

Acknowledgments

Ich möchte mich bei meinen Betreuern, Georg Duda und Hans-Dieter Volk, herzlich bedanken für die Möglichkeit eine Dissertation unter ihrer Anleitung erarbeiten zu können. Ich bin sehr dankbar, dass ich an eurem Experten-Wissen teilhaben durfte und ich immer Unterstützung erfahren durfte, wo immer ich sie brauchte. Ganz besonders möchte ich mich bei meiner Mentorin Kate Schmidt-Bleek bedanken, die mir unermüdlich zur Seite stand, mir freie Hand gelassen hat, damit ich meiner Phantasie freien Lauf lassen konnte, neues Ausprobieren durfte und mir dabei auch die Finger verbrennen durfte. Ich habe unglaublich viel gelernt, vielen lieben Dank Kate.

Auch ohne meine Arbeitskollegen wäre ich nie so weit gekommen, daher möchte ich mich bei Claudia Schlundt, Julia Berkmann, Lisa Burkhardt, Sabine Stumpp, Sebastian Wendler, Christine Figge und bei Sven Geissler bedanken für die Unterstützung auf Arbeit aber auch für die lustigen Stunden im Privaten. Besonders hervorheben möchte ich Norma Schulz, die es nicht immer einfach hatte mit mir, da ich zu oft Methoden neu etabliert und angepasst habe, vielen Dank für deine Unterstützung Norma.

Diese Dissertation widme ich meiner Familie, die immer für mich da ist, mich unterstützt bei meinen Flausen und der stetige Rückhalt meines Lebens ist. Mam, Pa, Anja, Matthias, Vreni: Merci viu mau für aues! Auch meinen Freunden gilt ein besonderer Dank, ihr habt es nicht immer leicht mit mir: Sven, Fyllis, Joelle, Jenny, Chregu, Susanne und Tommy vielen Dank für eure Freundschaft!